



International Journal of Computational Engineering Research

Volume 4, Issue 8, August, 2014

Open Access
JOURNAL



International Journal of Computational Engineering Research is an international, peer-reviewed journal publishing an overview of IT research and algorithmic processes that create, describe and transform information to formulate suitable abstractions to model complex systems.



International Journal of Computational Engineering Research under Open Access category aims to provide advance in the study of the theoretical foundations of information and computation and of practical techniques.



International Journal of Computational Engineering Research explicates the complicated aspects of Information Technology & Software Engineering and focusing on research and experience that contributes to the improvement of software development practices. The Journal has a dual emphasis and contains articles that are of interest both to practicing information technology professionals and to university and industry researchers.

International Journal of Computational Engineering Research - Open Access uses online manuscript submission, review and tracking systems for quality and quick review processing. Submit your manuscript at

<http://www.ijceronline.com/online-submission.html>

Editors & Editor's Board



DR. Qais Faryadi

USIM (Islamic Science University of Malaysia)

Dr. Lingyan Cao

University of Maryland College Park, MD, US

Dr. A.V.L.N.S.H. Hariharan

Gitam University, Visakhapatnam, India

Dr. Md. Mustafizur Rahman

Universiti Kebangsaan Malaysia (UKM)

Dr. S. Morteza Bayareh

Islamic Azad University Iran

Dr. Zahra Mekkioui

University of Tlemcen, Algeria

Dr. Yilun Shang

University of Texas at San Antonio, TX 78249

Lugen M. Zake Sheet

University of Mosul, Iraq

Mohamed Abdellatif

Graduate School of Natural Science and Technology



Meisam Mahdavi

University of Tehran Iran

Dr. Ahmed Nabih Zaki Rashed

Menoufia University, Egypt

Dr. José M. Merigó Lindahl

University of Barcelona, Spain

Dr. Mohamed Shokry Nayle

Faculty of Engineering Tanta University Egypt

Dr. Thanhtrung Dang

Hochiminh City University of Technical Education, Vietnam

Dr. Sudarson Jena

GITAM University, INDIA

Dr. S. Prakash

Professor, Sathyabama University, Chennai

Mr. J. Banuchandar

P.S.R Engineering College, Sivakasi, Tamilnadu

Dr. Vuda Sreenivasarao

Defence University College, Deberzeit, Ethiopia.



M. Chithik Raja

Salalah College of Technology, Oman

Md. Zakaria Mahub

Islamic University Of Technology (IUT), Bangladesh

Dr. Mohana Sundaram Muthuvalu

Universiti Malaysia Sabah, Malaysia

Dr. Virajit A. Gundale

SITCOE, Yadrav, Kolhapur Maharashtra

Mohamed Abdellatif

Graduate School of Natural Science and Technology

CONTENTS:

S.No.	Title Name	Page No.
Version I		
1.	Improving and Comparing the Coefficient of Performance of Domestic Refrigerator by using Refrigerants R134a and R600a Suresh Boorneni A.V.Satyanarayana	01-05
2.	On $(1,2)^*$ - $\pi g\theta$ -CLOSED SETS IN BITOPOLOGICAL SPACES C.Janaki M. Anandhi	06-12
3.	Enhancement of the Performance of Hydraulic Power Pack by Increasing Heat Dissipation M.L.R.Chaitanya Lahari DR.B.SRINIVASA REDDY	13-19
4.	A Brief Study on Usability Principles of Mobile Commerce Manjot Kaur	20-25
5.	Path Loss Prediction by Robust Regression Methods T. E. Dalkilic K. S. Kula B. Y. Hanci	26-35
6.	Stochastic Model to Find the Diagnostic Reliability of Gallbladder Ejection Fraction Using Normal Distribution P. Senthil Kumar A. Dinesh Kumar M. Vasuki	36-41
7.	Vehicle Theft Intimation Using GSM Minakshi Kumari Prof. Manoj Singh	42-47
8.	XML Retrieval: A Survey Hasan Naderi Mohammad Nazari Farokhi Nasredin Niazy Behzad Hosseini Chegeni Somaye Nouri Monfared Iran	48-54
9.	Prediction System for Reducing the Cloud Bandwidth and Cost G Bhuvaneswari Mr. K.Narayana Erasappa Murali	55-59
10.	A New Way of Identifying DOS Attack Using Multivariate Correlation Analysis R Nagadevi P Nageswara Rao Rameswara Anand	60-64
11.	An Efficient FB Addressing Protocol for Auto configuration of Ad Hoc Networks Kg Mohanavalli P Nageswara Rao Rameswara Anand	65-71
Version II		
	Effects Of Skewness On Three Span Reinforced Concrete T Girder Bridges Himanshu Jaggerwal Yogesh Bajpai	01-09

2.	Modelling Of Water Resources in Bakaru Hydropower Plant in Anticipating Load Increment in Sulsebar Power System Sri Mawar Said Salama Manjang M.Wihardi Tjaronge Muh. Arsyad Thaha	10-14
3.	Performance Analysis of Neighbour Coverage Probabilistic Rebroadcast to Reduce the Routing Overhead Over Ad-hoc On Demand Distance Vector Protocol Ms. Rajeshree Ambulkar Prof. Milind Tote	15-19
4.	Simulation of Two-Concentric Ring Microstrip Patch Antenna Dr. K. Kumar Naik Harini Appana Prasanth Palnati Priyanka Kotte	20-23
5.	Modeling of Dissolved oxygen and Temperature of Periyar river, South India using QUAL2K Lakshmi.E Dr.G. Madhu	24-31
6.	Design Of QOS Aware Light Path Planning And Technical Aspects In Wdm Networks Ashish Kumar Prof. R.L.Sharma	32-38
7.	Cuckoo Search Based Threshold Optimization for Initial Seed Selection in Seeded Region Growing M.Mary Synthuja Jain Preetha Dr. L.Padma Suresh M.John Bosco	39-42
8.	Development of Self Repairable Concrete System Sahebrao.G.Kadam Dr. M.A.Chakrabarti S.V.Kedare	43-48
9.	Case Study on Injection Moulding Windsor 650 Machine Parameters on Wall Thickness Variation Defect K. Raghavendra Kasyap M Subba Rao	49-53

Improving and Comparing the Coefficient of Performance of Domestic Refrigerator by using Refrigerants R134a and R600a

Suresh Boorneni¹ , A.V.Satyanarayana²,

¹Department of Mechanical Engineering, G.P.R College of Engineering, Andhra Pradesh, India)

²ASSOCIATE PROFESSOR (Department Of Mechanical Engineering, G.P.R College of Engineering, Andhra Pradesh, India)

ABSTRACT

The main objective in present dissertation has been focused on alternative refrigerant to conventional CFC refrigerant, CFC like R12, R22, R134a, etc... are not eco friendly. The emission of these refrigerants causes the depletion of ozone layer etc.... Hence to avoid above difficulty the alternative of refrigerant in the form of R600a has been choosing. R600a refrigerant are natural refrigerant consist of hydrocarbon. In the present work, the performance of the domestic refrigerator is determined using R600a (Isobutane) and comparison with R134a (Tetrafluoro-ethane) as the part of project work the refrigerator setup consists of evaporator, compressor, condenser and expansion valve are chosen with suitable specification. Also in the present work an attempt has been made to improve the coefficient of performance (cop) of the system, by incorporating a heat exchanger before admitting refrigerant into the compressor. Thus the compressor work reduces and it may results increase the performance of the refrigeration system.

KEYWORDS :Heat exchanger, coefficient of performance, Isobutane, depletion of ozone, alternative refrigerants.

I. INTRODUCTION

Vapor compression Refrigeration system is an improved type of Mechanical refrigeration system. The ability of certain liquids to absorb enormous quantities of heat as they vaporize is the basis of this system. Compared to melting solids (say ice) to obtain refrigeration effect, vaporizing liquid refrigerant has more advantages. To mention a few, the refrigerating effect can be started or stopped at will, the rate of cooling can be predetermined, the vaporizing temperatures can be governed by controlling the pressure at which the liquid vaporizes. Moreover, the vapor can be readily collected and condensed back into liquid state so that same liquid can be recirculated over and over again to obtain refrigeration effect. Thus the vapor compression system employs a liquid refrigerant which evaporates and condenses readily. The System is a closed one since the refrigerant never leaves the system. The coefficient of performance of a refrigeration system is the ratio of refrigerating effect to the compression work; therefore the coefficient of performance can be increased by increasing the refrigerating effect or by decreasing the compression work. The Vapor compression refrigeration system is now-a-days used for all purpose refrigeration. It is generally used for all industrial purposes from a small domestic refrigerator to a big air-conditioning plant.

1.2 Statement of Problem

The main components of refrigeration system are compressor, condenser, expansion valve and evaporator. In general refrigeration system the entire refrigeration circuit is exposed to atmosphere so that some losses may occur. So the entire refrigeration circuit is placed in the closed cabin. The emission of refrigerants like R12, R22, R134a etc... are causes the depletion of ozone layer. So that the refrigerant R600a has been chosen because it is natural refrigerant consist of hydrocarbon and eco friendly.

In the present dissertation work the heat exchanger is incorporated i.e. the capillary tube is insulated together with suction line of the compressor. So that the heat transfer occur between vapour refrigerant in the suction line and the liquid refrigerant in the capillary tube, so that some precooled liquid refrigerant can enter in to evaporator which is more efficient than regular refrigeration system. This change in temperature of liquid refrigerant entering in to evaporator will increase the coefficient performance of the system.

1.3 objective of the work

1. Determining the actual coefficient of performance of domestic refrigerator using refrigerants R-134a and R-600a.
2. Comparison the coefficient of performance of domestic refrigerators between refrigerants using R-134a and R-600a.
3. Experiments increasing coefficient of performance of vapour compression refrigeration system by incorporating heat exchanger.
4. Comparison the coefficient of performance of domestic refrigerators between refrigerants using R-134a and R-600a after incorporating heat exchanger.

II. EXPERIMENTAL SETUP AND DESIGN DETAILS

Different experimental and theoretical comparison is performed by many researchers to evaluate the performance of domestic refrigerator by using different refrigerants. In this experimental R-600a is compared with the R-134a in a domestic refrigeration system. To perform the experiment 165L refrigerator is selected which was designed to work with R-134a. It consists of an evaporator, air cooled condenser, reciprocating compressor. Heat exchanger incorporating in system, capillary tube rounded on the entire suction line of system. By the process rounding of capillary to the suction line we reduce that external type of heat exchanger.



Figure.1 Fabrication of Refrigeration Tutor before Heat Exchanger Incorporation

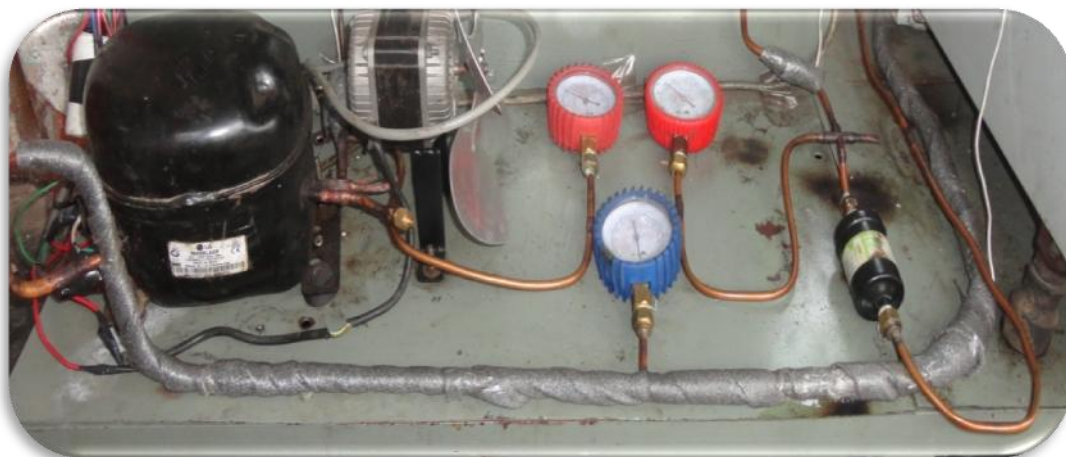


Figure.2 Fabrication of Refrigeration Tutor after Heat Exchanger Incorporation

III. EXPERIMENTAL PROCEDURE

While coming experiment two types of refrigerant using in the refrigerator R134a & R600a, Putting the freezer regulator at top position so that no need of cut-off easily taken for system. Take down which refrigerant is in application. Take down the energy meter reading no of seconds for 5 revolution of energy meter Take down the reading of compressor pressure discharge inlet & condenser outlet from the pressure gauges. Take down the temperature readings of compressor suction line, discharge temperature, temperature of evaporator and condenser outlet temperature of system. Calculate coefficient of performance & energy consumption. And the experiment is repeated for other refrigerant and the readings are tabulated in the tabular column.

IV. RESULTS AND DISCUSSION

Table reading taken from the experimental procedure of R134a refrigerant placed in the experimental setup. Note the reading of compressor inlet, compressor outlet condenser outlet, evaporator temperature pressure & of various parameters in the setup.

Table.1 Reading of R134a Refrigerant without Heat Exchanger

Operating freezer point	N (rev/sec)	T ₁ °c	T ₂ °c	T ₃ °c	P ₁ (bar)	P ₂ (bar)	P ₃ (bar)	C.O.P
1	61:07	-3.7	53	40	0.68	9.6	9.31	4.22
2	61:12	-5.9	56.9	42	0.62	10.34	9.65	4.20
3	60:00	-9.3	57.5	44	0.55	11.72	11.03	4.16
4	59:00	-11	60	46	0.55	11.72	11.03	3.81

Table .2 Reading of R134a Refrigerant with Heat Exchanger

Operating freezer point	N (rev/sec)	T ₁ °c	T ₂ °c	T ₃ °c	P ₁ (bar)	P ₂ (bar)	P ₃ (bar)	C.O.P
1	46:10	-7.9	54.8	44.3	0.68	17.24	16.55	4.55
2	49:18	-7.9	54.9	42.3	0.55	15.51	14.62	4.44
3	50:30	-9.6	55.6	41.6	0.58	15.72	15.03	4.30
4	49:29	-12	57	42.6	0.58	15.86	15.17	3.9
5	51:20	-15	58.5	43	0.37	15.17	14.48	3.87
6	53:12	-17.8	59.2	43.1	0.344	15.17	14.48	3.64
7	52	-19	60.1	43.1	0.310	14.48	14.13	3.40

Table reading taken from the experimental procedure of R600a refrigerant placed in the experimental setup. Note down reading as per procedure placed.

Table .3 Reading for R600a without Heat Exchanger

Operating freezer point	N (rev/sec)	T ₁ °c	T ₂ °c	T ₃ °c	P ₁ (bar)	P ₂ (bar)	P ₃ (bar)	C.O.P
1	54	-10.6	55.9	45.2	0.14	9.2	8.21	5.76
2	55	-11.6	57.4	45.1	0.13	8.9	8.12	4.12
3	54	-12.2	56.8	43.9	0.14	9.1	7.94	4.76
4	57	-14.1	57.2	43	0.07	8.06	7.79	3.9
5	60	-16.8	58.4	44	0.08	8.34	7.94	3.8
6	57	-17.7	59.3	43.8	0.07	8	7.35	3.7
7	60	-18.3	60	44.3	0.08	7.92	7.24	4.08

Table .4 Reading for R600a Refrigerant with Heat Exchanger

Operating freezer point	N (rev/sec)	T ₁ °c	T ₂ °c	T ₃ °c	P ₁ (bar)	P ₂ (bar)	P ₃ (bar)	C.O.P
1	55:10	-11.6	51.9	41.3	0.13	8.2	7.93	5.2
2	55:10	-11.9	51.7	39.4	0.13	8.4	7.93	5.19
3	56:60	-12.9	52.3	41.7	0.14	8.2	7.91	5.21
4	56:10	-14.6	53.6	39.6	0.06	8.06	7.79	4.15
5	60:20	-17.6	53.7	38	0.06	7.93	7.58	3.6
6	60:09	-19.2	53.3	39.2	0.07	7.44	7.24	4.01
7	60:05	-19.6	53.5	38.6	0.06	7.33	7.17	4.06

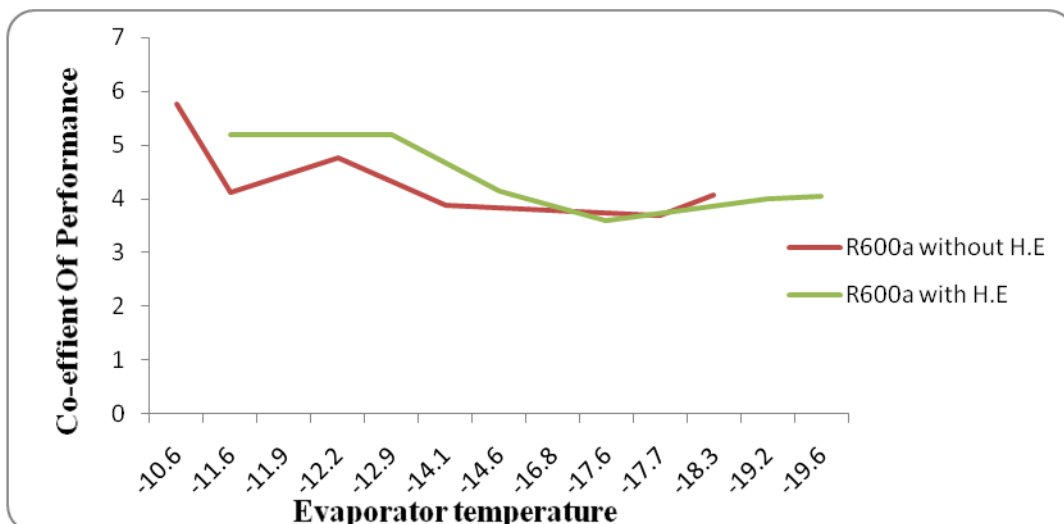


Figure .3 Shows R600a refrigerant Evaporator point V_s C.O.P
Colour Represent in graph Green colour : refrigerant with H.E
 Red colour : refrigerant without H.E

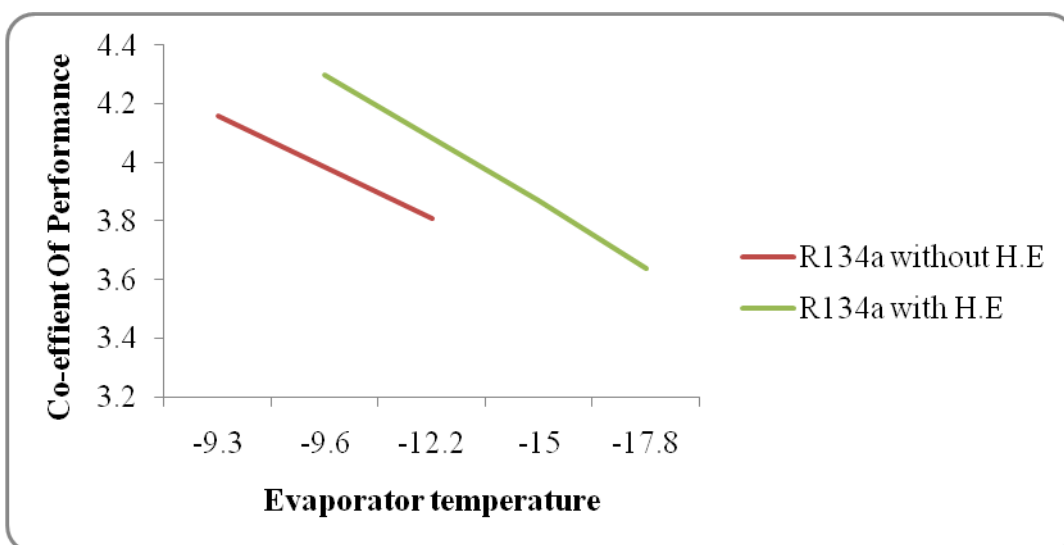


Figure .4 Shows R134a refrigerant Evaporator point V_s C.O.P

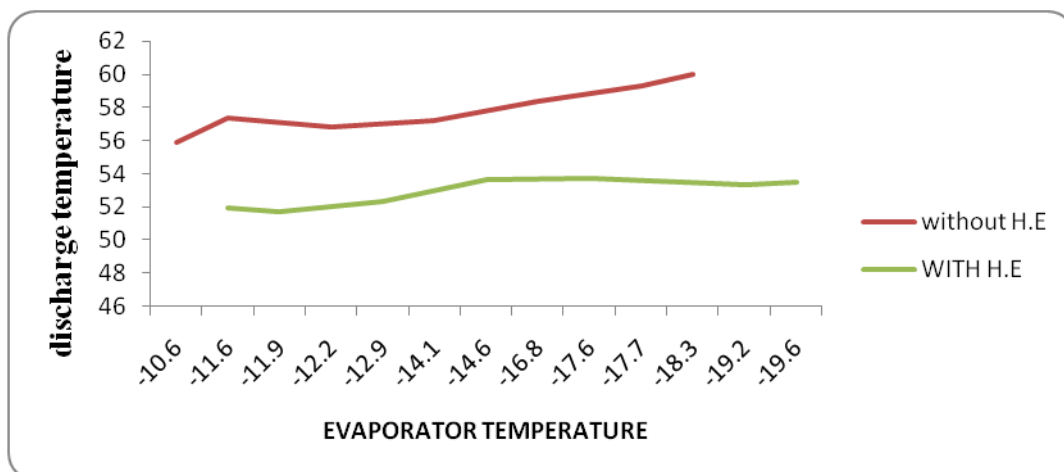


Figure .5 Represent R600a evaporator Temp V_s Discharge Temp

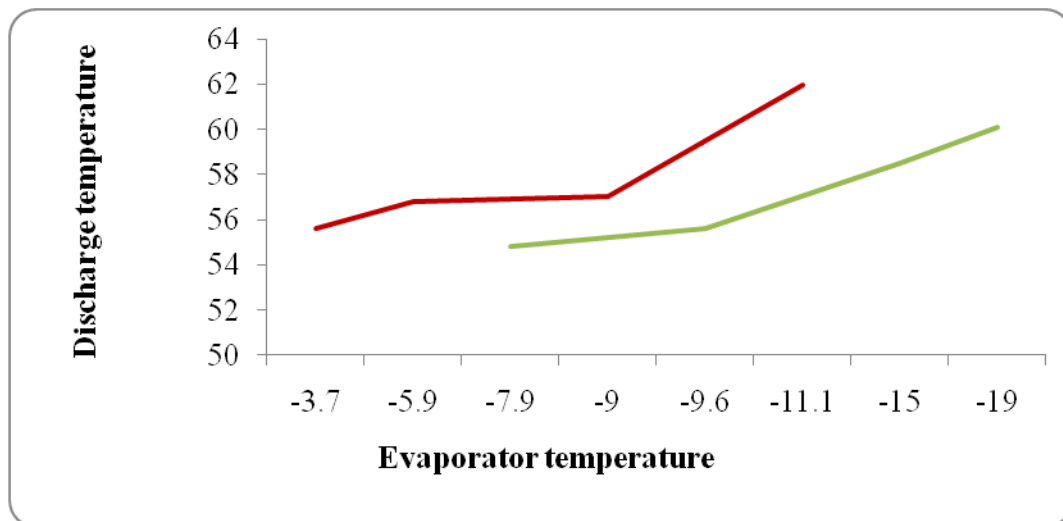


Figure .6 Represent R134a evaporator Temp Vs Discharge Temp

V. CONCLUSIONS

An experiment is conducted on domestic refrigerator by with & without incorporating heat exchanger in the system by using various refrigerants in the fabrication system and their coefficient of performance & energy consumption of the system is calculated.

- Refrigerator carried out using without & with heat exchanger of refrigerant R134a & R600a in system, in which coefficient of performance of refrigerator 0.95 increased by using heat exchanger.
- In the same way the discharge temperature of compressor is decreased with 10% by using heat exchanger , energy consumption refrigerator gradually increased with 3% of compared to normal domestic refrigerator.

REFERENCES

- [1] R. Yajima et al., 1994, "The Performance Evaluation of HFC Alternative Refrigerants for HCFC-22", IIR Joint meeting, CFCs The Day After, Padova
- [2] K. Furuhashi et al., 1994, "Performance Evaluation of Residential Air Conditioner with HFC32/125 Mixture, The International Symposium HCFC Alternative Refrigerants, Kobe
- [3] E. Johnson, Global warming from HFC, Environ. Impact Assessment Rev. 18 (1998) 485–492.
- [4] M.A. Hammad, M.A. Alsaad, The use of hydrocarbon mixtures as refrigerants in domestic refrigerators, Applied Thermal Engineering 19 (1999) 1181–1189.
- [5] Douglas J D, Braun J E, Groll E A and Tree D R (1999), "A Cost Method Comparing Alternative Refrigerant Applied to R-22 System", International Journal of Refrigeration, Vol. 22, pp. 107-125.
- [6] B. O. Bolaji, Experimental study of R152a and R32 to replace R134a in a domestic refrigerator, Energy 35 (2010) 3793–3798.

On $(1,2)^*$ - $\pi g\theta$ -CLOSED SETS IN BITOPOLOGICAL SPACES

C.Janaki¹, M. Anandhi²

^{1,2}Asst. Professor, Dept. of Mathematics, L.R.G Government Arts College For Women,
Tirupur-4, India.

Abstract

In this paper we introduce a new class of sets called $(1,2)^*$ - $\pi g\theta$ -closed sets in bitopological spaces. Also we find some basic properties of $(1,2)^*$ - $\pi g\theta$ -closed sets. Further, we introduce a new space called $(1,2)^*$ - $\pi g\theta$ - $T_{1/2}$ space. Mathematics Subject Classification: 54E55, 54C55

KEY WORDS: $(1,2)^*$ - $\pi g\theta$ -closed set, $(1,2)^*$ - $\pi g\theta$ -open set, $(1,2)^*$ - $\pi g\theta$ -continuity and $(1,2)^*$ - $\pi g\theta$ - $T_{1/2}$ space.

I. INTRODUCTION

Velicko[24] introduced the notions of θ -open subsets, θ -closed subsets and θ -closure, for the sake of studying the important class of H-closed spaces in terms of arbitrary filterbases. Dontchev and Maki [7] alone have explored the concept of θ -generalized closed sets. Regular open sets have been introduced and investigated by Stone [23]. Levine [4,14] introduced generalized closed sets and studied their properties. Bhattacharya and Lahiri [5], Arya and Nour [4], Maki et al.[15],[16] introduced semi-generalized closed sets, generalized semi-closed sets and α -generalized closed sets and generalized α -closed sets respectively. O.Ravi et al [21] have introduced the concepts of $(1,2)^*$ -semi-open sets, $(1,2)^*$ - α -open sets, $(1,2)^*$ -semi-generalized-closed sets and $(1,2)^*$ - α -generalized closed sets in bitopological spaces. This paper is an attempt to highlight a new type of generalized closed sets called $(1,2)^*$ - π generalized θ -closed (briefly $(1,2)^*$ - $\pi g\theta$ -closed) sets and a new class of generalized functions called $(1,2)^*$ - $\pi g\theta$ -continuous functions and $(1,2)^*$ - $\pi g\theta$ -irresolute functions. These findings result in procuring several characterizations of $(1,2)^*$ - $\pi g\theta$ -closed sets and as well as their application which leads to an introduction of a new space called $(1,2)^*$ - $\pi g\theta$ - $T_{1/2}$ space.

II. PRELIMINARIES

Throughout this paper (X, τ_1, τ_2) and (Y, σ_1, σ_2) represent bitopological spaces on which no separation axioms are assumed unless otherwise mentioned.

Definition 2.1 ([20]). A subset S of a bitopological space (X, τ_1, τ_2) is said to be $\tau_{1,2}$ -open if $S = A \cup B$ where $A \in \tau_1$ and $B \in \tau_2$. A subset S of X is $\tau_{1,2}$ -closed if the complement of S is $\tau_{1,2}$ -open.

Definition 2.2 ([20]). Let S be a subset of X . Then

- (i) The $\tau_1 \tau_2$ -interior of S , denoted by $\tau_1 \tau_2$ -int(S) is defined by $\bigcup \{G/G \subset S \text{ and } G \text{ is } \tau_{1,2}\text{-open}\}$.
- (ii) The $\tau_1 \tau_2$ -closure of S denoted by $\tau_1 \tau_2$ -cl(S) is defined by $\bigcap \{F/S \subset F \text{ and } F \text{ is } \tau_{1,2}\text{-closed}\}$.

Definition 2.3. A subset A of a bitopological space (X, τ_1, τ_2) is called

1. $(1,2)^*$ -semi-open[20] if $A \subset \tau_1 \tau_2$ -cl($\tau_1 \tau_2$ -int(A)).
2. $(1,2)^*$ -preopen [20] if $A \subset \tau_1 \tau_2$ -int($\tau_1 \tau_2$ -cl(A)).
3. $(1,2)^*$ - α -open [20] if $A \subset \tau_1 \tau_2$ -int($\tau_1 \tau_2$ -cl($\tau_1 \tau_2$ -int(A))).
4. $(1,2)^*$ -generalised closed (briefly $(1,2)^*$ -g-closed) [20] if $\tau_1 \tau_2$ -cl(A) \subset U whenever $A \subset U$ and U is $\tau_{1,2}$ -open in X .
5. $(1,2)^*$ -regular open[20] if $A = \tau_1 \tau_2$ -int($\tau_1 \tau_2$ -cl(A)).
6. $(1,2)^*$ -semi-generalised-closed (briefly $(1,2)^*$ -sg-closed) [20] if $(1,2)^*$ -scl(A) \subset U whenever $A \subset U$ and U is $(1,2)^*$ -semi-open in X .
7. $(1,2)^*$ -generalized semi-closed (briefly $(1,2)^*$ -gs-closed)[20] if $(1,2)^*$ -scl(A) \subset U , whenever $A \subset U$ and U is $\tau_{1,2}$ -open in X .

8. $(1,2)^*$ - α -generalized-closed (briefly $(1,2)^*$ - αg -closed) [20] if $(1,2)^*$ - $\text{acl}(A) \subset U$, whenever $A \subset U$ and U is $\tau_{1,2}$ -open in X .
9. $(1,2)^*$ -generalized α -closed (briefly $(1,2)^*$ - $g\alpha$ -closed)[20] if $(1,2)^*$ - $\text{acl}(A) \subset U$, whenever $A \subset U$ and U is $(1,2)^*$ - α -open in X .
10. a $(1,2)^*$ - θ -generalized closed (briefly, $(1,2)^*$ - θg -closed) set [11] if $(1,2)^*$ - $\text{cl}_\theta(A) \subset U$ whenever $A \subset U$ and U is $\tau_{1,2}$ -open in (X, τ_1, τ_2) .
11. $(1,2)^*$ - π generalized closed (briefly $(1,2)^*$ - πg -closed [8] if $(1,2)^*$ - $\text{cl}(A) \subset U$, whenever $A \subset U$ and U is $\tau_{1,2}$ - π -open.
12. $(1,2)^*$ - π generalized α -closed (briefly $(1,2)^*$ - $\pi g\alpha$ -closed)[3] if $(1,2)^*$ - $\text{acl}(A) \subset U$, whenever $A \subset U$ and U is $\tau_{1,2}$ - π -open.
13. $(1,2)^*$ - π generalized semi-closed (briefly $(1,2)^*$ - $\pi g s$ -closed)[4] if $(1,2)^*$ - $\text{scl}(A) \subset U$, whenever $A \subset U$ and U is $\tau_{1,2}$ - π -open.
14. $(1,2)^*$ - π generalized b-closed (briefly $(1,2)^*$ - $\pi g b$ -closed)[22] if $(1,2)^*$ - $\text{bcl}(A) \subset U$, whenever $A \subset U$ and U is $\tau_{1,2}$ - π -open.
15. $(1,2)^*$ - π generalized pre-closed (briefly $(1,2)^*$ - $\pi g p$ -closed)[19] if $(1,2)^*$ - $\text{pcl}(A) \subset U$, whenever $A \subset U$ and U is $\tau_{1,2}$ - π -open.

The complement of a $(1,2)^*$ -semi-closed (resp. $(1,2)^*$ - α -closed, $(1,2)^*$ - g -closed, $(1,2)^*$ - sg -closed, $(1,2)^*$ - gs -closed, $(1,2)^*$ - αg -closed $(1,2)^*$ - $g\alpha$ -closed, $(1,2)^*$ - θg -closed, $(1,2)^*$ - πg -closed, $(1,2)^*$ - $\pi g\alpha$ -closed, $(1,2)^*$ - $\pi g s$ -closed, $(1,2)^*$ - $\pi g b$ -closed, $(1,2)^*$ - $\pi g p$ -closed) set is called $(1,2)^*$ -semi open (resp. $(1,2)^*$ - α -open, $(1,2)^*$ - g -open, $(1,2)^*$ - sg -open, $(1,2)^*$ - gs -open, $(1,2)^*$ - αg -open, $(1,2)^*$ - $g\alpha$ -open, $(1,2)^*$ - θg -open, $(1,2)^*$ - πg -open, $(1,2)^*$ - $\pi g\alpha$ -open, $(1,2)^*$ - $\pi g s$ -open, $(1,2)^*$ - $\pi g b$ -open, $(1,2)^*$ - $\pi g p$ -open).

Definition 2.4 The finite union of $(1,2)^*$ -regular open sets[5] is said to be $\tau_{1,2}$ - π -open. The complement of $\tau_{1,2}$ - π -open is said to be $\tau_{1,2}$ - π -closed.

Definition 2. 5: A function $f: (X, \tau_1, \tau_2) \rightarrow (Y, \sigma_1, \sigma_2)$ is called

- (i) $\tau_{1,2}$ - π -open map[3] if $f(F)$ is $\tau_1 \tau_2$ - π -open map in Y for every $\tau_{1,2}$ -open set F in X .
- (ii) $(1,2)^*$ - θ -continuous[7] if $f^{-1}(V)$ is $(1,2)^*$ - θ -closed in (X, τ_1, τ_2) for every $(1,2)^*$ -closed set V in (Y, σ_1, σ_2) .
- (iii) $(1,2)^*$ - θ -irresolute[7] if $f^{-1}(V)$ is $(1,2)^*$ - θ -closed in (X, τ_1, τ_2) for every $(1,2)^*$ - θ -closed set V in (Y, σ_1, σ_2) .

III. $(1,2)^*$ - $\pi g\theta$ -closed set

We introduce the following definition.

Definition 3.1. A subset A of (X, τ_1, τ_2) is called $(1,2)^*$ - π generalized θ -closed set (briefly $(1,2)^*$ - $\pi g\theta$ -closed) if $\tau_1 \tau_2 \text{-cl}_\theta(A) \subset U$ whenever $A \subset U$ and U is $\tau_1 \tau_2$ - π -open.

The complement of $(1,2)^*$ - $\pi g\theta$ -closed is $(1,2)^*$ - $\pi g\theta$ -open..

Theorem 3.2:

1. Every $(1,2)^*$ - θ - closed set is $(1,2)^*$ - $\pi g\theta$ -closed.
2. Every $(1,2)^*$ - θg -closed set is $(1,2)^*$ - $\pi g\theta$ -closed.
3. Every $(1,2)^*$ - $\pi g\theta$ -closed set is $(1,2)^*$ - πg -closed.
4. Every $(1,2)^*$ - $\pi g\theta$ -closed set is $(1,2)^*$ - $\pi g\alpha$ -closed.
5. Every $(1,2)^*$ - $\pi g\theta$ -closed set is $(1,2)^*$ - $\pi g s$ -closed.
6. Every $(1,2)^*$ - $\pi g\theta$ -closed set is $(1,2)^*$ - $\pi g b$ -closed.
7. Every $(1,2)^*$ - $\pi g\theta$ -closed set is $(1,2)^*$ - $\pi g p$ -closed

Proof: Straight forward.

Converse of the above need not be true as seen in the following examples.

Example 3.3 Let $X = \{a, b, c\}$, $\tau_1 = \{ \emptyset, X, \{a\}, \{c\}, \{a, c\} \}$; $\tau_2 = \{ \emptyset, X, \{b, c\} \}$:
Let $A = \{b\}$. Then A is $\pi g\theta$ -closed but not θ -closed.

Example 3.4 Let $X = \{a, b, c, d\}$, $\tau_1 = \{ \emptyset, \{b\}, \{d\}, \{b, d\}, \{a, b, d\}, X \}$; $\tau_2 = \{ \emptyset, \{b, d\}, \{b, c, d\}, X \}$.
Then $A = \{a, d\}$.
Then A is $(1,2)^*$ - $\pi g\theta$ -closed but not $(1,2)^*$ - θg -closed.

Example 3.5 Let $X = \{a,b,c,d\}$, $\tau_1 = \{\phi, \{a\}, \{b\}, \{a,b\}, \{a,b,d\}, X\}$, $\tau_2 = \{\phi, \{a,c\}, \{a,b,c\}, X\}$. Let $A = \{c\}$. Then A is $(1,2)^*$ - πg -closed but not $(1,2)^*$ - $\pi g\theta$ -closed.

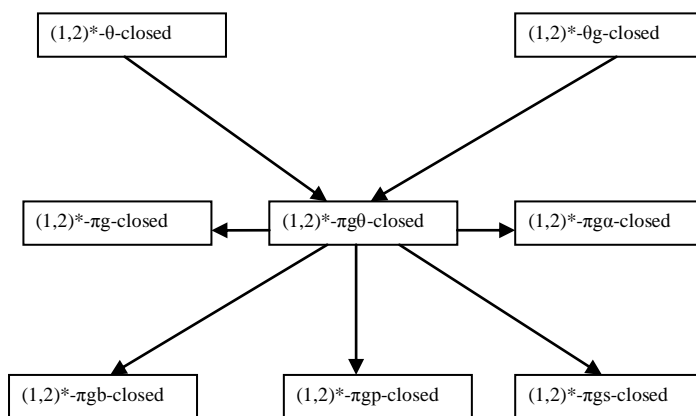
Example 3.6 Let $X = \{a,b,c,d\}$. $\tau_1 = \{\phi, \{a\}, \{d\}, \{a,d\}, X\}$; $\tau_2 = \{\phi, \{c,d\}, \{a,c,d\}, X\}$: Let $A = \{c\}$. Then A is $(1,2)^*$ - $\pi g\alpha$ -closed set but not $(1,2)^*$ - $\pi g\theta$ -closed.

Example 3.7 Let $X = \{a,b,c,d\}$. $\tau_1 = \{\phi, \{a\}, \{b\}, \{a,b\}, X\}$; $\tau_2 = \{\phi, \{a,b\}, \{a,b,d\}, X\}$; Let $A = \{a\}$. Then A is $(1,2)^*$ - $\pi g s$ -closed set but not $(1,2)^*$ - $\pi g\theta$ -closed.

Example 3.8 Let $X = \{a,b,c,d\}$. $\tau_1 = \{\phi, \{a\}, \{d\}, \{a,d\}, X\}$; $\tau_2 = \{\phi, \{c,d\}, \{a,c,d\}, X\}$; Let $A = \{a,c\}$. Then A is $(1,2)^*$ - $\pi g b$ -closed set but not $(1,2)^*$ - $\pi g\theta$ -closed.

Example 3.9 Let $X = \{a,b,c,d\}$. $\tau_1 = \{\phi, \{a\}, \{d\}, \{a,d\}, X\}$; $\tau_2 = \{\phi, \{c,d\}, \{a,c,d\}, X\}$: Let $A = \{c\}$. Then A is $(1,2)^*$ - $\pi g p$ -closed but not $(1,2)^*$ - $\pi g\theta$ -closed.

Remark 3.10 The above discussions are summarized in the following diagram.



Remark 3.11 $(1,2)^*$ - $\pi g\theta$ -closed is independent of $(1,2)^*$ -closedness, $(1,2)^*$ - α -closedness, $(1,2)^*$ -semi-closedness, $(1,2)^*$ -sg-closedness, $(1,2)^*$ -gs-closedness, $(1,2)^*$ -g-closedness, $(1,2)^*$ - αg -closedness and $(1,2)^*$ -g α -closedness, as seen in the following examples.

Example 3.12 Let $X = \{a,b,c,d\}$, $\tau_1 = \{\phi, \{a\}, \{b\}, \{a,b\}, X\}$; $\tau_2 = \{\phi, \{a,b,d\}, X\}$: Let $A = \{d\}$. Then A is $(1,2)^*$ - $\pi g\theta$ -closed but not $(1,2)^*$ -g-closed.

Example 3.13 Let $X = \{a,b,c,d,e\}$, $\tau_1 = \{\phi, \{a,b\}, \{a,b,c,d\}, X\}$; $\tau_2 = \{\phi, \{c,d\}, X\}$: Let $A = \{e\}$. Then A is $(1,2)^*$ -g-closed but not $(1,2)^*$ - $\pi g\theta$ -closed.

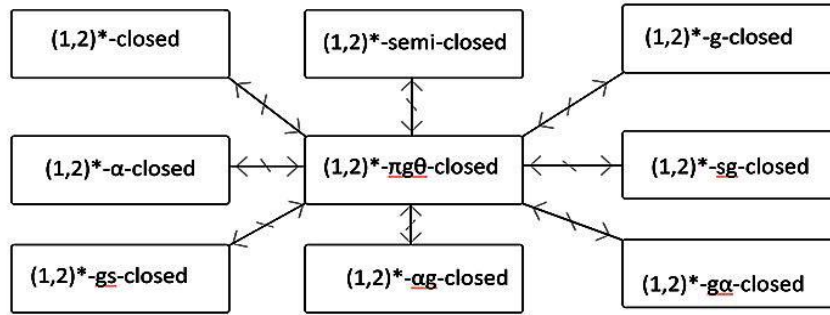
Example 3.14. Let $X = \{a,b,c\}$, $\tau_1 = \{\phi, \{a\}, \{b\}, \{a,b\}, X\}$; $\tau_2 = \{\phi, \{b,c\}, X\}$: Let $A = \{b\}$. Then A is $(1,2)^*$ - $\pi g\theta$ -closed but not $(1,2)^*$ -closed, $(1,2)^*$ - α -closed, $(1,2)^*$ -semi-closed.

Example 3.15 Let $X = \{a,b,c\}$, $\tau_1 = \{\phi, \{a\}, \{b\}, \{a,b\}, X\}$; $\tau_2 = \{\phi, \{b,c\}, X\}$: Let $A = \{a\}$. Then A is $(1,2)^*$ -closed, $(1,2)^*$ - α -closed, $(1,2)^*$ -semi-closed but not $(1,2)^*$ - $\pi g\theta$ -closed.

Example 3.16 Let $X = \{a,b,c,d\}$, $\tau_1 = \{\phi, \{a\}, \{b\}, \{a,b\}, \{a,b,c\}, X\}$; $\tau_2 = \{\phi, \{a,b,d\}, X\}$:
 (i) Let $A = \{a,b,c\}$. Then A is $(1,2)^*$ - $\pi g\theta$ -closed but neither $(1,2)^*$ -sg-closed nor $(1,2)^*$ -gs-closed.
 (ii) Let $A = \{a\}$. Then A is both $(1,2)^*$ -sg-closed and $(1,2)^*$ -gs-closed but not $(1,2)^*$ - $\pi g\theta$ -closed.

Example 3.17 Let $X = \{a,b,c,d\}$, $\tau_1 = \{\phi, \{c,d\}, \{a,c,d\}, X\}$, $\tau_2 = \{\phi, \{a\}, \{d\}, \{a,d\}, \{c,d\}, X\}$.
 (i) Let $A = \{b,d\}$. Then A is $(1,2)^*$ - $\pi g\theta$ -closed but neither $(1,2)^*$ - αg -closed nor $(1,2)^*$ -g α -closed.
 (ii) Let $A = \{c\}$. Then A is $(1,2)^*$ - αg -closed, $(1,2)^*$ -g α -closed but not $(1,2)^*$ - $\pi g\theta$ -closed.

Remark 3.18 The above discussions are summarized in the following diagram.



Remark 3.19 A finite union of $(1,2)^*$ - $\pi g\theta$ -closed sets is always a $(1,2)^*$ - $\pi g\theta$ -closed.

Proof: Let $A, B \in (1,2)^*$ - $\pi G\theta C(X)$. Let U be any $\tau_1\tau_2$ - π -open set such that $(A \cup B) \subseteq U$. Since $(1,2)^*$ - $cl_\theta(A \cup B) = (1,2)^*$ - $cl_\theta(A) \cup (1,2)^*$ - $cl_\theta(B) \subseteq U \cup U = U$. This implies $(1,2)^*$ - $cl_\theta(A \cup B) \subseteq U$. Hence $A \cup B$ is also a $(1,2)^*$ - $\pi g\theta$ -closed set.

Remark 3.20 The intersection of two $(1,2)^*$ - $\pi g\theta$ -closed sets need not be $(1,2)^*$ - $\pi g\theta$ -closed as seen in the following example.

Example 3.21 Let $X = \{a, b, c, d\}$, $\tau_1 = \{\phi, \{a\}, \{b\}, \{a, b\}, X\}$; $\tau_2 = \{\phi, \{a, b, d\}, X\}$:
Let $A = \{a, b, c\}$ and $B = \{a, b, d\}$. Clearly A and B are $(1,2)^*$ - $\pi g\theta$ -closed sets. But $A \cap B = \{a, b\}$ is not a $(1,2)^*$ - $\pi g\theta$ -closed set.

Proposition 3.22 Let A be $(1,2)^*$ - $\pi g\theta$ -closed in (X, τ) . Then $(1,2)^*$ - $cl_\theta(A) - A$ does not contain any non-empty $\tau_1\tau_2$ - π -closed set.

Proof: Let F be a non-empty $\tau_1\tau_2$ - π -closed set such that $F \subseteq (1,2)^*$ - $cl_\theta(A) - A$. Since A is $(1,2)^*$ - $\pi g\theta$ -closed, $A \subseteq X - F$ where $X - F$ is $\tau_1\tau_2$ - π -open implies $(1,2)^*$ - $cl_\theta(A) \subseteq (X - F)$. Hence $F \subseteq X - (1,2)^*$ - $cl_\theta(A)$. Now, $F \subseteq (1,2)^*$ - $cl_\theta(A) \cap X - (1,2)^*$ - $cl_\theta(A)$ implies $F = \phi$ which is a contradiction. Therefore $cl_\theta(A) - A$ does not contain any non-empty $\tau_1\tau_2$ - π -closed set.

Remark 3.23 The converse of Proposition 3.22 need not be true as shown in the following example.

Example 3.24 Let $X = \{a, b, c\}$. $\tau_1 = \{\phi, X, \{b\}\}$; $\tau_2 = \{\phi, X, \{c\}\}$:
Let $A = \{b, c\}$. Then $(1,2)^*$ - $cl_\theta(A) - A$ contains no non-empty $\tau_1\tau_2$ - π -closed set. However A is not $(1,2)^*$ - $\pi g\theta$ -closed.

Proposition 3.25 If A is a $\tau_{1,2}$ -regular open and $(1,2)^*$ - $\pi g\theta$ -closed subset of (X, τ_1, τ_2) , then A is a $(1,2)^*$ - θ -closed subset of (X, τ_1, τ_2) .

Proof. Since A is $\tau_{1,2}$ -regular open and $(1,2)^*$ - $\pi g\theta$ -closed, $(1,2)^*$ - $cl_\theta(A) \subseteq A$. Hence A is $(1,2)^*$ - θ -closed.

Proposition 3.26 Let A be a $(1,2)^*$ - $\pi g\theta$ -closed subset of (X, τ_1, τ_2) . If $A \subseteq B \subseteq (1,2)^*$ - $cl_\theta(A)$, then B is also a $(1,2)^*$ - $\pi g\theta$ -closed subset of (X, τ_1, τ_2) .

Proof. Let U be a $\tau_1\tau_2$ - π -open set of (X, τ_1, τ_2) such that $B \subseteq U$. Then $A \subseteq U$. Since A is a $(1,2)^*$ - $\pi g\theta$ -closed set, $(1,2)^*$ - $cl_\theta(A) \subseteq U$. Also since $B \subseteq (1,2)^*$ - $cl_\theta(A)$, $(1,2)^*$ - $cl_\theta(B) \subseteq (1,2)^*$ - $cl_\theta((1,2)^*$ - $cl_\theta(A)) = (1,2)^*$ - $cl_\theta(A)$. Thus $(1,2)^*$ - $cl_\theta(B) \subseteq U$. Hence B is also a $(1,2)^*$ - $\pi g\theta$ -closed subset of (X, τ_1, τ_2) .

Theorem 3.27 Let A be a $(1,2)^*$ - $\pi g\theta$ -closed sub set in X . Then A is $(1,2)^*$ - θ -closed if and only if $(1,2)^*$ - $cl_\theta(A) - A$ is $\tau_{1,2}$ - π -closed.

Proof. Necessity: Let A be $(1,2)^*$ - θ -closed subset of X . Then $(1,2)^*$ - $cl_\theta(A) = A$ and $(1,2)^*$ - $cl_\theta(A) - A = \phi$ which is $\tau_{1,2}$ - π -closed.

Sufficiency: Since A is $(1,2)^*$ - $\pi g\theta$ -closed, by proposition 3.22 $(1,2)^*$ - $cl_\theta(A) - A$ contains no non-empty $\tau_{1,2}$ - π -closed set. But $(1,2)^*$ - $cl_\theta(A) - A$ is $\tau_{1,2}$ - π -closed. This implies $(1,2)^*$ - $cl_\theta(A) - A = \phi$, which means $(1,2)^*$ - $cl_\theta(A) = A$ and hence A is $(1,2)^*$ - θ -closed.

IV. $(1,2)^*$ - $\pi g\theta$ -open sets

Definition 4.1 A subset A of (X, τ_1, τ_2) is called $(1,2)^*$ - $\pi g\theta$ -open if and only if A^c is $(1,2)^*$ - $\pi g\theta$ -closed in (X, τ_1, τ_2) .

Remark 4.2 For a subset A of (X, τ_1, τ_2) , $(1,2)^*$ - $cl_0(A^c) = [(1,2)^*$ - $int_0(A)]^c$

Theorem 4.3 A subset A of (X, τ_1, τ_2) is $(1,2)^*$ - $\pi g\theta$ -open if and only if $F \subset (1,2)^*$ - $int_0(A)$ whenever F is $\tau_1 \tau_2$ - π -closed and $F \subset A$.

Proof. Necessity: Let A be a $(1,2)^*$ - $\pi g\theta$ -open set in (X, τ_1, τ_2) . Let F be $\tau_1 \tau_2$ - π -closed and $F \subset A$. Then $F^c \supseteq A^c$ and F^c is $\tau_1 \tau_2$ - π -open. Since A^c is $(1,2)^*$ - $\pi g\theta$ -closed, $(1,2)^*$ - $cl_0(A^c) \subseteq F^c$. By remark 4.2, $[(1,2)^*$ - $int_0(A)]^c \subseteq F^c$. That is $F \subset (1,2)^*$ - $int_0(A)$.

Sufficiency: Let $A^c \subseteq U$ where U is $\tau_1 \tau_2$ - π -open. Then $U^c \subset A$ where U^c is $(1,2)^*$ - $\tau_1 \tau_2$ - π -closed. By hypothesis $U^c \subseteq (1,2)^*$ - $int_0(A)$. That is $[(1,2)^*$ - $int_0(A)]^c \subseteq U$. By remark 4.2, $(1,2)^*$ - $cl_0(A^c) \subseteq U$. This implies A^c is $(1,2)^*$ - $\pi g\theta$ -closed. Hence A is $(1,2)^*$ - $\pi g\theta$ -open.

Theorem 4.4 If $(1,2)^*$ - $int_0(A) \subseteq B \subseteq A$ and A is $(1,2)^*$ - $\pi g\theta$ -open, then B is also $(1,2)^*$ - $\pi g\theta$ -open.

Proof. $(1,2)^*$ - $int_0(A) \subseteq B \subseteq A$ implies $A^c \subseteq B^c \subseteq [(1,2)^*$ - $int_0(A)]^c$. By remark 4.2 $A^c \subseteq B^c \subseteq (1,2)^*$ - $cl_0(A^c)$. Also A^c is $(1,2)^*$ - $\pi g\theta$ -closed. By Proposition 3.26 B^c is $(1,2)^*$ - $\pi g\theta$ -closed. Hence B is $(1,2)^*$ - $\pi g\theta$ -open.

As an application of $(1,2)^*$ - $\pi g\theta$ -closed sets we introduce the following definition.

Definition 4.5 A space (X, τ_1, τ_2) is called a $(1,2)^*$ - $\pi g\theta$ - $T_{1/2}$ space if every $(1,2)^*$ - $\pi g\theta$ -closed set is $(1,2)^*$ - θ -closed.

Theorem 4.6 For a space (X, τ_1, τ_2) the following conditions are equivalent.

- (i) (X, τ_1, τ_2) is a $(1,2)^*$ - $\pi g\theta$ - $T_{1/2}$ space.
- (ii) Every singleton set of (X, τ_1, τ_2) is either $\tau_1 \tau_2$ - π -closed or $(1,2)^*$ - θ -open.

Proof. (i) \Rightarrow (ii). Let $x \in X$. Suppose $\{x\}$ is not a $\tau_1 \tau_2$ - π -closed set of (X, τ_1, τ_2) . Then $X - \{x\}$ is not a $\tau_1 \tau_2$ - π -open set. So X is the only $\tau_1 \tau_2$ - π -open set containing $X - \{x\}$. So $X - x$ is a $(1,2)^*$ - $\pi g\theta$ -closed set of (X, τ_1, τ_2) . Since (X, τ_1, τ_2) is a $(1,2)^*$ - $\pi g\theta$ - $T_{1/2}$ space, $X - x$ is a $(1,2)^*$ - θ -closed set of (X, τ_1, τ_2) or equivalently $\{x\}$ is a $(1,2)^*$ - θ -open set of (X, τ_1, τ_2) .

(ii) \Rightarrow (i). Let A be a $(1,2)^*$ - $\pi g\theta$ -closed set of X . Trivially $A \subset (1,2)^*$ - $cl_0(A)$. Let $x \in (1,2)^*$ - $cl_0(A)$. By (ii) $\{x\}$ is either $\tau_1 \tau_2$ - π -closed or $(1,2)^*$ - θ -open.

(a) Suppose that $\{x\}$ is $\tau_1 \tau_2$ - π -closed. If $x \notin A$, then $x \in (1,2)^*$ - $cl_0(A) - A$ contains a non-empty $\tau_1 \tau_2$ - π -closed set $\{x\}$. By proposition 3.6 we arrive at a contradiction. Thus $x \in A$.

(b) Suppose that $\{x\}$ is a $(1,2)^*$ - θ -open. Since $x \in (1,2)^*$ - $cl_0(A) = A$ or equivalently A is $(1,2)^*$ - θ -closed. Hence (X, τ_1, τ_2) is a $(1,2)^*$ - $\pi g\theta$ - $T_{1/2}$ space.

V. $(1,2)^*$ - $\pi g\theta$ -continuous and $(1,2)^*$ - $\pi g\theta$ -irresolute functions

Definition 5.1 A function $f: (X, \tau_1, \tau_2) \rightarrow (Y, \sigma_1, \sigma_2)$ is called $(1,2)^*$ - $\pi g\theta$ -continuous if every $f^{-1}(V)$ is $(1,2)^*$ - $\pi g\theta$ -closed in (X, τ_1, τ_2) for every $(1,2)^*$ - $\sigma_1 \sigma_2$ -closed set V of (Y, σ_1, σ_2) .

Definition 5.2 A function $f: (X, \tau_1, \tau_2) \rightarrow (Y, \sigma_1, \sigma_2)$ is called $(1,2)^*$ - $\pi g\theta$ -irresolute if $f^{-1}(V)$ is $(1,2)^*$ - $\pi g\theta$ -closed in (X, τ_1, τ_2) for every $(1,2)^*$ - $\pi g\theta$ -closed set V in (Y, σ_1, σ_2) .

Remark 5.3 $(1,2)^*$ - $\pi g\theta$ -irresolute function is independent of $(1,2)^*$ - θ -irresoluteness, as seen in the following examples.

Example 5.4 Let $X=Y=\{a,b,c,d\}$, $\tau_1=\{\emptyset, \{a\}, \{d\}, \{a,d\}, \{a,c,d\}, X\}$, $\tau_2=\{\emptyset, \{a,d\}, \{a,b,d\}, X\}$, $\sigma_1=\{\emptyset, \{a\}, \{d\}, \{a,d\}, X\}$, $\sigma_2=\{\emptyset, \{c,d\}, \{a,c,d\}, X\}$. Let $f: (X, \tau_1, \tau_2) \rightarrow (Y, \sigma_1, \sigma_2)$ be an identity function. Then f is $(1,2)^*$ - θ -irresolute but not $(1,2)^*$ - $\pi g\theta$ -irresolute, since $f^{-1}[\{b,c,d\}] = \{b,c,d\}$ is not $(1,2)^*$ - $\pi g\theta$ -closed in (X, τ_1, τ_2) .

Example 5.5 Let $X=Y=\{a,b,c,d\}$, $\tau_1=\{\phi, \{a\}, \{d\}, \{a,d\}, \{a,c,d\}, X\}$, $\tau_2 = \{\phi, \{a,d\}, \{a,b,d\}, X\}$, $\sigma_1 = \{\phi, \{a\}, \{c\}, \{a,c\}, \{c,d\}, \{a,c,d\}, X\}$, $\sigma_2 = \{\phi, \{d\}, \{a,b,d\}, X\}$. Let $f: (X, \tau_1, \tau_2) \rightarrow (Y, \sigma_1, \sigma_2)$ be an identity function. Then f is $(1,2)^*$ - $\pi g\theta$ -irresolute but not $(1,2)^*$ - θ -irresolute, since $f^{-1}[\{a,b,d\}] = \{a,b,d\}$ is not $(1,2)^*$ - θ -closed in (X, τ_1, τ_2) .

Remark 5.6: Every $(1,2)^*$ - θ -continuous is $(1,2)^*$ - $\pi g\theta$ -continuous. The converse of the above need not be true as seen in the following examples.

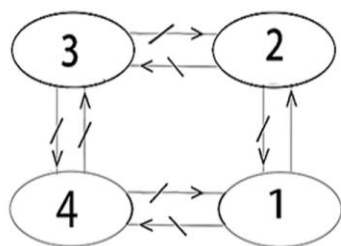
Example 5.7: Let $X=Y=\{a,b,c,d,e\}$, $\tau_1 = \{\phi, \{a,b\}, \{a,b,c\}, X\}$, $\tau_2 = \{\phi, \{c\}, X\}$, $\sigma_1 = \{\phi, \{a,b\}, \{a,b,c,d\}, X\}$, $\sigma_2 = \{\phi, \{c,d\}, \{a,b,c,d\}, X\}$. Let $f: (X, \tau_1, \tau_2) \rightarrow (Y, \sigma_1, \sigma_2)$ be an identity function. Then f is $(1,2)^*$ - $\pi g\theta$ -continuous but not $(1,2)^*$ - θ -continuous, since $f^{-1}[\{c,d,e\}] = \{c,d,e\}$ is not $(1,2)^*$ - θ -closed in (X, τ_1, τ_2) .

Remark 5.8 $(1,2)^*$ - $\pi g\theta$ -continuous is independent of $(1,2)^*$ - $\pi g\theta$ -irresolute as seen in the following examples.

Example 5.9 Let $X=Y=\{a,b,c,d,e\}$, $\tau_1 = \{\phi, \{a,b\}, \{a,b,c,d\}, X\}$, $\tau_2 = \{\phi, \{c,d\}, X\}$, $\sigma_1 = \{\phi, \{b\}, \{b,c\}, X\}$, $\sigma_2 = \{\phi, \{c\}, \{a,b\}, \{a,b,c\}, X\}$. Let $f: (X, \tau_1, \tau_2) \rightarrow (Y, \sigma_1, \sigma_2)$ be an identity function. Then f is $(1,2)^*$ - $\pi g\theta$ -continuous but not $(1,2)^*$ - $\pi g\theta$ -irresolute, since $f^{-1}[\{d\}] = \{d\}$ is not $(1,2)^*$ - $\pi g\theta$ -closed in (X, τ_1, τ_2) where $\{d\}$ is $\pi g\theta$ -closed in (Y, σ_1, σ_2) .

Example 5.10: Let $X=Y=\{a,b,c,d\}$, $\tau_1 = \{\phi, \{a\}, \{b\}, \{a,b\}, \{a,b,c\}, X\}$, $\tau_2 = \{\phi, \{b\}, \{c\}, \{b,c\}, \{a,c\}, \{a,b,c\}, \{a,b,d\}, X\}$, $\sigma_1 = \{\phi, \{a\}, \{b\}, \{a,b\}, \{a,d\}, \{a,b,d\}, X\}$, $\sigma_2 = \{\phi, \{c\}, \{a,c\}, \{b,c\}, \{a,b,c\}, \{a,c,d\}, X\}$. Let $f: (X, \tau_1, \tau_2) \rightarrow (Y, \sigma_1, \sigma_2)$ be an identity function. Then f is $(1,2)^*$ - $\pi g\theta$ -irresolute but not $(1,2)^*$ - $\pi g\theta$ -continuous, since $f^{-1}[\{b\}] = \{b\}$ is not $(1,2)^*$ - $\pi g\theta$ -closed in (X, τ_1, τ_2) where $\{b\}$ is closed in (Y, σ_1, σ_2) .

Remark 5.11 The above discussions are summarized in the following diagram.



Where (1) \Rightarrow $(1,2)^*$ - θ -continuous; (2) \Rightarrow $(1,2)^*$ - $\pi g\theta$ -continuous;
 (3) \Rightarrow $(1,2)^*$ - $\pi g\theta$ -irresolute; (4) \Rightarrow $(1,2)^*$ - θ -irresolute.

Remark 5.12 Composition of two $(1,2)^*$ - $\pi g\theta$ -continuous function need not be $(1,2)^*$ - $\pi g\theta$ -continuous.

Example 5.13 Let $X=Y=Z=\{a,b,c,d,e\}$, $\tau_1 = \{\phi, \{a,b\}, \{a,b,c\}, X\}$, $\tau_2 = \{\phi, \{c\}, X\}$, $\sigma_1 = \{\phi, \{a,b\}, X\}$, $\sigma_2 = \{\phi, \{c,d\}, \{a,b,c,d\}, X\}$, $\eta_1 = \{\phi, \{a,b,c,d\}, X\}$, $\eta_2 = \{\phi, \{e\}, X\}$. Let $f: (X, \tau_1, \tau_2) \rightarrow (Y, \sigma_1, \sigma_2)$ and $g: (Y, \sigma_1, \sigma_2) \rightarrow (Z, \eta_1, \eta_2)$ be the identity functions. Both f and g are $(1,2)^*$ - $\pi g\theta$ -continuous but $g \circ f$ is not $(1,2)^*$ - $\pi g\theta$ -continuous, since $(g \circ f)^{-1}[\{a,b,c,d\}] = \{a,b,c,d\}$ is not $(1,2)^*$ - $\pi g\theta$ -closed in (X, τ_1, τ_2) .

Theorem 5.14 Let $f: (X, \tau_1, \tau_2) \rightarrow (Y, \sigma_1, \sigma_2)$ be a function .

- (i) If f is $(1,2)^*$ - $\pi g\theta$ -irresolute and X is $(1,2)^*$ - $\pi g\theta$ - $T_{1/2}$ space, then f is $(1,2)^*$ - θ -irresolute.
- (ii) If f is $(1,2)^*$ - $\pi g\theta$ -continuous and X is $(1,2)^*$ - $\pi g\theta$ - $T_{1/2}$ space then f is $(1,2)^*$ - θ -continuous.

Proof: (i) Let V be $(1,2)^*$ - θ -closed in Y . Since f is $(1,2)^*$ - $\pi g\theta$ -irresolute, $f^{-1}(V)$ is $(1,2)^*$ - $\pi g\theta$ -closed in X . Since X is $(1,2)^*$ - $\pi g\theta$ - $T_{1/2}$ space, $f^{-1}(V)$ is $(1,2)^*$ - θ -closed in X . Hence f is $(1,2)^*$ - θ -irresolute.

(ii) Let V be closed in Y . Since f is $(1,2)^*$ - $\pi g\theta$ -continuous, $f^{-1}(V)$ is $(1,2)^*$ - $\pi g\theta$ -closed in X . By assumption, it is $(1,2)^*$ - θ -closed. Therefore f is $(1,2)^*$ - θ -continuous.

Theorem 5.15 If the bijective $f: (X, \tau_1, \tau_2) \rightarrow (Y, \sigma_1, \sigma_2)$ is $(1,2)^*$ - θ -irresolute and $\tau_1 \tau_2$ - π -open map, then f is $(1,2)^*$ - $\pi g\theta$ -irresolute.

Proof: Let V be $(1,2)^*$ - $\pi g\theta$ -closed in Y . Let $f^{-1}(V) \subset U$ where U is $\tau_1\tau_2$ - π -open in X . Then $V \subset f(U)$ and $f(U)$ is $\tau_1\tau_2$ - π -open implies $(1,2)^*$ - $cl_0(V) \subset f(U)$. This implies $f^{-1}((1,2)^*$ - $cl_0(V)) \subset U$. Since f is $(1,2)^*$ - θ -irresolute, $f^{-1}((1,2)^*$ - $cl_0(V))$ is $(1,2)^*$ - θ -closed. Hence $(1,2)^*$ - $cl_0(f^{-1}(V)) \subset (1,2)^*$ - $cl_0(f^{-1}((1,2)^*$ - $cl_0(V))) = f^{-1}((1,2)^*$ - $cl_0(V)) \subset U$. Therefore f is $(1,2)^*$ - $\pi g\theta$ -irresolute.

Theorem 5.16 : If $f: (X, \tau_1, \tau_2) \rightarrow (Y, \sigma_1, \sigma_2)$ is $(1,2)^*$ - $\pi g\theta$ -irresolute map and $g: (Y, \sigma_1, \sigma_2) \rightarrow (Z, \eta_1, \eta_2)$ is $(1,2)^*$ - $\pi g\theta$ -continuous map, the composition $g \circ f: (X, \tau_1, \tau_2) \rightarrow (Z, \eta_1, \eta_2)$ is a $(1,2)^*$ - $\pi g\theta$ -continuous map.

Proof: Let V be $\eta_1\eta_2$ -closed set in Z . Since $g: (Y, \sigma_1, \sigma_2) \rightarrow (Z, \eta_1, \eta_2)$ is a $(1,2)^*$ - $\pi g\theta$ -continuous map, $g^{-1}(V)$ is $(1,2)^*$ - $\pi g\theta$ -closed in Y . By hypothesis, $f^{-1}(g^{-1}(V)) = (g \circ f)^{-1}(V)$ is $(1,2)^*$ - $\pi g\theta$ -closed in X . Hence $g \circ f: (X, \tau_1, \tau_2) \rightarrow (Z, \eta_1, \eta_2)$ is a $(1,2)^*$ - $\pi g\theta$ -continuous map.

V. CONCLUSION

Through the above findings, this paper has attempted to compare $(1,2)^*$ - $\pi g\theta$ -closed with the other closed sets in bitopological spaces. An attempt of this paper is to state that the several definitions and results that shown in this paper, will result in obtaining several characterizations and enable to study various properties as well. It brings to limelight that the weaker form of continuity in bitopological settings is the future scope of study.

REFERENCES

- [1] M. E. Abd El-Monsef, S.Rose Mary and M.Lellis Thivagar $(1,2)^*$ - αg -closed sets in topological spaces, Assiut Univ. J. of Mathematics and Computer Science, Vol.36(1) (2007), 43-51.
- [2] M. Anandhi and C.Janaki: On $\pi g\theta$ -Closed sets in Topological spaces, International Journal of Mathematical Archive-3(11), 2012, 3941-3946.
- [3] I. Arockiarani and K. Mohana, $(1,2)^*$ - $\pi g\alpha$ -closed sets and $(1,2)^*$ -Quasi- α -normal Spaces in Bitopological settings, Antarctica j. Math.,7(3)(2010), 3465-355.
- [4] S. P. Arya and T. Nour: Characterizations of S-normal spaces, Indian J. Pure. Appl. Math., 21(1990), No. 8, 717-719.
- [5] P.Bhattacharya and B.K. Lahiri: Semi-generalised closed sets in topology, Indian J. Math., 29(1987), 375-382.
- [7] J. Dontchev and H. Maki, On θ -generalized closed sets, Internat. J. Math & Math.Sci. 22(2) (1999) 239-249.
- [8] J. Dontchev and T. Noiri, Quasi Normal Spaces and πg -closed sets, Acta Math. Hungar., 89(3)(2000), 211-219.
- [9] J. Dontchev and M. Przemski, The various decompositions of continuous and weakly continuous functions, Acta Math. Hungar., 71(1996), no. 1-2, 109-120.
- [10] E. Ekici and M. Caldas, Slightly-continuous functions, Bol. Soc. Parana. Mat. (3) 22 (2004), 63-74.
- [11] Govindappa Navalagi and Md. Hanif Page, θ -generalized semi-open and θ -generalized semi-closed functions Proyecciones J. of Math. 28,2 ,(2009) 111-123.
- [12] C.Janaki, Studies on $\pi g\alpha$ -closed sets in Topology, Ph.D Thesis, Bharathiar University, Coimbatore (2009).
- [13] N.Levine: Semi-open sets and semi-continuity in topological spaces, Amer. Math. Monthly, 70 (1963), 36-41.
- [14] N.Levine: Generalised closed sets in topology, Rend. Circ. Mat. Palermo, 19(1970), 89-96.
- [15] H. Maki, R.Devi and K.Balachandran: Semi-generalised closed maps and generalised semi-closed maps, Mem. Fac. Sci. Kochi Univ. Ser. A Math.,14(1993),41-54.
- [16] H. Maki, R. Devi and K. Balachandran generalised α -closed maps and α -generalised closed maps, Indian J. Pure. Appl. Math., 29(1998), No. 1, 37-49.
- [17] A.S. Mashhour, M. E. Abd El-Monsef and S.N. El Deeb: On pre continuous and weakly pre continuous mappings, Proc. Math. Phys. Soc. Egypt., 53(1982), 47-53.
- [18] O.Njastad: On some Classes of nearly open sets, Pacific J. Math.,15(1965),961-970.
- [19] J.H. Park, On $\pi g\theta$ -closed sets in topological spaces, Indian J. Pure. Appl. Math., (To appear).
- [20] O.Ravi and M.Lellis Thivagar, On Stronger forms of $(1,2)^*$ -quotient mappings on bitopological spaces, Internat. J. Math. Game Theory & Algebra 4(2004), No.6, 481-492.
- [21] O.Ravi, M.Lellis Thivagar and M.E.Abd El-Monsef, "Remarks on bitopological $(1,2)^*$ -quotient mappings", J. Egypt Math. Soc. Vol. 16, No.1, pp.17-25,2008.
- [22] D.Sreeja and C.Janaki, On $(1,2)^*$ - πgb -closed sets, Inter. J. of Computer Applicationz (0975-8887), Vol.42.,No.5.
- [23] M.H. Stone : Application of the theory of Boolean rings to general topology, Trans. Amer. Math. Soc., 41 (1937), 375-381.
- [24] N. V. Velicko, On H-closed topological spaces, Amer. Math. Soc. Transl.,78, (1968) 103-118.

Enhancement of the Performance of Hydraulic Power Pack by Increasing Heat Dissipation

*¹M.L.R.Chaitanya Lahari, DR.B.SRINIVASA REDDY²

¹,(Department of Mechanical Engineering, G.P.R College of Engineering, Andhra Pradesh, India)
²,Professor & Principal (Department Of Mechanical Engineering, G.P.R College of Engineering, Andhra Pradesh, India)

ABSTRACT

Hydraulic power units are main driving components of driving system. Consisting mainly a motor, a reservoir and a hydraulic pump these units can generate a tremendous amount of power to drive any kind of hydraulic ram. Hydraulic power units are based on Pascal's law of physics drawing their power from ratios of area and pressure. Heating of hydraulic oil in operation is caused by inefficiencies. Inefficiencies result in losses of input power, which are converted to heat. If the total input power lost to heat is greater than the heat dissipated, the hydraulic system will eventually overheat. In this work an attempt is made to reduce the unwanted temperature of oil by changing the construction and material of the tank and providing fins over it. Finally the improvement of efficiency of power pack by reducing heat losses has been studied and analyzed.

Keywords: Hydraulic Power Pack, Thermal Conductivity, Heat Transfer Coefficient, Heat Dissipation

I. INTRODUCTION

Hydraulic Power Pack Basic Circuit

A hydraulic system employs enclosed fluid to transfer energy from one source to another, and subsequently create rotary motion, linear motion, or force. Hydraulic power units apply the pressure that drives motors, cylinders, and other complementary parts of a hydraulic system. Unlike standard pumps, these power units use multi-stage pressurization networks to move fluid, and they often incorporate temperature control devices. The mechanical characteristics and specifications of a hydraulic power unit dictate the type of projects for which it can be effective.

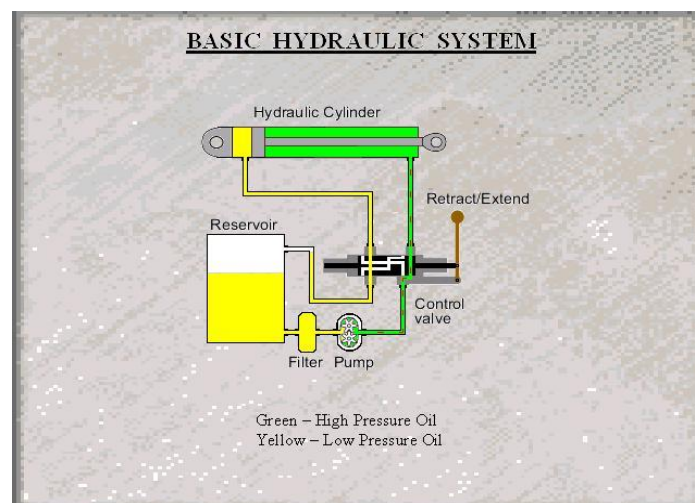


Figure 1 Basic Hydraulic System

Some of the important factors that influence a hydraulic power unit's performance are pressure limits, power capacity, and reservoir volume. In addition, its physical characteristics, including size, power supply, and pumping strength are also significant considerations. To better understand the operating principles and design features in a hydraulic power unit, it may be helpful to look at the basic components of a standard model used in industrial hydraulic systems.

As the temperature of hydraulic oil increases, input power falls – and if the total loss of power is greater than the heat dissipated, the hydraulic system will eventually overheat. And if oil overheats, it loses its lubricating properties and increases friction and wear on hydraulic components, meaning hardened seals and increased wear to the system. Another problem caused by high oil temperatures is reduced oil viscosity – which often leads to oil leakages. Because hydraulic components are constructed with very close tolerances, high heat and lubrication loss can also cause severe damage or seizure.

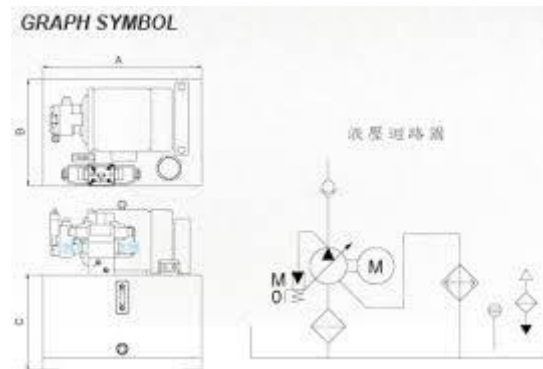


Figure 2 Circuit Diagram of Hydraulic Power Pack

Repairs can be costly and at worst, operations may have to close down. In many cases it is possible to do without cooling of the power unit because due to the reduced energy consumption the hydraulic fluid will not heat up excessively. This in turn allows a compacter design which reduces complexity and acquisition costs.

Reasons for Hydraulic Fluid Cooling:

The viscosity of hydraulic oil needs to be suitable during operation for both transmission of power and lubrication. This is very difficult to get right when there is a huge gaping hole between the temperatures of oil at a cold start, say 5°C, and that after continual running at 110°C. It's going to be hard to get hold of oil that can manage to perform in that type of scenario. Although seals and hoses are improving in design and materials all the time, they can still operate at their best with a temperature of 82°C before degradation begins. Even just 10°C above that temperature can have a huge effect on their lifespan. Hydraulic oil that gets very hot can suffer from oxidation (air) and hydrolysis (water). This is when there is air and water present in the system. The trouble comes when the temperature rises as according to Arrhenius's Law there is an increase in temperature of 10°C and reactions happen considerably faster. In summary, running a hydraulic system at such a high temperature does nothing for its lifespan or performance. It's a short cut to degradation and the receipt of several high priced maintenance related invoices.

RESERVOIR:

The design of the reservoir should be of sufficient capacity to contain all of the fluid in the hydraulic system with at least a 10% excess margin. For static hydraulic transmission systems the reservoir capacity of about 4 x the pump flow/minute should be available. On mobile units it is often necessary to have a smaller reservoir. The return line to the reservoir should be at the furthest end from the pump inlet feed to allow solid particle the drop out and entrained air to be released to the open surface. The return pipe can include a pepper pot arrangement well below the fluid surface level to encourage dispersion of flow. The reservoir should be designed with a safe working level such that the pump inlet and the system return pipe are continuously immersed at all times during the operating cycle. The oil flow through the reservoir should be at a low rate and preferable through perforated baffle plates to encourage air and precipitation of contaminants. The reservoir normally provides a cooling function, often eliminating the need for oil cooler. This chapter estimates the heat dissipated from a reservoir. The construction of the reservoir is generally based on a simple rectangular box with a floor sloping down to a drain plug. The tank should have internal corners suitably designed to ensure convenient cleaning and the surfaces should be descaled and painted with a paint which is corrosion resistant and suitable for the oil contained. The tank should include a sealed lid which includes a Filler/breather cap with air filter included and a sight level gauge on the side. Fluid power systems must have a sufficient and continuous supply of cool, uncontaminated fluid to operate efficiently. A hydraulic system has a reserve of fluid in addition

to that contained in the other components of the system. This reserve fluid compensates for changing fluid levels from system operation, loss of volume due to cooling and fluid compression from the pressure. This extra fluid is contained in a tank usually called a hydraulic reservoir. Most reservoirs have a capped opening for filling, an air vent, an oil level indicator or dip stick, a return line connection, a pump inlet or suction line connection, a drain line connection, and a drain plug.

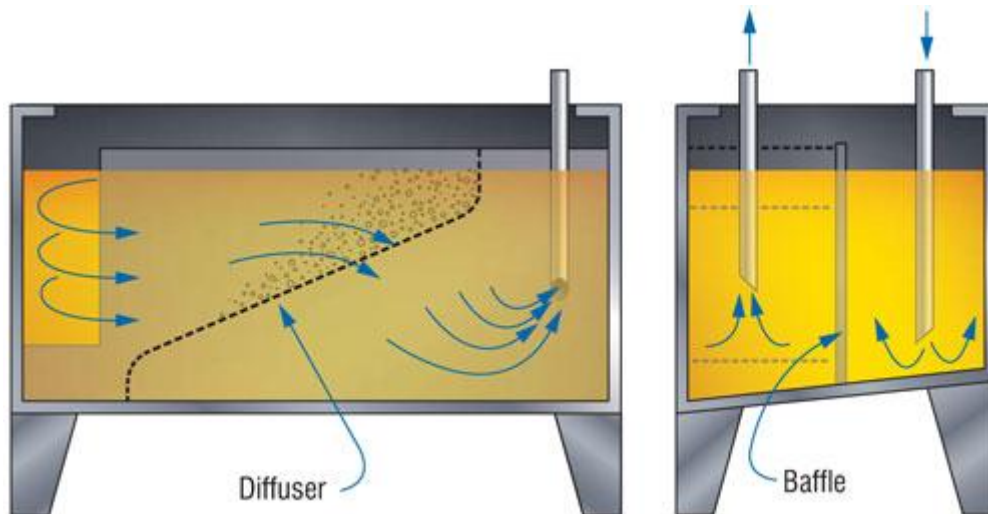


Figure 3: Reservoir of a Hydraulic Power Pack

A properly designed reservoir has internal baffles to prevent excessive sloshing of the fluid and to put a partition between the fluid return line and the pump suction line. The partition forces the returning fluid to travel farther around the tank before being drawn back through the pump inlet line. This does 3 things; it helps cool the fluid more effectively, aids in settling contaminants to the bottom and separates air from the fluid. Larger reservoirs are desirable as all 3 of the above benefits are further enhanced. As a rule of thumb the ideal reservoir will hold about 4 times the pump output per minute. The benefits of a large reservoir are sometimes sacrificed due to space limitations in mobile systems. As a minimum they must be large enough to accommodate thermal expansion of the fluid and changes in fluid level due to system operation. Reservoirs are of two general types - non-pressurized and pressurized. Propower manufactures non-pressurized hydraulic reservoirs and pressurized reservoirs operating up to 5 psi. Most systems are normally designed for equipment operating at normal atmospheric pressure. This includes hydraulic systems for truck or stationary installations. A typical reservoir for use in industrial installations is made of hot rolled steel plates, has welded seams and is not commonly used for mobile operation. The bottom of the reservoir is often convex, and a drain plug is incorporated at the lowest point. Most non-pressurized reservoirs are constructed in a cylindrical shape. The outer housing is manufactured from a strong corrosion-resistant metal. To keep the fluid clean filter elements are normally installed within the reservoir or externally to clean the returning fluid. Reservoirs that are filled by pouring fluid directly into them have a strainer in the filler well to strain out impurities when fluid is added. The quantity of fluid in the reservoir is indicated by a direct reading sight gauge, a clear tube, or a float/dial gauge.



Figure 4: MS Tank of a Hydraulic Power Pack



Figure 5: Al Tank of a Hydraulic Power Pack

2. Literature survey:

[1] Electric conveyor drives, brush drives, and soft clothe drives have gained a foothold because of the problems traditional hydraulics has caused. Most hydraulic systems in carwashes have used traditional petroleum based mineral oils as hydraulic fluids. Whenever these fluids leaked or a spill occurred it wreaked havoc. Mineral oil must be hand washed from the vehicle surface, brushes and soft clothe must be thoroughly cleaned or replaced, and free mineral oil can harm the water reclaim system. Also mineral oils are flammable and require hazardous storage. Larger spills may necessitate HAZMAT clean up. Mineral oil is not biodegradable and any spillage that winds up in the effluent may result in significant fines. However, the negative effects of mineral oil based hydraulic fluids can and have been rectified by using water based carwash hydraulic lubricants such as MRL Hydraulics' ENVIRO-GREEN II[®]. Now, I am ready to discuss efficiency. There are a number of steps that can be taken to improve hydraulic system efficiencies and improve performance. We need to look at where changes can be made and the impact that they will have on energy efficiencies.

If the system upgrade is coupled with a change to water based hydraulic fluid, such as ENVIRO-GREEN II[®]; the standard hydraulic carwash system becomes more energy efficient and eco-friendly. This becomes much more attractive to already installed systems where the hydraulics is pulled out and replaced with electrics. The conversion can be done with local fluid power and inverter drive professionals. The higher the local energy costs are the more imperative it becomes to make the transition.

[2] Fully powered flight controls are common among many aircraft, both military and commercial. Multiple pumps are generally employed to provide these flight controls with a redundant power source in addition to many other aircraft services. The prime hydraulic source in most cases is the engine-driven pump. It is driven directly by one of the aircraft's engines and offers the most efficient method of converting engine horsepower to hydraulic horsepower. The secondary hydraulic power source is generally not as efficient. It must derive its power from a source other than that which powers the prime pump. Present transport aircraft have utilized bleed air, ram air, electrical power, or hydraulic power to drive this redundant pump. All have demonstrated poor power-transfer efficiency when compared to a mechanically coupled pump. This inefficiency generally results in increased cost, weight, and complexity to the aircraft. The inadequate performance of existing hydraulic power transfer units was of particular concern. This paper will address the performance problem as well as the Douglas approach to improve it.

[3] With increased focus on the environmental impact of oil-based hydraulic systems, industry ry is seeking new technologies to provide cleaner power transmission sources. Researchers at Purdue University are responding to this demand by studying alternatives such as water hydraulic controls and water-based power transmission. One of the agricultural and biological engineering department's projects involves port design in a composite hydraulic cylinder to reduce cavitations during actuation. Cavitations are when formed and collapse in the hydraulic medium bubbles. This implosion of air bubbles can cause damage within hydraulic components. Purdue has developed a clear plastic cylinder with various port designs to allow capitation visualization during operation. Another university project focuses on developing a gear box with hydrostatic bearings using water as the working fluid. This concept includes using a nonmetallic bearing material.

[4] In this era of automation technologies manufacturing sectors have placed very high demands on fast and reliable production methods. This work is the evaluation & analysis of the existing clamping system. The current system uses manual clamping of fixtures for holding the work piece in the proper position while welding process is being done on the part. The evaluated system uses hydraulic vertical swing clamps for holding the work piece driven by hydraulic power pack. Thus the new system achieves automatic and simultaneous clamping of fixtures.

Table 1 Thermal properties of Mild steel and Aluminum

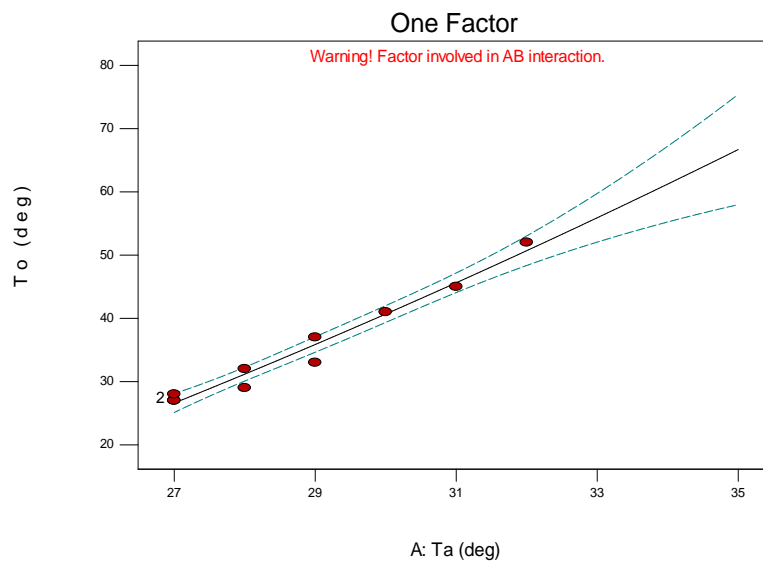
Properties	units	Mild steel	Aluminum
Density	10^3kgm^{-3}	7.86	2.70
Thermal Conductivity	$\text{Jm}^{-1}\text{K}^{-1}\text{s}^{-1}$	50	247
Thermal Expansion	10^{-6}K^{-1}	11.7	23.6
Young 'Modulus	GNm^{-2}	210	71
Tensile Strength	J/kg-k	350	310
% Elongation	MNm^{-2}	30	14

Temperature readings of hydraulic fluid for mild steel tank and Aluminum tank:

S.No	$T_a(^{\circ}\text{C})$	$T_{m_f}(^{\circ}\text{C})$	$\Delta T(^{\circ}\text{C})$ [$T_a \sim T_{m_f}$] ($^{\circ}\text{C}$)	$T_{a_l}(^{\circ}\text{C})$	$\Delta T(^{\circ}\text{C})$ [$T_a \sim T_{a_l}$] ($^{\circ}\text{C}$)
1	35	35	0	35	0
2	35	39	4	39	4
3	35	41	6	41	6
4	35	44	9	43	9
5	35	46	9	44	9
6	35	49	9	45	10
7	36	50	14	45	9
8	36	50	14	45	9
9	36	51	15	46	9
10	36	52	16	46	9
11	36	52	16	46	9
12	36	52	16	46	9

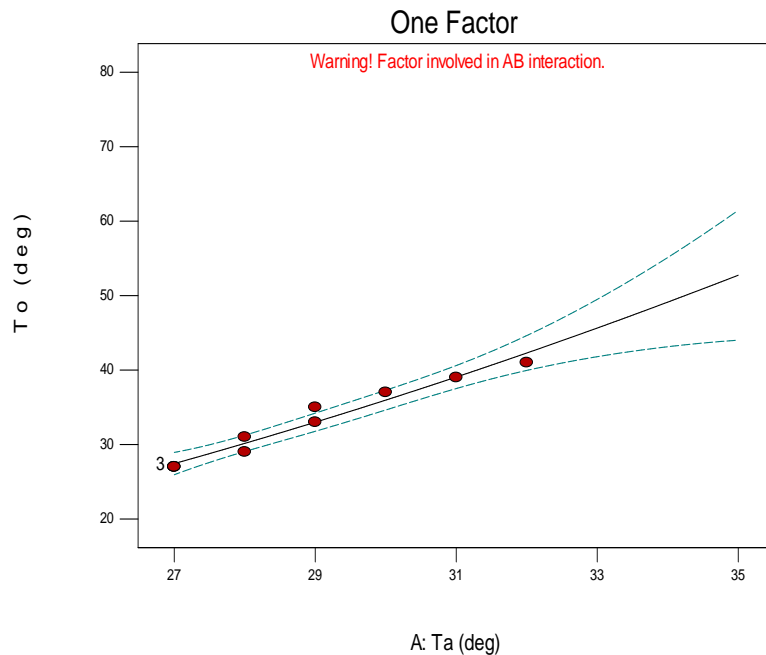
T_a versus T_o for MS:

Design-Expert® Software
 Factor Coding: Actual
 To (deg)
 • Design Points
 --- 95% CI Bands
 X1 = A: T_a
 Actual Factor
 B: M = MS



T_a versus T_o for Aluminum:

Design-Expert® Software
 Factor Coding: Actual
 To (deg)
 ● Design Points
 --- 95% CI Bands
 X1 = A: Ta
 Actual Factor
 B: M = Al



5. Results & Discussions

The total heat transfer rate has been improved by changing the material of the tank from Mild steel to Aluminum for the power pack and the simulation can be done even when the power pack of greater capacity is used. The limitation of the work is that the pressure bearing capacity is more for Mild Steel where the same is less for Aluminum.

Interpretation of the work has been analyzed using design expert software and error is only 0.01% where less than 0.05% indicates model terms are significant.

REFERENCES

- [1] Laamanen, A. & Linjama, M. (Eds.) Proceedings of the Third Workshop on Digital Fluid Power, October 13-14, 2010, Tampere, Finland, 170 p. (Tampere University of Technology, 2010) [1] S. S. Ngu, L. C. Kho, T. P. Tan & M. S. Osman, "Design of the Roller Clamp Robotic Assembly", World Academy of Science, Engineering and Technology, Vol-68, 2012.
- [2] Tudor Paunescu, "New solutions for driving the hydraulic fixtures", International Journal of Systems Applications, Engineering & Development, Issue 5, Volume 5, 2011.
- [3] U. Zuperl, F. Cus & D. Vukelic, "Variable clamping force control for an intelligent fixturing", Journal of Production Engineering, Vol-14, February 2011.
- [4] Emanuele Guglielmino, Claudio Semini, Helmut Kogler, Rudolf Scheidl & Darwin G. Caldwell, "Power Hydraulics - Switched Mode Control of Hydraulic Actuation", IEEE/RSJ International Conference on Intelligent Robots and Systems on October 18-22, 2010, Taipei, Taiwan.
- [5] Jeffrey J. Madden, P. Martin, Stowell Peilin, Wu Hongmiao & Li Lu He, "Welding Fixture with Active Position Adapting Functions", Huohzong Institute of Technology, 7/31/2007.
- [6] Guohua Qin, "Analysis and Optimal Design of Fixture Clamping Sequence", Sino-French Laboratory of Concurrent Engineering, Department of Aircraft Manufacturing Engineering, Northwestern Polytechnic University, 482 / Vol. 128, MAY 2006.
- [7] M. Vural, H.F. Muzafferoglu & U.C. Tapici, "The effect of welding fixtures on welding distortions", Mechanical Engineering Department, Istanbul Technical
- [2] Bishop, E. D. Digital Hydraulic Transformer – Approaching Theoretical Perfection in Hydraulic Drive Efficiency. CD-ROM Proceedings of the Ninth Scandinavian International Conference on Fluid Power, June 2-4, 2009, Linköping, Sweden, 19 p.
- [3] Pugh, B. The Hydraulic Age – Public Power Supplies before Electricity, 176 p. (Mechanical Engineering Publications Ltd., London, 1980)
- [4] A. Idrich, R. H. 1920. Unloading Mechanism. US Patent No 1334828.
- [5] Rickenberg, F. 1930. Valve. US Patent No. 1757059.

- [6] Murphy, R. & Weil, J. 1962. Hydraulic Control System. US Patent No. 3038449.
- [7] Virvalo, T. 1978. Cylinder Speed Synchronization. *Hydraulics & Pneumatics*, Dec 1978, pp. 55–57.
- [8] Ballard, R. L. 1968. System for Minimizing Skidding. US Patent No 3528708.
- [9] Wennmacher, G. Untersuchung und Anwendung schnellschaltender elektrohydraulischer Ventile für den Einsatz in Kraftfahrzeugen, Dissertation, RWTH Aachen, Germany, 1995.
- [10] Lauttamus, T., Linjama, M., Nurmi, M. & Vilenius, M. A novel seat valve with reduced axial forces. **In:** Johnston, D.N. & Edge, K.A. (eds.) *Power Transmission and Motion Control, PTMC 2006*, 13-15 September, 2006, Bath, UK, pp. 415-427.
- [11] Johnson, B., Massey, S. & Sturman, O. 2001. Sturman Digital Latching Valve. **In:** Palmberg, J.-O. (Ed.) *The Seventh Scandinavian International Conference on Fluid Power, SICFP'01*, pp. 299–314 (Vol. 3)
- [12] Anon. PVE Series 4 for PVG 32, PVG 100 and PVG 120, Technical Information. Sauer-Danfoss Prochure No 520L0553 Rev EA, May 2010, 32 p.
- [13] Suematsu, Y., Yamada, H., Tsukamoto, T. & Muto, T. Digital Control of Electrohydraulic Servo System Operated by Differential Pulse Width Modulation. *JSME International Journal, Series C*, Vol. 36 (1993), No. 1, pp. 61-68.
- [14] Becker, U. The Behavior of a Position Controlled Actuator with Switching Valves. *Proceedings of the Fourth Scandinavian International Conference on Fluid Power*, Sept. 26-29, 1995, Tampere, Finland, pp. 160-167.
- [15] Muto, T., Yamada, H. & Tsuchiya, S. A Precision Driving System Composed of a Hydraulic Cylinder and High-Speed ON/OFF Valves. *Proceedings of the 49th National Conference on Fluid Power*, March 19-21, 2002, Las Vegas, Nevada, USA, pp. 627-638.
- [16] Branson, D. T., Lumkes, J. H. Jr., Wattananithiporn, K. & Fronczak, F. J. Simulated and Experimental Results for a Hydraulic Actuator Controlled by Two High-Speed On/Off Solenoid Valves. *International Journal of Fluid Power*, Vol. 9 (2008), No 2, pp. 47-56.
- [17] Scheidl R., Riha G., Energy Efficient Switching Control by a Hydraulic „Resonance-Converter“. **In:** Burrows, C. R. & Edge K. A. (Eds.): *Proc. Workshop on Power Transmission and Motion Control (PTMC'99)*, Sept. 8-11, 1999, Bath, UK, pp. 267-273.

A Brief Study on Usability Principles of Mobile Commerce

Manjot Kaur

G.S.S.D.G.S. Khalsa College, Patiala-147001, PUNJAB, INDIA

ABSTRACT :

The widespread use of mobile commerce is no longer a fiction. The future is for mobile technology and mobile commerce. These emerging technologies are getting wide acceptance throughout the world. Mobile commerce getting fast popularity since it allows the freedom of movement and ease of access virtually from anywhere. The future of mobile commerce heavily depends upon how easy and how friendly is this service to use. An effective user friendly interface design plays central role in the success of mobile commerce. Therefore, the main purpose of my research is to evaluate the usability principles of mobile commerce. In this research paper firstly I discussed about the M-Commerce in detail. Definitions of Mobile Commerce given by various authors are explained in brief. In problem discussion various barriers to M-Commerce are identified such as security, tangibility and physical experience. After this, usability of M-Commerce is explained as one of the biggest challenging issue in the adoption of M-Commerce. Essential factors of the M-Commerce acceptance are also outlined. After this a model of attributes of system acceptability is described. In last research questions are defined with the suitable answers. After research it can be concluded that if mobile usability could be improved above "satisfactory" level, it will have direct and positive impact of m-commerce usage and increase in m-commerce business volume.

KEYWORDS: WAP usability, Usability Principles, Mobile commerce, User Interface Design, Principles to support usability, Usability Heuristics, Amazon.com, CNN.com

I. MOBILE COMMERCE-

According to Will (2004) E-Commerce can be defined as a monetary transaction conducted using the combination of internet and a desktop or laptop computer. Likewise, M-commerce is generally known as an extension of e-commerce. M-commerce can be defined as a monetary transactions that take place using wireless internet-enabled technology like handheld computers, mobile phones, personal digital assistant and palmtop computers that allow the freedom of movement for the end user. The Wi-Fi- Wireless Fidelity which is the transmission of short-ranged radio signals between a fixed- based station and an end user's mobile device is the operating technology that facilitates mobile commerce. Condos et al. (2002) describe that m-commerce combines the advantages of mobile-communication with existing Electronic Commerce applications to permit customers to shop for goods and services virtually from anywhere. The rapid development in telecommunication and innovative thinking about user interface design has greatly facilitated mobile users to take the full advantage of m-commerce. WAP is one of the key enabling technologies of m-commerce that allows mobile users to access the internet from mobile. As a result, the future consumer adoption of m-commerce relies heavily on how easy it is to use WAP in order to access and utilize these services.

II. PROBLEM DISCUSSION

Although, WAP has sufficiently influenced the life style of common people, however the boost in the use of WAP users has not been as fast as the marketer's expectations (Brewin, 2001). For instance, a report by two large mobile phone carriers found that only 10 percent of 400,000 WAP enabled phones in Asia were used to connect to the Internet, the major reasons are identified as, the poor data quality, slow connections, small screens and poor enjoyment experience has been on the top (Associated Press, 2001; Bangkok Post, 2001). The problems of user interface, limited menu options and screen resolution should be taken into account by the

senders of the information but only to a point since WAP device display screens are presently too small to provide enough information to foster ease of use. Jakob Nielsen (1993) has identified these potential issues of navigation barriers; he figure out that it took 20 clicks to locate a stock quote and 12 clicks to get the location of a Starbucks coffee store. Zaret (2001) conducted a research by providing a sample of WAP enabled mobile phone to users for a week and information on the available content, as result, 70 per cent of the handset holders said they would not use a WAP phone within the next 12 months. Similarly, a research conducted in Japan in May 2001 produced same results that the participants in a large-scale trial of 3G handsets in complained about the short usage periods before battery discharge and the phones were very hot to use due to heavy voltage drains. A commercial research conducted by TNS Interactive (2001) shows consistent results that show that the greatest barriers to m-commerce were, in order of priority:

- Security
- Tangibility and
- Physical experience

The WAP adoption has not been achieved up-to its assumptions even in those countries where internet usage is at its highest growth where internet usage is at its highest growth, for instance, Norway as first in internet usage with (63 per cent) USA being fourth (57 per cent) and Australia seventh (48 per cent), however despite there being almost twice as many cellular phone subscribers as internet households in the USA in 2001, just 12 per cent of the mobile phone owners use WAP shopping. In addition, Phillips (2001) figure out that 39 per cent of cellular phone users were not ready for WAP or did not want to use WAP for shopping. Here a question arises, that, how the marketers will meet the profile needs of cellular phones users to stimulate the WAP usage?

According to Whitfield (2003) the wireless technology and mobile computing applications has been overestimated in marketing. It was estimated that in the mobile of 2003 a million new consumers could make video calls, they could watching live football and check e-mail using their WAP enabled phones. The 3G- third generation technology is believed to be accountable for this revolution and new market promotion. However, there are numerous questions about this technology, for instance, what new marketing opportunities will emerge from this technology? What are the limitations of this new promising wireless mobile market? However, it has been noticed that the value creation to the user and to the customer is not always delivered using those emerging technologies

III. M-COMMERCE USABILITY

M-Commerce usability is one of the biggest challenging issues in adopting m-commerce (Ghinea and Angelides, 2004). Since, m-commerce has been deflated in the last few years therefore some doubts and concerns arose about its future (Jarvenpaa et al., 2000). In contrast to e-commerce, research shows new challenges in usability design in mobile commerce that are not limited to, the small screen size, limited screen resolution, limited processing capabilities, inadequate battery power of mobile devices, and bulky input mechanisms (Ghinea and Angelides, 2004).

Similar to Sears and Arora (2002) and Nielsen et al. (2001), Ozok and Wei (2004) has also identified additional usability difficulties with the use of mobile phones including one of the hands being occupied holding mobile phone while data entry is conducted with the other hand using a stylus pen or the keypad. In addition, more difficulties involve information retrieval such as graphics being too small to read and take long time to download. In online sales, the user interface features including web page and content designs are key factors to enhance sales (Cao et al., 2005). In order to satisfy internet commerce usability expectations, the websites needs to be customized according to user interface principles to satisfy both their sensory and functional needs (Bellman et al., 1999). According to Venkatesh et al. (2003) with the aim to establish a successful mobile commerce environment there are certain prerequisites to pursue. A simple conversion of a successful e-commerce business into mobile commerce is not a way of success. Therefore, a step-by-step content translation from e-commerce to m-commerce is not a best solution. There are numerous fundamental challenges needed for transferring websites from e-commerce to mobile commerce such as

- The first factor is related to the human issue connected with the small keypads and limited display interfaces of mobile phones; therefore, mobile commerce website designers should offer shrunk web pages with a limited number of features on the mobile interfaces rather than offering variety of features on e-commerce websites.
- Second factor is that the goal is different in mobile commerce, since the key in mobile commerce success is the ability to present content to users in a customized fashion, therefore, the goals mobile commerce customers wants to achieve are different than their goals in the e-commerce environment. Since, in mobile commerce environment goals are often associated with a limited time (Sadeh, 2002). Mobile commerce tends to provide services to support time-critical activities therefore designers have to leverage the desires for specific usability aspects of mobile commerce.
- The third factor is associated with cultural differences, Chau et al. (2002) has identified that while designing mobile commerce solution the designers should consider the cultural differences since people have been found as culturally sensitive.
- The fourth important factor in mobile commerce is security and privacy. Palen and Salzman (2002) has figure out security as part of the advancement of usability in m-commerce. The issue of information privacy is a growing concern from a customer perspective as in m-commerce the world is a global village.
- The fifth vital factor in mobile commerce is user trust. Ozok and Wei (2004) has identified that user trust in secure data transmission using mobile device is considerably high, as compare to e-commerce.

IV. ESSENTIAL FACTORS OF M-COMMERCE ACCEPTANCE

Choi et al.; (2008) has list down the essential factors of m-commerce acceptance in their study of m-commerce in Korea. They figure out that these factors have significant impact on customer satisfaction while using m-commerce. The factors such as ease of navigation ease of use, content quality, perceived usefulness, and mobile portal reliability strongly affect to decide whether the customer should revisit that mobile portal or not. If these factors are considered in mobile portal development it will increase m-commerce usability. Following Figure shows the detailed contents of these essential factors of m-commerce acceptance.

Factors	Description	Researchers
Convenience	Perceived ease of use Ease of Navigation	Cheong and Park (2005), Wu and Wang (2005), Kim et al, (2005)
Transaction Process	Transaction Time Transaction Process	Ghinea and Angelides (2004), Kim et al, (2005)
Mobile portal and Reliability	Systems Perceived risk Perceived system quality Compatibility Product Perceived content quality Degree of content up-to-date Variety of content	Cheong and Park (2005), Wu and Wang (2005), Kim et 1, (2005)
Information	Categorization of information Naming of information	Kim et al, (2005)
Price	Cost Perceived level of price	Ghinea and Angelides (2004), Cheong and Park (2005), Wu and Wang (2005)
Security/Privacy Usefulness	Perceived usefulness Usefulness of content	Cheong and Park (2005), Wu and Wang (2005), Kim et al, (2005)
Experience	Internet experience	Cheong and Park (2005)
User behavior	Attitude to m-internet Intention to use	Cheong and Park (2005), Wu and Wang (2005)
Representation	Size of image/text Readability of information Convenience of navigation	Kim et al, (2005)

Figure 1.1 Essential factors of m-commerce acceptance in the previous studies

Source: Choi et al.; (2008)

The above figure illustrates the essential factors of m-commerce acceptance such as “transaction process” and “customization” which lead customer satisfaction when connecting an m-commerce site. However it has unique aspects of “content reliability”, “availability”, and “perceived price level” of mobile Internet which build customers intention to use m-commerce site.

V. USABILITY AND SYSTEM ACCEPTABILITY

According to (Nielsen, 1993) system usability is relatively a minor concern as compared to the larger issues of system acceptability, which is the main question of whether the system is good enough to satisfy user needs and requirements and other potential stakeholders e.g. users, clients and managers. In general, acceptability of a computer system is again a combination of its social acceptability and practical acceptability; for instance, consider a system which investigates whether people applying for unemployment benefits are currently employed or unemployed to prevent fraudulent claims. This can easily be done by verifying information with other systems. Some people might appreciate this fraud-preventing system whereas some people might assume that it un-necessarily delays the benefits to deserving people. In this example, the system is not socially acceptable by peoples of later category; even though the system is practically acceptable since it prevent fraudulent claims.

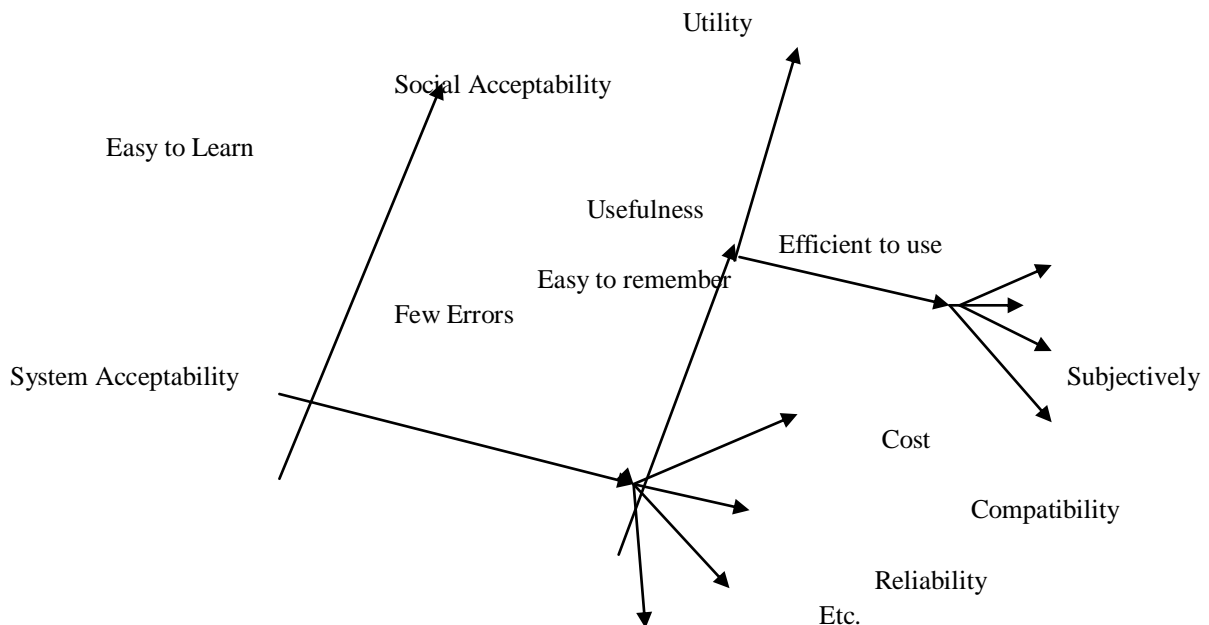


Figure 2.2 A model of attributes of system acceptability

Source: (Nielsen, 1993) page 25

In this figure, A model of attributes of system acceptability is given which illustrates the different elements of system acceptability. The model is based on four key attributes, included social acceptability, practical acceptability, usefulness, utility and usability, these elements are critical for the successful interface design. The main features of system acceptability also include sub-elements that describe the details against each key segment.

VI. RESEARCH QUESTIONS

Based on problem discussions, I have formulated two research questions which are as follows:

RQ1. Does the design of WAP services contain major usability flaws?

Research conducted by Ramsay 2001, Condos et al, 2002 and Nielsen 1993 is very much useful to answer our first research question to workout does the design of current WAP services contain major usability flaws?

Usability Principles for WAP Services defined by Condos et al., (2002)

- Avoid unnecessary use of graphics
- Avoid long lists and indicate the length of the list
- Make important options visible to the user
- Provide clear, helpful and meaningful error messages
- Avoid dead ends
- Format and present content appropriately
- Offer consistency in navigation and naming of menu options
- Provide the user with sufficient prompting
- Minimize user input
- Structure tasks to aid the user's interaction with the system

Usability Principles for WAP Services defined by Ramsay (2001)

- E-Navigation and Labeling
- Unnecessary browse time
- Minimize input
- Help Facility

RQ2. How the m-commerce interface design can be made user-friendly?

User centered interface design principles and usability principles plays key role to improve interface design. Since, my research is intended to first figure-out any existing flaws in WAP services and in second research question, I will attempt to propose solutions to improve the interface design with the help of valuable research conducted by Nielsen, 1990, Dix et al., 1993, and Preece et al., 1995.

Usability heuristics for User Interface Design: Jakob Nielsen (1990)

- Visibility of system status
- Use user's own language
- User control and freedom
- Consistency and standards
- Error prevention
- Recognition versus Recall
- Flexibility of use
- Aesthetic and minimalist design
- Sensible error messages
- Help and documentation

VII. CONCLUSION

Mobile commerce is one of the fastest and emerging fields of research. The importance of mobile commerce is an open reality; however a few studies are found on "usability of mobile commerce". Therefore, this field of research required immediate attention of passionate and enthusiastic researchers. Since, the mobile devices and technology itself changing very quickly, as a result, it open doors for the constant need for the improvement of mobile usability and mobile interface design principles. I would recommend that a future study should be conducted by taking different WAP Portals. Since, we believe that if mobile usability could be improved above "satisfactory" level, it will have direct and positive impact of m-commerce usage and increase in m-commerce business volume.

REFERENCES:

- [1]. Associated Press, (2001), "WAF services rarely used in Hong Kong", Taylor Nelson Sofres Interactive.
- [2]. Bellman, S., Lohse, G. and Johnson, E. (1999), "Predictors of online buying behaviour", Communications of the ACM, Vol. 42 No. 12, pp.32-8.
- [3]. Brewin, B (2001), "Mobile commerce loses luster", Info World, <http://www.infoworld.com/articles/hn/xml/01/05/11/010511hn1uster.xml? p=br&s=2>,
- [4]. Cao, M., Zhang, Q. and Seydel, J. (2005), "B2C e-commerce web site quality: an empirical examination", Industrial Management & Data Systems, Vol. 105 No.5, pp. 645-61.
- [5]. Chau, P., Cole, M., Massey, A., Motoya-Weiss, M. and O'Keefe, R. (2002), "Cultural differences in consumer's online behaviours", Communications of the ACM, Vol. 45 No. 10, pp. 45-50.
- [6]. Condos, Chris; James, Anne; Every, Peter; Simpson, Terry, (2002), "Ten usability principles for the development of effective WAP and m-commerce services", Journal: Aslib Proceedings: new information perspectives; Volume 54 No.6; 2002.
- [7]. Choi Jeewon, Hyeonjoo Seol, Sungjoo Lee, Hyunmyung Cho, Yongtae Park (2008), "Customer satisfaction factors of mobile commerce in Korea ", Journal of Internet Research, Vol. 18,No.3Page: 3}3-335
- [9]. Dix (1993), *Human-Computer Interaction*, Prentice-Hall, Englewood Cliffs, NJ.
- [10]. Ghinea, G. and Angelides, M. (2004), "A user perspective of quality of service in m-commerce": Multimedia Tools and Applications, Vol. 22, pp. 187-206.
- [11]. Jarvenpaa, S.L. and Staples, D.S. (2000), "The use of collaborative electronic media/or information sharing: an exploratory study of determinants?", Journal of Strategic Information Systems, Vol. 9, pp: 129-54.
- [12]. Nielsen, Jakob (1993) *Usability Engineering*, Academic Press, San Diego, CA, USA.
- [13]. Ozok, A.A. and Wei, J. (2004), "User perspectives of mobile and electronic commerce with a usability emphasis", Proceedings of the ISO One World 2004 Conference, Las Vegas, NE, Article 71.
- [14]. Palen, L. and Salzman, M. (2002), "Beyond the handset: designing for wireless communications usability", ACM Transactions on Computer-Human Interactions, Vol. 9 No.2, pp. 125-51.
- [15]. Phillips, M (2001), "Australians mystified by WAP", APT Strategies,
- [16]. <http://anywhereyougo.com/wap/Article.po?id=212280>
- [17]. Preece, Jenny (1995), *Human Computer Interaction*, Addison-Wesley Publishing Company.
- [18]. Ramsay, M. (2001), "Mildly irritating: a W AP usability study", *Aslib Proceedings*, Vol. 53 No.4, pp.141-58.
- [19]. Sadeh, N. (2002), *M-Commerce: Technologies, Services, and Business Models*, Wiley, New York, NY.
- [20]. Sears, A. and Arora, R. (2002), "Data entry for mobile devices: an empirical comparison of novice performance with Jot and Graffiti ", *Interacting with Computers*, Vol. 14 No.5, pp. 413-33.
- [21]. TNS Interactive (2001), *Global Ecommerce Report 2001*, Taylor Nelson Sofres Interactive, London, pp.1-229.:
- [22]. Venkatesh, V., Ramesh, V. and Massey, A. (2003), "Understanding usability in mobile commerce", Communications of the ACM, Vol. 46 No. 12, pp. 53-6.
- [24]. Will, G. (2004), "Upstart airline shows direction of industry", The Chicago Sun-Times, Chicago Sun Times Inc., Chicago, IL, available at: <http://web.lexis-nexis.com>.
- [25]. Whitfield, N. (2003), "The future of 3G, it wasn't supposed to be like this", T3, No. August, pp. 47-50.
- [26]. Zaret, E (2001), "Why WAP is whack", www.msnbc.com/news/506189.asp?cp1=1.

Path Loss Prediction by Robust Regression Methods

¹T. E. Dalkilic, ²K. S. Kula, ³B. Y. Hanci

¹Karadeniz Technical University, Faculty of Sciences, Department of Statistics and Computer Sciences,
Trabzon, Turkey.

²Ahi Evran University, Faculty of Sciences and Arts, Department of Mathematics, Kirsehir, Turkey.

³50 Kersey Crescent, RG141SZ, Speen, Newbury, UK.,

ABSTRACT.

Estimating the position of mobile terminals is an important problem for cellular networks. One of the methods of locating the mobile terminal is to use measurements of the radio path loss. This paper presents the results of robust regression methods for the prediction of path loss in a specific urban environment. Since the data set using in the application has outlier robust regression methods are used prediction of the path loss model. The performance of the path loss model which is obtained from robust regression methods are compared to Bertoni-Walfisch model, which is one of the best studied for propagation analysis involving buildings. This comparison based on the mean square error between predicted and measured values. In this study, propagation measurements were carried out at 900 MHz band in the city of Istanbul, Turkey.

KEY WORDS: Path Loss Model, Anfis, Robust Regression, Prediction

I. INTRODUCTION

Cellular mobile communication is the field of wireless communication which gets most attention and improves fast. The combination of flexibility of radio communication and digital transmission quality has an important role in the success of this system. Global Systems for Mobile Communications (GSM) has become the only global and fastest growing system standard for mobile communication in the world. Because, it is the system whose standards accepted by whole world and have the highest number of users. Communication between mobile unit and system is provided with base stations. One of the most important criteria in system design is that spread of radio sign transmitted from the transmitter antenna which is located on the base station to the mobile unit should be modeled. Walfisch and Bertoni, have study a theoretical model that encounters the effects of buildings on radio propagation. This model assumes that building heights and separation between buildings are equal [1]. Bertoni Walfish model is improved by Chrysanthou and Bertoni [2]. In the model, the effects of the difference of height and structures of buildings to the sign spread are given. In the study of Cerri G. it was studied on feed forward neural networks for path loss prediction in urban environment [3]. In the study of Ileana, neural network models for path loss prediction are comparison [4]. Xia, H.H. [5] a simplified analytical model for predicting path loss in urban and suburban environments was proposed. There are many studies on the usage of the adaptive network for parameter prediction. In the study of Chi-Bin, C., and Lee, E. S. it was studied on fuzzy adaptive network approach for fuzzy regression analysis [6]. Jhy-Shing R. J. studied on the adaptive networks based on fuzzy inference system [7]. In the study of Erbay, D.T., and Apaydin, A., adaptive network is used to parameter estimation where independent variables come from an exponential distribution [8]. Fuzzy adaptive network used for estimating the unknown parameters of regression model is based on fuzzy if-then rules and fuzzy inference system. In regression analysis, data analysis is very important. Because, every observation may be has large influence on the parameters estimates in regression model. When data set has outlier, robust M methods (Huber, Hampel, Andrews and Tukey), are used parameters estimates. In this study the path loss predictions are obtained by robust regression methods. The predictions from robust regression methods are compared with predictions from the model which is proposed by Bertoni-Walfisch path loss model. The Bertoni-Walfisch model is the most suitable theoretical model for the Cağaloğlu region, because of this model is consider the buildings database. The remainder of the paper is organized as follows. Section II introduces the measurements and the path loss models. In the Section III robust regression methods for path loss prediction are presented. In the Section IV the path loss model for real data collected from Cağaloğlu, which is urban area in Istanbul (Turkey), is obtain via robust regression methods. In Section V, a discussion and conclusion are provided.

II. THE MEASUREMENTS AND THE PATH LOSS MODELS

To optimize the most suitable propagation model the measurements are very important. The measurement equipments consist of the transmitter and the receiver. The narrow band CW (Continuous Wave) transmitter, which can be tuned to a specific test frequency, was used together with an omni antenna. The antenna was installed on the rooftops. In order to decrease cable losses, the transmitter was located near the antenna. The receiver is a high speed GSM scanner, with Walkabout data collection software from Saftco Technologies. The measurements were carried out at an approximate speed of 40 km/h, while the receiving antenna was at a height of 1.5 m from the ground. The receiver was moved through a variety of urban environments. The measurements data was recorded every 250 m. The route length and the number of points were approximately 161 km and 644 respectively. The signal level enrollments are collected from along the streets which are between the base station antenna and the mobile station antenna. A variety of experimentally or theoretically based models have been developed to predict radio propagation in land mobile system in the literature. Walfisch and Bertoni have published a theoretical model that encounters the effects of buildings on radio propagation [1]. In this study, Bertoni-Walfisch model will be used to comparison, because of this model is take into consideration the buildings between the antennas.

2.1. A. Bertoni - Walfisch Model. Bertoni - Walfisch proposed a semi - empirical model that is applicable to propagation through buildings in urban environments. The model assumes building heights to be uniformly distributed and the separation between buildings are equal. Propagation is then equated to the process of multiple diffractions past these rows of buildings. The expression of the Bertoni-Walfisch path loss model is in dB,

$$PL_{B-W} (dB) = 89.5 + 21 \log f + 38 \log(d) - 181 \log(h_t - h_b) + A_b \tag{2.1}$$

where,

h_r , is the mobile station antenna height,

h_b , building height,

d_c , is the center-to-center spacing of the rows of the buildings,

f , is the frequency MHz

h_t , is the base station antenna height [1].

The influence of building geometry is contained in term

$$A_b = 5 \log \left[\left(\frac{d_c}{2} \right)^2 + (h_b - h_r)^2 \right] - 9 \log d_c + 20 \log \left\{ \tan^{-1} [2(h_b - h_r) / d_c] \right\} \tag{2.2}$$

III. ROBUST REGRESSION METHODS FOR PATH LOSS PREDICTION

In the determining of test statistics and coefficients, the role of each observation must be taken into consideration. The data details must also be tested, because the results of the parameter estimation may be related to an observation, and removal of this observation from the data may change the result of the analysis. This kind of observation, which has a bigger residual value than the others, is called an outlier. In the event of an outlier value, robust methods are used that are less affected than the least square method (LSM) during the estimation of the regression model. In this section, we provide definitions of robust M methods and adaptive network based fuzzy inference systems which are commonly used in the literature [9, 10, 11, 12,13].

3.1. M methods. M method is minimizing the residual function. Regression coefficients $\hat{\beta}_j$ are obtained by minimizing the sum

$$\sum_{i=1}^n \rho \left[\left(y_i - \sum_{j=1}^p x_{ij} \hat{\beta}_j \right) / d \right] \tag{3.1}$$

where $x_i = (x_{i1}, x_{i2}, \dots, x_{ip},)$ are independent variables, y_i is depend variable and

$$d = \text{median} \left| r_i - \text{median} (r_i) \right| / 0.6745, r_i \text{ is the } i^{\text{th}} \text{ observed error.}$$

By taking the first partial derivative of the sum in Eq. (3.1) with respect to each $\hat{\beta}_j$ and setting it to zero, the regression coefficients are obtained from Eq. (3.2) [9, 10, 11, 12, 13].

$$\sum_{i=1}^n x_{ij} \psi \left[\left(y_i - \sum_{j=1}^p x_{ij} \hat{\beta}_j \right) / d \right] = 0 \tag{3.2}$$

3.1.1. Huber. Huber’s ρ function is defined as

$$\rho(z) = \begin{cases} \frac{z^2}{2} & |z| \leq k \\ k|z| - \frac{k^2}{2} & |z| > k \end{cases} \tag{3.3}$$

$$z = r_i / d$$

$$d = \text{median} \left| r_i - \text{median} (r_i) \right| / 0.6745$$

where k is called the tuning constant and k is set at 1.5 and r_i is the i^{th} observed error. Sometimes the numerator of d is called the median of the absolute deviations (MAD). The following function is obtained by taking the derivative of Eq. (3.3).

$$\psi(z) = \begin{cases} -k & z < -k \\ z & |z| \leq k \\ k & z > k \end{cases} \tag{3.4}$$

The function Ψ is the derivative of ρ . They are typically set up such that large residuals will be given only marginal or zero Ψ weights in Eq. (3.4). So Ψ is often labeled as "re-descending to zero" [9, 10, 11, 12, 13].

3.1.2. Hampel. The Hampel Ψ function is defined as

$$\psi(z) = (\text{sign } z) \begin{cases} |z| & 0 \leq |z| \leq a \\ a & a \leq |z| \leq b \\ a \left(\frac{c - |z|}{c - b} \right) & b \leq |z| \leq c \\ 0 & c \leq |z| \end{cases} \tag{3.5}$$

The constant values are selected as $a = 1.7, b = 3.4$ and $c = 8.5$ in general [9, 10, 11, 12, 13].

3.1.3. Andrews. Andrews (sin estimate) Ψ function is defined as

$$\psi(z) = \begin{cases} \sin(z / k) & |z| \leq k\pi \\ 0 & |z| > k\pi \end{cases} \tag{3.6}$$

where k is taken to be 1.54 or $k = 2.1$ [9, 10, 11, 12, 13].

3.1.4. Tukey. In Tukey’s biweight estimate, the Ψ function is defined as

$$\psi(z) = \begin{cases} z(1 - (z/k)^2)^2 & |z| \leq k \\ 0 & |z| > k \end{cases} \quad (3.7)$$

where k is selected as 5 or 6 [9, 10, 11, 12, 13].

3.2. Fuzzy Inference Systems and ANFIS.

3.2.1. Fuzzy Inference Systems. The fuzzy inference system forms a useful computing framework based on the concepts of fuzzy set theory, fuzzy reasoning, and fuzzy if-then rules. The fuzzy inference system is a powerful function approximator. The basic structure of a fuzzy inference system consists of three conceptual components; a rule base, which contains a selection of fuzzy rules, a database, which defines the membership functions used in the fuzzy rules, and a reasoning mechanism, which performs the inference procedure upon the rules to derive a reasonable output. There are several different types of fuzzy inference systems developed for function approximation. In this study, the Sugeno fuzzy inference system, which was proposed by Takagi and Sugeno [14], will be used. When the input vector X is $(x_1, x_2, \dots, x_p)^T$, then the system output Y can be determined by the Sugeno inference system as

$$R^L : \text{If } (x_1 \text{ is } F_1^L, \text{ and } x_2 \text{ is } F_2^L, \dots, \text{ and } x_p \text{ is } F_p^L), \text{ Then } (Y = Y^L = c_0^L + c_1^L x_1 + \dots + c_p^L x_p),$$

Where F_j^L is fuzzy set associated with the input x_j in the L th rule and Y^L is output due to rule R^L ($L = 1, \dots, m$). The parameters used to define the membership functions for F_j^L is called the premise parameters, and c_i^L are called the consequence parameters. For a real-valued input vector $X = (x_1, x_2, \dots, x_p)^T$, the overall output of the Sugeno fuzzy inference systems a weighted average of the Y^L

$$\hat{Y} = \frac{\sum_{L=1}^m w^L Y^L}{\sum_{L=1}^m w^L} \quad (3.8)$$

where the weight w^L is the truth value of the proposition $Y = Y^L$ and is defined as

$$w^L = \prod_{i=1}^p \mu_{F_i^L}(x_i) \quad (3.9)$$

where $\mu_{F_i^L}(x_i)$ is a membership function defined on the fuzzy set F_j^L .

3.2.2. ANFIS. The Adaptive-Network Based Fuzzy Inference System (ANFIS) is a neural network architecture that can solve any function approximation problem. An adaptive network is a multilayer feed forward network in which each node performs a particular function on incoming signals as well as a set of parameters pertaining to this node and it has five layers [15],[16]. Fuzzy rule number of the system depends on numbers of independent variables and class or fuzzy sets number forming independent variables. When independent variable number is indicated with p , if level number belonging to each variable is indicated with l_i ($i = 1, \dots, p$) fuzzy rule number is indicated with

$$L = \prod_{i=1}^p l_i \quad (3.10)$$

The detail of ANFIS which is used in the path loss prediction is located in [17].

3.2.3. An algorithm to path loss prediction. In this study, the path loss prediction problem has a three-dimensional input. One of them is comes from Gaussian distribution and the others are come from exponential distribution. Because of this condition, there will be used two different membership function, one of them is named Gaussian membership function whose parameters can be represented by parameter set $\{v_h, \sigma_h\}$ and the other one is produced for the inputs which are come from exponential distribution in this study, by the membership function suggested by Erbay, T.D. and Apaydin, A. [8]. The membership function has one parameter which is represented by $\{v_h\}$. The optimal membership function for the exponential distribution function is obtained in the shape of

$$\mu(x_i) = \begin{cases} 2ce^{-\frac{x_i}{v}} & \text{if } x_i > a(c)_i \\ 1 & \text{if } x_i \leq a(c)_i \end{cases} \quad (3.11)$$

where c ($c < 1$) is a constant element and v is a distribution parameter which is called a priori parameter. In the data set derived from the exponential distribution, the limit of the data belonging to the cluster with one membership degree is dependent on the fixed element c and the parameter v , which indicates the distribution. This limit, given with $a(c)$, is described by,

$$a(c) = \max\{0, v \ln(2(1 - c))\} \quad (3.12)$$

and the optimal membership function for Gaussian distrubition is

$$\mu_{F_h}(x_i) = \exp \left[- \left(\frac{x_i - v_h}{\sigma_h} \right)^2 \right] \quad (3.13)$$

Where $\{v_h\}$ is center and $\{\sigma_h\}$ is spread of fuzzy cluster.

The steps of the proposed algorithm for predicted path loss model are as follows:

Step 0: Optimal class numbers related to data set belonging to independent variables are determined. Optimal value of class number l_i , ($l_i=2, l_i=3, \dots, l_i=\max$) can be obtained by minimizing fuzzy clustering validity function S [18]. This function is expressed by

$$S = \frac{\frac{1}{n} \sum_{i=1}^{l_i} \sum_{j=1}^n (\mu_{ij})^m \|v_i - x_j\|^2}{\min_{i \neq j} \|v_i - v_j\|^2} \quad (3.14)$$

where, μ_{ij} are fuzzy membership, v_i cluster center, n observation numbers and m fuzziness index.

Step 1: Priori parameters are determined. Spreading is determined intuitively according to the space in which input variables gain value and to the fuzzy class numbers of variables gain value and to the fuzzy class numbers of variables Center parameters are based on the space in which variables gain value and fuzzy class number and it is defined with

$$v_i = \min(X_i) + \frac{\max(X_i) - \min(X_i)}{(l_i - 1)}(i - 1), \quad i = 1, \dots, p \quad (3.15)$$

Step 2: w^L weights are calculated which are used to form matrix B to be used in counting posteriori parameter set by Eq. (3.11) and Eq. (3.13). The \bar{w}^L sets are the normalizations of the sets which is indicated with w^L .

Step 3: On the condition that the independent variables are fuzzy and the dependent variables are crisp, a posteriori parameter set is obtained as crisp numbers in the shape of, $c_i^L = (a_i^L, b_i^L)$, $c_i^L = a_i^L$. In that condition,

$$Z = (B^T B)^{-1} B^T Y \tag{3.16}$$

equality is used for determining the a posteriori parameter set. Here B is weighted input matrix and, Y and Z defined as

$$Y = [y_1, y_2, \dots, y_n]^T$$

$$Z = [a_0^1, \dots, a_0^m, a_1^1, \dots, a_1^m, a_p^1, \dots, a_p^m]^T$$

Step 4: By using posteriori parameter set c_i^L obtained in Step 3, the system model indicated with

$$f_{4,L} = \overline{w}^L Y^L \tag{3.17}$$

Setting out from the models and weights specified in Step 2, prediction values are obtained with

$$\hat{Y} = \sum_{L=1}^m \overline{w}^L Y^L \tag{3.18}$$

Step 5: Error related to model is counted as

$$\varepsilon = \frac{1}{n} \sum_{k=1}^n \varepsilon_k^2 = \frac{1}{n} \sum_{k=1}^n (y_k - \hat{y}_k)^2 \tag{3.19}$$

If $\varepsilon < \phi$, then posteriori parameter has been obtained as parameters of models to be formed, the process is determinated. If $\varepsilon \geq \phi$, then, step 6 begins. Here ϕ is a law stable value determined by decision maker.

Step 6: Central priori parameters specified in Step 1, are updated with

$$v_i' = v_i \pm t \tag{3.20}$$

in a way that it increases from the lowest value to the highest and decreases from the highest value to the lowest. Here, t is size of step;

$$t = \frac{\max(x_{ji}) - \min(x_{ji})}{a} \quad j = 1, \dots, n \quad i = 1, \dots, p \tag{3.21}$$

and a is stable value which is determinant of size of step and therefore iteration number.

Step 7: Predictions for each priori parameter obtained by change and error criterion related to these predictions are counted with

$$\varepsilon_k = y_k - \hat{y}_k \tag{3.22}$$

The lowest of error criterion is defined. Priori parameters giving the lowest error specified, and prediction obtained via the models related to these parameters is taken as output.

IV. PREDICTION PATH LOSS MODEL

In this section, try to obtain the most suitable path loss model based on the value of signal level in 900 MHz frequency, in Cağaloğlu region. The obtained model will be compare with the Bertoni-Walfisch model. Because, this model is take into consideration the buildings database. To Cağaloğlu region, number of observation is 644, base station antenna height is 16m, route is 161km, the average of the building heights 14.656m, and the average of the center-to-center spacing of the rows of the buildings is 42.7083m. From the result of the residual analysis, the 278th,

335th, 414th, 420th, 427th, 547th, 615th, 639th and 644th, nine observations are outliers. Standardized residuals for these observations are greater than 2.5. Cağaloğlu region is urban area and it has regular building structure. The gabs between buildings along the streets are small. Figure 1

shows the histogram of the center-to-center spacing of the rows of the buildings d_c , the building height h_b , and the α , respectively Figure (1-a), Figure (1-b) and Figure (1-c), which are the independent variables used in the constitute path loss model. This is appearing from histograms, the building heights h_b , have gauss distribution and the center-to-center spacing of the rows of the buildings d_c and the propagation angle α have exponential distribution. Because of that, during the form of the path loss model by ANFIS, the membership function which is expressed in Eq. (3.11) and (3.13) is used. The algorithm which is proposed in section five was operated with a program written in MATLAB for data set from Cağaloğlu region. This data set has 745 observations. And the fuzzy rules to path loss model based on fuzzy inference system are obtained as

$$\begin{aligned}
 \hat{Y}_1 &= -7250 + 160 x_1 + 2630 x_2 + 10154 x_3 \\
 \hat{Y}_2 &= 4390 - 60 x_1 - 1750 x_2 + 13530 x_3 \\
 \hat{Y}_3 &= -12050 - 30 x_1 + 490 x_2 - 6210 x_3 \\
 \hat{Y}_4 &= 8360 + 10 x_1 - 340 x_2 + 210 x_3 \\
 \hat{Y}_5 &= -240 + 20 x_1 - 850 x_2 - 76350 x_3 \\
 \hat{Y}_6 &= 520 - 0.7 x_1 + 4301 x_2 - 18540 x_3 \\
 \hat{Y}_7 &= 3470 - 1.1 x_1 - 110 x_2 + 6060 x_3 \\
 \hat{Y}_8 &= -1500 - 0.7 x_1 + 50 x_2 + 440 x_3
 \end{aligned}
 \tag{4.1}$$

where

x_1 : the center to center spacing of the rows of the buildings (d_c),

x_2 : the building heights (h_b),

x_3 : the propagation angle (α).

The parameter estimation from M methods and least square method (LSM) are located in Table 1.

	LSM	Huber	Hampel	Tukey	Andrews
$\hat{\beta}_0$	57.7577	58.5896	58.3194	58.7315	58.1706
$\hat{\beta}_1$	-0.1148	-0.1237	-0.1221	-0.1248	-0.1193
$\hat{\beta}_2$	-0.1468	-0.1707	-0.1595	-0.1764	-0.1585
$\hat{\beta}_3$	-218.2631	-217.7969	-218.1587	-218.0822	-218.0103

TABLE 1. Parameter estimation from LSM and M method

The input variable number, which is according to independent variables are three and the fuzzy class number of each input variable is two, which is determinate in initial step in proposed algorithm. And then fuzzy rules number is eight from Eq. (3.10). The comparison of the predictions is based on the error criterion given with Eq. (3.22). The error related to predictions obtained via the models given with Eq. (4.1), which are formed by ANFIS, is found as

$$\varepsilon_{ANFIS} = \frac{1}{n} \sum_{k=1}^n (y_k - \hat{y}_k)^2 = 30.6540$$

The error related to predictions obtained via the model given with Eq. (2.1) which is proposed by Bertoni-Walfisch, is found as

$$\varepsilon_{B-W} = \frac{1}{n} \sum_{k=1}^n (y_k - \hat{y}_k)^2 = 112.1499$$

And the error related to predictions obtained via M methods and the LMS are found as

$$\begin{aligned}
 \varepsilon_{Huber} &= 45.9195 \\
 \varepsilon_{Hampel} &= 45.8920 \\
 \varepsilon_{Andrews} &= 45.9365 \\
 \varepsilon_{Tukey} &= 45.8728 \\
 \varepsilon_{LMS} &= 45.8572
 \end{aligned}
 \tag{4.2}$$

The graphs of errors obtained via proposed algorithm, M methods and Bertoni- Walfisch model are shown in Figure 2. In Figure (2-a), errors from Bertoni-Walfisch model, in Figure (2-b), errors from LSM, in Figure (2-c), errors from fuzzy adaptive network which is related to proposed algorithm in this work, in Figure (2-d) to (2-g) errors from Huber, Hampel, Tukey and Andrews are shown respectively.

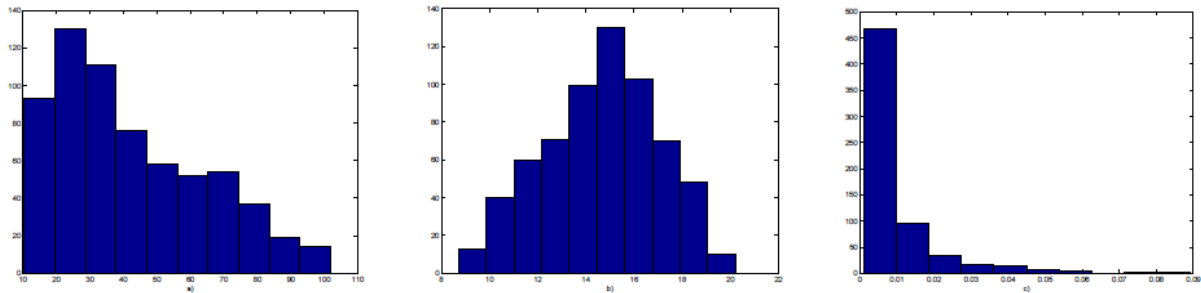


FIGURE 1. (a-b-c) Histograms of the independent variables.

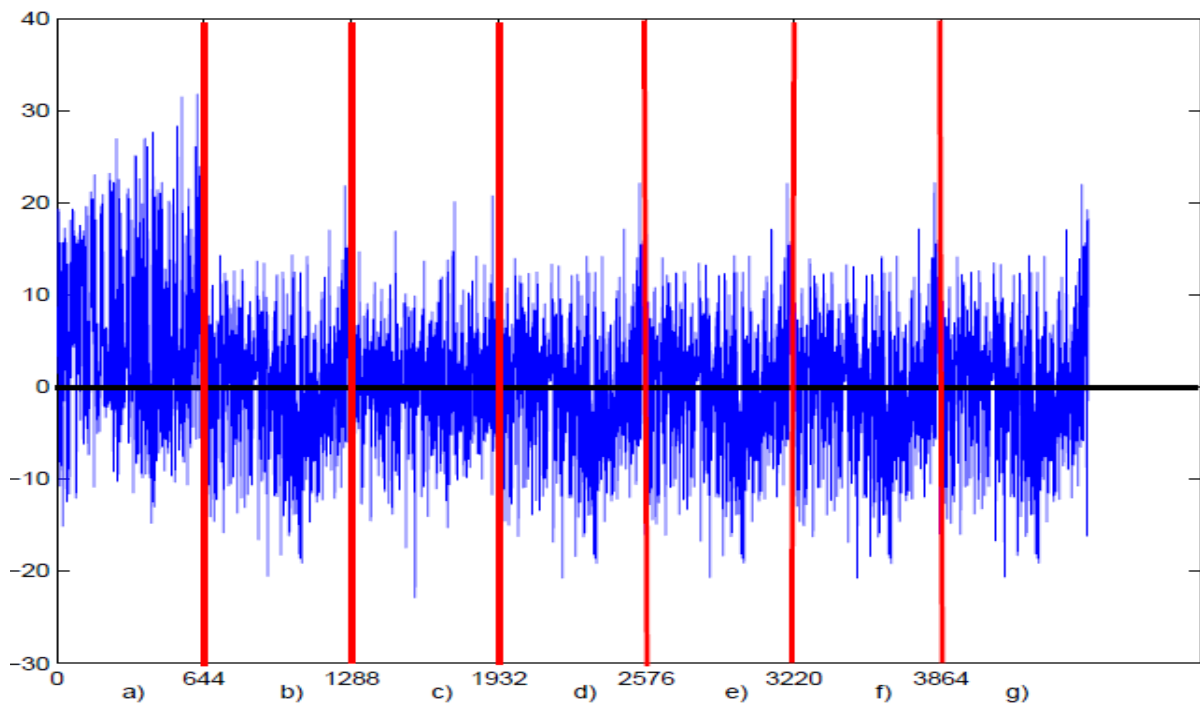


FIGURE 2. Errors from Prediction.

V. CONCLUSIONS

The path loss model prediction for the 900 MHz band is achieved depends on the measurements for Cağaloğlu which is the urban area in Istanbul. For the each measurement which are obtained from 644 different point in Cağaloğlu, the building height (h_b), center-to-center spacing of the rows of the buildings (d_c), propagation angle between base station antenna and mobile station antenna in radian (α) are counted. And they are used as the input variable in the robust regression methods. The Bertoni-Walfisch model is first model which is taking into consideration the effect of the buildings in path loss modeling. Because of the measurements are collecting from the urban are, the predictions from proposed algorithm are compared whit the predictions from Bertoni-Walfisch Model. The predictions from robust regression methods are compared with the Bertoni-Walfisch Model. And according to the indicated error criterion, which is expressed in Eq. (3.22) the errors related to the predictions that are obtained from the robust regression methods are less than the errors that are obtained from the Bertoni-Walfisch Model. The robust methods don't necessitate the equality of the heights and distance of buildings, it can be used for the different areas which have the similar characteristics of the area studied on.

Acknowledgment: The authors would like to thank to the GSM Operator Vodafone Turkey for providing the measurement equipment and locations of transmitter.

REFERENCES

- [1] Walfisch, J. and Bertoni, H.L.: A theoretical model of UHF propagation in urban environments, *IEEE Trans. Antennas and Propagation* 36 (12), 1788-1796, (1988).
- [2] Chrysanthou, C. and Bertoni, H.L.: Variability of sector averaged signals for UHF propagation in cities, *IEEE Trans. Veh. Technol.* 39 (4),352-358, (1990).
- [3] Cerri, G.: Feed forward neural networks for path loss prediction in urban environment, *IEEE transaction on Antennas and Propagation*, 52(11), 3137-3139, (2004).
- [4] Ileana, P. Iona, P. N. and Philip,C.: Comparison of neural network models for path loss prediction, *Wireless and Mobile Computing, Networking and Communications*, IEEE International Conference 1, 44-49, 22-24 Aug. (2005).
- [5] Xia,H.H.: A simplified analytical model for predicting path loss in urban and suburban environments, *IEEE Trans. Antennas and Propagation*, 40(2),170-177, (1992).
- [6] Chi-Bin, C. and Lee, E.S.: Applying fuzzy adaptive network to fuzzy regression analysis, *An International Journal Computers and Mathematics with Applications*, 38, 123-140, (1999).
- [7] Jyh-Shing, R.J.: ANFIS: adaptive network based fuzzy inference system, *IEEE Transaction on Systems, Man and Cybernetics*, 23(3),665-685, (1993).
- [8] Erbay, T.D. and Apaydn, A.: A fuzzy adaptive network approach to parameter estimation in cases where independent variables come from an exponential distribution, *Journal of Computational and Applied Mathematics*,233, 26-45 (2009).
- [9] Hampel, F.R., Ronchetti, E.M., Rousseeuw, P.J., and Stahel, W.A.: *Robust Statistics*, John- Willey and Sons, New-York, (1986).
- [10] Hogg, R.V.: Statistician robustness: One View of Its Use in Applications Today. *The American Statistician*, 33, 108-115, (1979).
- [11] Huber, P.J.: *Robust statistics*". John Willey and Son, (1981).
- [12] Huynh, H.: A Comparison of For Approaches to Robust Regression, *Psychological Bulletin*, 92, 505-512, (1982).
- [13] Kula, K.S.and Apaydn, A.: Fuzzy robust regression analysis based on the ranking of fuzzy sets, *International Journal of Uncertainty, Fuzziness and Knowledge-Based Systems* 16 (2008).
- [14] Takagi, T. and Sugeno,M. : Fuzzy identification of systems and its applications to modeling and control, *IEEE Trans. on Systems, Man and Cybernetics*, 15(1), 116-132, (1985).
- [15] Hisao, N. Manabu: Fuzzy regression using asymmetric fuzzy coefficients and fuzzied neural networks, *Fuzzy Sets and Systems*, 119, 273-290, (2001).
- [16] Ishibuchi, H. and Tanaka,H.: Fuzzy regression analysis using neural networks, *Fuzzy Sets and Systems*, 50,257-265, (1992).
- [17] Dalkilic, E. T., Hanci, B.Y. and Apaydin, A.: Fuzzy adaptive neural network approach to path loss prediction in urban areas at GSM-900 band, *Turkish Journal of Electrical Engineering and Computer Sciences*, 18(6), 1077-1094, (2010).
- [18] Xie, X.L. and Beni, G.: A validity measure for fuzzy clustering, *IEEE Trans Pattern Anal. Machine Intell*, 13(8), 841-847, (1991).

Stochastic Model to Find the Diagnostic Reliability of Gallbladder Ejection Fraction Using Normal Distribution

P. Senthil Kumar*, A. Dinesh Kumar** & M. Vasuki***

*Assistant Professor, Department of Mathematics, Rajah Serfoji Government College (Autonomous), Thanjavur, Tamilnadu, India.

**Assistant Professor, Department of Mathematics, Dhanalakshmi Srinivasan Engineering College, Perambalur, Tamilnadu, India

***Assistant Professor, Department of Mathematics, Srinivasan College of Arts and Science, Perambalur, Tamilnadu, India.

Abstract: To assess the diagnostic reliability of gallbladder ejection fraction in patients with suspected biliary pain. For a class of nonlinear diffusion equations we use the Painleve analysis. In some cases we find that it has only the conditional Painleve property and in other cases, just the painleve property. We also obtained special solutions of Painleve analysis. In that, one of the solution (i.e) the reduction of nonlinear diffusion equation to Riccati equation was used for the gallbladder ejection fraction.

Key Words: Gallbladder Ejection Fraction, Normal Distribution, Painleve Property, Riccati Equation, Cholecystokinin, Chronic Acalculous Cholecystitis.

2010 Mathematics Subject Classification: 60H99, 60G99

1. Introduction:

Measurement of gallbladder emptying with either oral fatty meal or intravenous administration of octapeptide of cholecystokinin (CCK-8) is a standard procedure in the evaluation of patients with varieties of gallbladder diseases. When quantitative cholescintigraphy was introduced nearly 30 years ago, 10ng/kg of CCK-8 was infused intravenously over a three minute period and an ejection fraction value of 35% or greater was considered as normal. Intravenous infusion of CCK-8 has become more popular than ingestion of a fatty meal.

Quantitative cholescintigraphy is critical in the evaluation of hepatobiliary diseases [5], and biliary dyskinesia. Since biliary dyskinesia is purely a functional abnormality, traditional method of correlation with other imaging test such as ultrasound does not appear appropriate, and therapeutic outcome studies become critical for assessment of accuracy of diagnostic techniques. We undertook the current study in fairly large number of patients with abdominal pain to find out the therapeutic outcome results by infusing CCK-8 for three minutes. Merit of any diagnostic test depends upon its ability to separate normal subjects from those with the underlying disease [4].

In recent years, much attention has been focused on higher order non linear partial differential equations, known as evolution equations. Such nonlinear equations often occur in the description of chemical and biological phenomena. Their analytical study has been drawing immense interest. In [1], a nonlinear partial differential equation is integrable if all its exact reductions to ordinary differential equations have the Painleve property: that is, to have no movable singularities other than poles.

This approach poses an obvious operational difficulty in finding all exact reductions. The reduction of $u_t = \mu u^2 u_x + Du u_{xx} + Du_x^2$ to Riccati equation was used to find the gallbladder ejection fraction.

2. Notations:

$GBCF$	-	Gallbladder Ejection Fraction
$CCK - 8$	-	Cholecystokinin
β	-	Intensity
φ	-	Arbitrary Function
η	-	Resonances

A	-	Shape Parameter
B	-	Scale Parameter

3. Painleve Analysis:

In [1], a nonlinear partial differential equation is integrable if all its exact reductions to ordinary differential equations have the Painleve property: that is, to have no movable singularities other than poles. This approach poses an obvious operational difficulty in finding all exact reductions. This difficulty was circumvented by [12] by postulating that a partial differential equation has the Painleve property if its solutions are single - valued about a movable singular manifold

$$\varphi(z_1, z_2, \dots, z_n) = 0$$

where φ is an arbitrary function. In other words, a solution $u(z_i)$ of a partial differential equation should have a Laurent - like expansion about the movable singular manifold $\varphi = 0$:

$$u(z_i) = [\varphi(z_i)]^\alpha \sum_{j=0}^{\infty} u_j(z_i) \varphi(z_i)^j \tag{1}$$

where α is a negative integer. The number of arbitrary functions in expansion (1) should be equal to the order of the partial differential equation. Inserting expansion (1) into the targeted equation yields a recurrence formula that determines $u_n(z_i)$ for all $n > 0$, except for a finite number of $r_1, r_2, \dots, r_j > 0$, called resonances. For some

equations, the recurrence formulas at the resonance values may result in constraint equations for the movable singular manifold which implies that it is no longer completely arbitrary. In such cases, one can say that the equation has the Conditional Painleve Property [6]. The Painleve property is a sufficient condition for the integrability or solvability of equations. Meanwhile, various authors have applied this approach to other nonlinear partial differential equations to decide whether or not these equations are integrable. Recent investigations of [2] regarding the Painleve analysis also yield a systematic procedure for obtaining special solutions when an equation possesses only the conditional Painleve property. From [3] proposed the nonlinear diffusion equation

$$u_t = D u_{xx} + \beta u(1 - u) \tag{2}$$

as a model for the propagation of a mutant gene with an advantageous selection of intensity β . From [6] has considered the extended form of equation (2) as

$$u_t = \beta u^p(1 - u^q) + D(u^m u_x)_x \tag{3}$$

For Painleve analysis and obtained special solutions for various cases of p, q and m .

In this paper we consider

$$u_t = \beta u^p(1 - u^q) + \mu u^s u_x + D(u^m u_x)_x \tag{4}$$

This is a generalization of (3) for the Painleve analysis. This equation has several interesting limiting cases which have already been studied:

- (i) When $\mu = m = 0, p = 1$ and $q \neq 0$, equation (4) is reduced to the generalized Fisher equation. For $q = 1$, equation (4) reduces to the Fisher equation and for $q = 2$, (4) reduces to the Newell Whitehead equation.
- (ii) If we take $\beta = m = 0$, then equation (4) is reduced to the generalized Burgers equation. With $s = 1$ and $\beta = m = 0$, equation (4) gives the Burgers equation, which describes the far field of wave propagation in nonlinear dissipative systems [13].
- (iii) When $m = 0, p = 1$ and $q = s$, equation (4) is reduced to the generalized Burger - Fisher equation [11].

The behavior of solutions of equation (4) at a movable singular manifold,

$$\varphi(x, t) = 0$$

is determined by a leading order analysis where by one makes the substitution

$$u(x, t) = u_0(x, t)[\varphi(x, t)]^\alpha \tag{5}$$

and balances the most singular or dominant terms. Substituting (5) into (4), we obtain three possible values for α as follows:

Case (i):

$p + q > m \geq s$: Balancing the dominant terms $u^{p+q}, \mu u^{m-1} u_x^2$ and $u^m u_{xx}$, we obtain

$$\alpha = -2/(p + q - m - 1) \tag{6}$$

and

$$\beta u_0^{p+q-m-1} = 2D(p + q + m + 1)\varphi_x^2/(p + q - m - 1)^2$$

Case (ii):

$p + q > s > m = 0$: Balancing the dominant terms u^{p+q} and $u^s u_x$, we obtain

$$\alpha = -1/p + q - s - 1$$

and

$$\beta u_0^{p+q-s-1} = (-\mu/p + q - s - 1)\varphi_x$$

For $p + q = -m + 2s + 1 > s > m$,

$$\alpha = -1/(s - m) \tag{7}$$

Here we have two branches for u_0 as follows:

Branch (i): $u_0 = -(k + 1)\varphi_x$ & Branch (ii): $u_0 = k\varphi_x$ where $k = 1, 2, 3, \dots$

$$m = ((2k + 1)^2 - 9)/4 \text{ and } \beta = \mu = D = 1 \tag{8}$$

Case (iii):

$s > m \geq p + q$: Balancing the dominant terms $u^s u_x$, $\mu u^{m-1} u_x^2$ and $u^m u_{xx}$, we obtain

$$\alpha = -1/(s - m)$$

and

$$u_0^{s-m} = (D/\mu)((1 + s)/(s - m))\varphi_x \tag{9}$$

We have the following lemma as a result.

Lemma:

For all combinations of integer values of p, q, m and s , the leading order singularity of equation (4) is

- (i) A movable pole for all combinations with $(p + q - m - 1)$ is equal to 1 or 2 for case (i), with $(p + q - s - 1)$ being equal to 1 for case (ii), and with $s - m$ being equal to 1 for case (iii).
- (ii) A rational branch point for all combinations with $(p + q - m - 1) > 2$ for case (i), $(p + q - s - 1) > 1$ for case (ii) and $s - m > 1$ for case (iii).

The powers of φ , at which the arbitrary coefficient appears in the series, that is, the resonances are determined by setting

$$u(x, t) = u_0(x, t)(\varphi(x, t))^\alpha + p(\varphi(x, t))^{\alpha+r}$$

and balancing the most singular terms of equation (4) again. We obtain for case (i), using the value of α given by (6),

$$p\{(r + \alpha)^2 + (2m\alpha - 1)(r + \alpha)[m\alpha(\alpha - 1) + m(m - 1)\alpha^2 - 2(p + q)(p + q + m + 1)/(p + q - m - 1)^2]\} = 0$$

with solutions

$$r = -1, \quad 2[1 - \alpha(m + 1)]$$

However, for case (ii), with value α given in (7) and for a particular value of m given by (8), we obtain for branch (i)

$$p\{(2m\alpha(r + \alpha) + \alpha^2 m(m - 1) + (r + \alpha)(r + \alpha - 1) + \alpha(\alpha - 1)m) - (s\alpha + (r + \alpha))(k + 1) - (-m + 2s + 1)(k + 1)^2\} = 0$$

with solutions

$$r = -1, \quad (k + 3) - 2\alpha(m + 1)\}$$

and for branch (ii)

$$p\{(2m\alpha(r + \alpha) + \alpha^2m(m - 1) + (r + \alpha)(r + \alpha - 1) + \alpha(\alpha - 1)m) + (s\alpha + (r + \alpha))k + (-m + 2s + 1)k^2\} = 0$$

with solutions

$$r = -1 \ \& \ (2 - k) - 2\alpha(m + 1)$$

For case (iii), we get

$$p\{r^2 + r(2\alpha(m + 1)) - r + \alpha^2(1 + m)^2 - \alpha(1 + m) + \alpha s(r + \alpha)u_0^{s-m}\} = 0$$

with solutions

$$r = -1 \ \& \ -\alpha(1 + s) \tag{10}$$

By using the above lemma, we consider the following cases;

- (i) $m = 0, s = 0, p = 1, q = 2$
- (ii) $m = 0, s = 1, p = 1, q = 2$
- (iii) $m = 0, s = 1, p = 0, q = 0$
- (iv) $m = 1, s = 2, p = 0, q = 0$
- (v) $m = 2, s = 3, p = q = 1,$

In which equation (4) has a movable pole as leading order singularity, and therefore, it may have a valid Laurent Expansion.

Now consider the case (iv): Equation (4) with $m = 1, s = 2, p = q = 0$

In this case, equation (4) becomes

$$u_t = \mu u^2 u_x + D u u_x + D u_x^2 \tag{11}$$

Using (9) and (10), we obtain

$$u_0 = (3D/\mu)\varphi_x$$

and the resonances are $r = -1$ and 3 . Hence, we take the Laurent expansion of the form

$$u = u_0\varphi^{-1} + u_1 + u_2\varphi + u_3\varphi^2 \tag{12}$$

Substituting (12) into (11) and collecting coefficients of equal powers of φ , we have

$$\begin{aligned} \varphi^{-4}: \quad u_0 &= (3D/\mu) \\ \varphi^{-3}: \quad u_1 &= 0 \\ \varphi^{-2}: \quad u_2 &= (-1/3D)\sigma_t \\ \varphi^{-1}: \quad 0Xu_3 &= 0 \end{aligned} \tag{13}$$

Equation (13) shows that u_3 is an arbitrary function. Therefore (11) possesses the Painleve property.

4. Reduction of $u_t = \mu u^2 u_x + D u u_x + D u_x^2$ to Riccati Equation:

Let $u = f(z)$, where

$$z = x - ct \tag{14}$$

Substituting (14) into (11) with $\mu = D = 1$ we obtain

$$cf' + f^2 f' + f f'' + f'^2 = 0 \tag{15}$$

Integrating (15) once, we get

$$f' = -(c + (f^2/3)) \tag{16}$$

Equation (16) is a Riccati Equation, which can be linearized through the transformation

$$f = 3y'/y \tag{17}$$

Substituting (17) into (16), we get

$$y'' = (-c/3)y(z) \tag{18}$$

which is a second order linear differential equation. Solving (18), we obtain

$$y(z) = A \cos \sqrt{(c/3)}z + B \sin \sqrt{(c/3)}z \tag{19}$$

Using (19) then (17) becomes

$$f(z) = \sqrt{3c} \left(\frac{-A \sin \sqrt{(c/3)}z + B \cos \sqrt{(c/3)}z}{A \cos \sqrt{(c/3)}z + B \sin \sqrt{(c/3)}z} \right) \tag{20}$$

5. Example:

Total of 140 subjects (113 women, 27 men) with a mean age of 46 years were selected retrospectively from a list of 444 patients. Hepatic extraction fraction and excretion half-time were determined as described [5]. Differential hepatic bile flow into gallbladder versus small intestine was calculated by dividing the total gallbladder counts by the sum of gallbladder and small intestinal counts at 60 minutes after radiotracer injection. Gallbladder phase study was obtained separately between 61 to 90 minutes by collecting data on the same size computer matrix at one frame/minute. Octapeptide of cholecystokinin (CCK-8), 10ng/kg, was infused over three minutes through an infusion pump, infusion beginning at 65 minutes after radiotracer injection (Figure 1). Gallbladder ejection fraction (GBEF) was calculated in the standard fashion [4] & [7-10].

Figure 1: In a normal subject, the gallbladder empties with an ejection fraction of 59%

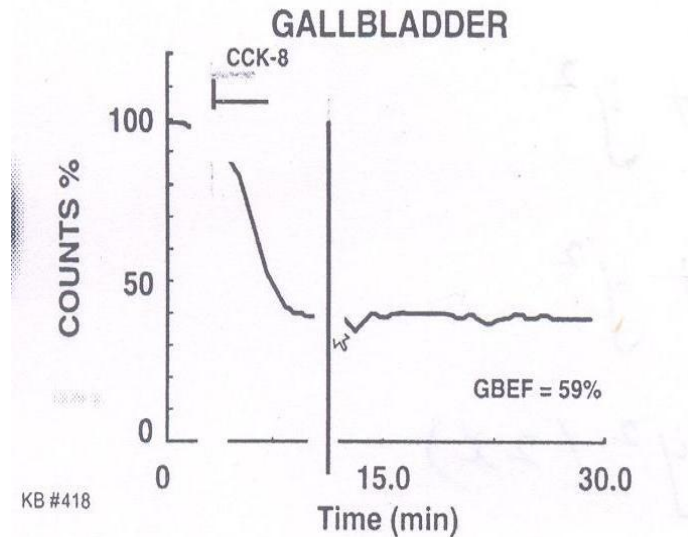
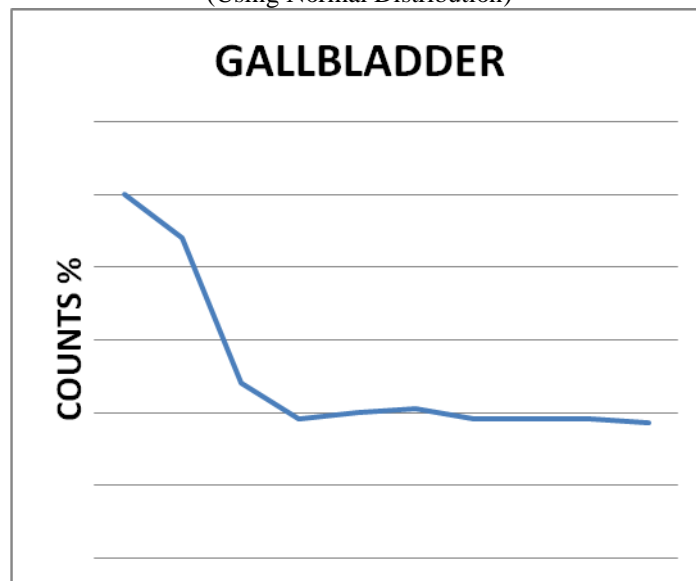


Figure 2: In a normal subject, the gallbladder empties with an ejection fraction of 59% (Using Normal Distribution)



6. Conclusion:

3 minute infusion of 10ng/kg of CCK-8 and a cut off value of 35% as the lower limit of GBEF carries a sensitivity of 95%, specificity of 89% with an overall accuracy of 92% in the evaluation of patients with chronic acalculous cholecystitis (CAC). Excellent therapeutic outcome was achieved in CAC patients with laparoscopic cholecystectomy, performed solely on the basis of low ejection fraction; gallbladder ejection fraction with three minute intravenous infusion of 10ng/kg CCK-8 carries both high sensitivity and specificity and clearly separates normal gallbladder from those patients with CAC. The test is simple and reliable. This model is fairly fitted with the non linear diffusion equation by using normal distribution. The medical report {Figure (1)} is beautifully fitted with the mathematical model {Figure (2)}; (i.e) the results coincide with the mathematical and medical report.

7. References:

- [1] Ablowitz M J, Ramani A & Segur H, "A Connection between Nonlinear Evolution Equations and Ordinary Differential Equations of P-type I", *Journal of Math. Physics*, 21, 715-721, 1980.
- [2] Cariello F & Tabor M, "Painleve Expansions for non integrable Evolution Equations", *Physica D*, 39, 77-94, 1989.
- [3] Fisher R A, "The wave of Advance of Advantages Genes", *Ann. Engenics* 7, 355-369, 1937.
- [4] Gerbail T Krishnamurthy & Shakuntala Krishnamurthy, "Diagnostic Reliability of Gallbladder Ejection Fraction", *IJNM*, 13-17, 2002.
- [5] Krishnamurthy G T & Krishnamurthy Ss, "A Text Book of Hepatobiliary Diseases", New York, Springer, 2000.
- [6] Roy Choudhury S, "Painleve Analysis and Partial Integrability of a Class of Reaction Diffusion Equations", *Nonlinear Analysis, TMA* 18, 445-459, 1992.
- [7] Senthil Kumar P & Umamaheswari N, "Stochastic Model for the Box Cox Power Transformation and Estimation of the Ex-Gaussian Distribution of Cortisol Secretion of Breast Cancer due to Smoking People", *Antarctica Journal of Mathematics*, Volume 11, 99-108, 2014.
- [8] P. Senthil Kumar, A. Dinesh Kumar & M. Vasuki, "Stochastic Model to find the Gallbladder Motility in Acromegaly Using Exponential Distribution", *International Journal of Engineering Research and Applications (IJERA)*, Volume 4, Issue 8 (Version 2), August 2014, Page Number 29-33.
- [9] P. Senthil Kumar, A. Dinesh Kumar & M. Vasuki, "Stochastic Model to Find the Gallbladder Dynamics with Gallstones Results Using Exponential Distribution", *IFRSA's International Journal of Computing (IJC)*, Volume 4, Issue 3, July 2014, Page Number 619-622.
- [10] P. Senthil Kumar, A. Dinesh Kumar & M. Vasuki, "Stochastic Stochastic Model to Find the Multidrug Resistance in Human Gallbladder Carcinoma Results Using Uniform Distribution", *International Journal Emerging Engineering Research and Technology (IJERT)*, Volume 2, Issue 4, July 2014, Page Number 416-421.
- [11] Wang X Y, Zhu Z S & Lu Y K, "Solitary Wave Solutions of the Generalized Burgers- Huxley Equation", *J. Phys. A: Math. Gen.* 23, 271-274, 1990.
- [12] Weiss J, Tabor M & Carnevale G, "The Painleve Property for Partial Differential Equations", *J. Math. Phys.* 24, 522-526, 1983.
- [13] Whitham G B, "Linear and Nonlinear Waves", Wiley, New York, 1974.

Vehicle Theft Intimation Using GSM

¹, Minakshi Kumari, ², Prof. Manoj Singh

^{1,2}, Computer Science and Engineering (Information Security)
Disha institute of Management and Technology Raipur, India

ABSTRACT:

This project uses a wireless technology for automobiles using GSM modem. With the help of GSM modem, we can stop the automobile engine when someone tries to steal the vehicle. When unauthorised person tries to unlock the door of car, then a programmable microcontroller 8051 gets an interrupt and order to GSM modem to send a SMS. GSM modem that stores owner's number upon a miss call for the first time sends an alert SMS to that authorized number. If owner reply to "stop the engine" then the control instruction is given to the microcontroller through interface that the output from which activates a relay driver to trip the relay that disconnects the ignition of the automobile resulting in stopping the vehicle.

Keywords - Step down transformer 230/12V, Bridge Rectifier, Voltage Regulator 7805, Microcontroller 8051 and GSM modem.

I. INTRODUCTION

GSM (Global System for Mobile communications) is an open, digital cellular technology used for transmitting mobile voice and data services. GSM differs from first generation wireless systems in that it uses digital technology and Time Division Multiple Access (TDMA) transmission methods. GSM is a circuit-switched system that divides each 200kHz channel into eight 25kHz time-slots. GSM operates in the 900MHz and 1.8GHz bands in Europe and the 1.9GHz and 850MHz bands in the US. The 850MHz band is also used for GSM and 3GSM in Australia, Canada and many South American countries. GSM supports data transfer speeds of upto 9.6 kbit/s, allowing the transmission of basic data services such as SMS (Short Message Service). Another major benefit is its international roaming capability, allowing users to access the same services when travelling abroad as at home. This gives consumers seamless and same number connectivity in more than 210 countries. GSM satellite roaming has also extended service access to areas where terrestrial coverage is not available Global System for Mobile Communications. The first European digital standard, developed to establish cellular compatibility throughout Europe.

It's success has spread to all parts of the world and over 80 GSM networks are now operational. It operates at 900 MHz.

- GSM stands for **G**lobal **S**ystem for **M**obile **C**ommunication and is an open, digital cellular technology used for transmitting mobile voice and data services.
- The GSM emerged from the idea of cell-based mobile radio systems at Bell Laboratories in the early 1970s.
- The GSM is the name of a standardization group established in 1982 to create a common European mobile telephone standard.
- The GSM standard is the most widely accepted standard and is implemented globally.
- The GSM is a circuit-switched system that divides each 200kHz channel into eight 25kHz time-slots. GSM operates in the 900MHz and 1.8GHz bands in Europe and the 1.9GHz and 850MHz bands in the US.
- The GSM is owning a market share of more than 70 percent of the world's digital cellular subscribers.
- The GSM makes use of narrowband Time Division Multiple Access (TDMA) technique for transmitting signals.
- The GSM was developed using digital technology. It has an ability to carry 64 kbps to 120 Mbps of data rates.
- Presently GSM supports more than one billion mobile subscribers in more than 210 countries throughout the world.

- The GSM provides basic to advanced voice and data services including Roaming service. Roaming is the ability to use your GSM phone number in another GSM network.

Throughout the evolution of cellular telecommunications, various systems have been developed without the benefit of standardized specifications. This presented many problems directly related to compatibility, especially with the development of digital radio technology. The GSM standard is intended to address these problems.

From 1982 to 1985 discussions were held to decide between building an analog or digital system. After multiple field tests, a digital system was adopted for GSM. The next task was to decide between a narrow or broadband solution. In May 1987, the narrowband time division multiple access (TDMA) solution was chosen.

1. GSM Modem



Fig 1. GSM Modem

Global system for mobile communication (GSM) is a globally accepted standard for digital cellular communication. GSM is the name of a standardization group established in 1982 to create a common European mobile telephone standard that would formulate specifications for a pan-European mobile cellular radio system operating at 900 MHz. A GSM modem is a wireless modem that works with a GSM wireless network. A wireless modem behaves like a dial-up modem. The main difference between them is that a dial-up modem sends and receives data through a fixed telephone line while a wireless modem sends and receives data through radio waves. The working of GSM modem is based on commands, the commands always start with AT (which means ATtention) and finish with a <CR> character. For example, the dialing command is ATD<number>; ATD3314629080; here the dialing command ends with semicolon. The AT commands are given to the GSM modem with the help of PC or controller. The GSM modem is serially interfaced with the controller with the help of MAX 232.

II. NEW APPROACHES

Recently, a GPS based system is use for automobile security. This GPS system helps to find out the exact location of the vehicle and find out the direction of the vehicle. This system uses geographic position and time information from the Global Positioning Satellites. The system has an "On-Board Module" which resides in the vehicle to be tracked and a "Base Station" that monitors data from the various vehicles. But this system is not able to give protection to the vehicle. To overcome this problem, a GSM Modem based project introduced in this security system. The main aim of this project is to use a wireless technology for automobiles using GSM modem. The main scope of this project is to stop the automobile engine with the help of GSM modem when any person tries to steal the vehicle. When unauthorised person tries to unlock the door of car, then a programmable microcontroller 8051 gets an interrupt and order to GSM modem to send a sms. GSM modem that stores owner's number upon a miss call for the first time, sends an alert sms to that authorized number. If owner reply to "stop the engine" then the control instruction is given to the microcontroller through interface that the output from which activates a relay driver to trip the relay that disconnects the ignition of the automobile resulting in stopping the vehicle.

Global usage: Originally GSM had been planned as a European system. However the first indication that the success of GSM was spreading further afield occurred when the Australian network provider, Telstra signed the GSM Memorandum of Understanding.

Frequencies: GSM networks operate in a number of different carrier frequency ranges (separated into GSM frequency ranges for 2G and UMTS frequency bands for 3G), with most 2G GSM networks operating in the 900 MHz or 1800 MHz bands. Where these bands were already allocated, the 850 MHz and 1900 MHz bands were used instead (for example in Canada and the United States). In rare cases the 400 and 450 MHz frequency bands are assigned in some countries because they were previously used for first-generation systems. Most 3G networks in Europe operate in the 2100 MHz frequency band. For more information on worldwide GSM frequency usage, see GSM frequency bands. Regardless of the frequency selected by an operator, it is divided into timeslots for individual phones. This allows eight full-rate or sixteen half-rate speech channels per radio frequency. These eight radio timeslots (or burst periods) are grouped into a TDMA frame. Half-rate channels use alternate frames in the same timeslot. The channel data rate for all 8 channels is 270.833 kb/s, and the frame duration is 4.615 ms. The transmission power in the handset is limited to a maximum of 2 watts in GSM 850/900 and 1 watt in GSM 1800/1900.

III. GSM NETWORK

The network architecture of GSM can be broadly divided into these main areas –

- Mobile station
- Base-station subsystem
- Network and switching subsystem
- Operation and support subsystem.

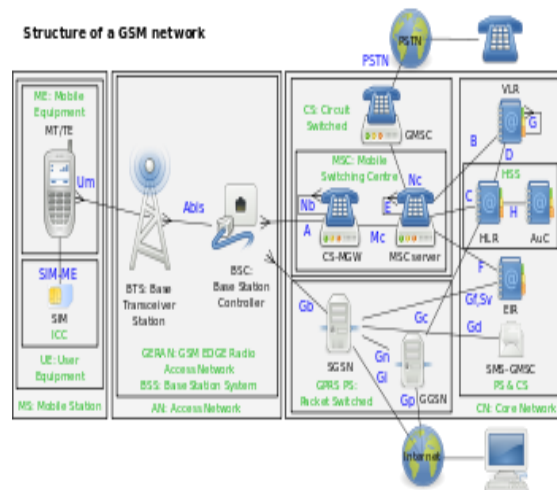


Fig 3.GSM Network

GSM is a cellular network, which means that cell phones connect to it by searching for cells in the immediate vicinity. There are five different cell sizes in a GSM network—macro, micro, pico, femto, and umbrella cells. The coverage area of each cell varies according to the implementation environment. Macro cells can be regarded as cells where the base station antenna is installed on a mast or a building above average rooftop level. Micro cells are cells whose antenna height is under average rooftop level; they are typically used in urban areas. Picocells are small cells whose coverage diameter is a few dozen metres; they are mainly used indoors. Femtocells are cells designed for use in residential or small business environments and connect to the service provider’s network via a broadband internet connection. Umbrella cells are used to cover shadowed regions of smaller cells and fill in gaps in coverage between those cells.

Cell horizontal radius varies depending on antenna height, antenna gain, and propagation conditions from a couple of hundred metres to several tens of kilometres. The longest distance the GSM specification supports in practical use is 35 kilometres (22 mi). There are also several implementations of the concept of an extended cell, where the cell radius could be double or even more, depending on the antenna system, the type of terrain, and the timing advance. Indoor coverage is also supported by GSM and may be achieved by using an indoor picocell base station, or an indoor repeater with distributed indoor antennas fed through power splitters, to deliver the radio signals from an antenna outdoors to the separate indoor distributed antenna system. These are typically deployed when significant call capacity is needed indoors, like in shopping centers or airports. However, this is not a prerequisite, since indoor coverage is also provided by in-building penetration of the radio signals from any nearby cell.

IV. SPECIFICATIONS OF GSM

The GSM specification is listed below with important characteristics.

A. Modulation:

Modulation is a form of change process where we change the input information into a suitable format for the transmission medium. We also changed the information by demodulating the signal at the receiving end. The GSM uses Gaussian Minimum Shift Keying (GMSK) modulation method.

B. Access Methods:

GSM chose a combination of TDMA/FDMA as its method. The FDMA part involves the division by frequency of the total 25 MHz bandwidth into 124 carrier frequencies of 200 kHz bandwidth. One or more carrier frequencies are then assigned to each BS. Each of these carrier frequencies is then divided in time, using a TDMA scheme, into eight time slots. One time slot is used for transmission by the mobile and one for reception. They are separated in time so that the mobile unit does not receive and transmit at the same time.

C. Transmission Rate:

The total symbol rate for GSM at 1 bit per symbol in GMSK produces 270.833 K symbols/second. The gross transmission rate of the time slot is 22.8 Kbps. GSM is a digital system with an over-the-air bit rate of 270 kbps.

D. Frequency Band:

The uplink frequency range specified for GSM is 933 - 960 MHz (basic 900 MHz band only). The downlink frequency band 890 - 915 MHz (basic 900 MHz band only).

E. Channel Spacing:

This indicates separation between adjacent carrier frequencies. In GSM, this is 200 kHz.

F. Speech Coding:

GSM uses linear predictive coding (LPC). The purpose of LPC is to reduce the bit rate. The LPC provides parameters for a filter that mimics the vocal tract. The signal passes through this filter, leaving behind a residual signal. Speech is encoded at 13 kbps.

G. Duplex Distance:

The duplex distance is 80 MHz. Duplex distance is the distance between the uplink and downlink frequencies. A channel has two frequencies, 80 MHz apart.

H. Misc:

- Frame duration: 4.615 ms
- Duplex Technique: Frequency Division Duplexing (FDD) access mode previously known as WCDMA.
- Speech channels per RF channel: 8.

V. COMPARISONS:

	GPS based System	Vehicle Theft Intimation Using GSM Modem
Definition	GPS stands for "Global positioning System". It is a satellite-based navigation system that was developed by the United States Department of Defence.	It is a specification of wireless network infrastructure. The system has been developed by the European Telecommunications Standards Institute.
Technology	Triangulation to at least three or four of the 24 satellites that orbit the earth.	An object's position is determined using signal strength and triangulation from base stations.

Features	GPS system helps to find location and tracking of the vehicle	This project can stop the vehicle when unauthorised person tries to steal the vehicle.
Vehicle Tracking	Digital maps, etc. are used to track the location in real time.	Phone's international mobile equipment identity number, etc. are used to track the location of a vehicle.
Accuracy	Comparatively difficult in area surrounded by tall buildings.	Base stations are capable of providing locations in areas like tunnel and dense areas.
Advantage	<ul style="list-style-type: none"> • Provides the exact location • Provides the exact latitude and longitude • Helps in searching the local area for nearby amenities • Assists in improving the accuracy for weather forecasts. 	<ul style="list-style-type: none"> • World wide roaming • The facilities of GSM are highly protected • Reasonable Devices and Facilities • The GSM expertise usages five bands of MHz rate; 450, 850, 900, 1800 and 1900 MHz.

VI. FUTURE WORK

Vehicle tracking system is becoming increasingly important in large cities and it is more secured than other systems. Now a day's vehicle Stealing is rapidly increasing. Nowadays, GPS tracking system is used in the vehicle. But this security is not enough for security. Due to this reason, this project is introducing the wireless technology effectively for the automotive environments by using the GSM Modem. It is used in sending sms intimation to owner in case of theft of vehicle. When a person trying to steal the vehicle. At that time, programmable microcontroller 8051 gets an interrupt and microcontroller that stores owner's number upon a miss call for the first time, sends an alert sms to that authorized number. When someone tries to steal the car then microcontroller gets an interrupt and orders GSM Modem to send the sms, the owner receives a SMS that his car is being stolen then the owner sends back the SMS to the GSM modem to 'stop the engine', while the vehicle will be stopped. The control instruction is given to the microcontroller through interface, the output from which activates a relay driver to trip the relay that disconnects the ignition of the automobile resulting in stopping the vehicle. This project can be more effective when this is use in bank for security purpose. When unauthorized person tries to unlock bank locker then a security locker which is also available in bank locker automatically get locked. So that theft cannot able to open the bank locker. For this, we can also provide security in the bank.

VII. RESULT AND CONCLUSION

For fast development of the country transportation of men & materials is urgently require. For transportation of men & material in very large amount large numbers vehicle is of high capacity is required .The cost high capacity vehicle is very high .The Chances of theft vehicle is also increased due to high cost of vehicle, non availability of garage ,guards & parking space in the town or city. To stop the theft of the car /vehicle is urgently required for fast movement of the vehicle/car & also to control criminal activity. At present we are using GPS system for tracking the theft vehicle. GPS system is not full prove system for arresting the theft of vehicle or car. It only track the theft vehicle/car after theft.GPS system is also very costly system and needs internet connection for tracking the vehicles.

My project is based on GSM modem, which is a full prove system for arresting the theft of vehicles without using GPS system and internet connection. My system is based on wireless technology. This project is to use wireless technology to intimate the owner of the vehicle about any unauthorized door entry into the vehicle. This is done by sending an auto-generated SMS to the owner. An added advantage of this project is that, the owner can send back the SMS to the system, which will disable the ignition of the vehicle. Theft intimation of the vehicle over SMS using GSM modem by user programmable number upon a miss-call , to the owner, while unauthorized door entry is made in the vehicle. Owner can send command through his mobile to the system to stop the engine by activating the relay interfaced to a microcontroller along with the GSM modem used for the purpose. My system can be used remotely for stoppage the ignition of engine of the vehicles which will completely stop the theft of vehicle .The cost of my GSM modem system is very low in comparison to present GPS system and it is also very handy and light weighted. The circuit of my GSM modem is very simple, which can be repaired very easily. In my GSM modem system, we are providing separate power system through 12v battery. There will be no any connection in my GSM system through car/vehicle battery. It will be a hidden system fitted in the car/vehicles.

REFERENCES

- [1] "GSM Global System for Mobile Communications". 4G Americas. Retrieved 2014-03-22.
- [2] "GSM UMTS 3GPP Numbering Cross Reference". ETSI. Retrieved 30 December 2009.
- [3] Introduction to GSM: Physical Channels, Logical Channels, Network, and Operation by Lawrence Harte.
- [4] GSM Switching, Services and Protocols by Hans-Jorg Vogel, Christian Bettstetter
- [5] An Introduction to GSM (Mobile Communications Library) by Siegmund H. Redl, Matthias Weber, Malcolm W. Oliphant
- [6] GSM Networks: Protocols, Terminology and Implementation (Mobile Communications Library) by Gunnar Heine
- [7] Radio Interface System Planning for GSM/GPRS/UMTS
- [8] Fundamentals of Cellular Network Planning and Optimisation
- [9] GSM, GPRS and EDGE Performance: Evolution Towards 3G/UMTS
- [10] HSDPA/HSUPA for UMTS: High Speed Radio Access for Mobile Communications
- [11] Intelligent Networks for the GSM, GPRS and UMTS Network
- [12] National Research Council (U.S.). Committee on the Future of the Global Positioning System; National Academy of Public Administration (1995). *The global positioning system: a shared national asset: recommendations for technical improvements and enhancements*.
- [13] The Global Positioning System: Assessing National Policies, p.245. RAND Corporation

XML Retrieval: A Survey

Hasan Naderi¹, Mohammad Nazari Farokhi², Nasredin Niazy³,
Behzad Hosseini Chegeni⁴, Somaye Nouri Monfared⁵

¹Department of Computer Engineering, Iran University Science and Technology, Tehran, Iran

^{2, 3, 4, 5} Department of Computer Engineering, Science and Research Branch, Islamic Azad University, Lorestan, Iran

ABSTRACT:

Nowadays in the world of the Internet and the Web, great amounts of information in various forms and different subjects are available to users. The available information can be divided into three categories: structured, unstructured and semi-structured. Information retrieval systems traditionally retrieve information from unstructured text which is a text without marking up. XML retrieval is content-based retrieval of structured documents with XML. The aim of XML retrieval is restoring related parts of an XML document that by exploiting the document structure can respond to users' needs. In this research we will examine the XML retrieval. Moreover, models, challenges and retrieve methods exactly are studied.

Keywords: Cas, Co, ComRank, Inex, Information Retrieval, Trec, XML Retrieval

I. INTROUCTION:

By rapid development of using extensible language and XML development on the Internet, retrieval of XML data has become one of the most interesting research matters. Since the XML documents are increasingly expanding, engines for search and retrieval can be developed into a set of XML documents in order to perform the search. XML documents have not only textual information, but also contain information about the logical structure of the documents. The logical structure in fact is a tree-like structure that is encrypted by the XML labels. In XML retrieval, elements and components of document are retrieved, not the whole document. Content-based retrieval of XML documents over the past few years has been the most highly regarded which mainly has emerged from the NEXI initiative design [1]. The aim of XML retrieval is restoring related parts of an XML document that by exploiting the document structure can respond to users' needs [2]. Information retrieval systems are often inconsistent with relational databases. In XML retrieval, information needs of users determine as queries, includes key phrases and structured points. Structure, specifies XML elements tracks marked in the set from which system should restore the information [3]. In XML documents and texts, structure and content are separable [4]. An information retrieval system in response to a query returns a ranked list of documents. Then, user examine in the linear case each of them that are in a higher rank [5]. Since the numbers of XML components are generally high, it is necessary that users have systems to retrieve XML, so that components of content have become retrieved and reviewed. One approach could involve the use of summarization that is useful in interactive information retrieval. In interactive XML retrieval, a summary can connect by any one of its document parts which has returned via XML retrieval system [6].

II. THE STRUCTURE OF TEXTUAL INFORMATION

Textual information based on the structure can be divided into three categories:

2.1. Unstructured data: unstructured data means raw text, which through of markings and syntactic labels are separated.

2.2. Structured data: structured data is including data that are already defined. In structured data the user can find out exact and specified respond from their needs.

2.3. Semi-structured data: semi-structured data is between structured data and unstructured data and has stronger structure than unstructured data. We need to incorporate structured information in semi-structured data.

III. INEX

INEX is an international association for the study of XML retrieval. Available approaches of XML retrieval for current structure in ranking and scoring elements are related to returning structures in memory and timing parameters. One approach only returns logical elements such as sections and paragraphs in the search results. Another approach allows users to specify their Structural preferences that consist of structural limitations [7]. INEX can be used in connection with the Xpath to retrieve the XML structural tracks based on what the user specifies in the query. On the other hand, by adding the function about () expands its, which this function is used to filter components [8].

In INEX keywords are combined with structural adverbs. Thus, in response to a question, a ranked list of XML components presents that must contain the following conditions:

1. At least comprising one of the keywords.
2. Also has the considered adverbs [4].

3.1. Our track goals at INEX

In INEX any response is studied to a target. Different track goals are as follows [9]:

- ✓ Adhoc Track
- ✓ Language Processing
- ✓ Interactive Track
- ✓ Multimedia Track
- ✓ Use Case Track
- ✓ Entity Ranking
- ✓ Book Search
- ✓ Link The Wiki
- ✓ Question Answering

IV. CO AND CAS

Users' information needs at INEX are expressed in two ways, CAS and CO. CO approach, shows key phrases based on an approach that is typically used for retrieval information on the Internet. CAS approach, is used a combination of structural and textual marks. In recent years, much work has been done in connection with the CAS that as four sub- tasks was implemented in 2005:

4.1. VVCAS: the target element and limitations of the support elements unclearly were studied.

4.2. SVCAS: limitation of target element explicitly was examined but the limitation of support element is vaguely followed.

4.3. VSCAS: target element and limitation of support element were considered vaguely but limitation of support element is explicitly followed.

4.4. SSCAS: Both limitations of the target element and support element are explicitly considered.

If structural remarks are generated in information needs, in order to demonstrate these two marks, two vague or explicit methods are represented [10]. CAS questions can be solved by analyzing the INEX expressions and decide which indexes used in search. The fundamental ways in analysis CAS questions include the vector space model, DMMS and display XML documents by trees [11]. CO questions are suitable for ordinary users with limited programming skills, and users to achieve the desired information do not need to learn the combination of complex questions from before Xquery and Xpath [12].

4.5. CAS questions are identified in three types:

4.5.1. Routes based questions: route based questions are defined based on Xpath queries such as NEXI.

4.5.2. Clause based questions: clause-centric questions are usually developed from Xquery language.

4.5.3. Parts based questions: sections based questions used XML for the retrieval of XML documents [13, 14].

V. COMRANK SYSTEM IN XML RETRIEVAL :

ComRank system is an Intermediary Search system used for automatic ranking in XML retrieval systems [15]. ComRank system have used a free approach for Intermediary Search so that its results obtained from several systems, its main systems have high ranking, furthermore its results are achieved from systems which compared with other systems have better operation [16]. Comrank is alike a voting system based on consensus [17].

VI. TREX:

TREX is an XML retrieval system that can use of several summarized structures including the newly defined. TREX can itself manage great but small features, and thus accelerate the assessment of workload to the TOP-K questions. TREX has three methods of comprehensive retrieval, TA and integration. In TREX, summarized structure and reverse lists which are shown in the two tables are stored as the names of elements and sent lists. Evaluation of a NEXI query in the TREX is performed in the two ways of recovery and interpretation [18]. The TREX function in search engine TOPX is generalization of the markup function [19].

VII. RE IN XML RETRIEVAL

Relevant feedback is a technique that allows users to provide feedback on the initial search. The purpose of relevant feedback is that the user's needs express more precisely. RF approaches are proposed to XML retrieval. These approaches by adding extracted words from whole texts and documents enrich questions [20]. In fact, it can be said that relevant feedback is employed to improve results accuracy including extract keywords from documents. In RF, for ranking components from AQR algorithm, separate indexes for each component are created [22].

VIII. EVALUATION OF XML RETRIEVAL

Evaluation of XML retrieval is determined by the member coverage and subject relevance. Member coverage is defined as follow in four ways:

8.1. Exact coverage (E): The principal subject of component is searching for information which components are also.

8.2. Small coverage (S): The principal subject of component is searching for information, but components are not meaningful units of information.

8.3. Large coverage (L): Seeking information on components is presented, but is not the main issue.

8.4. No coverage (N): searching information is not the components subject.

Also, the dimension of subject relevance has four levels which are as follow:

-Highly relevance with the number 3 is specified.

-Relatively relevance with the number 2 is specified.

-Slightly relevance with the number 1 is specified.

-No relevance with the number 0 is specified.

In subject relevance, components are judged in both dimensions and then judgment is combined in a letter - digits code. The composition of relevance coverage is specifying as follows:

$$Q(\text{rel}, \text{cov}) = \begin{cases} 1.00 & \text{if } (\text{rel}, \text{cov}) = 3E \\ 0.75 & \text{if } (\text{rel}, \text{cov}) \in \{2E, 3L\} \\ 0.50 & \text{if } (\text{rel}, \text{cov}) \in \{1E, 2L, 2S\} \\ 0.25 & \text{if } (\text{rel}, \text{cov}) \in \{1S, 1L\} \\ 0.00 & \text{if } (\text{rel}, \text{cov}) = 0N \end{cases}$$

Formula 1.the compositions of relevant c [23].

2S is a rather relevant part, i.e. it is so small. 2S component provides incomplete information, but answers the question trivially. 3E is a much related component that has much accurate coverage. An unrelated component cannot have precise coverage, so composition of 3N is impossible.

The quantized Q function dose not imposes a dual selection of related / unrelated, and permits to categorize component as low relevance. Some related Components for retrieval set of A are calculated as follows [23].

$$\#(\text{the retrieval relevant cases}) = \sum_{c \in A} Q(\text{rel}(c), \text{cov}(c))$$

Formula 2. relevant components in retrieval set[23].

IX. CHALLENGES IN XML RETRIEVAL:

Challenges in XML retrieval are proposed as follows:

- ✓ parts of the document must be retrieved
- ✓ parts of the document that should be indexed
- ✓ nested element
- ✓ statistical terms
- ✓ heterogeneity model

9.1. Parts of the document must be retrieved

XML retrieval should return the following:

- ✓ parts of documents or XML elements
- ✓ All documents not return

Existing solutions to this challenge is to retrieve documents in a structured way which in fact a system should retrieve the certain part of a document.

9.1. parts of the document that should be indexed

This challenge in the unstructured retrieval, usually is straight, but in structured retrieval has four approaches including of total to detail, of detail to total ,indexing all elements, and lack of interaction in Pseudo-documents . Approach of total to detail is a two-step process that begins with the largest element as a indexing unit, leading to find sub-elements from each element. In this method relevance of a larger element is not necessarily a good predictor of the sub-elements contained in it. The method of detail to total, by considering all of the leaves select the most relevant leaves and expand them into larger units. The approach of indexing all elements, is the most strict approach. In approach of lacking interaction in Pseudo-documents, documents may be meaningless to the user since the units are not contiguous.

9.3. Nested Elements

In this challenge all elements that are small and are not relative leave aside and we keep the elemans which are useful for result.

9.4. Statistical Terms

This challenge has problem in distribution and can be trusted to estimate the frequency distribution of the documents. Calculating the idf term is available solution for the pair of XML documents.

9.5. Heterogeneity Model

It is in two ways of ideal and similar elements in different patterns. In Ideal case, only one model is needed that this model be realized for user. Similar elements are determined in different patterns fall into two different names and different elements in the structure.

X. INDEXING OF XML RETRIEVAL

Several indexing strategies for XML retrieval have been developed as follows:

- ✓ Element-based indexing: allow to each element which based on direct text and generation text, indexing is done. The indexing has one major drawback. Text that appears at the nth logical structure of XML, n-order indexing, thus requiring more index space [24, 25].
- ✓ Only indexing leaf: only allow indexing leaves by the element or elements that are directly related to the leaves.
- ✓ Expanse-axis indexing: text in one continuous element, is used to estimate a statistical expression [26].
- ✓ Selective indexing: includes removal of small elements and selective element type.
- ✓ Distributed indexing: separately for each type of element is created. Ranking model for each indicator separately runs and retrieves a list of ranked elements [22].

XI. RANKING PATTERNS OF XML RETRIEVAL

The ranking patterns are chosen based on indexing strategies and the specific mechanisms, such as expansion and density that at them only leaf elements, are listed. Most of ranking methods create a list of elements with limited or no structural constraints on the associated element in question are ranked.

Distribution or publication of scores for ranking items based on the curve of the leaves is used [27]. Then scores are published upwards to the parent. Ranking model should be applied to each indicator separately and retrieve ranked lists of elements [28].

XII. XML RETRIEVAL MODELS

12.1. Language model

This model combine estimations based on the whole text components and the compact expression components, as well as for improving efficiency and recovery, use from appearance a component in document and main text, and duration of that way.

Sigurbjornsson by using a language model, evaluated different indexing strategies and for retrieving elements created four indicators:

- ✓ Indicator element with traditional overlying elements.
- ✓ Length based on the index, in which the elements of a length pre-set threshold crossed over and are just indexing.
- ✓ Index based on Qrel, where elements specified by heading elements to indexing.
- ✓ Section index, which also indexing other unoverlying pages based on structure [30].

12.2. The vector space model (VSM)

Vector space model is the best and most efficient information retrieval models for retrieving unstructured documents [31]. Example of the vector space model is relationship- building tree techniques where the set of document is considered as a tree and documents are under the tree. Question is also a tree, and instead of returning a ranked list of documents from the elements, a ranked list of documents returned [32].

A simple measure of the similarity of the C_q in route search and route of C_d in a document, is the CR similarity function:

$$CR(c_q, c_d) = \begin{cases} \frac{1+|c_q|}{1+|c_d|} & \text{if } c_q \text{ matches } c_d \\ 0 & \text{if } c_q \text{ does not match } c_d \end{cases}$$

Formula 3. vector space model[32].

Where C_q and C_d are the number of the curves in the search path, and the document path respectively. The final score for a document is computed as a variable of the cosine measure that specifies by SIMNOMERGE, and be defined as follows:

$$SIMNOMERGE(q, d) = \sum_{c_k \in B} \sum_{c_l \in B} CR(c_k, c_l) \sum_{t \in V} \text{weight}(q, t, c_k) \frac{\text{weight}(d, t, c_l)}{\sqrt{\sum_{c \in B, t \in V} \text{weight}^2(d, t, c)}}$$

Formula 4. Final score for document[32].

Where V non-structural terms, B the set of all fields of XML and $\text{weight}(q, t, c)$ and $\text{weight}(d, t, c)$ are the weight of terms t in XML field to searching q and document d .

12.3. Models based on okapi

Let nE element, $e = 1, 2, \dots, nE$ are the C set. El is the length of element and the $avel$ is the length of average element. Weight for query term j in document d in the collection c , e element is calculated by the following formula:

$$W_j(e, d, c) = \frac{(K_1 + 1) + f_{e,j}}{k_1 \left((1 - b) + b \frac{el}{avel} \right) + tf_{e,j}} \log \frac{N - df_j + 0.5}{df_j + 0.5}$$

Formula5. Formula okapi[9].

Where $tf_{e,j}$ is equal to the frequency of query terms j in element e , df_j is the frequency of documents for query j and N specifies the number of documents [33].

Okapi to calculate the retrieval rate for an element x in a query q using the following formula:

$$Okapi(q, X) = \sum_{j=1}^q W_{j,x} \frac{(K_1 + 1) + f_{x,j}}{k_1 \left((1 - b) + b \frac{el}{avel} \right) + tf_{e,j}} \times \frac{(k_2 + 1)qt f_j}{k_2 + qt f_j}$$

Formula 6. Okapi for calculating the retrieval rate for an element[9].

Where:

$$W_{j,x} = \log \frac{M - ef_j + 0.5}{pf_j + 0.5}$$

Where q is the length and ef_j is element frequency of the term j [34].

12.4. Logistic regression model

The relevant probability in any document or document component is estimated according to a series of statistic in a set of document for a series of queries into a series of connected scales to statistics.

The probability $P(R | Q, C)$ to the log-odds of relevance $\text{LogO}(R | Q, C)$ can be computed for any two events A and B is a deformation of simple probability $P(A | B) / P(A' | B)$ is as follows:

$$\log O(R|Q, C) = b_0 + \sum_{i=1}^S b_i s_i$$

$$P(R|Q, C) = \frac{e^{\log O(R|Q, C)}}{1 + e^{\log O(R|Q, C)}}$$

Formula 7. Logistic regression model[9].

b_0 is the intercept term, b_i coefficients statistics and S_i is the S series.

XIII. TREE MATCHING IN THE XML RETRIEVAL

Many problems should be examined with retrieval systems in relation to the problem of tree matching and structured search. Documents may be very large in size and when the search is not selective, the response may be composed of many results.

Xml document collection may include documents that are not specifically adapted to the structural search. Therefore, one of the key issues is how to choose the components that are approximately consistent with the limitations of search [35]. Tree matching algorithms are associated with the XML retrieval divided into two main sections. The first section covers the exact algorithms to find all patterns in a database XML. The second part describes and shows in detail approximation algorithm [36]. Branching pattern of the XML existing algorithms can be divided to the two-step algorithms of analysis approaches and one step algorithms of navigation approach. Evaluation of tree matching algorithms and approaches can be done in two ways for evaluating the performance and effectiveness. The exact tree matching approach is directly related to the efficiency while the approximate tree matching is more associated with effective [37].

XIV. CONCLUSION

At first, information retrieval was a matter for medical professionals, law, and library science. Users who worked less in secret, and more were seeking to study in the domain, were limited few via the companies of static documents and linguistic tools. But by appearance the era of information and expand use of the Internet, an abrupt mutation of the users number is developed, in general leading to the importance of discipline.

The World Wide Web and the Internet have brought to us a huge flood of data flow and aspects of life. So, unprecedented demand for efficient techniques to handle the enormous amounts of data is available. Nowadays querying the data and extracting relevant documents, is not enough. Users want to focus more on certain information even the smallest details that are irrelevant. XML that is seemed as semi-structured data, a potential candidate to meet these requirements.

This study is summarized on recent efforts in the field of XML retrieval. Also, the database community presents methods based on the use of traditional database techniques to XML data. Topics of interest include query languages such as SQL and referential data integrity problems. On the other hand, the IR community applies IR standard techniques with some variations to Centralized retrieval on the level of element. Despite some similarities with unstructured text, XML requires special attention, an aspect of determining relationship between the elements of the user's query and methods for its evaluation.

REFERENCES

- [1] N. Fuhr, M. Lalmas, S. Malik, and G. Kazai, *Advances in XML Information Retrieval and Evaluation: 4th International Workshop of the Initiative for the Evaluation of XML Retrieval, INEX 2005, Dagstuhl ... Papers (Lecture Notes in Computer Science)*: Springer-Verlag New York, Inc., 2006.
- [2] R. van Zwol and T. van Loosbroek, "Effective Use of Semantic Structure in XML Retrieval," in *Advances in Information Retrieval*. vol. 4425, G. Amati, C. Carpineto, and G. Romano, Eds., ed: Springer Berlin Heidelberg, 2007, pp. 621-628.
- [3] M. S. Ali, M. P. Consens, and B. Helou, "Improving the Effectiveness of XML Retrieval with User Navigation Models," in *Data Engineering, 2009. ICDE '09. IEEE 25th International Conference on*, 2009, pp. 1584-1587.
- [4] M. P. Consens, G. Xin, Y. Kanza, and F. Rizzolo, "Self Managing Top-k (Summary, Keyword) Indexes in XML Retrieval," in *Data Engineering Workshop, 2007 IEEE 23rd International Conference on*, 2007, pp. 245-252.
- [5] N. Naffakhi and R. Faiz, "Using Bayesian networks theory for aggregated search to XML retrieval," presented at the *Proceedings of the 2nd International Conference on Web Intelligence, Mining and Semantics, Craiova, Romania, 2012*.
- [6] Z. Szlávik, A. Tombros, and M. Lalmas, "Investigating the use of summarisation for interactive XML retrieval," presented at the *Proceedings of the 2006 ACM symposium on Applied computing, Dijon, France, 2006*.
- [7] A. Trotman and B. Sigurbjörnsson, "Narrowed Extended XPath I (NEXI)," in *Advances in XML Information Retrieval*. vol. 349, N. Fuhr, M. Lalmas, S. Malik, and Z. Szlávik, Eds., ed: Springer Berlin Heidelberg, 2005, pp. 16-40.
- [8] A. Trotman and B. Sigurbjörnsson, "NEXI, Now and Next," in *Advances in XML Information Retrieval*. vol. 3493, N. Fuhr, M. Lalmas, S. Malik, and Z. Szlávik, Eds., ed: Springer Berlin Heidelberg, 2005, pp. 41-53.

- [9] S. Pal and M. Mitra, "XML Retrieval: A Survey," Citeseer2007.
- [10] J. Pehcevski, J. Thom, S. M. M. Tahaghoghi, and A.-M. Vercoustre, "Hybrid XML Retrieval Revisited," in *Advances in XML Information Retrieval*. vol. 3493, N. Fuhr, M. Lalmas, S. Malik, and Z. Szlávik, Eds., ed: Springer Berlin Heidelberg, 2005, pp. 153-167.
- [11] L. M. de Campos, J. M. Fernández-Luna, J. F. Huete, and C. Martín-Dancausa, "Managing structured queries in probabilistic XML retrieval systems," *Information Processing & Management*, vol. 46, pp. 514-532, 9//2010.
- [12] W. Yanlong, L. Xinkun, C. Xiangrui, Z. Ying, and Y. Xiaojie, "XML Retrieval with Structural Context Relaxation," in *Emerging Intelligent Data and Web Technologies (EIDWT)*, 2013 Fourth International Conference on, 2013, pp. 747-752.
- [13] S. Amer-Yahia, N. Koudas, Am, I. Marian, D. Srivastava, et al., "Structure and content scoring for XML," presented at the Proceedings of the 31st international conference on Very large data bases, Trondheim, Norway, 2005.
- [14] D. Carmel, Y. S. Maarek, M. Mandelbrod, Y. Mass, and A. Soffer, "Searching XML documents via XML fragments," presented at the Proceedings of the 26th annual international ACM SIGIR conference on Research and development in information retrieval, Toronto, Canada, 2003.
- [15] M. Salem, A. Woodley, and S. Geva, "IR of XML Documents – A Collective Ranking Strategy," in *Advances in XML Information Retrieval*. vol. 3493, N. Fuhr, M. Lalmas, S. Malik, and Z. Szlávik, Eds., ed: Springer Berlin Heidelberg, 2005, pp. 113-126.
- [16] A. Woodley and S. Geva, "ComRank: metasearch and automatic ranking of XML retrieval system," in *Cyberworlds, 2005. International Conference on*, 2005, pp. 8 pp.-154.
- [17] J. A. Aslam and M. Montague, "Models for metasearch," presented at the Proceedings of the 24th annual international ACM SIGIR conference on Research and development in information retrieval, New Orleans, Louisiana, USA, 2001.
- [18] G. Kazai, N. Gövert, M. Lalmas, and N. Fuhr, "The INEX Evaluation Initiative," in *Intelligent Search on XML Data*. vol. 2818, H. Blanken, T. Grabs, H.-J. Schek, R. Schenkel, and G. Weikum, Eds., ed: Springer Berlin Heidelberg, 2003, pp. 279-293.
- [19] M. S. Ali, M. Consens, X. Gu, Y. Kanza, F. Rizzolo, and R. Stasiu, "Efficient, Effective and Flexible XML Retrieval Using Summaries," in *Comparative Evaluation of XML Information Retrieval Systems*. vol. 4518, N. Fuhr, M. Lalmas, and A. Trotman, Eds., ed: Springer Berlin Heidelberg, 2007, pp. 89-103.
- [20] Y. Mass and M. Mandelbrod, "Relevance Feedback for XML Retrieval," in *Advances in XML Information Retrieval*. vol. 3493, N. Fuhr, M. Lalmas, S. Malik, and Z. Szlávik, Eds., ed: Springer Berlin Heidelberg, 2005, pp. 303-310.
- [21] J. Kamps, M. Marx, M. d. Rijke, r. Sigurbj, et al., "Structured queries in XML retrieval," presented at the Proceedings of the 14th ACM international conference on Information and knowledge management, Bremen, Germany, 2005.
- [22] Y. Mass and M. Mandelbrod, "Component Ranking and Automatic Query Refinement for XML Retrieval," in *Advances in XML Information Retrieval*. vol. 3493, N. Fuhr, M. Lalmas, S. Malik, and Z. Szlávik, Eds., ed: Springer Berlin Heidelberg, 2005, pp. 73-84.
- [23] C. D. Manning, P. Raghavan, H. Sch and tze, *Introduction to Information Retrieval*: Cambridge University Press, 2008.
- [24] S. Geva, "GPX – Gardens Point XML IR at INEX 2005," in *Advances in XML Information Retrieval and Evaluation*. vol. 3977, N. Fuhr, M. Lalmas, S. Malik, and G. Kazai, Eds., ed: Springer Berlin Heidelberg, 2006, pp. 240-253.
- [25] H. Tanioka, "A Fast Retrieval Algorithm for Large-Scale XML Data," in *Focused Access to XML Documents*, F. Norbert, K. Jaap, L. Mounia, and T. Andrew, Eds., ed: Springer-Verlag, 2008, pp. 129-137.
- [26] P. Ogilvie and J. Callan, "Hierarchical Language Models for XML Component Retrieval," in *Advances in XML Information Retrieval*. vol. 3493, N. Fuhr, M. Lalmas, S. Malik, and Z. Szlávik, Eds., ed: Springer Berlin Heidelberg, 2005, pp. 224-237.
- [27] Y. Mass and M. Mandelbrod, "Using the INEX Environment as a Test Bed for Various User Models for XML Retrieval," in *Advances in XML Information Retrieval and Evaluation*. vol. 3977, N. Fuhr, M. Lalmas, S. Malik, and G. Kazai, Eds., ed: Springer Berlin Heidelberg, 2006, pp. 187-195.
- [28] J. Lafferty and C. Zhai, "Document language models, query models, and risk minimization for information retrieval," presented at the Proceedings of the 24th annual international ACM SIGIR conference on Research and development in information retrieval, New Orleans, Louisiana, USA, 2001.
- [29] F. Huang, "Using Language Models and Topic Models for XML Retrieval," in *Focused Access to XML Documents*. vol. 4862, N. Fuhr, J. Kamps, M. Lalmas, and A. Trotman, Eds., ed: Springer Berlin Heidelberg, 2008, pp. 94-102.
- [30] B. o. Sigurbjornsson, J. Kamps, and M. de Rijke, "University of Amsterdam at INEX 2005: AdHoc Track," in *Advances in XML Information Retrieval and Evaluation: Fourth Workshop of the INitiative for the Evaluation of XML Retrieval (INEX 2005)*, 2006.
- [31] C. Crouch, A. Mahajan, and A. Bellamkonda, "Flexible Retrieval Based on the Vector Space Model," in *Advances in XML Information Retrieval*. vol. 3493, N. Fuhr, M. Lalmas, S. Malik, and Z. Szlávik, Eds., ed: Springer Berlin Heidelberg, 2005, pp. 292-302.
- [32] T. Schlieder and H. Meuss, "Querying and ranking XML documents," *J. Am. Soc. Inf. Sci. Technol.*, vol. 53, pp. 489-503, 2002.
- [33] T. Wichaiwong and C. Jaruskulchai, "A simple approach to optimize XML Retrieval," in *Computer Information Systems and Industrial Management Applications (CISIM)*, 2010 International Conference on, 2010, pp. 426-431.
- [34] W. Lu, S. Robertson, and A. MacFarlane, "Field-Weighted XML Retrieval Based on BM25," in *Advances in XML Information Retrieval and Evaluation*. vol. 3977, N. Fuhr, M. Lalmas, S. Malik, and G. Kazai, Eds., ed: Springer Berlin Heidelberg, 2006, pp. 161-171.
- [35] M. A. Tahraoui, K. Pinel-Sauvagnat, C. Laitang, M. Boughanem, H. Kheddouci, and L. Ning, "A survey on tree matching and XML retrieval," *Computer Science Review*, vol. 8, pp. 1-23, 2013.
- [36] C. Zhang, J. Naughton, D. DeWitt, Q. Luo, and G. Lohman, "On supporting containment queries in relational database management systems," presented at the Proceedings of the 2001 ACM SIGMOD international conference on Management of data, Santa Barbara, California, USA, 2001.
- [37] S. Al-Khalifa, H. V. Jagadish, N. Koudas, J. M. Patel, D. Srivastava, and W. Yuqing, "Structural joins: a primitive for efficient XML query pattern matching," in *Data Engineering, 2002. Proceedings. 18th International Conference on*, 2002, pp. 141-152.

Prediction System for Reducing the Cloud Bandwidth and Cost

¹G Bhuvaneswari, ² Mr. K.Narayana, ³Erasappa Murali

¹computer Science And Engineering,

²asso.Professor & Hod Cse, Seshachala Institute Technology

³asst.Professor, Sistk, Puttur

ABSTRACT:

In this paper, we present AACK (Anticipating ACKs), a novel end-to-end traffic redundancy elimination (TRE) system, designed for cloud computing customers. Cloud-based traffic redundancy elimination needs to apply a judicious use of cloud resources so that the bandwidth cost reducing is combined with the additional bandwidth cost of traffic redundancy elimination computation and storage would be reduced. AACK's main advantage is its capability of offloading the cloud- server traffic redundancy elimination effort to end-clients, thus minimizing the processing costs induced by the traffic redundancy elimination algorithm. Unlike previous solutions, AACK does not require the server to continuously maintain clients' status. This makes AACK very suitable for pervasive computation environments that combine client mobility and server migration to maintain cloud elasticity. AACK is based on a novel traffic redundancy elimination technique, which allows the client to use newly received packets to identify previously received packet chains, which in turn can be used as reliable predictors to future transmitted packets. We present a fully functional ACK implementation, transparent to all TCP-based applications and net-work devices. Finally, we analyze AACK benefits for cloud users, using traffic traces from various sources.

Keywords: Anticipating ACKs, AACK, Traffic Redundancy Elimination, TCP, TRE

I. INTRODUCTION

Cloud computing provides its customers an economical and convenient anything as a service model, known also as usage-based pricing [3]. Cloud customers pay only for what they actually use resources, storage, and bandwidth, according to their changing needs, utilizing the cloud's scalable and elastic computational capabilities. data transfer costs i.e., bandwidth is an important problem when trying to reduce costs [3]. Consequently, cloud customers, applying a careful use of the cloud's resources, are motivated to use various traffic reduction techniques, in particular traffic redundancy for reducing bandwidth costs.

Traffic redundancy stems from common end-users' activities, such as repeatedly accessing, downloading, uploading (i.e., backup), distributing, and modifying the same or similar information items (documents, data, Web, and video). traffic redundancy elimination is used to eliminate the transmission of redundant content and, there-fore, to significantly reduce the network cost. In most common traffic redundancy elimination solutions, both the sender and the receiver examine and compare signatures of data packets, parsed according to the data content, prior to their transmission. When redundant packets are detected, the sender replaces the transmission of each redundant packet with its strong signature [3–5]. Commercial traffic redundancy elimination solutions are popular at enterprise networks, and involve the deployment of two or more proprietary- protocol, state synchronized middle-boxes at both the intranet entry points of data centers and branch offices, eliminating repetitive traffic between them

In this paper, we are presenting a novel receiver-based end-to-end traffic redundancy elimination solution that depends on the strenght of predictions to eliminate redundant traffic between the cloud and its end-users. In this solution, each receiver observes the incoming traffic redundancy elimination and tries to match its packets with a previously received packet chain or a packet chain of a local file. Using the long- term packets' meta-data information kept locally, the receiver sends to the server predictions that include packets' signatures and easy-to-verify hints of the sender's future data. The sender first examines the hint and performs the traffic redundancy elimination operation only on a hint- match. The purpose of this procedure is to avoid the expensive traffic redundancy elimination computation at the sender side in the absence of traffic redundancy. When redundancy is identified, the sender then sends to the receiver only the ACKs to the predictions, instead of sending the data.

II. RELATED WORK

Several traffic redundancy elimination techniques have been explored in recent years. A protocol - independent traffic redundancy elimination was proposed in [4]. The paper describes a AACK-level traffic redundancy elimination, utilizing the algorithms presented in [3].

Several commercial traffic redundancy elimination solutions described in [6] and [7] have combined the sender-based traffic redundancy elimination ideas of [4] with the algorithmic and implementation approach of [5] along with protocol specific optimizations for middle- boxes solutions. In particular, [6] describes how to get away with three-way handshake between the sender and the receiver if a full state synchronization is maintained.

III. AACK ALGORITHM

For the sake of clarity, we first describe the basic receiver-driven operation of the AACK protocol. Several enhancements and optimizations are introduced in below sections.

A. Receiver Packet Store

AACK uses a new chains scheme, described in Fig. 1, in which packets are linked to other packets according to their last received order. The AACK receiver maintains a packet store, which is a large size cache of packets and their associated metadata. Packet's metadata includes the packet's signature and a (single) pointer to the successive packet in the last received traffic redundancy elimination containing this packet. Caching and indexing techniques are employed to efficiently maintain and retrieve the stored packets, their signatures, and the chains formed by traversing the packet pointers.

B. Receiver Algorithm

Upon the arrival of new data, the receiver computes the respective signature for each packet and looks for a match in its local packet store. If the packet's signature is found, the receiver determines whether it is a part of a formerly received chain, using the packets' metadata. If affirmative, the receiver sends a prediction to the sender for several next expected chain packets. The prediction carries a starting point in the bytes traffic redundancy elimination (i.e., offset) and the identity of several subsequent packets (PRED command).

Proc. 1: Receiver Segment Processing 2 if segment carries payload data then 3 calculate packet

4 if reached packet boundary then
5 activate predAttempt ()
6 end if
7 else if PRED-ACK segment then
8 processPredAck ()
9 activate predAttempt ()
10 end if

Proc. 2: predAttempt ()

8 if received packet matches one in packet store then 9 if foundChain(packet) then
10 prepare PREDs
11 send single TCP ACK with PREDs according to Options free space
12 exit
13 end if
14 else
15 store packet
16 link packet to current chain
17 end if
18 send TCP ACK only

Proc. 3: processPredAck() for all offset \in PRED-ACK do read data from packet
store put data in TCP input buffer end for

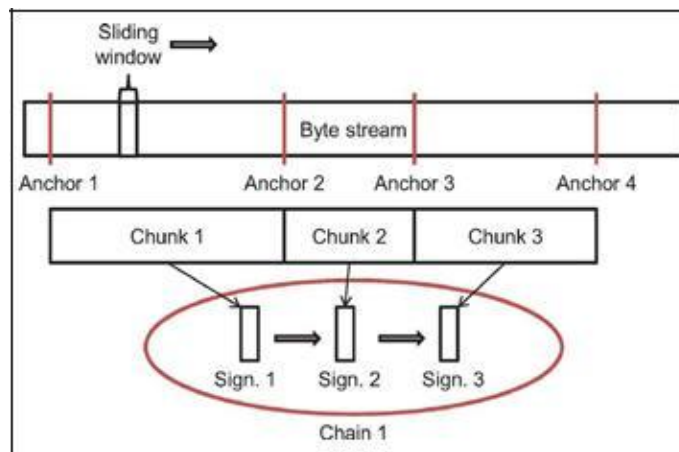


Fig. 1: From S-traffic redundancy elimination to Chain

C. Sender Algorithm

When a sender receives a PRED message from the receiver, it tries to match the received predictions to its buffered (yet to be sent) data. For each prediction, the sender determines the corresponding TCP sequence range and verifies the hint. Upon a hint match, the sender calculates the more computationally intensive SHA-1 signature for the predicted data range and compares the result to the signature received in the PRED message. Note that in case the hint does not match, a computationally expensive operation is saved. If the two SHA-1 signatures match, the sender can safely assume that the receiver's prediction is correct. In this case, it replaces the corresponding outgoing buffered data with a PRED-ACK message.

D. Wire Protocol

In order to conform with existing firewalls and minimize overheads, we use the TCP Options field to carry the AACK wire protocol. It is clear that AACK can also be implemented above the TCP level while using similar message types and control fields.

IV. OPTIMIZATIONS

For the sake of clarity, Section III presents the most basic version of the AACK protocol. In this section, we describe additional options and optimizations.

A. Adaptive Receiver Virtual Window

AACK enables the receiver to locally obtain the sender's data when a local copy is available, thus eliminating the need to send this data through the network. We term the receiver's fetching of such local data as the reception of virtual data.

Proc. 4: predAttemptAdaptive()—obsoletes Proc. 2

1. {new code for Adaptive}
2. if received packet overlaps recently sent prediction then
3. if received packet matches the prediction then
4. predSizeExponent()
5. else
6. predSizeReset()
7. end if
8. end if
9. if received packet matches one in signature cache then
10. if foundChain(packet) then
11. {new code for Adaptive}
12. prepare PREDs according to predSize
13. send TCP ACKs with all PREDs
14. exit
15. end if

16. else
17. store packet
18. append packet to current chain
19. end if
20. send TCP ACK only

B. Cloud Server as a Receiver

In a growing traffic redundancy elimination, cloud storage is becoming a dominant player [13-14]—from backup and sharing services [5] to the American National Library [6], and e-mail services [7-8]. In many of these services, the cloud is often the receiver of the data.

C. Hybrid Approach

AACK's receiver-based mode is less efficient if changes in the data are scattered. In this case, the prediction sequences are frequently interrupted, which, in turn, forces the sender to revert to raw data transmission until a new match is found at the receiver and reported back to the sender. To that end, we present the AACK hybrid mode of operation, described in Proc. 6 and Proc. 7. When AACK recognizes a pattern of dispersed changes, it may select to trigger a sender-driven approach in the spirit of [4], [6-7], and [12].

V. MOTIVATING A RECEIVER-BASED APPROACH.

The objective of this section is twofold: evaluating the potential data redundancy for several applications that are likely to reside in a cloud, and to estimate the AACK performance and cloud costs of the redundancy elimination process.

Our evaluations are conducted using: 1) video traces captured at a major ISP; 2) traffic obtained from a popular social network service; and 3) genuine data sets of real-life workloads. In this section, we relate to an average packet size of 8 KB, although our algorithm allows each client to use a different packet size.

VI. IMPLEMENTATION

In this section, we present AACK implementation, its performance analysis, and the projected server costs derived from the implementation experiments.

Our implementation contains over 25 000 lines of C and Java code. It runs on Linux with Net filter Queue [3]. The AACK implementation architecture. At the server side, we use an Intel Core 2 Duo 3 GHz, 2 GB of RAM, and a WD1600AAJS SATA drive desktop. The clients laptop machines are based on an Intel Core 2 Duo 2.8 GHz, 3.5 GB of RAM, and a WD2500BJKT SATA drive.

A. Server Operational Cost

We measured the server performance and cost as a function of the data redundancy level in order to capture the effect of the TRAFFIC REDUNDANCY ELIMINATION mechanisms in real environment. To isolate the TRAFFIC REDUNDANCY ELIMINATION operational cost, we measured the server's traffic volume and CPU utilization at maximal throughput without operating a TRAFFIC REDUNDANCY ELIMINATION. We then used these numbers as a reference cost, based on present Amazon EC2 [9] pricing. The server operational cost is composed of both the network traffic volume and the CPU utilization, as derived from the EC2 pricing.

B. AACK Impact on the Client CPU

To evaluate the CPU effort imposed by AACK on a client, we measured a random client under a scenario similar to the one used for measuring the server's cost, only this time the cloud server traffic redundancy elimination videos at a rate of 9 Mb/s to each client. Such a speed throttling is very common in real-time video servers that aim to provide all clients with stable bandwidth for smooth view.

C. AACK Messages Format

In our implementation, we use two currently unused TCP option codes, similar to the ones defined in SACK [2]. The first one is an enabling option AACK permitted sent in a SYN segment to indicate that the AACK option can be used after the connection is established. The other one is a AACK message that may be sent over an established connection once permission has been granted by both parties.

VII. CONCLUSION

Cloud computing is expected to trigger high demand for TRAFFIC REDUNDANCY ELIMINATION solutions as the amount of data exchanged between the cloud and its users is expected to dramatically increase. The cloud environment redefines the TRAFFIC REDUNDANCY ELIMINATION system requirements, making proprietary middle -box solutions inadequate. Consequently, there is a rising need for a TRAFFIC REDUNDANCY ELIMINATION solution that reduces the cloud's operational cost while accounting for application latencies, user mobility, and cloud elasticity.

In this paper, we have presented AACK, a receiver-based, cloud-friendly, end - to-end TRAFFIC REDUNDANCY ELIMINATION that is based on novel speculative principles that reduce latency and cloud operational cost. AACK does not require the server to continuously maintain clients' status, thus enabling cloud elasticity and user mobility while preserving long -term redundancy. Moreover, AACK is capable of eliminating redundancy based on content arriving to the client from multiple servers without applying a three-way handshake.

Our evaluation using a wide collection of content types shows that AACK meets the expected design goals and has clear advantages over sender -based TRAFFIC REDUNDANCY ELIMINATION, especially when the cloud computation cost and buffering requirements are important. More-over, AACK imposes additional effort on the sender only when redundancy is exploited, thus reducing the cloud overall cost.

Two interesting future extensions can provide additional benefits to the AACK concept. First, our implementation maintains chains by keeping for any packet only the last observed sub-sequent packet in an LRU fashion. An interesting extension to this work is the statistical study of chains of packets that would enable multiple possibilities in both the packet order and the corresponding predictions. The system may also allow making more than one prediction at a time, and it is enough that one of them will be correct for successful traffic elimination. A second promising direction is the mode of operation optimization of the hybrid sender-receiver approach based on shared decisions de-rived from receiver's power or server's cost changes.

REFERENCES

- [1] E. Zohar, I. Cidon, O. Mokryn, "The power of prediction: Cloud bandwidth and cost reduction", In Proc. SIGCOMM, 2011, pp. 86–97.
- [2] M. Armbrust, A. Fox, R. Griffith, A. D. Joseph, R. Katz, A. Konwinski, G. Lee, D. Patterson, A. Rabkin, I. Stoica, M. Zaharia, "A view of cloud computing", Commun. ACM, Vol. 53, No. 4, pp. 50–58, 2010.
- [3] U. Manber, "Finding similar files in a large file system", in Proc. USENIX Winter Tech. Conf., 1994, pp. 1–10.
- [4] N. T. Spring, D. Wetherall, "A protocol-independent technique for eliminating redundant network traffic", In Proc. SIGCOMM, 2000, Vol. 30, pp. 87–95.
- [5] A. Muthitacharoen, B. Chen, D. Mazières, "A low-bandwidth net-work file system", In Proc. SOSP, 2001, pp. 174–187.
- [6] E. Lev-Ran, I. Cidon, I. Z. Ben-Shaul, "Method and apparatus for reducing network traffic over low bandwidth links", US Patent 7636767, Nov. 2009.
- [7] S. Mccanne and M. Demmer, "Content-based segmentation scheme for data compression in storage and transmission including hierarchical segment representation", US Patent 6828925, Dec. 2004.
- [8] R. Williams, "Method for partitioning a block of data into subblocks and for storing and communicating such subblocks", US Patent 5990810, Nov. 1999.
- [9] Juniper Networks, Sunnyvale, CA, USA, "Application accel-eration", 1996 [Online] Available: <http://www.juniper.net/us/en/products-services/application-acceleration/>
- [10] Blue Coat Systems, Sunnyvale, CA, USA, "MACH5", 1996 [Online] Available: <http://www.bluecoat.com/products/ mach5>

A New Way of Identifying DOS Attack Using Multivariate Correlation Analysis

R Nagadevi¹, P Nageswara Rao², Rameswara Anand³

1(Dept of Cse, Swetha Institute of Technology and Science, Tirupati)

2(Associate Professor & Head, Dept Of Cse, Swetha Institute Of Technology And Science, Tirupati)

3(Professor, Dept of Cse, Swetha Institute Of Technology And Science, Tirupati)

ABSTRACT

This paper talked about the results of MCA on the Distributed DoS detection and suggests an example, a covariance analysis model for detecting SYN flooding attacks. The imitation end results show that this method is highly accurate in detecting malicious system traffic in Distributed DoS attacks of different forces. This technique can effectively distinguish between ordinary and attack traffic. To be sure, this technique can identify even very fine attacks only a little different from normal behaviors. The linear difficulty of the method makes its immediate detection practical. The covariance model in this document to some area verifies the effectiveness of multivariate correlation analysis (MCA) for Distributed DoS detection. Some open problem still exists in this model for further research.

Key words: *Wireless DoS, MCA, malicious node, jammer, learning patterns.*

I. INTRODUCTION

In modern days, securities have been precedence throughout the transmission of data in wireless network, be it through ad hoc, Wi-Fi or wireless sensor network (WSN). As of the reality of hacking and further malicious activities that happen now like any other common day-to-day routine. Due to the growth in technology, wireless networks are coming into reality as they've become more inexpensive and easily reachable through the off-the-shelf machinery. So they are some tools to interrupt these developments. While wireless networks are easy handier for the use of internet in the next to past and future, it is more weak to attacks than wired network.

The broadly known authenticity about the wireless network is its easy accessibility and sharable nature of intermediate. This reality is together the in favor of and cheat when it comes to a wireless network i.e., it is very simple for the competitor to start an attack. This attack can be the disturbance of network functions and flooding the user and kernel buffers. It is termed as Denial of service attack or jamming, depending on whether one looks at the consequence or the cause of attack. A most common example of such an attack is while browsing the internet, the page that is to be unlocked is not catching loaded properly and the refresh push button is clicked a number of times than necessary. This is an example of jamming or the Denial of Service attack that is done accidentally. This attack can also be done purposely. For example, one can use a mobile device to send volume of SMS in hinterland. This is sufficient to block announcement among a few wireless nodes.

In fact, it has happen to extra like a contest between the enemy to attack a network and the security experts to invent efficient techniques to block the attack. The networks have to be able of broadcast of data between the valid nodes irrelevant of the attack encouraged by the enemy. There must not be any intermission between the genuine users. Intimation about the presence of an attacker must be given to the top of the network. It is also not decently and with honesty accepted if the legitimate node/ user communicate with the attacker. On such times the node complicated in such a trick must be recognized and advised of any other ambiguous behavior in the network could cooperate both the network and the data.

Our paper is organized as follows: In section II, we discuss the related theory about the jamming and various techniques. Section III comprises of the system design and proposed system. Section IV describes about the algorithms for Multivariate Correlation Analysis. Section V will conclude the paper.

II. RELATED THEORY

Denial of service attack is mainly done in categorize to block a node from receiving genuine data or to block the node entirely from another genuine node. This blocking is able to be done either with the data sent frequently or by sending radio signal indications or by some other means of transmission signal congestion. Many authors who have discussed about the various congestion techniques and their detection and/ or prevention techniques.

In [1], the authors have analyzed the different types of denial of service attacks and the shown issues due to the DoS attack in all networks. They have provided a number of intrusion detection methods in their survey and have mentioned that there must be system implementation to avoid real world opponent. In all of the congestion techniques and the detection algorithms, throughput is 0 which successfully reduces the performance of the network.

In [2], the authors have detailed about the selective congestion where the opponent chooses the data to squeeze preferentially a high priority data when it concerns protection and privacy. They do so by performing packet classification at the physical layer. The authors have appraised the property of packet hiding by measuring the effective throughput of the

TCP connection in the following states:

1. No packet hiding (N.H.).
2. MAC-layer encryption with a static key (M.E).
3. SHCS (C.S.).
4. Time-lock CPHS (T.P.).
5. Hash-based CPHS (H.P.).
6. Linear AONT-HS (L.T.).
7. AONT-HS based on the package transform.

In [3], data forwarding without any delay in the defending congestion in a wireless sensor network is proposed. This offer consists of sensor nodes as clusters used for a exacting frequency rate. Now when a frequency rate where data promoting occurs is blocked, the cluster of sensor nodes in to frequency turn into inoperative and the other clusters act as backup.

[4] Discusses the system of game theory. This Game theory method offers powerful tools to form and evaluate such attacks. This technique talked about a class of such congestion games played at the MAC layer among a set of transmitters and squeezers. The stability strategies ensuing from these congestion games characterize the expected performance under DoS attacks and motivate robust network protocol design for secure wireless communications. A key characteristic of the distributed wireless access networks is that users do not have complete information regarding the other user's character, the traffic lively, the control channel characteristics, or the rates and rewards of other clients.

The whole detection process consists of three major steps as shown in Fig. 1. Step 1: The basic features are generated from ingress network traffic to the internal network where protected servers reside in and are used to form traffic records for a well-defined time period. Observing and analyzing at the destination network diminish the overhead of detecting cruel activities by concentrating only on related inbound traffic. This as well allows our detector to give protection which is the best fit for the targeted internal network because legitimate traffic profiles used by the detectors are developed for a smaller number of network services. Step 2: Multivariate Correlation Analysis, in which the "Triangle Area Map Generation" module is applied to extract the correlations between two distinct features within each traffic record coming from the first step or the traffic record normalized by the "Feature Normalization" module in this step (Step 2). The occurrence of network intrusions cause changes to these correlations so that the changes can be used as indicators to identify the intrusive activities. All the removed relationships, that is to say triangle areas lay up in Triangle Area Maps (TAMs), are then used to replace the original

Basic features or the standardized features to represent the traffic report. This provides higher discriminative information to differentiate between legitimate and illegal traffic reports. Our MCA method and the quality normalization technique are explained in Sections 3 and 5 respectively. Step 3: The anomaly-based detection mechanism is adopted in result creation. It makes easy the detection of any DoS attacks without requiring any attack related knowledge. Also, the manual attack analysis and the frequent update of the attack signature database in the case of misuse-based detection are avoided. Meanwhile, the mechanism enhances the robustness of the proposed detectors and makes them harder to be evaded because attackers need to generate attacks that match the normal traffic profiles built by a specific detection algorithm. This, however, is a manual task and needs expertise in the targeted detection algorithm. Particularly, two phases (i.e., the "Training Phase"

and the “Test Phase”) are involved in Decision Making. The “Normal Profile Generation” module is operated in the “Training Phase” to generate profiles for various types of legitimate traffic records, and the generated normal profiles are stored in a database. The “Tested Profile Generation” module is used in the “Test Phase” to build profiles for individual observed traffic documentation. Next, the tested profiles are passed over to the “Attack Detection” section, which evaluates the individual tested profiles with the own stored normal profiles. A threshold-based classifier is employed in the “Attack Detection” section module to distinguish DoS attacks from legitimate traffic.

III. MULTIVARIATE CORRELATION ANALYSIS

DoS attack traffic behaves differently from the legitimate network traffic and the behavior of network traffic is reflected by its geometric assets. To well describe these statistical properties, here a novel Multivariate Correlation Analysis (MCA) moves toward in this section. This MCA approach use triangle area for remove the correlative data between the features within an observed data object (i.e., a traffic record).

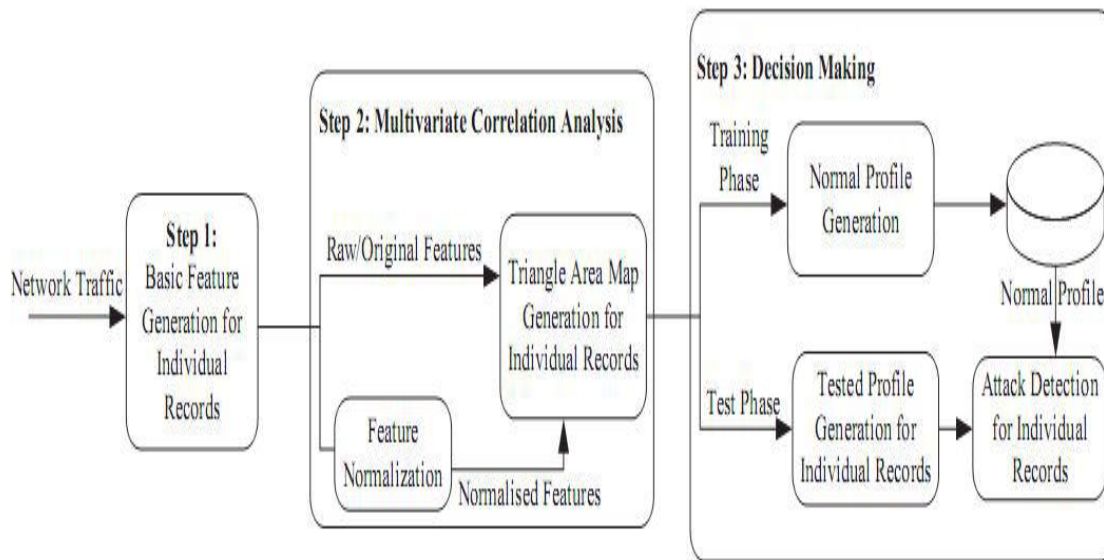


Figure 1: SYSTEM ARCHITECTURE

IV. DETECTION MECHANISM

In this section, we present a threshold-based on anomaly detector, whose regular profiles are produced using purely legal network traffic records and utilized for future comparisons with new incoming investigated traffic report. The difference between a fresh arriving traffic record and the individual normal outline is examined by the planned detector. If the difference is greater than a pre-determined threshold, then the traffic record is colored as an attack. If not, it is marked as a legal traffic record. Clearly, normal profiles and threshold points have direct power on the performance of a threshold-based detector. A low down quality normal shape origins an mistaken characterization to legitimate network traffic. Thus, we first apply the proposed triangle area- based MCA approach to analyze legitimate network traffic, and the created TAMs be then used to supply quality features for normal profile generation.

4.1 Normal Profile Generation

Assume there is a set of g legitimate training traffic records $X_{normal} = \{X_{normal1}, X_{normal2}, \dots, X_{normalg}\}$. The triangle-area-based MCA approach is applied to examine the records. The produced lesser triangles of the TAMs of the set of g legitimate training traffic records are denoted by $X_{normal} TAM_{lower} = \{TAM_{normal,1lower}, TAM_{normal,2lower}, \dots, TAM_{normal,glower}\}$.

Mahalanobis Distance (MD) is adopted to measure the dissimilarity between traffic proceedings. This is for the reason that MD has been successfully and widely used in cluster studies, categorization and multivariate outlier detection techniques. Unlike Euclidean distance and Manhattan distance, it assesses distance linking two multivariate information objects by taking the correlations between variables into account and removing the dependency on the scale of measurement during the calculation.

4.2 Threshold Selection

The threshold point is used to distinguish attack traffic from the legal one.

Threshold = $\mu + \sigma * \alpha$. (16)

For a normal distribution, α is usually ranged from 1 - 3. This means that detection decision can be made with a certain level of confidence varying from 68% to 99.7% in association with the selection of different values of α . Thus, if the MD between an observed traffic record $X_{observed}$ and the respective normal profile is greater than the threshold point value, then it will be measured as an attack.

4.3 Attack Detection

To detect DoS attacks, the lower triangle ($TAM_{observed\ lower}$) of the TAM of an observed record needs to be generated using the proposed triangle-area-based MCA move toward. Next, the MD among the $TAM_{observed\ lower}$ and the $TAM_{normal\ lower}$ stored in the respective pre-generated normal profile Pro is computed. The detailed detection algorithm is shown in Fig. 2.

Require: Observed traffic record $X_{observed}$, normal profile

$Pro : (N(\mu, \sigma^2), TAM_{normal\ lower})$

$lower, Cov$ and parameter

α

- 1: Generate $TAM_{observed\ lower}$ for the observed traffic record $x_{observed}$
- 2: $MD_{observed\ lower} \leftarrow MD(TAM_{observed\ lower}, TAM_{normal\ lower})$
- 3: if $(\mu - \sigma * \alpha) \leq MD_{observed\ lower} \leq (\mu + \sigma * \alpha)$ then
- 4: return Normal
- 5: else
- 6: return Attack
- 7: end if

Fig. 2. Algorithm for attack detection based on Mahalanobis distance.

V. EVALUATION OF THE MCA-BASED DOS ATTACK DETECTION SYSTEM

The estimate of our projected DoS attack detection system is conducted using KDD Cup 99 dataset [17]. Despite the dataset is criticised for redundant records that prevent algorithms from learning infrequent harmful records [21], it is the only publicly available labeled benchmark dataset, and it has been widely used in the domain of intrusion detection research. Testing our approach on KDD Cup 99 dataset contributes a convincing evaluation and makes the comparisons with other state-of-the-art techniques equitable. Additionally, our detection system innately withstands the negative impact introduced by the dataset because its profiles are built purely based on legitimate network traffic. Thus, our system is not affected by the redundant records. During the evaluation, the 10 percent labeled data of KDD Cup 99 dataset is worn, here we have three types of legitimate traffic (TCP, UDP and ICMP traffic) and six different types of DoS attacks (Teardrop, Smurf, Pod, Neptune, Land and Back attacks) are available. All of these records are first filtered and then are further grouped into seven clusters according to their labels (see Table 9 in Appendix 4 in the supplemental file to this paper for details).

The general evaluation procedure is in depth as follows.

First, the proposed triangle-area-based MCA approach is assessed for its capability of network traffic characterization. Second, a 10-fold cross-validation is conducted to evaluate the detection performance of the proposed MCA-based detection system, and the entire filtered data subset is used in this assignment. In the training stage, we utilize only the Normal records. Normal profiles are built with respect to the different types of legitimate traffic using the algorithm presented in Fig. 2. The corresponding thresholds are determined according to (16) given the parameter α varying from 1 to 3 with an addition of 0.5. In the test phase, together the Normal records and the attack records are taken into account. As given in Fig. 3, the observed samples are examined against the respective normal profiles which are built based on the legitimate traffic records carried using the same type of Transport layer procedure. Third, four metrics, namely True Negative Rate (TNR), Detection Rate (DR), False Positive Rate (FPR) and Accuracy (i.e. the proportion of the overall samples which are classified correctly), are used to evaluate the proposed MCA-based detection system. To be a good candidate, our proposed detection system is required to achieve a high detection accuracy.

5.1 Problems with the Current System and Solution

Even though the detection system reaches a moderate overall detection performance in the above evaluation, we want to explore the causes of degradation in detecting the Land, Teardrop and Neptune attacks.

Our analysis shows that the problems come from the data used in the evaluation, where the basic features in the non-normalized original data are in different scales. Therefore, even though our triangle-area-based MCA approach is promising in characterization and clearly reveals the patterns of the various types of traffic report, our detector is silent ineffective in various of the attacks. For instance, the Land, Teardrop and Neptune attacks whose patterns are different than the patterns of the legitimate traffic. However, the level of the dissimilarity between these attacks and the respective normal profiles are close to that between the legitimate traffic and the respective normal profiles. Moreover, the changes appearing in some other more important features with much smaller ideals can only just take effect in unique the DoS attack traffic from the legal traffic, since the overall variation is subject by the features with large values. Nevertheless, the non-

normalized original data have zero values in several of the features (both the important and the less important features), and they confuse our MCA and make many new generated features equal to zeros. This vitally degrades the discriminative power of the new feature set (TA lower), which is not supposed to happen. Apparently, an appropriate data normalization technique should be employed to eliminate the bias. We adopt the statistical normalization technique [20] to this work. The statistical normalization takes both the mean scale of attribute values and their statistical distribution into description. It exchanges data derived from any normal allocation into standard normal distribution, inside which 99.9% samples of the attribute are scaled into $[-3, 3]$. In addition, statistical normalization has been proven improving detection performance of distance-based classifiers and outperforming other normalization methods, such as mean range $[0, 1]$, ordinal normalization etc

VI. CONCLUSION AND FUTURE WORK

This paper has presented a MCA-based DoS attack detection system which is powered by the triangle-area based MCA technique and the anomaly-based detection technique. The former technique extracts the geometrical correlations hidden in individual pairs of two distinct features within each network traffic record, and offers more accurate characterization for network traffic behaviors. The latter technique facilitates our system to be able to distinguish both known and unknown DoS attacks from legitimate network traffic.

Evaluation has been conducted using KDD Cup 99 dataset to verify the effectiveness and performance of the proposed DoS attack detection system. The influence of original (non-normalized) and normalized data has been studied in the paper. The results have revealed that when working with non-normalized data, our detection system achieves maximum 95.20% detection accuracy although it does not work well in identifying Land, Neptune and Teardrop attack records. The problem, however, can be solved by utilizing statistical normalization technique to eliminate the bias from the data. The results of evaluating with the normalized data have shown a more encouraging detection accuracy of 99.95% and nearly 100.00% DRs for the various DoS attacks. Besides, the comparison result has proven that our detection system outperforms two state-of-the-art approaches in terms of detection accuracy. In addition, the computational complexity and the time cost of the proposed detection system have been analyzed and shown in Section 6. The proposed system realizes equal or better performance in comparison with the two state-of-the-art approaches. To be part of the future work, we will further test our DoS attack detection system using actual world data and spend more sophisticated arrangement performances to further alleviate the false positive rate.

REFERENCES

- [1] V. Paxson, "Bro: A System for Detecting Network Intruders in Realtime," *Computer Networks*, vol. 31, pp. 2435-2463, 1999
- [2] P. Garcia-Teodoro, J. Daz-Verdejo, G. Maci-Fernandez, and E. Vzquez, "Anomaly-based Network Intrusion Detection: Techniques, Systems and Challenges," *Computers & Security*, vol. 28, pp. 18-28, 2009.
- [3] D. E. Denning, "An Intrusion-detection Model," *IEEE Transactions on Software Engineering*, pp. 222-232, 1987.
- [4] K. Lee, J. Kim, K. H. Kwon, Y. Han, and S. Kim, "DDoS attack detection method using cluster analysis," *Expert Systems with Applications*, vol. 34, no. 3, pp. 1659-1665, 2008.
- [5] A. Tajbakhsh, M. Rahmati, and A. Mirzaei, "Intrusion detection using fuzzy association rules," *Applied Soft Computing*, vol. 9, no. 2, pp. 462-469, 2009.
- [6] J. Yu, H. Lee, M.-S. Kim, and D. Park, "Traffic flooding attack detection with SNMP MIB using SVM," *Computer Communications*, vol. 31, no. 17, pp. 4212-4219, 2008.
- [7] W. Hu, W. Hu, and S. Maybank, "AdaBoost-Based Algorithm for Network Intrusion Detection," *Trans. Sys. Man Cyber. Part B*, vol. 38, no. 2, pp. 577-583, 2008.
- [8] C. Yu, H. Kai, and K. Wei-Shinn, "Collaborative Detection of DDoS Attacks over Multiple Network Domains," *Parallel and Distributed Systems*, *IEEE Transactions on*, vol. 18, pp. 1649-1662, 2007.
- [9] G. Thatte, U. Mitra, and J. Heidemann, "Parametric Methods for Anomaly Detection in Aggregate Traffic," *Networking*, *IEEE/ACM Transactions on*, vol. 19, no. 2, pp. 512-525, 2011.
- [10] S. T. Sarasamma, Q. A. Zhu, and J. Huff, "Hierarchical Kohonenet for Anomaly Detection in Network Security," *Systems, Man, and Cybernetics, Part B: Cybernetics*, *IEEE Transactions on*, vol. 35, pp. 302-312, 2005.
- [11] S. Yu, W. Zhou, W. Jia, S. Guo, Y. Xiang, and F. Tang, "Discriminating DDoS Attacks from Flash Crowds Using Flow Correlation Coefficient," *Parallel and Distributed Systems*, *IEEE Transactions on*, vol. 23, pp. 1073-1080, 2012.
- [12] S. Jin, D. S. Yeung, and X. Wang, "Network Intrusion Detection in Covariance Feature Space," *Pattern Recognition*, vol. 40, pp. 2185-2197, 2007.
- [13] C. F. Tsai and C. Y. Lin, "A Triangle Area Based Nearest Neighbors Approach to Intrusion Detection," *Pattern Recognition*, vol. 43, pp. 222-229, 2010.
- [14] A. Jamdagni, Z. Tan, X. He, P. Nanda, and R. P. Liu, "RePIDS: A multi tier Real-time Payload-based Intrusion Detection System," *Computer Networks*, vol. 57, pp. 811-824, 2013.
- [15] Z. Tan, A. Jamdagni, X. He, P. Nanda, and R. P. Liu, "Denialof- Service Attack Detection Based on Multivariate Correlation Analysis," *Neural Information Processing*, 2011, pp. 756-765.
- [16] Z. Tan, A. Jamdagni, X. He, P. Nanda, and R. P. Liu, "Triangle- Area-Based Multivariate Correlation Analysis for Effective Denialof- Service Attack Detection," *The 2012 IEEE 11th International Conference on Trust, Security and Privacy in Computing and Communications*, Liverpool, United Kingdom, 2012, pp. 33-40.
- [17] S. J. Stolfo, W. Fan, W. Lee, A. Prodromidis, and P. K. Chan, "Costbased modeling for fraud and intrusion detection: results from the JAM project," *The DARPA Information Survivability Conference and Exposition 2000 (DISCEX '00)*, Vol.2, pp. 130-144, 2000.
- [18] G. V. Moustakides, "Quickest detection of abrupt changes for a class of random processes," *Information Theory*, *IEEE Transactions on*, vol. 44, pp. 1965-1968, 1998.
- [19] A. A. Cardenas, J. S. Baras, and V. Ramezani, "Distributed change detection for worms, DDoS and other network attacks," *The American Control Conference*, Vol.2, pp. 1008-1013, 2004.

An Efficient FB Addressing Protocol for Auto configuration of Ad Hoc Networks

Kg Mohanavalli¹, P Nageswara Rao², Rameswara Anand³

1(Dept of Cse, Swetha Institute of Technology and Science, Tirupati)

2(Associate Professor & Head, Dept Of Cse, Swetha Institute Of Technology And Science, Tirupati)

3(Professor, Dept Of Cse, Swetha Institute Of Technology And Science, Tirupati)

ABSTRACT

Address assignment is a main challenge in ad hoc networks due to the lack of groundwork. Self-determining addressing protocols require a distributed and automatic mechanism to avoid address collisions in a aggressive network with piling channels, usual partitions, and adding/deleting nodes. We propose and evaluate a lightweight protocol that configures mobile ad hoc nodes based on a shared address database stored in filters that decreases the control load and makes the proposal potent to packet losses and network partitions. We evaluate the achievement of our protocol, considering adding nodes, partition merging events, and network declaration. Simulation results show that our protocol resolves all the address collisions and also decreases the control traffic when compared to previously proposed protocols.

Index Terms— *FB, Ad hoc networks, computer based network management*

I. INTRODUCTION

Ad hoc networks do not require any previous groundwork and rely on dynamic multihop topologies for passage forwarding. Sensing, Internet access to deprived communities, and disaster recovering are called as the distributed applications. To makes these several applications it requires centralized administration. An essential issue of ad hoc networks is the frequent network partitions. Frequent partitions, caused by node mobility, fading channels [1], and joining nodes and leaving nodes in the network, can interrupt the distributed Network control. Because of the lack of servers in the network [2], Network initialization is the key challenge in Ad hoc Network.

As other wireless networks, ad hoc nodes also need a unique network address to enable multihop routing and full connectivity. Address assignment is key challenging in ad hoc networks, due to the self-organized nature of these situations. Centralized mechanisms, such as the Dynamic Host Configuration Protocol (DHCP) or the Network Address Translation (NAT), conflict with the distributed nature of ad hoc networks and do not address network detachment and integration. In this paper, we propose and analyze an efficient approach called Filter-based Addressing Protocol (FAP) [3]. The proposed protocol maintains a distributed database stored in filters containing the currently allocated addresses in a compressed manner. We consider Sequence filter contains both Sequence filter and proposed filter, to design a FB protocol that assures both the univocal address configuration of the nodes joining the network and the detection of address conflict after merging detachment. In filter-based approach simplifies the univocal address allocation and the detection of address conflict because every node can easily check whether an address is already assigned or not. We also propose to use the hash filter as a partition identifier, to provide an important feature for an easy detection of network detachment. Hence, we introduce the filters to store the allocated addresses without sustaining in high storage transparency. The filters are distributed maintained by exchanging the hash of the filters between neighbors. This allows nodes to detect with a small control transparency neighbors using different filters, which could affect address conflict. Because of these reason, our proposed method as a robust addressing scheme because it guarantees that all nodes share the same allocated list.

We compare FAP performance with the main address auto configuration proposals for ad hoc networks [4]–[6]. Analysis and simulation experiments show that FAP achieves low communication transparency and low latency, resolving all address conflict even in network partition merging events. These results are mainly associated to the use of filters because they reduce the number of tries to allocate an address to a combination node, as well as they reduce the number of false positives in the partition integration of events, when comparing to other proposals, which diminish message transparency.

II. RELATED WORK

The lack of servers hinders the use of centralized addressing schemes in ad hoc networks. In simple disseminated addressing schemes, however, it is hard to shun duplicated addresses since a random choice of an address by each node would result in a high conflict probability, as established by the birthday paradox [7]. The IETF Zero conf working group proposes a hardware-based addressing scheme [8], which assigns an IPv6 network address to a node based on the machine MAC address. However, if the number of bits in the address suffix is smaller than number of bits in the MAC address, which is forever factual for IPv4 addresses, this key must be adjusted by hashing the MAC address to fit in the address suffix. Hashing the MAC address, though, is similar to a random address preference and does not guarantee a collision-free address allocation.

Address auto configuration proposals that do not store the list of allocated addresses are typically based on a distributed protocol called Duplicate Address Detection (DAD) [4]. In this protocol, every joining node randomly chooses an address and floods the network with an Address Request message (AREQ) for a number of times to guarantee that all nodes receive the new allocated IP address. If the arbitrarily selected address is already allocated to another node, this node advertises the replica to the joining node sending an Address Reply message (AREP). When the joining node receives an AREP, it arbitrarily selects another address and repeats the overflowing process. Otherwise, it allocates the selected address. This proposal, nevertheless, does not take into account network divisions and is not suitable for ad hoc networks.

A few extensions to the Duplicate Address Detection (DAD) protocol use Hello messages and partition identifiers to handle network partitions [5], [9]. These identifiers are random numbers that identify each network partition. A collection of nodes modifies its partition identifier whenever it identifies a partition or when partitions merge. Fan and Subramanian propose a protocol based on DAD to solve address collisions in the presence of network integration of events. This protocol thinks that two partitions are merging when a node receives a Hello message with a partition identifier different from its own identifier or when the neighbor set of any node changes [5].

Other proposals use routing information to work around the addressing problem. Weak DAD [10], for instance, routes packets correctly even if there is an address conflict. In this protocol, every node is recognized by its address and a key. DAD is executed on the single-hop region, and collisions with the other nodes are identified by information from the steering protocol. If several nodes select the same address and key, nevertheless, the address conflict is not detected. Likewise, Weak DAD depends on modifying the routing protocols.

Other more complex protocols were proposed to improve the performance of network merging detection and address reallocation [6], [11]. In these protocols, nodes store additional data structures to run the addressing protocol. MANET conf [6] is a stateful protocol based on the concepts of mutual exclusion of the Ricart–Agrawala exclusion algorithm. In that the protocol, nodes store two field of address lists: the Allocated list and the assigned Pending list. A combination node asks for an address to a neighbor, which be converted into a leader in the address allocation procedure. The leader decides an available address, accumulates it on the Allocated Pending list, and floods the network. If all MANET conf nodes accept the allocation request and positively answer to the leader, followed by the leader report to the allocated address to the joining node, progress the distributed address to the assigned list, and floods the network again to authenticate the address allocation. After accept this message, each node moves the address from the distributed Pending list to Allocated list. MANET conf handles address reallocation; however network division detection depends on interrupted flooding. Hence this protocol acquires in a high control overhead.

Another stateful protocol is the Dynamic Address assignment Protocol (DAP) in mobile ad hoc networks [11], which is based on presented-address sets, Hello communication, and partition identifiers. In DAP; a node subdivides its available address set with a joining node whenever it is argued for an address by the fusion node. As node has a vacant address set, it rises for an address set reallocation. This reallocation and the recognition to give address is not being used any longer can foundation a high control load in the network, Based on how the addresses are circulated between nodes. DAP involves the use of DAD in integration events not only for the distributed addresses; however available address list stored in every node, improves the control load.

Prophet [12] allocates addresses based on a pseudo-random function through high entropy. The original node in the network, identified as prophet, selects seed for arbitrary sequence and assigns addresses to any joining node that contacts it. The combination of nodes starts to allocate addresses to other nodes from different points of the arbitrary sequence, building an address assignment tree. Prophet does not overflow the network

and, the arbitrary consequence, generates a low control load. The protocol, however, requires an address range much larger than the previous protocols to support the same number of nodes in the group of network. Likewise, it is based on the feature of the pseudo-random generator to evade duplicated addresses. Hence, it needs DAD mechanism, to detect duplicated addresses, which enhances the protocol intricacy and eliminates the advantage of a low control message transparency.

Our proposal aims to reduce the control load and to improve partition merging detections without requiring high storage capability. These intentions are achieved through small filters and an accurate dispersed mechanism to update the states in nodes. Moreover, we propose the use of the filter signature (i.e., a hash of the filter) as a partition identifier in preference to random numbers. The filter signature signifies the set of all the nodes within the partition. Consequently, if the set of allocated addresses changes, the filter signature also will change. Essentially, when using random numbers to identify the partition in preference to hash of the pass through a filter, the identifier does not change with the set of assigned addresses. Hence, filter signatures increases the capability to detect and merge partitions.

III. FAP

The proposed protocol aims to dynamically auto configure network addresses determine collisions with a low control load, yet in joining or merging events. To achieve these objectives, FAP uses a distributed compact filter to signify the current set of distributed addresses. This filter is present at every node to abridge frequent node joining events and reduce the control transparency essential to solve address collisions intrinsic in random obligations. Furthermore, we propose the filter signature, which is the hash of the address filter, as a partition identifier. The address filter signature is an significant feature for easily identifying network merging events, in which address collision may occur. FAP uses two different filters, depending on the scenario: the Bloom filter, which is support on hash functions, and the Sequence filter, which reduces data based on the address sequence.

A. Bloom Filters

The Bloom filter is a compact data structure used on distributed applications [13], [14]. The Bloom filter is composed of an m -bit vector that represents a set $A = \{a_1, a_2, a_3, \dots, a_n\}$ collection of elements. This elements are inserted into the filter which is through a set of independent hash functions, $h_1, h_2, h_3, \dots, h_k$, whose outputs are uniformly distributed over the m bits

$$P_{fp} = (1-p_0)^k \quad (1)$$

B. Sequence Filters

The other filter structure that we propose is called Sequence filter, and it stores and compress the addresses based on the sequence of addresses. This filter is produced by the concatenation of the first address of the address sequence, which we call primary element, with an m -bit vector, where m is the address range size. In this filter, each address suffix is represented by one bit, indicate to give the distance between the initial element suffix and the current element suffix. If a bit is in 1, then the address with the given suffix is considered as inserted into the filter; if not, the bit in 0 indicates that the address does not go to the filter. Consequently, there are neither false positives nor false negatives in the Sequence filter since each available address is deterministically represented by its relevant bit.

C. Procedures of FAP

1) Network Initialization: The network initialization procedure deals with the auto configuration of the primary set of nodes. Two different circumstances can happen at the initialization: the joining nodes appear one after the other with a long sufficient interval among them, called gradual initialization, or all the nodes appear at the same time, called abrupt initialization. Most protocols assume the gradual scenario with a large time interval between the arrival of the first and the second joining nodes. If all nodes join the network approximately at the equivalent time, each partition will choose a different partition identifier. This triggers many partition merging procedures concurrently, which creates a high control load and it cause inconsistency in the address assignment procedure, generating address conflicts. We dispute that address allocation protocols must operate lacking any restriction to the way the nodes join the network. Our FB proposal fits well for both gradual and rapid initialization scenarios, called Hello and AREQ messages, shown in Fig. 3(a) and (b). The Hello message is used by a node to advertise its current association status as division of identifier. The AREQ message is used to broadcast that the existing address is now allocated. Each AREQ has an unique number, which is used to differentiate AREQ messages produced by different nodes, but with the similar address.

In FAP, a node trying to join the network listens to the medium for a period T_L . If the node does not receive a Hello message within this period T_L , then it starts the network, acting as the initiator node. An initiator node may start the network only, or with other originator nodes. or else, if the node receives a Hello message, then the network previously survives and the node acts as a joining node. An initiator node randomly selects an address, assuming the address range defined by the bits of the network prefix, constructs an empty address filter, and initiates the network initialization phase. In this phase, the node floods the network N_F times with AREQ messages to improve the possibility that all originator nodes receive the AREQ message. If there are other initiator nodes, they also send their AREQ N_F times, promoting their randomly selected addresses. After waiting a period T_W without listening to AREQs from other originator nodes, suppose if they exist, the node disappears the initialization phase and introduce on the address filter all the available addresses accepted with AREQs. After the node begin to send Hello messages through the address filter signature, which is a hash of the filter. This signature recognize the network and is used to detect partitions, if they occur. If the initiator node receives any AREQ with the similar address that it has selected, however with a different identifier number, which means that there is an address conflict, the node waits for a period T_C and then selects another existing address and pass another AREQ. During the period T_C the node receives more AREQs with other already allocated addresses. Therefore, after T_C , the node knows a more complete list of distributed address, which reduces the probability of selecting used address. Therefore, the periods T_C reduce the probability of address conflicts and, accordingly, decrease the network control load.

After the initialization of FAP, all initiator nodes have selected a unique address due to the arbitrary address choice and the substantiation using AREQ messages with identifier numbers. Moreover, each node knows all presently allocated addresses with a high possibility due to the N_F times flooding the network. Therefore, each node create an address filter including all the assigned addresses.

2) *Node Ingress and Network Merging Events:* After the FAP initialization, every node begin to transmit periodic Hello messages including its address filter signature. Ahead the function of a Hello, neighbors estimate whether the signature in the message is the same as its own signature to sense merging events. Only the nodes that have already merged network are capable to send Hello messages, receive a request of a node to join the network, and sense merging events.

The node ingress procedure is illustrated in Fig. 4(a). When a node turns on, it listens to the medium for a period T_L . If the node eavesdrops to a Hello, there is at least single node with an address filter, and the network already be present. Consequently the node knows that it is a combination node instead of an originator node. The merging node then asks for the source of the first snooped Hello message(the host node) to send the address filter of the network using an Address Filter (AF) message, shown in Fig. 3(c).When the host node retrieves the AF, it checks bit I , which specifies whether the message is individually used for a node-merging procedure or a partition-joining procedure. If $I=1$, the message came from a merging node. Then, the host node replies the request with another AF with bit set to 1, indicate that the AF is an answer to a existing filter request. When the joining node retrieves the AF response message, it stores the address filter, selects a arbitrary existing address, and floods the network with an AREQ to assign the new address. When the other nodes retrieve the AREQ, they include the new address in their filters and modernize their filter signatures with the hash of the revised filter.

Joining events are also identified depend on Hello and AF messages, as illustrated in Fig. 4(b). Nodes in dissimilar partitions select their address depends only on the group of addresses of their network partition. Consequently, nodes in dissimilar partitions can select the similar address, which may origin address conflicts after the partitions joined. In FAP protocol, when a node retrieves a Hello, it verifies whether the filter signature on the message is dissimilar than its present signature. Hence, the node knows that they have different sets of allocated addresses.

IV. SIMULATION RESULTS

We implemented FAP in the Network Simulator-2 (NS-2) and evaluated it considering the Shadowing model for radio propagation and the NS-2 IEEE 802.11 model for the MAC. These replicas account for making a circumstances related to a real neighborhood network, using constraints of profitable equipments. Hence, the constraints are used for our simulations are: an average broadcasting range of 18.5 m, a highest carrier logic range of 108 m, and a density of 0.0121 nodes/m [16]. We measured the control traffic, the delays

TABLE I: PARAMETERS OF FAP (F), DAD-PD (PD), DAD (D), AND MCONF (M)

Variable	Description	Value	Protocol
T_L	Max. time listening to the medium	1.0 s	F, PD
T_P	Partition merging min. interval	3.0 s	F, PD
T_W	AREQ/AREP waiting time	1.2 s	F, PD, D
T_R	Message replication interval	0.3 s	F, PD, D
T_H	Hello Timer	1.0 s	F, PD, M
T_C	Waiting time before changing address	0.3 s	F
T_S	Generated-filter-signature storage time	0.5 s	F
$T_{S'}$	Received-filter-signature storage time	3.0 s	F
T_M	Min. interval between filter renews	5.0 s	F
T_F	Max. time waiting for a filter	0.5 s	F
T_{MA}	Address Allocation Timer	0.7 s	M
T_{MR}	Request Reply Timer	0.3 s	M
T_{MN}	Neighbor Reply Timer	0.35 s	M
T_{MAP}	Allocation Pending Timer	1.0 s	M
T_{MP}	Partition Timer	2.0 s	M
N_F	Transmissions of a flooding message	2	F, PD, D
N_T	Neighbor Reply Threshold	3	F, M
N_{MR}	Request Reply Retry	2	M
N_{MI}	Initiator Request Retry	2	M
N_{MP}	Partition Identifier Threshold	3	M

and the number of address collisions in FAP, considering a confidence level of 95% in the consequences. We also realized in Network Simulators-2 the addressing protocols projected by Perkins *et al.* [4], called DAD, by Fan and Subramani [5], which we call DAD-PD, and by Nesargi and Prakash [6], called MANET conf and indicated in the outcomes by Mconf.3 while DAD does not work in network partition-level locations, we estimated this protocol since it is a simple proposal with low transparency. Our main intention is to show that our proposal also near by a low transparency and works in any development. Comparing FAP to DAD-PD, we observe the performance collision of the use of the hash of the address filters as a substitute of mediated partition identifiers to sense partition merging events. In the original DAD-PD, but, the new partition identifier after a partition joining is given by the sum of network partition identifiers, which causes volatility in the protocol. Hence, we increased the protocol performance by selecting the huge partition identifier in network joining events in preference to sum them, which decrease the number of negative partition joining detections. Additionally, when compared FAP to MANET conf because both proposals use an allocated address list. The protocol constraints are shown in Table. These parameters were selected based on experiments to improve all the four protocols routine and also on proposals from the authors of the other proposals. Therefore, we have chosen these values edging on decreasing the delays and the transparency while at rest evading instabilities in the simulated scenario. Particularly, includes the time listening to the medium before the node choose if it is alone or not. Consequently, this phase must be, at least, equal to the Hello Timer .

The minimal interval between partition merging events, avoids high overheads in FAP in environments prone to high forwarding delays and/or many packet failures. This value is even more significant for the DAD-PD protocol, in which partition joining mechanisms are frequently called. We estimate this constraint choice throw simulations. Likewise, both the constraints , which identifies the intermission among retransmissions of flooding messages, and , which decreases the address conflicts during the initialization phase, contacts on FAP performance and are also appraised in the following simulations. The constraints is used through FAP initialization to identify when a node is allowed to use its selected address. Therefore, this interval identifies the period that a node should wait for more AREQs before

terminating the initialization phase, and does not hamper in the protocol stabilization interruption. The values and avoid wrong detections of partition joining events through the new node and partition joining events. The use of high values provisionally increases the storage transparency. The minimum interval among filter restores, collisions FAP transparency only if the network is full. This interval defines the frequency in which the filter is checked to discover if any node has left the network to provide addresses for merging nodes. A small implies on a frequent substantiation, which improves the transparency, while a high involves in low transparency, but long wait for new nodes to merge an almost complete network. The value controls the time a merging node waits until the chosen neighbor sends the present address filter. This timer only presents flexibility to fault nodes or to neighbors that leave the transmission range of the joining node, and then it usually does not influence on protocol performance. The number of transmissions of a flooding message, , also impacts FAP performance and is evaluated through simulations. Finally, the last FAP parameter, , has a resilience function similar to and presents a small impact over FAP performance.

Both FAP and DAD-PD use equal-sized Hello messages because we assume that both partition identifier and filter signature are composed of 4 B. We assume an address range of 150 addresses and a network with a maximum of 100 nodes to guarantee that the address range is not a constraint that can cause instabilities for any practice. Based on these parameters, we have used Sequence Filter of 23 B. We first evaluate the collision of one node merging the network. Therefore We have considered a rectangular space with nodes dispersed in grid.

We evaluate the control load after the last node merge the network and the involve delay to acquire an address, as revealed in Fig. 6. In the consequences, we monitor that our proposal, FAP, current an transparency larger than DAD since our protocol uses Hello messages to notice partitions. DAD-PD currents the greatest control transparency for more than 36 nodes since unnecessary partition joining practices are be ginned caused by mistakes in partition joining event detection after a node merge the network. in fact, DAD-PD has a partition detection mechanism that is depend on partition identifiers. When a new node merge the network, the partition identifier must be altered to signify the new set of assigned addresses. The modernize of this value, yet, can root negative partition joining detections which improve the control load transparency. For other than

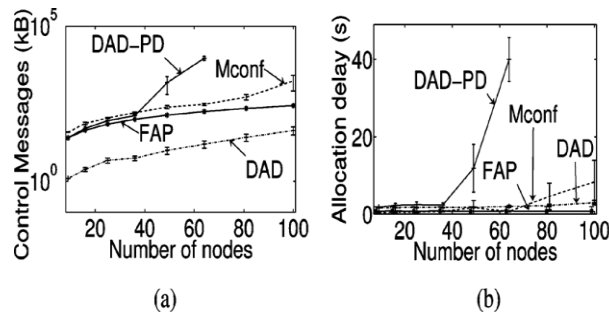


Fig. 1. Collision of a joining node procedure followed to the many number of nodes

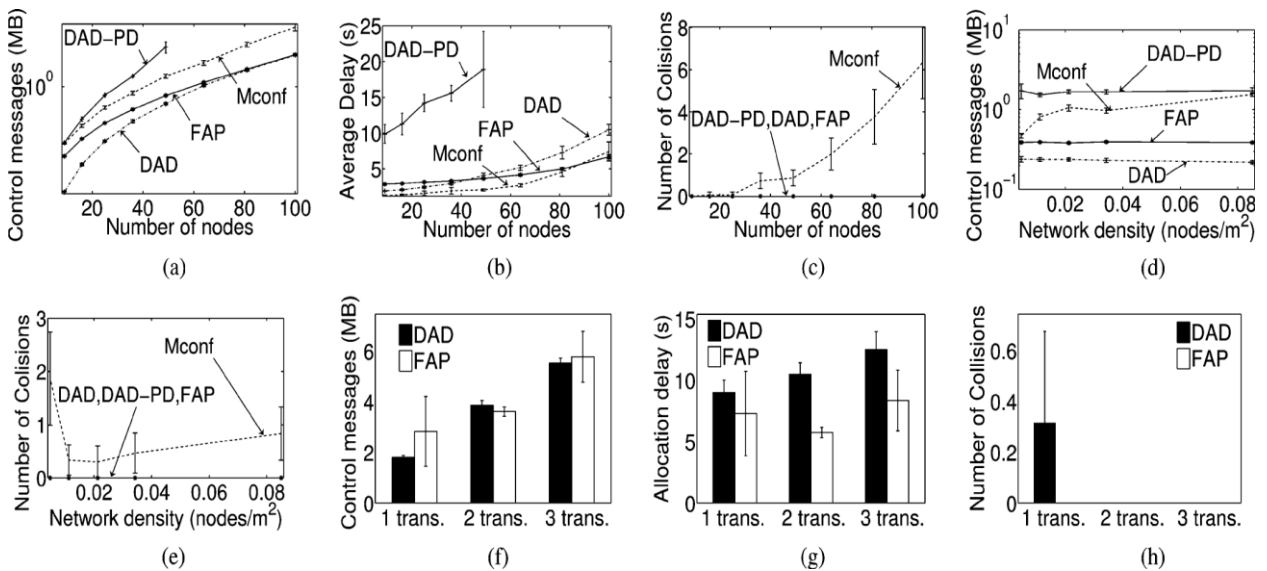


Fig. 7. Collision over the network of the number of nodes, the density, and the number of broadcasts of flooding messages (N_F) in a network rapidly initialized. (a) Control transparency according to the number of nodes. (b) Average interruption according to the many number of nodes. (c) Number of address conflicts based on the number of nodes. (d) Control transparency is depend on network density $N=36$, nodes. (e) Number of collisions according to network density $N=36$, nodes. (f) Control overhead according to $N_F, N=100$, nodes. (g) Average delay according to $N_F, N=100$, nodes. (h) Number of collisions according to $N_F, N=100$, nodes.

since this protocol switches joining events, but it could not evade all the address conflicts. FAP presented no address collision, but DAD-PD offered a small probability of conflict caused by packet losses. FAP omits this kind of address conflict because of the mechanism that detects packet losses and begins fake joining methods until all the nodes have retrieved the similar information. since a result, FAP determines all the conflicts and also presented a minimal control load. In Fig. 7, we have guessed the collision of the retransmissions of flooding packets in network initialization. Now, we analyze the collision of the delay among flooding message retransmission, the time waiting before selecting a new address in the initialization and the minimal interval among partition joining events. First, we have analyzed the conflict of the network with 100 nodes. We illustrated in Fig. 9(a) that a huge partition decreases the transparency since the nodes learn more allocated addresses before selecting a new address. However, this also improves the delays in the network, as illustrated in Fig. 9(b). An intermediate value in this scenario is s , which was used in the other simulations. In the same scenario, we analyze and observed that a small reduces both the overhead and the delay. We repeated the partition merging scenario with four partition merging events. Fig. 9. Analyzing performance according to different values of FAP parameters. (a) Control overhead. (b) Average delay to obtain an address. In this scenario, . We observe in Fig. 9(a) that a small s is better for FAP, but is very prejudicial for DAD-PD. Indeed, FAP presents a better partition merging event detection than DAD-PD. DAD-PD performs many unnecessary partition merging mechanisms and a greater s reduces these false detection events. Nevertheless, a greater s also increases the stabilization time of DAD-PD during network initialization. Then, we selected an intermediate value for s to balance the requisites of both protocols.

V. CONCLUSION

We proposed a distributed and self-managed addressing protocol, called as FB Addressing protocol, which is robust for dynamic ad hoc networks with fading channels, numerous partitions, and merging/leaving nodes. Our key idea is to use address filters to omit address conflicts, which decrease the control load, and reduce the address allocation interruption. We have also proposed to use the hash of the filter as the partition identifier, providing an easy and accurate feature for partition detection with a small number of control messages. Moreover, our filter-based protocol improves the protocol vigorousness to message losses, which is an main issue for ad hoc networks with fading channels and high bit error rates.

The use of the hash of the filter instead of a random number as the partition identifier creates a better representation of the group of nodes. Therefore, a change in the group of nodes is mechanically reflected in the partition identifier. This identifier is occasionally presented, allowing neighbors to identify if they belong to different sets of nodes. In the other proposals, mechanism to change the arbitrated partition identifier is requested, which increases the complexity and the packet overhead of the protocol.

The proposed protocol efficiently resolves all address collisions even during merging events, as showed by simulations. This is achieved because FAP is able to detect all merging events and also because FAP is robust to message failures. FAP initialization practice is straightforward and proficient, requiring a control load related to the control pack of DAD, which is a protocol with a small transparency but that does not handle network partitions. Moreover, FAP presents smaller delays in the joining node procedure and on network partition merging events than the other applications, designating that the proposed protocol is more appropriate for very dynamic environments with frequent partition merging and node joining events.

REFERENCES

- [1] D. O. Cunha, O. C. M. B. Duarte, and G. Pujolle, "A cooperation-aware routing scheme for fast varying fading wireless channels," *IEEE Commun. Lett.*, vol. 12, no. 10, pp. 794–796, Oct. 2008.
- [2] N. C. Fernandes, M. D. Moreira, and O. C. M. B. Duarte, "A self-organized mechanism for thwarting malicious access in ad hoc networks," in *Proc. 29th IEEE INFOCOM Miniconf.*, San Diego, CA, Apr. 2010, pp. 1–5.
- [3] N. C. Fernandes, M. D. Moreira, and O. C. M. B. Duarte, "An efficient filter-based addressing protocol for autoconfiguration of mobile ad hoc networks," in *Proc. 28th IEEE INFOCOM*, Rio de Janeiro, Brazil, Apr. 2009, pp. 2464–2472.
- [4] C. E. Perkins, E. M. Royers, and S. R. Das, "IP address autoconfiguration for ad hoc networks," *Internet draft*, 2000.
- [5] Z. Fan and S. Subramani, "An address autoconfiguration protocol for IPv6 hosts in a mobile ad hoc network," *Comput. Commun.*, vol. 28, no. 4, pp. 339–350, Mar. 2005.
- [6] S. Nesargi and R. Prakash, "MANETconf: Configuration of hosts in a mobile ad hoc network," in *Proc. 21st Annu. IEEE INFOCOM*, Jun. 2002, vol. 2, pp. 1059–1068.
- [7] B. Parno, A. Perrig, and V. Gligor, "Distributed detection of node replication attacks in sensor networks," in *Proc. IEEE Symp. Security Privacy*, May 2005, pp. 49–63.
- [8] S. Thomsson and T. Narten, "IPv6 stateless address autoconfiguration," RFC 2462, 1998.
- [9] M. Fazio, M. Villari, and A. Puliafito, "IP address autoconfiguration in ad hoc networks: Design, implementation and measurements," *Comput. Netw.*, vol. 50, no. 7, pp. 898–920, 2006.
- [10] N. H. Vaidya, "Weak duplicate address detection in mobile ad hoc networks," in *Proc. 3rd ACM MobiHoc*, 2002, pp. 206–216.
- [11] H. Kim, S. C. Kim, M. Yu, J. K. Song, and P. Mah, "DAP: Dynamic address assignment protocol in mobile ad-hoc networks," in *Proc. IEEE ISCE*, Jun. 2007, pp. 1–6.

Effects Of Skewness On Three Span Reinforced Concrete T Girder Bridges

¹Himanshu Jaggerwal , ²Yogesh Bajpai

^{#1}Student- M.Tech (Structural Engineering), Civil Engineering Department, GGITS Jabalpur M.P,
India

^{#2}Associate Professor- Civil Engineering Department, GGITS Jabalpur M.P, India

ABSTRACT:

A very limited study has been carried out in the field of skew bridges and even that does not hold much relevance in Indian perspective due to difference in design live load standards and type of bridges being built there. Therefore it does not provide any help to designers regarding the quick estimation of design bending moments and shear forces which are of prime interest. In this paper an attempt has been made to study the effect of skewness directly on the design parameters i.e. B.M, Shear Force and Maximum Reaction in simply supported RC T-Beam 3 lane bridges. For this purpose a parametric study of Simply Supported 3-Lane T-Beam Bridge has been performed in STAAD PRO. The parameters varied were span and skew angle. The effect of same was observed on maximum live load bending moment, maximum live load shear force and maximum live load reaction at critical locations. Live Load “Class 70R Tracked” and “Class 70R Wheeled” were applied as per IRC 6 guidelines. The spans used were 10 m, 15 m, 20 m and 25 m. The skew angles were taken at an interval of 15° starting from 0° up to a maximum of 60°. Bridges with skew angle more than 45° are rare. From the study it was observed that as the skew angle increases from 0° to 60° there is a consistent reduction in Moment Distribution Factor (MDF) of the inner longitudinal girder of bridge. Similar trend of reduction in MDF were observed for other spans. This suggests that skew bridges designed, ignoring the skew effect is conservative with respect to the bending moment. The effect of skew angle was also studied on the shear coefficients. The shear coefficients as increases almost linearly with skew angle and span. Hence it can be concluded that proper estimation should be made in the live load shear when designing skew bridges.

KEYWORDS: Skew angle, distribution factor, T Beam Bridge, grillage analogy, bending moment,

I. INTRODUCTION

Most of the bridges in elder days were straight and skew bridges were preventing as far as feasible. Lack of information about the structural behaviour and construction difficulty were obvious reasons contributing to the designer's choice to help in a straight line bridges rather than skew bridges. But in the recent circumstances there is a rising trend of providing skew bridges rather than curved or straight bridges with long approach road at oblique intersections. There is immense pressure of increasing population due to which the cost of land acquisition for approach roads has hiked many folds. It is difficult for them to negotiate on curve roads even at low speeds. The introduction of curves also increases the distance travelled by the vehicle which in turn affects the economy. In hilly regions also due to topographic conditions, it is very difficult to provide curved approaches and many times skew bridge remains the only option. The railway and roadway intersection are also often oblique and requires approach road if skew bridge is to be avoided. Also old and overcrowded city due to be short of space, bridges have to be skew in nature if the intersection is not orthogonal. Hence there is need to study the behavior of skew bridges so as to facilitate quick estimation of design BM, shear force and support reactions and thus obviating the need of a rigorous analysis. The results have been presented in the form of ready to use design charts. In the present thesis behaviour of RC T Beam Bridge having skew angle from 0-60° has been investigated. Further on the basis of a parametric study an attempt has been made to develop suitable design charts for quick estimation of design forces in skew bridges.

II. METHODOLOGY

With the advancement in modeling and computing facilities world over, it has now become possible to perform a near exact analysis of any kind of bridge. The commercially available software packages like ANSYS, ABAQUS, SAP etc has made it possible to use the methods of Finite Element Analysis, etc with much ease. In spite of the fact that these methods are highly efficient and accurate, these methods are often criticized also for the reason that the efficiency is achieved at the cost of exorbitant computations and time requirement. Hence, care must be taken in selection of the appropriate method of analysis, appropriate to the type of bridge depending upon the required accuracy in the parameters under investigation. Grillage Analogy on the other hand presents a sufficiently accurate method to analyze slab-beam bridges for estimation of design bending moment, torsion, shear force etc. It is a comparatively simpler method to analyze the bridge decks and gives an excellent visualization of distribution of forces among different longitudinal and transverse girders in a bridge. It can easily handle complicated geometric features of a bridge such as skew, edge stiffening, and deep haunches over support, continuous and isolated supports etc with ease. It is a versatile method and can also take into account the contribution of kerb beams, footpaths and the effect of differential sinking of girder ends over yielding supports. The method has proved to be reliable and versatile for a wide variety of bridge decks. It do possess some limitations such as inability to take into account the effects like shear lag, warping and distortional effects for which more sophisticated methods like FEM have to be used.

Basically grillage analogy method uses stiffness approach for analyzing the bridge decks. The whole bridge deck is divided into no of longitudinal and transverse beams. The intersection of longitudinal and transverse beams is called as node. Each node has six degrees of freedom, namely 3 rotations and three translations. But if we assume the slab to be highly stiff in its own plane, which is actually the case in most of the bridges, the degrees of freedom are reduced to three i.e. 1- vertical translation and 2-rotations about the axes in plane of the bridge deck. The properties of cross-section such as beam moment of Inertia about their principal axes, Torsional constant, Effective Area etc are calculated and the grid is solved for the unknown degrees of freedom using the matrix stiffness method. After the nodal displacements are known, the forces in the grid members are calculated using the force displacement relationship. The overall equations of equilibrium are given below.

$$\{p\} = [k] \{u\} + \{q\} \quad \text{At member level}$$

$$\{P\} = [K] \{U\}, \quad \text{At structural level}$$

Where,

P represents the unknown nodal forces (BM, Torsion, and SF), K is the assembled stiffness matrix of the structure and U represents the vector of nodal displacements or degrees of Freedom at structural level. Similarly p, k, u are the representatives at member level, which are in respect to local coordinate system. Represents equivalent member end forces due to member loads.

Conceptually, grillage analogy method attempts to discretized the continuous or dispersed stiffness of bridge and concentrates it into discrete longitudinal and transverse members. The degree of structural similarity between the original bridge and grillage so formed depends on the fineness of the grid formed. But practically it is observed that after a certain degree of fineness in the grillage mesh, law of diminishing returns is followed and further reducing the size of grillage doesn't significantly add to the accuracy. The choice of the designer is the best judge to decide grid fineness.

The solution of grillage mesh involves a large no. of equations, which is beyond the scope of the manual solution. Hence it becomes mandatory to take aid of computer programs in the grillage analogy method. Commercially available software package like Staad Pro, are very helpful in analyzing bridges with grillage analogy method considering all the 6-DOFs i.e. 3 translations and 3 rotations per node. The use of same has been made in this study.

2.1 Gridlines, their locations, direction and properties: Gridlines are the beams representing the discretized stiffness and other structural properties of the slab portions which it replaces. Strictly speaking, gridlines represents the lines of strength. So they must be provided at all the locations where there is concentration of stiffness. Therefore gridlines must be provided at the centre of each longitudinal and transverse girder, running along them. Where isolated bearings are provided, gridlines should also be provided along the lines joining the bearings. Generally gridlines must coincide with the centre of gravity of the section but some shift may be permitted for the ease of calculation. A few guidelines for the Grillage Idealizations for slab T beam bridges are as follows.

- (a) Generally longitudinal gridlines are parallel to the free edge of Deck. (For straight bridges without skewness)
- (b) For skew Bridges with skew angle less than 15° the transverse girders are provided parallel to the support lines so the gridlines should also be parallel to the support lines. But for skew angles exceeding 15 degrees, where transverse diaphragms perpendicular to the longitudinal girders are provided as they are found to be more efficient in transverse load distribution amongst longitudinal Girders. Hence gridlines should be along the transverse diaphragms i.e perpendicular to the longitudinal beams.
- (c) End transverse gridlines must be provided along the center lines of bearings on each side of span.
- (d) For determining the sizes of gridlines aid form relevant IRC code can be taken.

III. PARAMETRIC STUDY OF RC T BEAM BRIDGE

A 3 lane RC T-Beam Bridge has been chosen for the study. Spans have been varied from 12m to 21 m with an increment of 3m. The no. of longitudinal girders has been kept as three. Cross Girders are hindrance in the speed of construction as they pose practical problems in construction. So their spacing is generally kept not less than 4 m and for this reason the spacing of cross girders is kept between 4.5 m to 6 m. For skew bridges of 0° and 10° , the cross girders (& transverse gridlines) are parallel to the abutment, while for 20° , 30° , and 40° , the cross girder (& transverse gridlines) are provided orthogonal to longitudinal girders for the reason explained in above section. The cross-section shown in Fig 1 has been chosen. The sizes of longitudinal and cross beams is given in Table 1

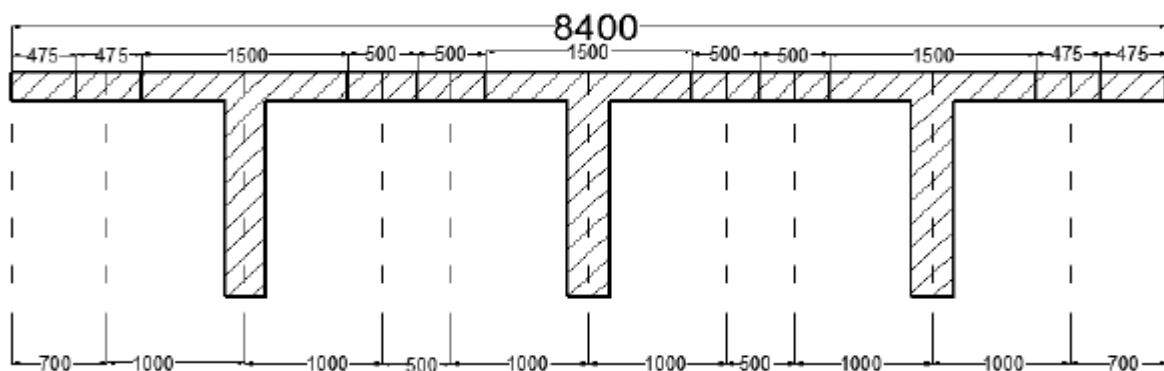


Figure 1 Division of bridge cross-section into equivalent grillage

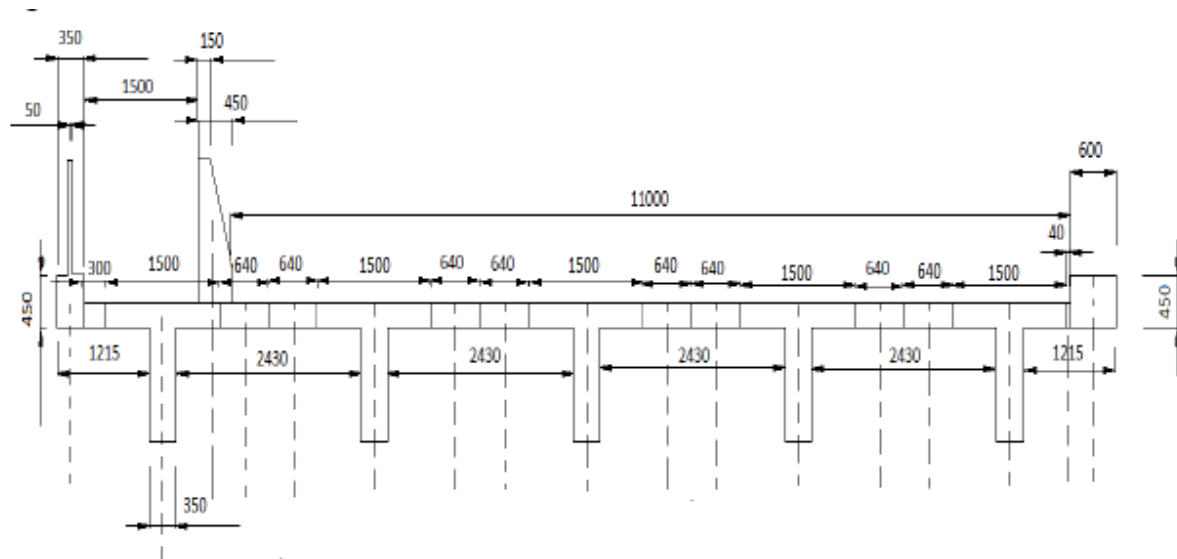
3.1 Grillage Idealization Of Bridge:

In grillage analogy method, the continuous bridge deck is discretized into a no of longitudinal and transverse beams. Since the distribution of bending stress in the flange of the T-Beam bridge is not uniform as suggested by the simple bending theory, so the effective width concept is used to define the flange of the T-section. For this purpose assistance from IRC 21: 2000 clause 305.15 was sought in the selection of sizes of T-Beam. It suggests

$$b_e = b_w + l_o / 5 \dots \dots \dots \text{IRC 21: 2000 clause 305.15}$$

Where, b_e = effective flange width of T-Beam; b_w = width of T-Beam and l_o = distance between the points of contra flexure.

Exact modelling of bridge is difficult so some approximations were made in grillage idealizations and the slab was assumed to be of uniform thickness taking partially into account the effect of kerbs. Figure 2 shows the grillage idealization of the bridge in longitudinal direction. Same method was used for discretizing the bridge in transverse direction also.



GRILLAGE IDEALIZATION OF CROSS SECTION OF THREE LANE ONE WAY BRIDGE

Figure 2: Grillage Idealization of the cross section of bridge. All dim in mm

IV. LIVE LOAD (LL) APPLICATION ON THE BRIDGE

The Bridge deck was analyzed for “Class A”, “Class 70R Tracked” and “Class 70R Wheeled” vehicles. As per IRC 6: 2000 Table 2, a two lane bridge should be loaded with either one lane of “Class 70R” or two lanes of “Class A”. For the transverse placement of the vehicle, guidelines of IRC 6: 2000 clause 207 were followed which suggests that the minimum spacing of vehicle from the face of the kerb is 1.2 m for “Class 70R” and 0.15 m for “Class A” loading. Many other trials of the transverse placement of vehicles were also made to obtain the maximum LL moments and maximum LL shear force and maximum LL reactions in the bridges. Following observations were made during these trials.

- For “Class 70R Wheeled” and “70R Tracked” the maximum bending moment in the bridge is always obtained in the outer girder when the vehicle is placed at minimum spacing from the kerb.
- For maximum bending moment in the middle girder the vehicle is placed both eccentrically and centrally as it does not always occur for same transverse placement loads.
- For all Class of loading, the maximum LL shear occurs in the outer girder, near the obtuse corner.
- For “Class 70R Wheeled” and “70R Tracked” the maximum LL support reaction occurs in the middle girder when the vehicle is placed centrally.

The loads were placed accordingly to obtain maximum bending moment, maximum shear and reaction in the bridge.

4.1 Idealization of Vehicle : The details of vehicles have been given in IRC 6: 2000. The Class 70 R Tracked vehicle has been simulated as train of 20 equal point loads as shown below in figure 3. The load values shown in the longitudinal details are the axle loads and since there are two wheels on each axle, so the values are halved when seen in the transverse view.

- 70R Wheeled Vehicle

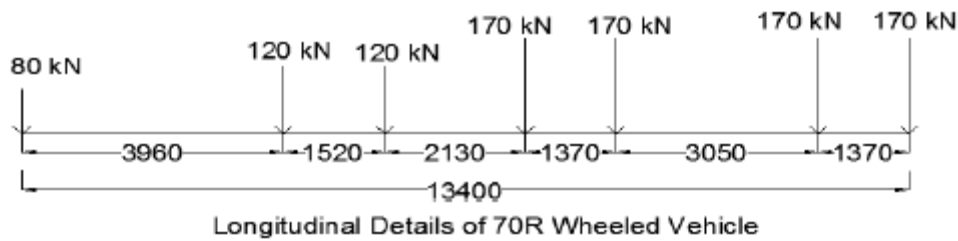
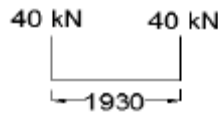


Figure 3: Class 70R Wheeled Vehicle



Rear Axle

(2) 70R Tracked Vehicle

The tracked vehicle was idealized as shown below. The uniformly distributed load, 4570 mm has been converted into equivalent train of 20 equal point loads for ease in application.

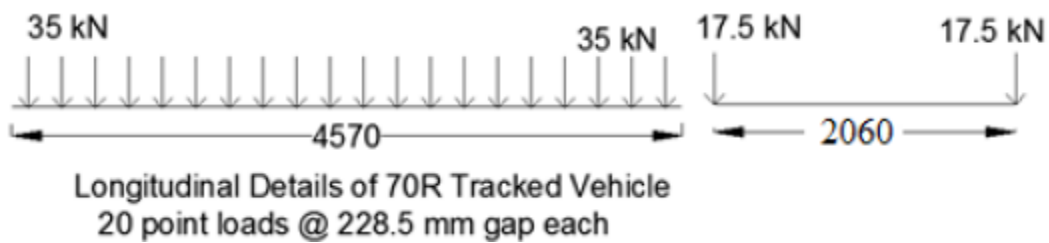


Figure 4: Class 70R Tracked Vehicle

4.2 Impact Factor : Provision for impact or dynamic action shall be made by an increment of the live load by an impact allowance expressed as a fraction or a percentage of the applied live load.

(1) For Class 70R Loading: for 70R Wheeled and 70R Tracked impact factor determined according to IRC: 6-2000 Clause 211.3 The impact factor for 70R Wheeled, 70R Tracked and Class A and for all span are given below in Table 4.1.

Table 1: Impact factor

Span (m)	10 m	15 m	20 m	25 m
70 R Wheeled	0.28	0.21	0.17	0.14
70 R Tracked	0.10	0.10	0.10	0.10

V. RESULTS AND DISCUSSION

Bridges of span 10 m, 15 m, 20m, and 25m were analyzed for skew angles 0°, 15°, 30°, 45° and 60°. The results are shown below. All the moment values are for live load only and the word “moment” is synonymously used for “maximum moment” at many places of this chapter. Also the abbreviation G1, G2, G3, G4, & G5 are shown in Results and Discussions Figure 23

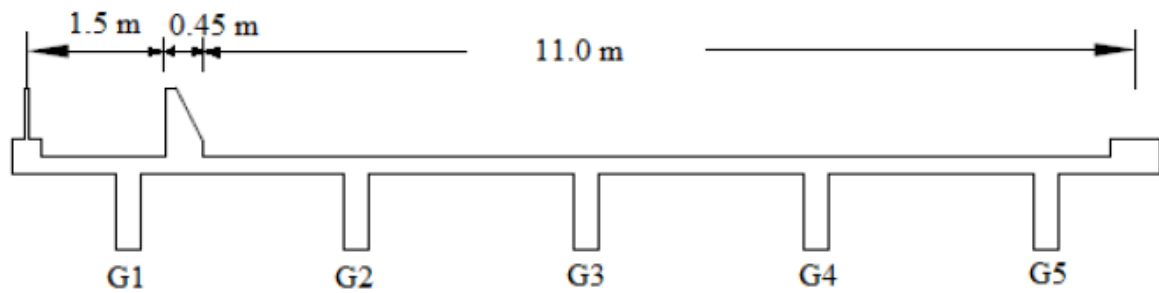


Figure 5: Cross section of three lane T-Girder bridge

G1 is the outer longitudinal girder on the left side of the middle girder.
 G2 is the inner longitudinal girder on the left side of the middle girder.
 G3 is the middle longitudinal girder.
 G4 is also the inner longitudinal girder but on right side of the middle girders.
 G5 is also the outer longitudinal girder but on right side of the middle girder.

5.1 Effect of Arrangement of Loading

5.1.2 Class 70R Wheeled with Class A Vehicle : The Class 70R Wheeled vehicle was placed centrally on G3 & G4 and Class A vehicle was placed at a minimum spacing of 1.2m (minimum spacing specified in IRC: 6 - 2000 for Class A vehicle) from 70R Wheeled Vehicle and moved over the span (Figure of placement of IRC loading over bridge is given in Annexure B). The maximum moments obtained in the girders G1, G2, G3, G4 and G5 were recorded. The maximum moment occurred simultaneously in all girders for 0° skew angle but for other skew angles it occurred with some lag due to skew effects. The lag increased with skew angle. A total of 1000 KN load was applied in this loading on 13.4m distance.

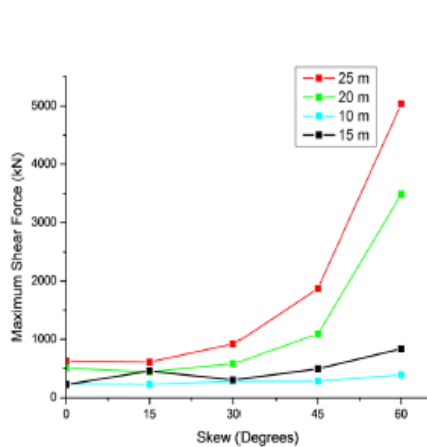


Figure 6: Maximum Shear Force Class70RW+A

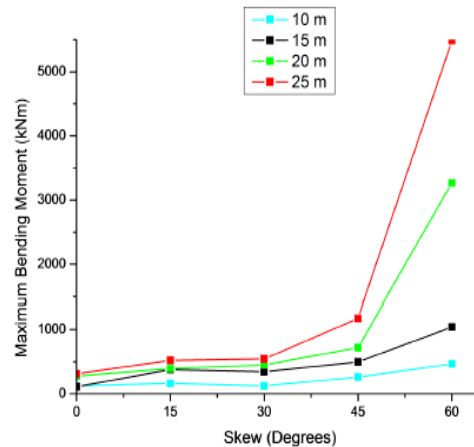


Figure 7: Maximum BM Class70RW+A

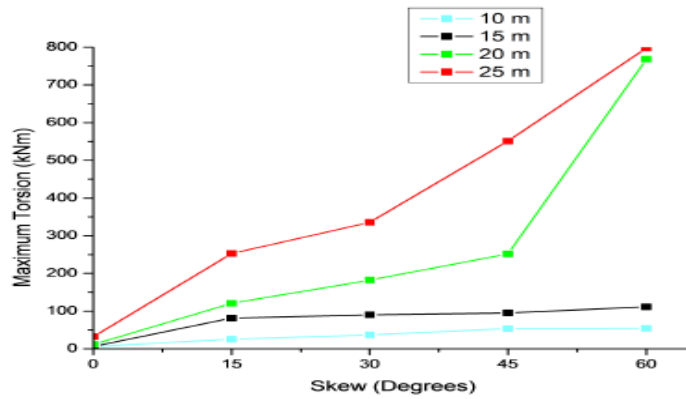


Figure 8: Maximum Torsion Class70RW+A

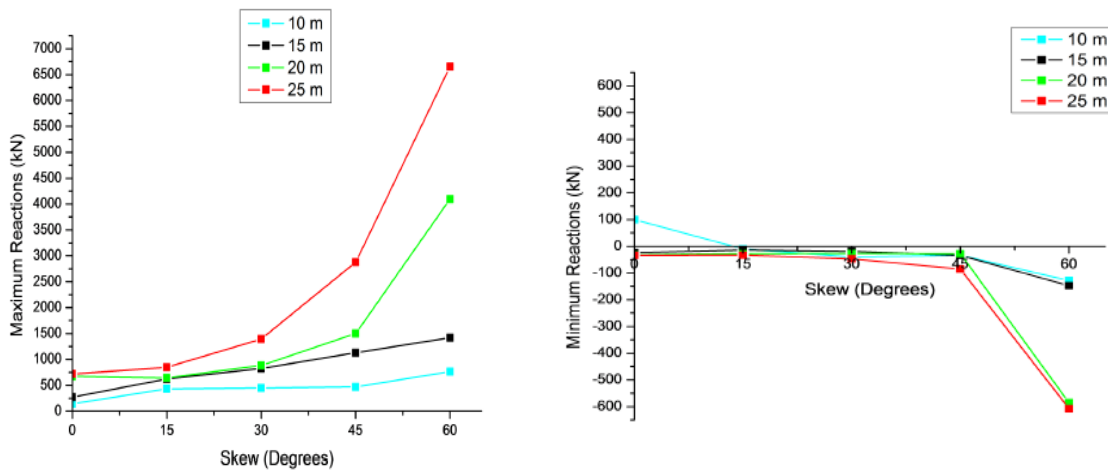


Figure 9: Maximum Positive Reaction Class70RW+A Figure 10: Maximum Negative Reaction Class70RW+A

5.1.3 Class 70R Tracked with Class A Vehicle : The Class 70R Tracked vehicle was placed centrally on G3 & G4 and Class A vehicle was placed at a minimum spacing of 1.2m (minimum spacing specified in IRC: 6 - 2000 for Class A vehicle) from 70R Wheeled Vehicle and moved over the span (Figure of placement of IRC loading over bridge is given in Annexure B). The maximum moments obtained in the girders G1, G2, G3, G4 and G5 were recorded. The maximum moment occurred simultaneously in all girders for 00 skew angle but for other skew angles it occurred with some lag due to skew effects. The lag increased with skew angle. A total of 700 KN load was applied in this loading on 4.57m distance

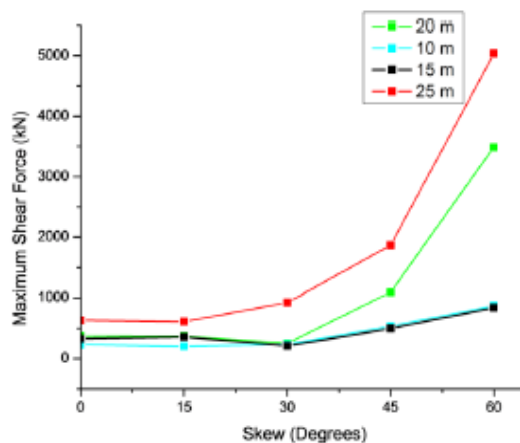


Figure 11: Maximum SF Class70RT+A

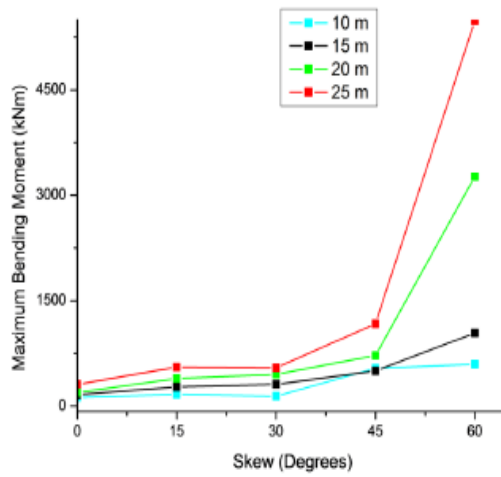


Figure 12: Maximum BM Class70RT+A

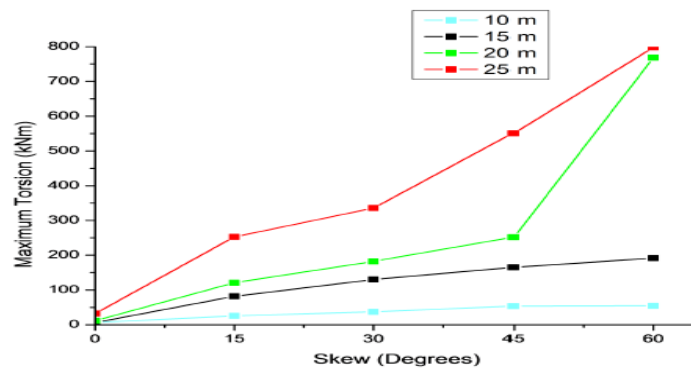


Figure 13: Maximum Torsion Class70RT+A

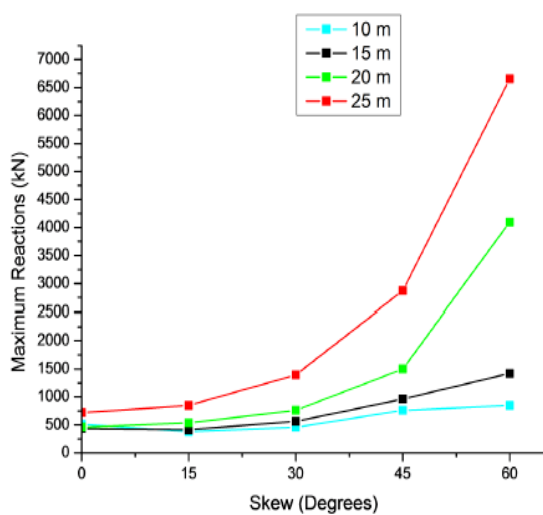


Figure 14: Maximum Positive Reaction Class70RT+A

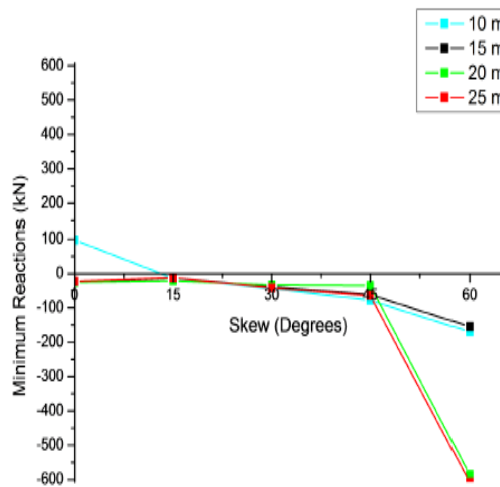


Figure 15: Maximum Negative Reaction Class70RT+A

VI. CONCLUSION

The analysis of bridges and comparisons of the results of different span and skew angles have led to the following conclusions.

- [1] For skew bridges the arrangement of cross girders perpendicular to the longitudinal girders is more effective in transverse load distribution as compared to the arrangement in which the cross girders are parallel to the abutments.
- [2] Grillage analogy method, based on stiffness matrix approach, is a reliably accurate method for a wide range of bridge decks. The method is versatile, easy for a designer to visualize and prepare the study for a grillage.
- [3] The increase in BM up to 40 degree skew angle is less. At higher skew angle sharp increase is observed. Results show that end girder placed in centre of skew span has maximum BM.
- [4] Torsion, with increase of skew angle increases appreciably in all directions.
- [5] Maximum positive and negative reactions are noted in skew bridges ,very close to each other
- [6] Results of SF shows mixed pattern i.e. value of maximum SF do not follow a regular pattern. However the difference of SF, as the span increases, decrease.
- [7]

REFERENCES

- [1] Trilok Gupta and AnuragMisra (2007) "Effect of Support Reaction of T-Beam Skew Bridges" ARPN Journal of Engineering and Applied Sciences, Vol 2, No.1, Feb (2007)
- [2] C. Menassa, M. Mabsout, K. Tarhini, and G. Frederick, "Influence of Skew Angle on Reinforced Concrete Slab Bridges" Journal of Bridge Engineering(ASCE) Vol. 12 (2007)
- [3] S. Maleki and V Bisadi, "Orthogonal effects in seismic analysis of skew bridges." Journal of Bridge Engineering(ASCE) Vol. 9 (2006)
- [4] Haoxiong H., Shenton, H. W and Chajes M. J., " Load Distribution for a Highly Skewed Bridge: Testing and Analysis" Journal of Bridge Engineering(ASCE) Vol. 9 No.6, Nov1(2004)
- [5] Khalo, A.R., and Mirzabozorg H "Load Distribution Factors in Simply Supported Skew Bridges." Journal of Bridge Engineering (ASCE), Vol. 8, No.4, July 1(2003).
- [6] Prestressed Concrete Institute (PCI manual) chapter 7.
- [7] Prestressed Concrete Institute (PCI manual) chapter 12.
- [8] Harrop J, "Ultimate Load Design of Skew Slabs by the Strip Method" Building Science Vol. 5 pp 117-121 (1970)
- [9] Alfred G. Bishara, "Wheel Load Distribution on simply supported Skew I Beam composite Bridges, Journal of Structural Engineering,(1993)
- [10] Ajit Singh, "Analysis of skew effects on slab bridges", M.Tech Dissertation (2006) IIT Roorkee.
- [11] PranayVasantRaoUrewar, "Analysis of skew effects on T-Girder Bridges", M.Tech Dissertation (2006) IIT Roorkee.
- [12] Mohammad A. Khaleel and Rafik Y. Itani, "Live-Load Moments for Continuous Skew Bridges" Journal of Structural Engineering, (ASCE) Vol 116 (1990)
- [13] BaidarBakht, "ANALYSIS OF SOME SKEW BRIDGES AS RIGHT BRIDGES" Journal of Structural Engineering, (ASCE) Vol 114 (1988)
- [14] Victor D J, "Essential's of Bridge Engineering" Oxford and IBH Publishing, New Delhi
- [15] C S Surana& R Agarwal, "Grillage Analogy in Bridge Deck Analysis", Narosa Publishing House, New Delhi
- [16] IRC 5-1998, "Standard Specification and Code of Practice for Road Bridges", Section 1 "General features of design", Indian Road Congress, New Delhi
- [17] IRC 6-2000, "Standard Specification and Code of Practice for Road Bridges", Section II "Loads And Stresses", Indian Road Congress, New Delhi
- [18] IRC 21-2000, "Standard Specification and Code of Practice for Road Bridges", Section III "Cement Concrete (plain & reinforced)", Indian Road Congress, New Delhi

Modelling Of Water Resources in Bakaru Hydropower Plant in Anticipating Load Increment in Sulsebar Power System

¹Sri Mawar Said , ²Salama Manjang , ³M.Wihardi Tjaronge , ⁴Muh. Arsyad Thaha

¹S3 students Civil Engineering , Electrical Engineering Lecture

² Civil Engineering Lecturer

³Hasanuddin University, Makassar-Indonesia.

ABSTRACT

Bakaru hydro power plan water resources model will describe a model in anticipating load growth in Sulsebar Power System until year 2030. Bakaru hydro power plan is supplied by Mamasa, Sumarorong, and Lembang watershed, water supply is influenced with rain fall volume, topography condition (steep slope, type of soil, and land use) of a water catchment area. A model is constructed using Fuzzy logic in water water inflow is $Y = 0,0687X^2 - 4,279X + 82,917$ and erosion inflow is $Y = -0.0001X^2 + 0.0106X + 0.117$, the model shows that increment in operation time at catchment area where there are changes in land uses will affected lower water inflow and bigger erosion inflow.

KEYWORD: watershed, Fuzzy logic, catchment area

I. INTRODUCTION

Bakaru hydro power plan is a power plan supplied by Garugureservoir which located at $3^{\circ}30'00'' - 2^{\circ}51'00''$ LS dan $119^{\circ}15'00'' - 119^{\circ}45'00''$ BT. The water resource is supplied by Mamasa watershed which the water flowing from Mamasa river in West Sulawesi to South Sulawesi. Bakaru hydro power plan is produce power to Sulsebar power system, power plan capacity is 2 x 63 MW with reservoir capacity is 6.919.000 m³ which is predict will be available for 50 years. Otherwise the power planreabilityin producing enery is decreased by year, because the disability of reservoir in saving maximal water volume. According to this situation it is really important to study the continuity of water supply by predicted the water inflow and erotion inflow inMamasa watershed.

II. REVIEW OF LITERATURE

Modelling of water resources of a hydro power plan is using the hydrolic side such as rainfall volume in water catchment area, and using the watershed characteristic. The watershed evaluated in the study is Mamasa, Sumarorong, and Lembang. The rainfall volume is really affected to water discharges in Bakaru power plan. The rainfall is records using Mamasa, Sumarorong, and Lembang recording station. The result of watershed characteristic (steep slope, type of soil, and land use) is described below.

Rainfall : Rainfall data of Mamasa, Sumarorong, and Lembang station reported from Metereology, Climatology and Geofisic department in Marosfrom year 1990 to 2012 is using to predict the rainfall for year 2013 to year 2030. The result is shown in table 1 below.

Table 1.Data Base and Data Result of Mamasa Watershed

Year	Data Base and Data Result of Mamasa Watershed (mm)											
	Mamasa Station				Sumarorong Station				Lembang Station			
	1995	2012	2017	2030	1995	2012	2017	2030	1995	2012	2017	2030
January	201	210	152	193	295	249	334	341	286	261	379	184
February	297	113	103	111	399	173	196	309	514	458	624	149
March	142	77	227	160	276	423	425	306	310	376	469	361
April	183	246	296	290	395	445	358	375	354	313	643	470
May	193	99	170	128	407	296	201	252	375	211	313	233
June	247	135	174	128	490	370	281	181	192	231	251	339
July	141	44	69	66	202	195	153	200	209	175	197	180
August	45	22	44	94	70	423	425	306	8	19	152	164
September	86	116	25	132	192	173	195	193	135	62	200	189
October	198	218	107	152	319	296	201	252	32	220	163	169
November	440	223	206	228	501	370	281	181	319	478	345	342
December	62	63	97	148	208	303	315	287	308	527	503	227

Topography : Topography of Bakarwater catchment area is describe the steep slope, type of soil, and land use of Mamasa, Sumarorong, and Lembang. Steep slope is classified as flat, ramps, rather steep, steep andvery steep. The steep slope is shown in table 2 below.

Table 2.Steep Slope of Mamasa Watershed

Steep Slope of Mamasa Watershed		
Mamasa Area	Sumarorong Area	Lembang Area
Kanora Village: 45 - 60 % (steep – very steep)	Salubalo Village: 20 – 45 % (rather steep – steep)	Bakaru Village: 10 – 20 % (ramps – rather steep)
Minangatalu Village: 17 – 25 % (rather steep)	Lepangan Village: 12 – 25 % (ramps – rather steep)	Kaluku Village: 12 – 25 % (ramps – rather steep)
Rantetambola Village: 20 - 45 % (rather steep – steep)	Pakawan Village: 15 – 25 % (ramps - rather steep)	Rampusa Village: 45 - 60 % (steep – rather steep)
Salumata Village: 25 – 45 % (rather steep – steep)	Paladan Village: 8 – 15 % (ramps)	Bakka Village: 20 – 45 % (rather steep – steep)
Pena Village: 10 – 25 % (ramps – rather steep)	Beting Village: 17 - 25 % (rather steep)	Lamba Village: 45 - 60 % (steep – very steep)
	Salinduk Village: 17 – 30 % (rather steep – steep)	Katumbangan Village: 20 – 45 % (rather steep – steep)
Average: 31.7 % (rather steep)	Average: 18.9 % (rather steep)	Average: 37.7 % (steep)

Type of soil of Bakarwater catchment area generally sensitivy to erosion, this is effected by land variety, that construct the area which is Litosol and Lateric. The description is shown in table 3.

Table 3.Type of Soil of Mamasa Watershed

Type of Soil of Mamasa Watershed		
Mamasa Area	Sumarorong Area	Lembang Area
Kanora Village: Laterik – Litosol (sensitive: score 60 – very sensitive: score 30)	Salubalo Village: Laterik – Litosol (sensitive: score 60 - very sensitive: score 30 - sensitive: score 30)	Bakaru Village: Litosol – Cacao forest (rather sensitive: score 30 – medium sensitive: score 45)
Minangatalu Village: Litosol (rather sensitive: score 30)	Lepangan Village: Litosol – Laterik (rather sensitive: score 30 - sensitive: score 30)	Kaluku Village: Litosol – Laterik (rather sensitive: score 30 - sensitive: score 30)
Rantetambola Village: Laterik – Litosol (sensitive: score 60 – very sensitive: score 30)	Pakawan Village: Litosol (very sensitive: score 75)	Rampusa Village: Laterik – Litosol (sensitive: score 60 – very sensitive: score 30)
Salumata Village: Laterik – Litosol (sensitive: score 60 – very sensitive: score 30)	Paladan Village: Planosol - Litosol (not sensitive: score 15 - rather sensitive: score 30)	Bakka Village: Laterik – Litosol (sensitive: score 60 – very sensitive: score 30)
Pena Village: Litosol - Cacao forest (rather sensitive: score 30 – medium sensitive: score 45)	Beting Village: Litosol (rather sensitive: score 30)	Lamba Village: Laterik – Litosol (sensitive: score 60 – very sensitive: score 30)
	Salinduk Village: Laterik – Litosol (sensitive: score 60 – very sensitive: score 30)	Katumbangan Village: Laterik – Litosol (sensitive: score 60 – very sensitive: score 30)
Average: score 54 (sensitive)	Average: score 48 (medium sensitive)	Average: score 63 (sensitive)

The land uses in Bakarwater watershed are dominated by forest, pine forest and moor. The description of land used is shown in table 4.

Tabel 4.Land Use of Mamasa Watershed

Land Use of Mamasa Watershed		
Mamasa Area	Sumarorong Area	Lembang Area
Kanora Village: forest (score 10) - moor (score 30)	Salubalo Village: forest(score 10) - moor (score 30)	Bakaru Village: forest(score 10) - moor (score 30)
Minangatalu Village:forest (score 10) - moor (score 20)	Lepangan Village: forest (score 10) - moor (scorer 20)	Kaluku Village: forest (score 10) - moor (score 20)
Rantetambola Village: forest (score 15) - moor (score 25)	Pakawan Village: forest (score 10) - moor (score 30)	Rampusa Village: forest (score 15) - moor (score 25)
Salumata Village: forest (score 15) - moor (score 35)	Paladan Village: forest (score 15) - moor (score 35)	Bakka Village: forest (score 15) - moor (score 35)
Pena Village: forest (score 10) - moor (score 10)	Beting Village: forest (score 10) - moor (score 20)	Lamba Village: forest (score 10) - moor (score 20)
	Salinduk Village: forest (score 15) - moor (score 35)	Katumbangan Village: forest (score 15) - moor (score 35)
Average: score 18 (forest - moor)	Average: score 20 (forest - moor)	Average: score 20 (forest - moor)

III. RESEARCH METHOD

Modelling Water Resources : Modelling water resource using Fuzzy logic, with input parameter are rainfall, steep slope, type of soil and land use, the flowchart of power plan inflow is shown in picture 1 below.

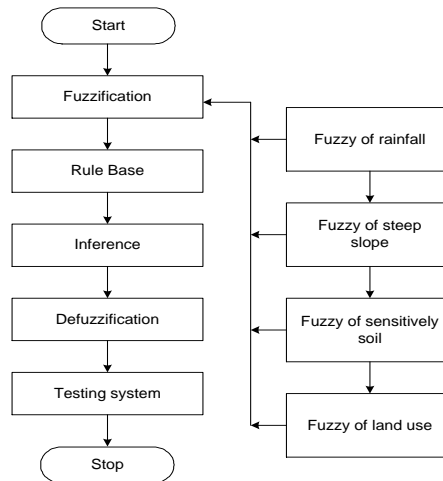


Figure 1.Flowchart inflow Hydro Power Plan

The result of water inflow and erotion inflow in Bakar hydro power plan is the accumulative of inflow prediction result of Mamasa, Sumarorong, and Lembang. The result is shown in table 5 and table 6.

Table 5.Water Inflow in Bakar Power Plan

Results of water inflow (m ³ /sec.)					
Year	Inflow	Year	Inflow	Year	Inflow
1995	74.16	2007	46.80	2019	19.90
1996	67.25	2008	52.34	2020	18.63
1997	44.28	2009	19.05	2021	18.79
1998	83.16	2010	19.25	2022	17.49
1999	68.81	2011	20.54	2023	18.37
2000	57.81	2012	20.93	2024	17.92
2001	60.96	2013	21.02	2025	18.17
2002	63.23	2014	20.31	2026	16.32
2003	57.58	2015	20.08	2027	17.94
2004	59.25	2016	19.72	2028	17.88
2005	59.16	2017	19.93	2029	19.43
2006	35.64	2018	19.78	2030	16.00

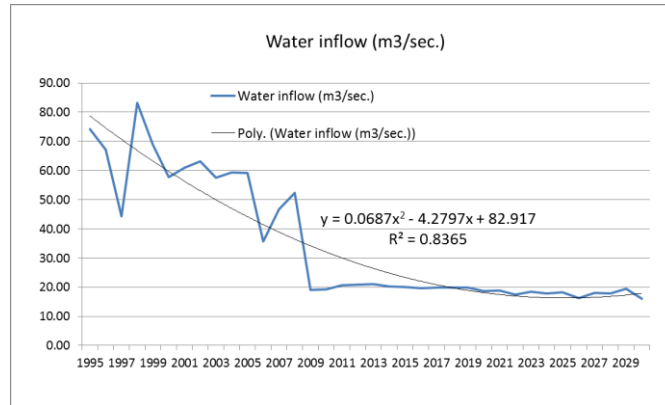


Figure 3. Water Inflow Curve of Bakaru Power Plan

Table 6. The Erosion Inflow Result of Bakaru Power Plan

Results of erosion inflow (m3/sec.)					
Year	Inflow	Year	Inflow	Year	Inflow
1995	0.11	2007	0.35	2019	0.31
1996	0.13	2008	0.67	2020	0.33
1997	0.15	2009	0.25	2021	0.34
1998	0.18	2010	0.25	2022	0.32
1999	0.18	2011	0.27	2023	0.33
2000	0.18	2012	0.26	2024	0.32
2001	0.19	2013	0.27	2025	0.32
2002	0.19	2014	0.26	2026	0.33
2003	0.20	2015	0.28	2027	0.34
2004	0.21	2016	0.33	2028	0.32
2005	0.21	2017	0.28	2029	0.35
2006	0.21	2018	0.29	2030	0.33

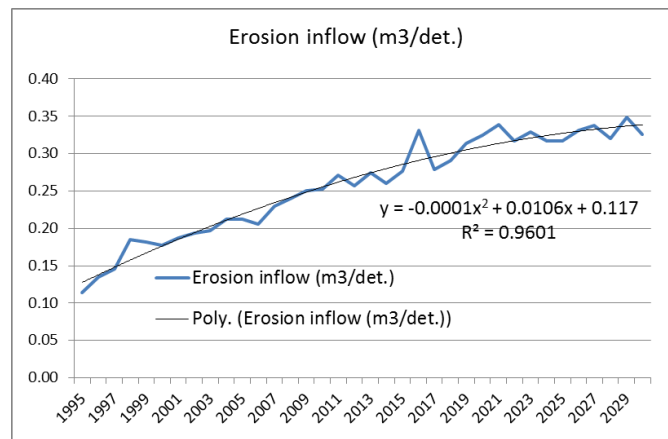


Figure 4. Erosion Inflow Curve of Bakaru Power Plan

IV. CONCLUSIONS

Water resources model of Bakarupower plan could be describe as polynomial model $Y = 0,0687X^2 - 4,279X + 82,917$ and erosion inflow could be describe as $Y = - 0.0001X^2 + 0.0106X + 0.117$, the model shows that by the increment of operate time of hydro power plan where there are changes in land use at catchment area will affected the decresement in water inflow and the increment in erosion inflow.

Average power produce by Bakaru hydro power plan in year 2013 to 2030 is 1 x 63 MW or half of its capacity, therefore the energy produce is decreased.

REFERENCE

- [1] Abdul wahid, "Sendiment Rate Progress Model in Bakaru Reservoir Caused by Sub DAS Mamasa Erotion - *Model Perkembangan Laju Sedimentasi di waduk Bakaru Akibat Erosi yang Terjadi di Hulu Sub DAS Mamasa*", Smartek Journal, volume 7. N0. Pebruari 2009: 1-12, <http://jurnal.untad.ac.id/jurnal/index.php/SMARTEK/article/view/576>, accesed on February 7th 2013.
- [2] Sri Mawar Said, "Arima Application as an Alternative Method of Rainfall Forecasts In Watershed Of Hydro Power Plant", International Journal of Computational Engineering Research, www.ijceronline.com/papers/Vol3_issue9/part%201/I0391068073.pdf.
- [3] Sri Mawar Said, "Optimization Model of Water Resources in Bakaru Hydro Power Plan in Anticipating Load Increment in Sulsebar power System" - Model Optimasi Sumber Daya Air PLTA Bakaru dalam Mengantisipasi Perkembangan Beban pada Sistem Kelistrikan Sulsebar" National Seminar Informatics Techniques (SNATIKA) 2013 www.unhas.ac.id/elektro/snatika.
- [4] Sri Mawar Said, "The Role of Mamasa Watershed Towards Bakaru Power Plan Water Resources" Seminar on Intelligent Technology and its Application (SITIA) 2014, Electrical Engineering Departement Faculty of Industrial Technology Institut Teknologi Sepuluh Nopember (ITS), <http://www.its.ac.id>

Performance Analysis of Neighbour Coverage Probabilistic Rebroadcast to Reduce the Routing Overhead Over Ad-hoc On Demand Distance Vector Protocol

Ms. Rajeshree Ambulkar¹, Prof. Milind Tote²

¹ Dept. of Comp. Science & Engg, Nuva College of Engineering, & Technology, Nagpur, R. T. M. Nagpur
University Nagpur, Maharashtra, India

² Computer Science & Engineering, Gurunanak College of Engineering, Nagpur, R. T. M. Nagpur University
Nagpur, Maharashtra, India

ABSTRACT:

MOBILE ad hoc networks (MANETs) consist of a collection of mobile nodes which can move freely. These nodes can be dynamically self-organized into arbitrary topology networks without a fixed infrastructure. One of the fundamental challenges of MANETs is the design of dynamic routing protocols with good performance and less overhead. Many routing protocols, such as Ad hoc On-demand Distance Vector Routing (AODV) [1] and Dynamic Source Routing (DSR) [2], have been proposed for MANETs. The above two protocols are on demand routing protocols, and they could improve the scalability of MANETs by limiting the routing overhead when a new route is requested [3]. However, due to node mobility in MANETs, frequent link breakages may lead to frequent path failures and route discoveries, which could increase the overhead of routing protocols and reduce the packet delivery ratio and increasing the end-to-end delay [4]. Thus, reducing the routing overhead in route discovery is an essential problem. Existing routing protocol for MANETS has a problem that they used broadcasting which induces excessive redundant retransmissions of RREQ packet and causes the broadcast storm problem, which leads to a considerable number of packet collisions, especially in dense networks. Because of this routing overhead of network increases which leads to broadcast storm problem. Therefore the proposed system try to reduce this routing overhead.

KEYWORDS: Mobile ad hoc networks, neighbor coverage, network connectivity, probabilistic rebroadcast, routing overhead.

I. INTRODUCTION

The ad hoc WLANs do not need any fixed infrastructure. MANETs are self-organizing and adaptive in that the topology of a formed network can change on-the-fly without the intervention of a system administrator [4, 9]. Although MANETs share many of the properties of the traditional wired networks, they possess certain unique characteristics which derive from the inherent nature of their wireless communication medium and the distributed function of their medium access mechanisms. The issues involved may be categorized as follows. Wireless Channel: The wireless communication medium (or channel) is susceptible to a variety of transmission impediments such as path loss, interference and blockage [10,11]. These factors restrict the range, data rate and reliability of the wireless transmission. A signal is considered successfully received at a node if the measured signal to interference and noise ratio (SINR) is large enough to be decoded. Typically, the transmitted signal has a direct path component between the transmitter and receiver [10]. Other components of the transmitted signal referred to as multi-path components are signals reflected, diffracted or scattered by the environment, and arrive at the receiver shifted in amplitude, frequency and phase with respect to the direct-path component [10].

II. AD HOC ON-DEMAND DISTANCE VECTOR (AODV) ROUTING

AODV is a reactive routing protocol that establishes a route to a destination on an on-demand basis, i.e. a route is established only when it is required by a source node for transmitting data packets. This is beneficial to mobile environments such as MANETs since fully up-to-date knowledge of all routes from every node implies large communication overhead. The routing mechanism of AODV consists of two processes; route discovery and route maintenance. When a source node needs to send data, but does not already have a valid

route to the destination, it initiates a route discovery process in order to locate the destination. A route request (RREQ) packet is disseminated throughout the entire network via simple flooding [7]. The RREQ packet contains the following main fields: source identifier, destination identifier, source sequence number, destination sequence number (created by the destination to be included along with any route information it sends to requesting nodes), broadcast identifier and time-to-live. The destination sequence number is used by AODV to ensure that routes are loop-free and contain the most recent route information [6, 7]. Each intermediate node that forwards an RREQ packet creates a reverse route back to the source node by imprinting the next hop information in its routing table. Once the RREQ packet reaches the destination or an intermediate node with a valid route, the destination or intermediate node responds by unicasting a route reply (RREP) packet to the source node using the reverse route. The validity of a route at the intermediate nodes is determined by comparing its sequence number with the destination sequence number. Each node that participates in forwarding the RREP packet back to the source creates a forward route to the destination by imprinting the next hop information in the routing table. Nodes along the path from source to destination are not required to have knowledge of which nodes are forming the path other than the next hop nodes to the source and destination. The next phase of the routing mechanism is the route maintenance process. After the route discovery process and as long as the discovered route is used, the intermediate nodes along the active route maintain an up-to-date list of their 1-hop neighbors by means of a periodic exchange of "hello" packets. Also, when the route becomes inactive, i.e. no data is sent over it, a timer is activated, after the expiration of which the route is considered stale and expires. If the routing agent (i.e. AODV) at a node becomes aware of a link breakage for an active route, a Route Error (RERR) packet is generated at the point of breakage. This is then disseminated to the appropriate nodes participating in the route's formation and those nodes actively using the route. The nodes affected by the invalid route mark it for expiration since it is no longer useful. In this fashion, the RERR packet propagates to the source node which can then initiate a new route discovery phase.

III. Neighbour Coverage Probabilistic Protocol (NCPR)

To implement new approach, the Neighbor Coverage-based Probabilistic Rebroadcast protocol is used for reducing routing overhead in route discovery. To implement the the NCPR protocol we modify the source code of AODV in NS-2.32. and also we have to calculate the uncovered neighbor set and rebroadcast delay. To obtain the neighbor information the proposed NCPR protocols Required HELLO packets and also requires to carry the neighbor list in RREQ packets. So we implement the following algorithm called it as NCPR algorithm, which described as follows.

Algorithm

Definition:

RREQ_v: RREQ packet received from node v

R_v.id: The unique identifier (id) for RREQ_v

N(u): NEIGHBOR SET OF NODE u

U(u,x): Uncovered neighbors set of node u for RREQ whose id is x.

Timer (u,x): Timer of node u for RREQ packet whose id is x.

{Note: In the actual implementation of NCPR protocol every different RREQ needs a UCN set and a Timer }

1. If n_i receive a new RREQ_s from s then
 2. {compute initial uncovered neighbors set U (n_i, R_s. id) for RREQ_s }
 3. $U (n_i, R_s. id) = N(n_i) - [N(n_i) \cap N(s)] - \{s\}$
 4. { compute rebroadcast delay T_d(n_i) }
- $$T_p(n_i) = 1 - \frac{|N(s) \cap N(n_i)|}{|N(s)|}$$
5. T_d(n_i) = MaxDelay × T_p(n_i)
 6. Set a timer (n_i, R_s. id) according to T_d(n_i)
 7. End if
 8. While n_i receive a duplicate RREQ_j from n_j before Timer (n_i, R_s. id) expire do
 9. { Adjust U(n_i, R_s. id): }
 10. $U(n_i, R_s. id) = U(n_i, R_s. id) - [U(n_i, R_s. id) \cap N(n_j)]$
 11. Discard (RREQ_j)
 12. End while
 13. If timer (n_i, R_s. id) expire then
 14. {compute the rebroadcast probability P_{re}(n_i)}
 15. $R_a(n_i) = \frac{|U(n_i)|}{|N(n_i)|}$

- $$F_c(n_i) = \frac{N_c}{|N(n_i)|}$$
16. $F_c(n_i) = \frac{N_c}{|N(n_i)|}$
 17. $Pre(n_i) = F_c(n_i) \cdot Ra(n_i)$
 18. If $Random(0,1) \leq Pre(n_i)$ then \
 19. Broadcast (RREQs)
 20. Else
 21. Discard (RREQs)
 22. End if
 23. End if

Protocol Implementation

We modify the source code of AODV in NS-2 (v2.30) to implement our proposed protocol. Note that the proposed NCPR protocol needs Hello packets to obtain the neighbour information, and also needs to carry the neighbour list in the RREQ packet. Therefore, in our implementation, some techniques are used to reduce the overhead of Hello packets and neighbour list in the RREQ packet, which are described as follows: . In order to reduce the overhead of Hello packets, we do not use periodical Hello mechanism. Since a node sending any broadcasting packets can inform its neighbours of its existence, the broadcasting packets such as RREQ and route error (RERR) can play a role of Hello packets. We use the following mechanism [12] to reduce the overhead of Hello packets: Only when the time elapsed from the last broadcasting (RREQ, RERR, or some other broadcasting packets) is greater than the value of Hello Interval, the node needs to send a Hello packet. The value of Hello Interval is equal to that of the original AODV.. In order to reduce the overhead of neighbour list in the RREQ packet, each node needs to monitor the variation of its neighbour table and maintain a cache of the neighbour list in the received RREQ packet. We modify the RREQ header of AODV, and add a fixed field `num_neighbours` which represents the size of neighbour list in the RREQ packet and following the `num_neighbours` is the dynamic neighbour list. In the interval of two close followed sending or forwarding of RREQ packets, the neighbour table of any node n_i has the following three cases: - if the neighbour table of node n_i adds at least one new neighbour n_j , then node n_i sets the `num_neighbours` to a positive integer, which is the number of listed neighbours, and then fills its complete neighbour list after the `num_neighbours` field in the RREQ packet. It is because that node n_j may not have cached the neighbour information of node n_i , and, thus, node n_j needs the complete neighbour list of node n_i ;- if the neighbour table of node n_i deletes some neighbours, then node n_i sets the `num_neighbours` to a negative integer, which is the opposite number of the number of deleted neighbours, and then only needs to fill the deleted neighbours after the `num_neighbours` field in the RREQ packet; - if the neighbour table of node n_i does not vary, node n_i does not need to list its neighbours, and set the `num_neighbours` to 0. The nodes which receive the RREQ packet from node n_i can take their actions according to the value of `num_neighbours` in the received RREQ packet: - if the `num_neighbours` is a positive integer, the node substitutes its neighbour cache of node n_i according to the neighbour list in the received RREQ packet; - if the `num_neighbours` is a negative integer, the node updates its neighbour cache of node n_i and deletes the deleted neighbours in the received RREQ packet; - if the `num_neighbours` is 0, the node does nothing. Because of the two cases 2 and 3, this technique can reduce the overhead of neighbours list listed in the RREQ packet.

IV. PERFORMANCE ANALYSIS OF NEIGHBOUR COVERAGE PROBABILISTIC ROUTING PROTOCOL OVER AD-HOC ON DEMAND DISTANCE VECTOR ROUTING PROTOCOL.

4.1 Performance of NCPR over AODV of End –to-End Delay

Table 1 shows the end-to-end delay by using Ad-hoc on demand .Distance Vector Protocol and Neighbor Coverage Probabilistic Routing Protocol (NCPR). It shows that the Neighbor Coverage Probabilistic Routing Protocol (NCPR) reduce the end to end delay in between nodes as compare to Ad-hoc on demand.

Sr. No.	No. Of Nodes	End- to- End Delay in AODV	End- to- End Delay in NCPR
1	50	0.05	0.15
2	100	0.07	0.09
3	150	0.21	0.05
4	200	0.29	0.18
5	250	0.52	0.10
6	300	1.21	0.27

Table 1. End- to- End Delay in AODV & NCPR

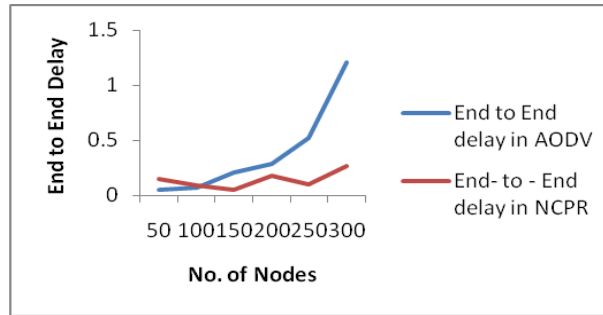


Figure 1. Graphical representation on End to End delay in NCPR & AODV

Distance Vector Protocol on X- axis shows the number of nodes and on Y-axis shows the end to end delay, also red lines shows the end to end delay with Neighbor Coverage Probabilistic Protocols where the green lines shows the end to end delay with Ad-hoc On Demand Distance Vector Protocol.

4.2 Performance of NCPR over AODV of Normalizing Routing Overhead

Table 2 shows the difference in Routing Overhead in route discovery by using Ad-hoc On demand Distance Vector Protocol (AODV) and Neighbour Coverage Probabilistic Routing Protocol (NCPR)., It shows that the routing overhead in route discovery is reduced by the Neighbor Coverage Probabilistic Routing Protocol (NCPR).

Sr. No.	No. Of Nodes	Normalizing Routing Overhead in AODV	Normalizing Routing Overhead in NCPR
1	50	0.63	0.55
2	100	2.58	1.22
3	150	3.63	1.50
4	200	4.70	2.01
5	250	7.09	3.73
6	300	20.87	7.59

Table 2. Normalizing Routing Overhead in AODV & NCPR

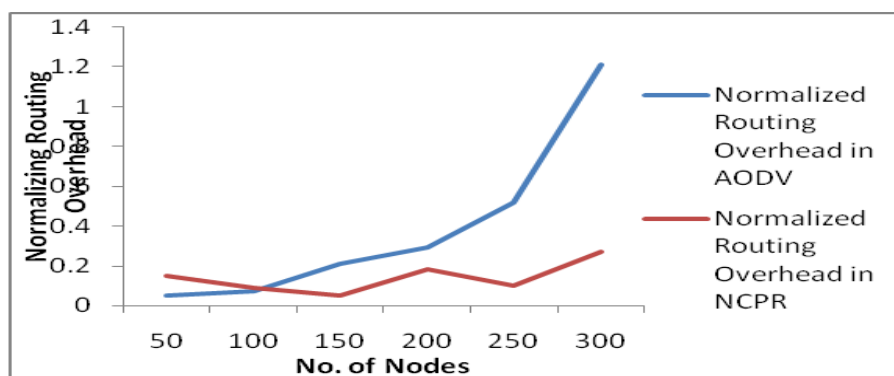


Figure 2. Graphical Representation of Normalizing Routing Overhead in AODV & NCPR

On X- axis shows the number of nodes and on Y-axis shows the Routing Overhead , also red lines shows the end to end delay with Neighbor Coverage Probabilistic Protocols where the green lines shows the end to end delay with Ad-hoc On Demand Distance Vector Protocol

4.3. Performance of NCPR over AODV of Packet Delivery Ratio in NCPR

Table 3 shows the difference in Packet Delivery Ratio by Ad-hoc On demand Distance Vector Protocol (AODV) and Neighbor Coverage Probabilistic Routing Protocol (NCPR)., It shows that the Packet Delivery Ratio is increases by the Neighbor Coverage Probabilistic Routing Protocol (NCPR).

Sr. No.	No. Of Nodes	Packet Delivery Ratio in AODV	Packet Delivery Ratio in NCPR
1	50	98.93	98.14
2	100	97.28	98.31
3	150	97.26	98.22
4	200	96.84	95.78
5	250	90.49	98.08
6	300	82.34	88.23

Table 3. Packet Delivery Ratio of AODV & NCPR

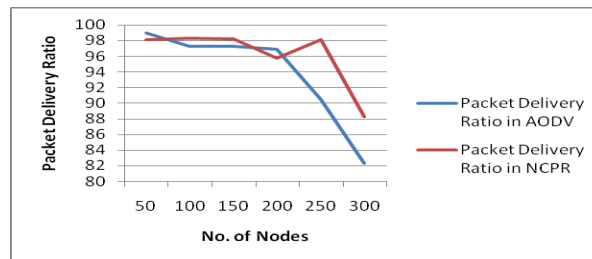


Figure 3. Graphical Representation of Packet Delivery Ratio in AODV & NCPR

On X- axis shows the number of nodes and on Y-axis shows the Packet delivery Ratio, also red lines shows the end to end delay with Neighbor Coverage Probabilistic Protocols where the green lines shows the end to end delay with Ad-hoc On Demand Distance Vector Protocol

V. CONCLUSION AND FUTURE SCOPE

Because of less redundant rebroadcast, the proposed protocol mitigates the network collision and contention, so as to increase the packet delivery ratio and decrease the average end-to-end delay. The simulation results also show that the proposed protocol has good performance when the network is in high density or the traffic is in heavy load. Because of node mobility in MANETs, always there is a greater chance of frequent link breakages between nodes. These frequent link breakages will cause a number of rebroadcasts between nodes and routing overhead. The proposed system robust for reducing routing overhead in MANETs, which uses additional coverage ratio, connectivity factor and high signal strength. Because of less redundant rebroadcast the proposed protocol mitigates the network connection, so as to increase the packet delivery ratio and decrease the average end-to-end delay, thus Quality of service (QOS) routing is maintained. In future this method can be used to check the suitability in VANETS and the same has to be implemented.

REFERENCES

- [1] C. S. L. M. S. Committee, "Wireless LAN Medium Access Control (MAC) and Physical Layer (PHY) Specifications," IEEE Standard 802.11-1997. Retrieved on January 2, 2008, from IEEE 802.11 Wireless Local Area Networks Website:<http://www.ieee802.org/11>, 1997.
- [2] J. D. Day and H. Zimmerman, "The OSI reference model," Proceedings of the IEEE, vol. 71, pp. 1334-1340, December, 1983.
- [3] P. S. Henry and H. Lou, "Wi-Fi: what's next," IEEE Communications Magazine, vol. 40, pp. 66-72, December 2002.
- [4] C. S. R. Murphy and B. S. Manoj, Ad Hoc Wireless Networks: Architectures and Protocols. New Jersey: Prentice Hall PTR, May 24, 2004.
- [5] P. Rauschert, A. Honarbacht, and A. Kummert, "On the IEEE 802.11 IBSS and its timer synchronization function in multi-hop ad hoc networks," Proceedings of 1st International Symposium on Wireless Communication Systems'207, pp. 304-308, September, 2004.
- [6] C. E. Perkins and P. Bhagwat, "Highly dynamic destination-sequenced distance vector routing (DSDV) for mobile computers," Proceedings of ACM SIGCOMM'94, pp. 234-244, September 1994.
- [7] C. Perkins, E. Belding-Royer, and S. Das, "Ad hoc On-Demand Distance Vector (AODV) Routing," IETF Mobile Ad Hoc Networking Working Group INTERNET DRAFT, RFC 3561, July 2003, <http://www.ietf.org/rfc/rfc3561.txt>. Experimental RFC, retrieved in October 2007.
- [8] S. Basagni, M. Conti, S. Giordano, and I. Stojmenovic, Mobile Ad hoc Networking. Hoboken, NJ; [Chichester]: John Wiley, 2004.
- [9] C. K. Toh, Ad-hoc Mobile Wireless Networks: Protocols and Systems, 1st ed: Prentice Hall, Inc., December 3, 2001.
- [10] S. Y. Tan, M. Y. Tan, and S. H. Tan, "Multipath delay measurements and modeling for interfloor wireless communications," IEEE Transactions on Vehicular Technology, vol. 49, pp. 1334-1341, July, 2000.
- [11] G. Lin, G. Noubir, and R. Rajamaran, "Mobility Models for Ad hoc Network Simulation," Proceedings of 23rd Conference of the IEEE Communications Society (INFOCOM 2003), vol. 1, pp. 454-463, March 2004.
- [12] V. Ramasubramanian, "SHARP: A Hybrid Adaptive Routing Protocol for Mobile Ad Hoc Networks," Proceedings ACM Mobihoc, pp. 303-314, June 2003.

Simulation of Two-Concentric Ring Microstrip Patch Antenna

Dr. K. Kumar Naik¹, Harini Appana², Prasanth Palnati³, Priyanka Kotte⁴

¹Professor, ^{2,3,4}Student, Department of Electronics and Communication Engineering,
K L University, Vaddeswaram, Guntur District, A.P, India.

ABSTRACT:

In this paper, we are analyse a two-concentric microstrip patch antenna for GPS application. In the literature survey, most of the literatures are available on different types of antennas, but few publications are available on microstrip patch antenna for GPS application. Microstrip patch antennas are very compact and low in cost. The concentric array has high directivity when compared to the linear array and this concept is applied to the microstrip patch. We are able to obtain low return loss. In view of that, we are designed a concentric circular microstrip patch antenna.

I. INTRODUCTION

There are various ways to model a microstrip patch. This modelling is used to predict characteristics of a microstrip patch such as resonant frequency, bandwidth, radiation pattern, etc. Each GPS satellite transmits signals on two frequencies: L1 (1575.42 MHz) and L2 (1227.60 MHz). The L1 frequency contains the civilian Coarse Acquisition (C/A) Code as well as the military Precise (P) Code. The L2 frequency contains only the P code. The P code is encrypted by the military using a technique known as anti-spoofing and is only available to authorized personnel.

A novel coupling technique for circularly polarized square ring patch antenna is developed and discussed in [1]. The circular polarization (CP) radiation of the square-ring patch antenna is achieved by a simple microstrip feed line through the coupling of a square patch on the same plane of the antenna. Proper positioning of the coupling square patch excites two orthogonal resonant modes with 90 phase difference, and a pure circular polarization is obtained. The dielectric material is a square block of ceramic with a permittivity of 58 and that reduces the size of the antenna.

The prototype has been designed, fabricated and found to have an impedance bandwidth of 1.1% and a 3-dB axial-ratio bandwidth of about 0.03% at GPS frequency of 1573 MHz. The characteristics of the proposed antenna have been studied by simulation software HFSS and experiments. The measured and simulated results are in good agreement. In article [2], the authors have endeavoured to design a gap-coupled concentric ARMSA on the basis of equivalent circuit model. The inner ring is a feed, and the outer ring is a parasitic element. The effect of mutual coupling is also taken into account along with variation of feed point and gap between the rings. The gap-coupled ARMSA can be used for dual band operation and especially in mobile communication. The main focus is on the effect of the gap length and feed point on the radiation pattern of the gap-coupled ARMSA.

A new defected ground structure (DGS) presented [3, 4] consisting of concentric circular rings in different configurations is experimentally studied to examine the stop-band characteristics. Unlike previous DGS designs, a metallic shielding is introduced at the back of the DGS to suppress any leakage or radiation, and this would be advantageous for microwave circuit applications. A wide stop band is demonstrated with a set of prototypes designed for X-band is presented. Its application to suppressing mutual coupling in microstrip patch arrays is demonstrated. The author [5] describes a novel compact solution for integrating a Global Positioning System (GPS) and a Satellite Digital Audio Radio Service (SDARS) antenna in a very small volume to satisfy the requirements of the automotive market. The GPS antenna is a classic small commercial ceramic patch, and the SDARS antenna is designed in order to fit in the reduced space without affecting radiation and band performance of the GPS antenna. The SDARS basic geometry is a square-ring microstrip antenna operating in the frequency range 2.320–2.345 GHz with left-hand circular polarization (LHCP), and it is wrapped around the GPS patch, which receives a right-hand circular polarization (RHCP) signal at 1.575 GHz. The overall volume of the presented integrated antenna solution is only 30X30X7.6mm³, rendering it attractive for the automotive market.

Several authors [6-11] has presented different models to obtain the optimum design. The analysis and design of two-concentric ring antenna has proposed dual-band for GPS applications. Here, we considered different dielectric materials to obtain dual-bands.

II. ANALYSIS OF TWO-CONCENTRIC RING MICROSTRIP ANTENNA:

There are various ways to model a microstrip patch. This modelling is used to predict characteristics of a microstrip patch such as resonant frequency, bandwidth, radiation pattern, etc. In this section the transmission line model and is presented. This model is based on some assumptions, which simplify the calculations at the cost of less accuracy.

Figure 1 shows the proposed antenna consists of two-concentric rings arranged in a single plane above a single substrate. In the concentric circular ring microstrip patch antenna, the structure having physical gap is shown. The inner ring is fed coaxially, while the outer ring is a parasitic element. Now, this can also be shown as a parallel gap-coupled radiator using planar waveguide mode for inner ring and outer ring as shown in figure. The characteristic impedance of the two gap-coupled concentric circular ring microstrip patch antenna radiator can be analyzed by applying the theory of coupled microstrip antenna.

The input impedance characteristics of the gap-coupled circular ring microstrip patch antenna can be analyzed. Figure which shows two-gap coupled annular ring antennas in which inner one is fed at point $(x, 0)$ by a coaxial cable ($a1 < x < b1$), where $a1$ and $b1$ are inner and outer radii of the inner ring and outer ring, respectively. The thickness of the substrate h is small as compared to the difference between the inner and outer radii of the inner ring

The reflection coefficient can be calculated as

$$\rho = \frac{Z_{in} - Z_0}{Z_{in} + Z_0} \quad (1)$$

Z_0 is impedance of the coaxial feed = 50 ohms

Z_{in} is input impedance of microstrip antenna

$$VSWR = \frac{1 + |\rho|}{1 - |\rho|} \quad (2)$$

The return loss of the antenna is

$$RL = -10 \log \left(\frac{1}{\rho^2} \right) \quad (3)$$

Radiation pattern of antenna can be calculated by

$$E_{\theta} = \left[\sum_{t=1}^N a_t E_{at} J_1'(ka_t \sin \theta) - \sum_{t=1}^N b_t E_{bt} J_1'(kb_t \sin \theta) \right] \cos \phi \quad (4)$$

Where, E_{at} and E_{bt} are the inner and outer peripheries of the t^{th} ring respectively, a_t , b_t , has two ring radius, k is wave number, J_1' is Bessel function.

From the above results it is evident that the above mentioned prototype isn't best suitable for our GPS system. As it is said in abstract, Antennas performance should be precise so that it is compatible with our required system. The main disadvantages of above proposed model is that it gives very high return loss. From the plot of return loss it is seen that there isn't sudden transition in plot which is required at resonant frequency of L1 and L2 band. Even Gain, Directivity, Radiation pattern are less for this model to be compatible.

In order overcome above mentioned problem, we came up with another model which the same concept of two-concentric circular microstrip patch antenna. Some of reasons for selecting this model is that it has less return loss (i.e. more number with negative sign), more gain with polar plot of directivity and gain being same, we now concentrate on the return loss. With different dielectric constants return losses are observed and these materials results are presented here: Ethylene Glycol, Methanol.

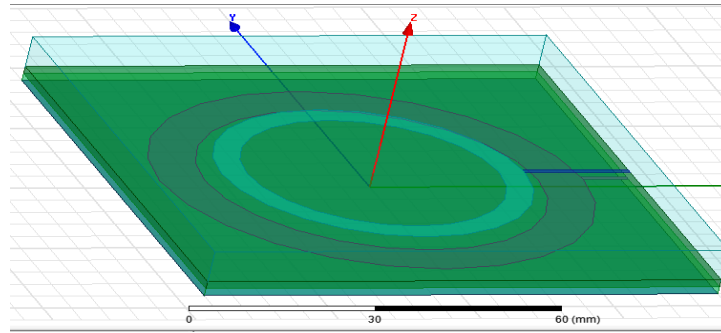


Figure 1. Proposed model of two-concentric ring microstrip antenna

Above figure shows the model of the second proposed antenna. Antenna consists of two-concentric rings arranged in a different plane (patch is sandwiched between two substrates).

III. RESULTS AND DISCUSSIONS

Figure 1 shows the proposed antenna. Using (3-4) return loss and gain has evaluated. It has the specifications of proposed two-concentric ring microstrip antenna are as follows:

Effective relative permittivity ϵ_{eff} is 12.76, thickness of dielectric substrate-1 $h_1=1.6\text{mm}$, thickness of dielectric substrate-2 $h_2=1.6\text{mm}$, inner radius of inner ring $a_1=22.1\text{ mm}$, outer radius of inner ring $b_1=26.1\text{ mm}$, inner radius of outer ring $a_2=29.1\text{mm}$, outer radius of outer ring $b_2=37.1\text{mm}$.

Feed line for this type of antenna is transmission line which is applied for the outer ring. The most important point in this two-concentric circular ring is that inner ring radiates at L1 band (1.22GHz) and outer ring radiates at L2 band (1.57GHz). Using HFSS the simulations are carried out and the results are presented in figs. (2-4). The gain plot has shown in fig. 2. The return loss of Ethylene Glycol ($\epsilon_r=37$), Methanol ($\epsilon_r=33$) dielectric materials are found for Ethylene Glycol is - 12.48, Methanol is - 23.23, these are shown in fig. (3-4). Methanol has dual-band frequency suitable for GPS application.

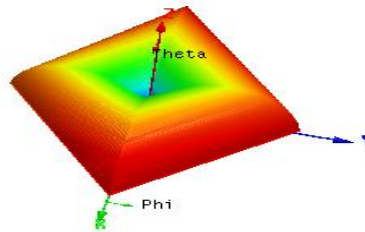
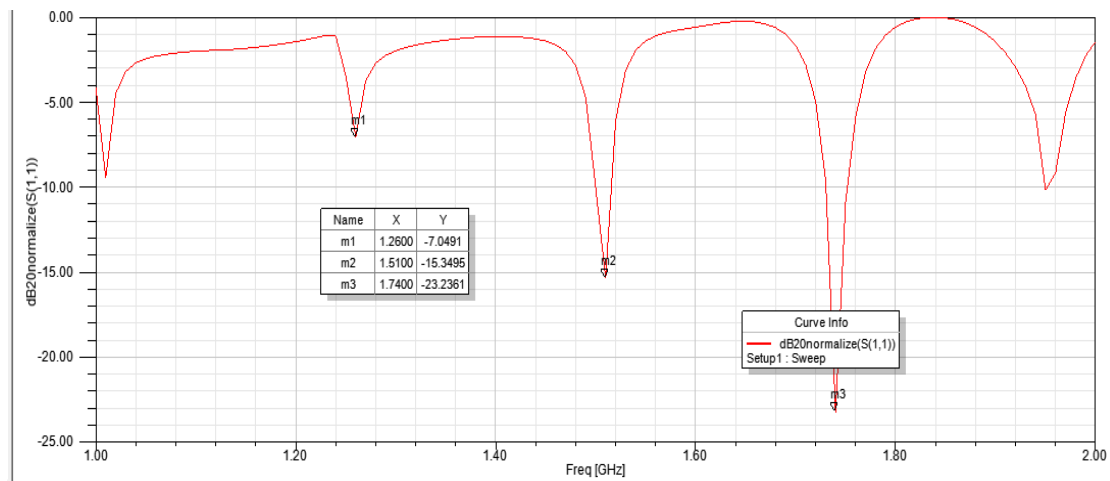
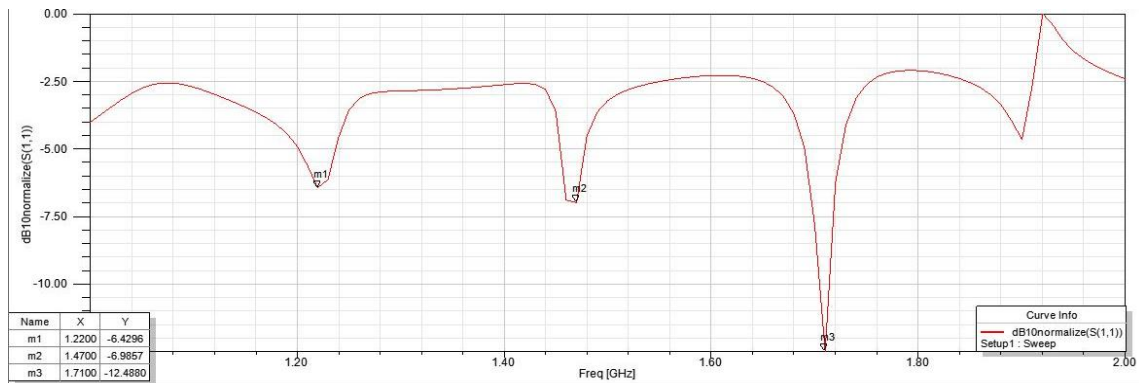


Figure 2. Polar plot-Gain of

Figure 3. Methanol $\epsilon_r=33$

Figure 4. Ethylene Glycol $\epsilon_r=37$

IV. CONCLUSIONS

Here, the materials used as substrates were changed and results were obtained. Upon thorough perusal with different materials, we came to a conclusion that Methanol and Ethylene glycol suited the best characteristic parameters. The overall working of antennas was studied. The major parameters that affect the design are studied and their implications were observed for return loss -23.23dB . The designed two-concentric circular ring microstrip antenna is operated at the desired frequency and power levels. Several patch antennas were simulated and the desired level of optimization was obtained. It was concluded that the software results we obtained matched the theoretically predicted results for Ethylene Glycol, Methanol materials.

REFERENCES

- [1] Hua- Ming Chen "Microstrip-fed circularly polarized square-ring patch antenna for GPS applications". IEEE Antennas Wireless Propag. , vol. 57, 2009.
- [2] Binod Kumar Kanaujia, "Analysis and Design of Gap-Coupled Annular Ring Microstrip Antenna". International Journal of Antennas and Propagation, 2008, Article ID 792123.
- [3] Debatosh Guha "Concentric Ring-Shaped Defected Ground Structures for Microstrip Applications". IEEE Antennas Wireless Propag. Lett., vol. 5, 2006.
- [4] S. Biswas, M. Biswas, D. Guha, and Y. M. M. Antar, "New defected ground structure for microstrip circuit and antenna applications". Proc. XXVIIIth URSI General Assembly, Oct. 2005.
- [5] Francesco Mariotini, "Design of a compact GPS and SDARS integrated antenna for automotive applications". IEEE Antennas and Wireless Propagation, vol. 9, 2010.
- [6] Y. Chung, S. S. Jeon, D. Ahn, J. I. Choi, and T. Itoh, "High isolation dual polarized patch antenna using integrated defected ground structure". IEEE Microw. Compon. Lett., vol. 14, no. 1, pp. 4–6, Jan. 2004.
- [7] J.-S. Lim, C.-S. Kim, Y.-T. Lee, D. Ahn, and S. Nam, "A spiral shaped defected ground structure for coplanar waveguide". IEEE Microw.Compon. Lett., vol. 12, no. 9, pp. 330–332, 2002.
- [8] Y.-Q. Fu, N.-C. Yuan, and G.-H. Zhang, "A novel fractal microstrip PBG structure". Microw. Opt. Technol. Lett., vol. 32, pp. 136–138, 2002.
- [9] C. Caloz, H. Okabe, T. Iwai, and T. Itoh, "A simple and accurate model for microstrip structures with slotted ground plane". IEEE Microw.Compon. Lett., vol. 14, no. 4, pp. 133–135, Apr. 2004.
- [10] D. Guha, "Resonant frequency of circular microstrip antennas with and without air gaps". IEEE Trans. Antennas Propag., vol. 49, no. 1, pp.55–59, Jan. 2001.
- [11] D. Guha, Y. M. M. Antar, J. Y. Siddiqui, and M. Biswas, "Resonant resistance of probe and microstrip line-fed circular microstrip patches". Proc. IEE Microwave Antennas Propagation, vol. 152, pp.481–484, Dec. 2005.

Modeling of Dissolved oxygen and Temperature of Periyar river, South India using QUAL2K

Lakshmi.E¹, Dr.G. Madhu²

1 Research Scholar, School of Environmental Sciences, Mahatma Gandhi University, Kottayam, Kerala, India,
2 Dr.G.Madhu, Principal, School of Engineering, Cochin University of Science and Technology, Kochi, Kerala, India.

ABSTRACT:

Numerous studies has been done on the water quality of river Periyar, South India. Most of the studies are done when a pollution event occurs. Such random analysis does not suffice the need for a management plan. Inorder to prepare a management plan, understanding past and present trend of the river is very much important. Moreover, prediction of future will give a clear pathway in preparing the framework for conservation of river. Here, in this article, variation of water temperature and dissolved oxygen through 28 year time period is evaluated using trend analysis. Then, surface water temperature and dissolved oxygen are modeled using QUAL 2K with 2007-2008 monthly data. WEAP water quality model was used for forecasting of QUAL 2k model. From the analysis, we could find that there is an annual increase in surface water temperature and decrease in dissolved oxygen per year. QUAL 2K model shows that the trend of surface water temperature and dissolved oxygen in the river is in agreement with the calibrated 2008 and 2013 data. From the WEAP analysis, we could observe that by 2030 surface water temperature of the river would be 29°C and dissolved oxygen would be 3.7mg/l. Such studies will help in evaluating new management plans for the future health of the river.

Keywords: Dissolved oxygen, Forecast, QUAL2K, Surface water temperature, Trend analysis, WEAP, Water quality modeling.

I. INTRODUCTION

Research on regional and global climate changes and variabilities and their impacts on water resources have received considerable attention in recent years. Potential impacts of climate change and its effects have been much in discussion but relatively fewer studies are being done on changes in water quality. From a global perspective, climate change is usually perceived as an increase in average air temperature. So with increase in air temperature, surface water temperature increases (Hassan et al 1998; and Hammond & Pryce 2001). This affects the water quality of river. Most of the bacteriological activities and chemical activities of the river increase with increase in water temperature, which reduces the dissolved oxygen in the river.

The 2007 conference of the parties to the United Nations Framework Convention on Climate Change in Bali and the latest Intergovernmental Panel on Climate Change (IPCC) report (2007) confirmed the consensus among scientists and policy makers that human induced global climate change is now occurring. However, there is uncertainty in the magnitude of future temperature changes both at global and regional scale. So here, an attempt is made to model the dissolved oxygen and water temperature of river Periyar. Assessing the trend and modeling of dissolved oxygen and water temperature is essential to understand the water quality of Periyar river with increasing water temperature. Kerala is the land of rivers and backwaters that criss-cross the state physique like blood veins. They fertilize the land and turn the waste into the wealth of rich, black alluvial soil. The lowlands or coastal area, made up of river deltas, back waters and the Arabian coast, is eventually a land of coconuts and rice. Aggressive human intervention, especially indiscriminate sand mining in almost all of Kerala's major rivers including Periyar, Pampa, Manimala, Achankovil etc has driven almost all the tributaries, which once used to facilitate agriculture activities and water transport in the region, to the verge of death. Periyar river, the largest river in Kerala, originates in the Sivagiri hills along the border of Kerala-Tamil Nadu. It eventually, flows into the Vembanadu Lake and to the Arabian Sea. The famous Thattekadu wildlife and bird sanctuary is situated on the bank of Periyar river at the side of Mullaperiyar river dam. Unlike other rivers, Periyar flows through ecologically sensitive areas as well as through Kerala's highest industrial belt.

The stretch between Angamaly and Kochi is highly critical as it is an industrialized zone along the river basin. Eloor, an island of 11.21 sq km within this riverine system at this region itself accommodates more than 247 industries of which 106 produce chemicals, including Hindustan Insecticide Limited (HIL), Fertilizers and Chemicals Travancore Ltd (FACT), Indian Rare Earths Ltd, Travancore Cochin Chemicals, Cochin Minerals and Rutile Ltd (CMRL) etc. Hence the Eloor - Edayar region along the Periyar river about 20 km from the point where the Periyar River meets the Lakshadweep Sea, presents a typical example of industrial pollution. According to the report of Green peace 2003 year, the industries take considerable amount of fresh water from Periyar River and discharge treated or partially treated effluents that amount to more than 170 million litres per day. Analysis of the past trend and present status of the river is imperative for establishing strategies for future health and management of the rivers.

Mathematical modeling is a useful tool to validate the estimations of pollutant loads into an aquatic environment, to establish cause-effect relations between pollution sources and water quality and also to assess the response of the aquatic environment to different scenarios. The simulation results are a useful management tool that can assist policy makers in determining realistic strategies that take into account the basin specific conditions and also in predicting the effect of accidental discharges or additional pollutant loads.

QUAL2K is a one dimensional, steady-state model of water quality and in-stream flow. It is neither stochastic nor dynamic simulation model. The QUAL2K model can simulate up to 16 water quality determinants along a river and its tributaries (Brown and Barnwell 1987). The river reach is divided into a number of subreaches of equal length. The model uses the following assumptions: (a) the advective transport is based on the mean flow, (b) the water quality indicators completely are completely mixed over the cross-section and (c) the dispersive transport is correlated with the concentration gradient. The model allows the user to simulate any combination of the following determinants: (a) Dissolved Oxygen, (b) Temperature, (c) Phosphorous, (d) Nitrate, Nitrite, Ammonium and Organic Nitrogen, (e) Chlorophyll-a, (f) up to three conservative solutes, (g) one non-conservative constituent solute, and (h) coliform bacteria.

II. METHODOLOGY

Secondary data of variables from the Periyar River during 1980-2008 was obtained from the Kerala State Pollution Control Board, Indian Meteorological Department, Neeleswaram station of Central Water Commission, Kochi for surface water temperature & dissolved oxygen, air temperature respectively. In order to understand the relation between dissolved oxygen and hydro climatic variables in the river especially surface water temperature, primarily a trend analysis was performed for all the variables. Thirty years annual average data of surface water temperature, air temperature and dissolved oxygen are used for analyzing the trend. 30 years is taken as the time period and average annual data as the time unit. Difference of data between the first year and second year are recorded. Continuing in this manner, the recording for the difference in data between each time unit is carried out until the 30 year time period is over. Add all the data to get total for all the time units. Divide the sum total by the number of time units over the time period. This data is then subjected to correlation and simple linear regression statistical analysis using SPSS 6.1 software. The equations obtained from the linear regression analysis are used to predict values of surface water temperature and dissolved oxygen of the river from the air temperature

QUAL2Kw is one-dimensional, steady state stream water quality model and is implemented in the Microsoft Windows environment. It is well documented and is freely available (<http://www.epa.gov/>). The model can simulate a number of constituents including temperature, pH, carbonaceous biochemical demand, sediment oxygen demand, dissolved oxygen, organic nitrogen, ammonia nitrogen, nitrite and nitrate nitrogen, organic phosphorus, inorganic phosphorus, total nitrogen, total phosphorus, phytoplankton and bottom algae.

QUAL2Kw is one-dimensional, steady state stream water quality model and is implemented in the Microsoft Windows environment. It is well documented and is freely available (<http://www.epa.gov/>). The model can simulate a number of constituents including temperature, pH, carbonaceous biochemical demand, sediment oxygen demand, dissolved oxygen, organic nitrogen, ammonia nitrogen, nitrite and nitrate nitrogen, organic phosphorus, inorganic phosphorus, total nitrogen, total phosphorus, phytoplankton and bottom algae.

QUAL2K is a river and stream water quality model (Brown and Barnwell 1987) and is similar to the older version in the following respects:

- One dimensional. The channel is well-mixed vertically and laterally.
- Branching. The system can consist of a main stem river with branched tributaries.
- Steady state hydraulics. Non-uniform, steady flow is simulated.
- Diel heat budget. The heat budget and temperature are simulated as a function of meteorology on a diel time scale.
- Diel water-quality kinetics. All water quality variables are simulated on a diel time scale.
- Heat and mass inputs. Point and non-point loads and withdrawals are simulated.

For QUAL2K modeling, the river is divided into 7 reaches. Reach of the river is decided based on the effluent discharge point to the river. First reach of the river is the upstream of the river with no industries along the river. Second reach starts with the beginning of industries along the river to the Pathalam earthen bund. The third reach begins from the Pathalam bund to the discharge point of Sudchem. The Fourth reach starts from the discharge point of sudchem to Travancore Cochin Chemicals. The Fifth reach is from the Travancore Cochin Chemicals to the Pallikadavu discharge point, which is devoid of any industry. The sixth reach starts from Pallikadavu to Eloor ferry. The seventh reach of the river is from the discharge point of the Kuzhikandam canal to Eloor Ferry. Temperature and Dissolved Oxygen was modeled using QUAL 2K. Data collected from the sampling site and secondary data from the literature were used for modeling.



Figure 1: Showing of sample site.

Here, initial parameter set is selected from the analysis result of the sample collected, followed by revisions to improve agreement between model results and measured data. Final parameters are then chosen to optimize the agreement between the modeled results and the measured data. Ideally, the range of feasible values is determined by measured data. For some parameters, however no observations are available. Then, the feasible range is determined by parameter values employed in similar models or by the judgment of the modeler (Ceres and Cole, 1994).

Prediction of these parameters to the periyar river is done using WEAP water quality model. WEAP is a microcomputer tool for integrated water resources planning. Developed by the Stockholm Environmental Institute (SEI), the WEAP model provides a tightly integrated planning and water resources simulation environment that draws upon expertise in policy and decision making, water resources, and financial analysis (Sieber et al., 2005).

Here using WEAP, the water temperature and dissolved oxygen are predicted. Two steps are involved in the process. Current accounts year is chosen to serve as the base year of the model. Then, a reference scenario is established from the current accounts to simulate likely evolution of the system. The predicted data range from 2009-2030.

III. RESULT

River has its own behavioral trend across time. Analysing the trend helps in understanding the river. In order to plan the future course of action we need to analyze the past. Here, we have collected secondary data of surface water temperature, air temperature and dissolved oxygen of Periyar river and it is given in the table below.

Table1: showing 28 year data for Air temperature, Water temperature and Dissolved Oxygen

Year	Air Temperature	Water Temperature	Dissolved Oxygen
1980	28.02	29.3	3.58
1981	27.81	31.1	7.05
1982	27.9	30.4	5.1
1983	27.91	29.6	6.67
1984	27.48	28.5	7.04
1985	27.67	30.3	6.63

1986	26.46	31.4	7.0
1987	28.41	28.8	6.66
1988	27.97	29.0	6.65
1989	27.54	28.3	6.5
1990	27.66	28.8	7.11
1991	27.86	28.6	6.55
1992	27.43	27.4	6.59
1993	27.53	27.4	6.84
1994	27.54	27.4	7.0
1995	27.61	26.5	7.17
1996	27.72	28.2	7.26
1997	28.02	28.7	6.8
1998	28.13	28.8	6.7
1999	27.42	24.9	6.84
2000	27.44	26.1	6.84
2001	27.49	26.5	6.62
2002	27.73	27.8	5.08
2003	27.91	28.3	5.41
2004	27.604	28.08	5.98
2005	28.69	27.9	5.7
2006	27.65	28.0	6.19
2007	27.7	27.75	5.54
2008	27.68	28.83	5.14

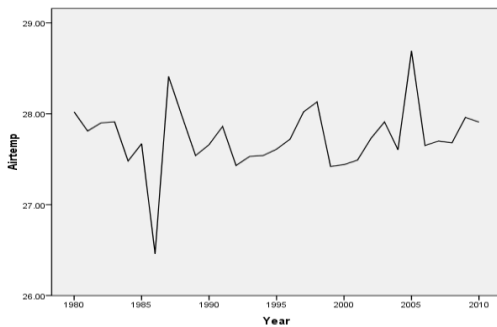


Figure 2: Variation of Air Temperature 2008

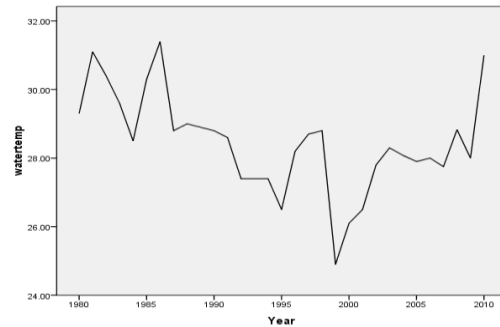


Figure 3: Variation of Water Temperature from 1980-2008

From the graph, we could observe that air temperature displayed values within 27 °C and 29 °C with one exception during 1986, where the temperature went below 27 °C. The historical data analysis shows that air temperature and water temperature increases through the years till 1999 after which temperature dips down and then increases after 2000. Dissolved oxygen graph indicates a zig- zag variation but the overall trend of dissolved oxygen in the river is decreasing.

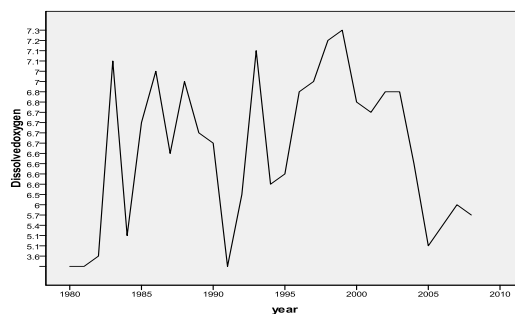


Figure 4: variation of dissolved oxygen from 1980-2008

Table 2: Result of Trend analysis variable

S.No	Variable	Trend
1	Water temperature	+0.012°C/yr
2	Air temperature	+0.018°C/yr
3	Dissolved Oxygen	- 0.065mgO2/l/yr

Relationship between hydro climatic variables air temperature, water temperature and dissolved oxygen are studied using correlation coefficient (SPSS 16.1). Correlation analysis of air temperature and water temperature shows positive correlation that is increase in one variable invariably, increases the other variable. Whereas correlation analysis between dissolved oxygen and water temperature shows negative correlation that is, increase in water temperature decreases dissolved oxygen in the river. Furthermore, to establish the relation between variables, simple linear regression analysis was performed between air temperature and water temperature, dissolved oxygen and water temperature and equations are derived. The regression equations are as follows;

$$\text{Water Temperature} = 22.858 + 0.202 \times \text{Air temperature} \quad \text{----I}$$

$$\text{Dissolved oxygen} = 9.197 - 0.103 \times \text{Water temperature} \quad \text{-----II}$$

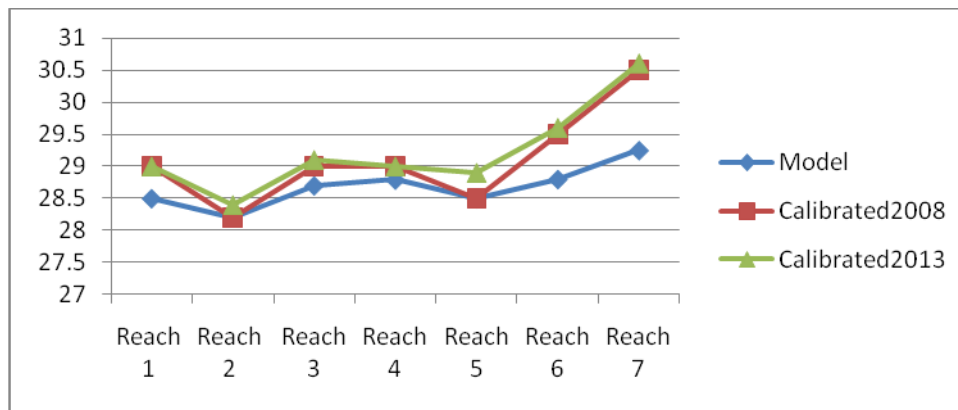


Fig 5: Graph of Temperature Modeling

Table 3: Temperature Model Data

	Model	Calibrated2008	Calibrated2013
Reach 1	28.5	29	29
Reach 2	28.2	28.2	28.4
Reach 3	28.7	29	29.1
Reach 4	28.79	29	29
Reach 5	28.5	28.5	28.9
Reach 6	28.8	29.5	29.6
Reach 7	29.25	30.5	30.6

From the graph we could observe that the calibration using the April – may 2008 (average) data is in sync with the model data except for the last two reaches of the river. Using Qual 2k we could develop a good temperature model. Graph of temperature model with April 2007 – March 2008 as model data and April – May 2008 & 2013 average as calibrated (observed) data. In this temperature model also we could find that the observed temperatures of the last two reaches are not in corroboration with the model. Observed temperature values of the last two reaches are slightly above the model in which temperature of the last reach is above the maximum temperature data. Graph controlling the model, calibration data of 2008 and 2013 shows that calibrated data of all reaches are in agreement with the model data. Temperature model is found to slightly decrease towards the lower reaches 5, 6 & 7. Temperature is found to decrease slightly towards the reach 5 and then increase towards reach 6 and 7. Calibration model and the calibration values are very low in the reach 1 and are found to increase for reach 2 and 3. Model is found to be steady towards reaches 3 and 4, then the graph lowers slightly towards reach 5 and then the graph increases steadily. Calibration data of 2008 and 2013 shows similar trend with the model.

3.1 Dissolved Oxygen Model of the River Periyar

Model was prepared with monthly dissolved oxygen data of river Periyar from April 2007 – May 2008 the data was calibrated with dissolved oxygen April – May 2008 & 2013.

Table 4: showing Dissolved oxygen model data

Model data	Calibration data 2008	Calibration data 2013
6.9	6.08	5.9
6.5	5.3	5.5
6.62	6.68	5.6
6.4	5.67	5.1
6.7	6.4	6.0
3.78	5.47	4.0
3.27	2.33	2.0

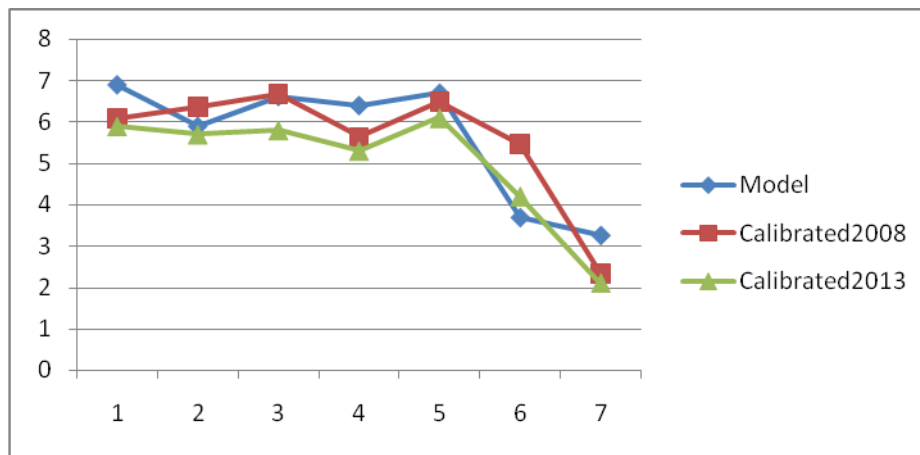


Fig 6: Graph of Dissolved Oxygen modeling

From the graph it is clear that the model developed shows that it is very much in agreement with the calibrated DO value of 2008 and 2013 (April – May average) values vary from the calibrated /observed values of the model for the model reaches 1, 6, & 7. Forecasting of temperature data is done using WEAP (Water Evaluation and assessment program).

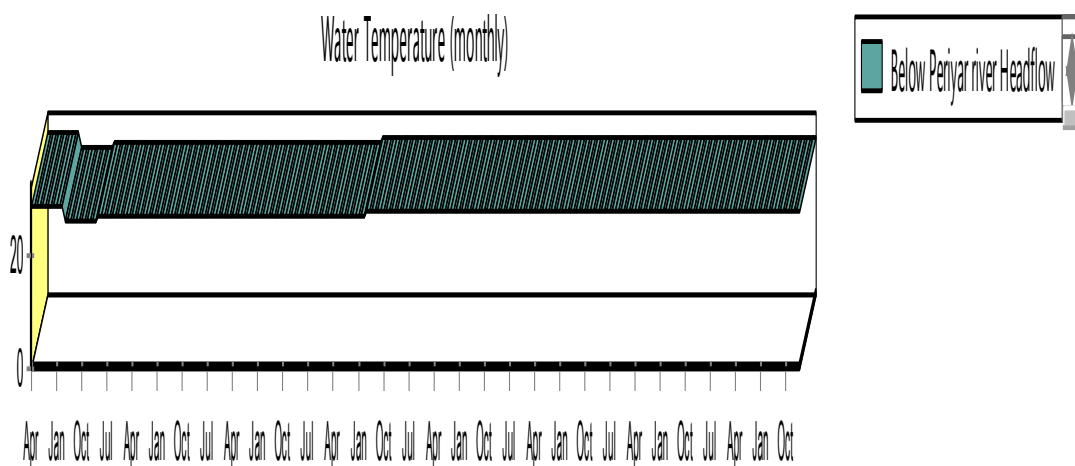


Fig 7: Graph showing Forecasting of Temperature Using WEAP.

From the graph we could observe that the surface water temperature will be 29°C by 2030. Forecasting of dissolved oxygen is done to the 1980-2007 data through time series forecasting of water quality model, water Evaluation and Assessment Program (WEAP)

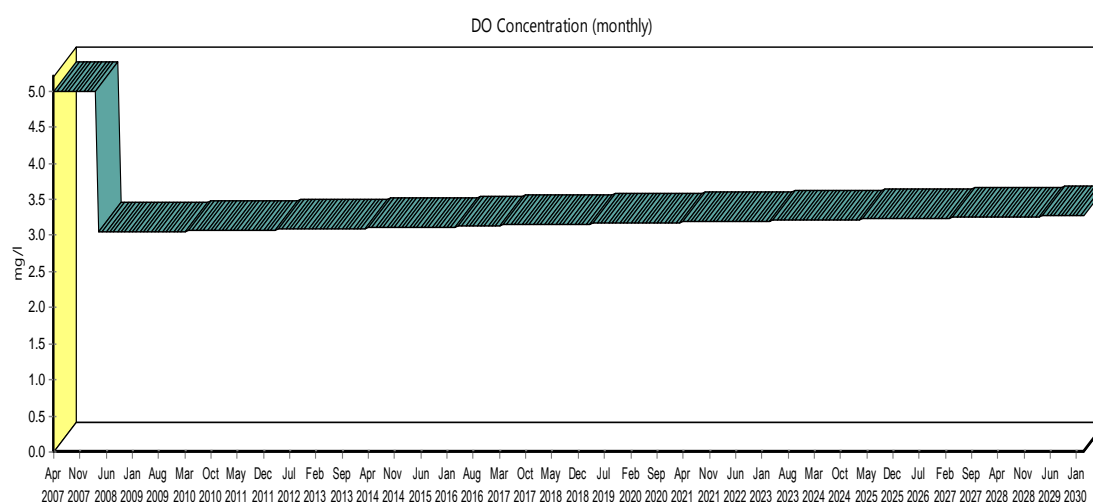


Fig 8: Graph Showing Forecasting of Dissolved Oxygen using WEAP

From the graph we could observe that by 2030 dissolved oxygen of the river would be 3.7 mg oxygen /l.

IV. DISCUSSION

Trend analysis of 30 year surface water temperature shows an increase of $+0.012^{\circ}\text{C}/\text{yr}$ and dissolved oxygen of $-0.065\text{mg oxygen}/\text{yr}$. So, with increase in surface water temperature, the dissolved oxygen in the river is decreasing. Temperature model of the river with qual2k indicates that the calibrated values (2008 and 2013) are slightly higher from the model data, but the trend along each reach is similar for both model and calibrated data. For dissolved oxygen model, the calibrated values (2008 and 2013) are slightly lower than the model data, but the trend is similar to the model along each reach throughout the river. Forecasting using WEAP water quality model clearly indicates that the average surface water temperature will be 29°C whereas dissolved oxygen will be $3.7\text{mg oxygen}/\text{l}$ by 2030.

Currently the river receives $25314\text{m}^3/\text{day}$ of effluent discharge. As water temperature increases, the rate of chemicals discharged to the river increase its reactions, which in turn affects the biological activity, further lowering the dissolved oxygen in the river. Inter governmental Panel on Climate Change projects that an increase in average temperature of several degrees as a result of climate change will lead to an increase in average global precipitation over the course of the 21st century. With increase in runoff and precipitation water will carry higher levels of nutrients, pollutants and pathogens, which will reduce the water quality. Moreover, increase in water temperature can lead to a bloom in microbial populations which affects the health of the river.

With increase in water temperature, self-purifying capacity of the river decreases further reducing the dissolved oxygen. With surface water temperature at 29°C , dissolved oxygen at $3.7\text{mg}/\text{l}$ and with effluent discharge to the river continuing at the present scenario, by 2030 the Periyar river will be in grave condition. Immediate plans and management action needs to be done in regeneration and sustenance of dissolved oxygen in Periyar river.

REFERENCE

- [1] N.W. Arnell and Wilby et al. Climate change and global water resources. *Global Environmental change*. 9, 31-49, 2004,1994.
- [2] N.J. Baggaley, S.J. Langan, M.N. Fulter, S.M. Dunn.2009. Long term trends in hydro-climatology of a major Scottish mountain river. *Science Total Environment*. 407 (16), 4633-41, 2009.
- [3] D.Caissie, N. El- Jabi, A. St-Hilaire. Stochastic modeling of water temperatures in a small stream using air to water relations. *Canadian Journal of Civil Engineering*. 25, 250-260, 1998.
- [4] D.Caissie, N. El-jabi, and M.G. Satish . Modeling of maximum daily water temperature in a small Stream using air temperatures. *Journal of Hydrology*. 251, 14-28,2001.
- [5] D. Caissie, M.G. Satish and El-Jabi N. Predicting river water temperatures using the equilibrium temperature concept with application on Miramichi River catchments (New Brunswick, Canada). *Hydrological Processes* 19: 2137-2159, 2005.
- [6] S.C. Chapra, S.C. Surface water quality modeling. McGraw-Hill: New York,1997.
- [7] T.R. Carter, S. Fronzek .Assessing uncertainties in climate change impacts on resource potential for Europe based on projections from RCMs and GCMs. 81, 357-371, 2007.
- [8] Central Pollution Control Board.1978. National Water Quality Monitoring, Global Environment Monitoring System (GEMS) water program, 1978.

- [9] Climate change. Working Group I. 2007. The Physical Science Basis, 2007
- [10] B.A. Cox and P.G. Whitehead. Impacts of climate change scenarios on dissolved oxygen in the river Thames, UK, Hydrology Research. 4(2-3), 138-152, 2009.
- [11] G.J. Edinger, D.W. Duttweiler and J.C. Geyer. The response of water temperatures to meteorological condition. Water Resources Research. 4 (5), 1137-1143, 1968.
- [12] T.R. Erickson, H.G. Stefan. Correlation of Oklahoma stream temperatures with air temperatures. Project report No.398. University of Minnesota. St Anthony Falls Laboratory: Minneapolis, MN, 1996.
- [13] M. Huber. Climate changes: Snakes tell a torrid tale. Nature Journal. 457, 669-671, 2009.
- [12] M. Hulme, E.M. Barrow, P.A. Harrison, T.E. Downing and T.C. Johns. Relative impacts of human induced climate change and natural climate variability. Nature. 397, 688-691, 1999.
- [13] H. Mathew. Climate change: Snakes tell a torrid tale. Nature Journal. 457, 669-671, 2009.
- [14] J. McCarthy, O.F. Canziani, N.A. Leary, D.J. Dokken and K.S. White (eds). 2001. IPCC Climate change: Vulnerability, impacts and adaptation, Contribution of Working Group II to the third assessment report of the Intergovernmental Panel on climate change. In: Cambridge University Press. Cambridge. UK. 1032, 2001.
- [15] D. Jacob, L. Barring, O. Christensens, B. Christensen, J.H. de Castro, M. Deque, M. Giorgi, F. Hagemann, S. Hirschi, M. Jones, R. Kjellstrom, E. Lenderink, G. Rockel, B. Sanchez, E. Schar, C. Seneviratne, S.I. Somot, S. Van Ulden, A. Van den Hurk, B. An inter-comparison of regional climate models for Europe: model performance in present day climate. Journal of climate change, 2007.
- [16] Z. James. New evidence of global warming in Earth's past supports current models for how climate responds to greenhouse gases. Science expresses, 2003.
- [17] K.S. Kim, S.C. Chapra. Temperature model for highly transient shallow streams. Journal of Hydraulic Engineering. American Society of Civil Engineers. 123(1), 30-40, 1997.
- [18] S.J. Langan, L. Johnston, M.J. Donaghy, A.F. Youngson, D.W. Hay, C. Soulsby. Variation in river water temperatures in an upland stream over a 30 year period. Science of the Total Environment. 265, 195-207, 2001.
- [19] A.P. Mackey, A.D. Berrie. The prediction of water temperatures in chalk streams from air temperatures. Hydrobiologia. 210, 183-189, 1991.
- [20] R. Marce and J. Armengol. Modeling river water temperature using deterministic, empirical and hybrid formulations in a Mediterranean stream. Hydrological processes. 22, 3418-3430, 2008.
- [21] O. Mohseni, Erickson and H.G. Stefan. Sensitivity of stream temperatures in the United States to air temperatures projected under a global warming scenario. Water Resources Research. 35, 3723-3733, 1999.
- [22] O. Mohseni, H.G. Stefan and T.R. Erickson. A non-linear regression model for weekly stream temperatures, Water Resources Research. 34, 2685-2692, 1998.
- [23] O. Mohseni, H.G. Stefan. Stream temperature/ air temperature relationship: a physical interpretation. Journal of Hydrology. 218, 128-141, 1999.
- [24] J.M. Pilgrim, Fang. H.G. Stefan, H.G. Stream temperature correlations with air temperatures in Minnesota: Implications for climate warming. Journal of American Water Resources Association. 34(5), 1109-1121, 1998.
- [25] S. Rehana, P.P. Mujumder. River Water quality response under hypothetical climate change scenarios in Tunga-Bhadra River, India. Hydrological processes. Wiley online library, 2011.
- [26] J. Schnoor. Environmental modeling, fate and transport of pollutants in water, Air, and Soil. Wiley Inter science, 1996.
- [27] R.H. Shumway and D.S. Stoffer. Time series analysis and its applications, Springer Verlag, New York, 2000.
- [28] K. Smitha. The prediction of river water temperatures. Hydrological Sciences Bulletin. 26, 19-32, 1981.
- [29] R. Stringer, I. Labunska, K. Brigden. Pollution from Hindustan Insecticide Limited and other factories in Kerala, India: A follow-up study. Green Peace Research Laboratories, University of Exeter, UK, 2003.
- [30] K. Sullivan, J. Tooley, Doughty. J.E. Caldwell and P. Knudsen. Evaluation of prediction models and characterization of stream temperature regimes in Washington, Report No. TFW-WQ3-90-006, Washington Department of natural resources: Olympia. WA. 224, 1990.
- [31] N.T. Vanrheenen, A.W. Wood, R.N. Palmer, D.P. Lettenmaier. Potential Implications of PCM climate change scenarios for Sacramento-San Joaquin river basin hydrology and water resources. Climate Change. 62, 257-281, 2004.
- [32] R.W. Wagner, L.R. Stacey. Brown and M. Dettinger. 2011. Statistical Models of temperature in the Sacramento-San Joaquin delta under climate-change scenarios and ecological implications. Estuaries and Coasts. 34, 544-556, 2011.
- [33] B.W. Webb, P.D. Clack, D.E. Walling. Water – Air temperature relationships in a Devon river system and the role of flow. Hydrological Processes. Wiley Inter Science. 17, 3069-3084, 2003
- [34] R. Prakash, S.L. Kannel, R.K. Sushil, S.L. Young, and A. Kyu-H. Application of Qual 2Kw for water quality modeling and dissolved oxygen control in the river Bagmati. Environment monitoring and assessment. 125:201-217, 2007.
- [35] B. Oliveir, J. Bola, P. Quinteiro, H. Nadais and L. Arroja. 2011. Application of Qual2Kw model as a tool for water quality management: Certima River as a case study. Environment Monitoring and Assessment, 2011.
- [36] R. Nipunika, S. Ravindra Kumar, P. Kriteswar, K. Dilip Kumar. Assessment of temporal variation in water quality of some important rivers in middle Gangetic plains, India. Environment Monitoring and Assessment. 174: 401-415, 2011.
- [37] K.K. Vass, M. K. Das, P.K. Srivastava, and S. Dey. 2009. Assessing the impact of climate change on inland fisheries in river Ganga and its plains in India. Aquatic Ecosystem Health and Management. 12:2, 138-151, 2009.

Design Of QoS Aware Light Path Planning And Technical Aspects In Wdm Networks

Ashish Kumar¹, Prof. R.L.Sharma²

¹M.TechStudent²ProfessorDepartmentofElectronics&CommunicationEngineering
AjayKumarGargEngineeringCollege,Ghaziabad

ABSTRACT:

In this work, the issue of connection provisioning and performance analysis in wavelength division multiplexing (WDM) network is considered. We ensured the quality of service (QoS) requirement of the connection requests from the client in the optical networks. While designing WDM system, the physical layer impairments (PLIs) incurred by non-ideal optical transmission media, accumulates long the optical path degraded the QoS. For high transmission speed Dispersion become a considerable degradation factor and in this work will be concentrated on the effects of dispersion on fibered sign parameters such as band width, delay etc. The overall effect of dispersion is described in terms of quality factor (Q-Factor) and improvement in blocking probability is observed over proposed algorithms and traditional algorithms. In this work the light path provisioning mechanism is based on both Q-Factor and blocking probability. Each path is provisioned that satisfy the requirement of client in the network model. A proposed algorithm and the traditional algorithm provide the improvement in blocking probability for incoming requests while considering impairment issues. In this work, the impact of dispersion on transmission performance of WDM network, by ensuring the QoS requirements, is evaluated. It is necessary to provide the best service to the customers. The aspect WDM network model can be specified in terms of QoS parameters such as bandwidth and delay. The QoS requirement, in terms of Q-Factor, is associated with the optimum light path. For high transmission speed, the dispersion becomes a considerable degradation factor. This work improves the blocking probability while performing the optimum routing.

KEYWORDS: Blocking probability, Disjoint Path, OVPN, PMD, Q-Factor, Shortest path, WDM. etc.

I. INTRODUCTION

The efficient optical virtual path network (OVPN) is the recent provisioning mechanism over WDM mesh network by considering the effect of polarization mode dispersions (PMD) [1]. The competitive market pressures demand that service provider continuously upgrade and maintain their networks to ensure they are able to deliver higher speed, higher quality application and services to the customers. The QoS based disjoint path (DJP) algorithm for dynamic routing in WDM network improves the blocking probability [2]. The WDM routed networks provide an optical connection layer which consists of several light paths. Light waves traversing through a wavelength-routed optical network encounter progressive linear and non-linear interactions [3]. The delay model and its application for fiber material selection in order to optimize a suitable OVPN connection with minimum delay [4]. A light path is defined as an optical connection from the source to destination node. In WDM network, the most important issue is routing and wavelength assignment. In this paper a new algorithm for provisioning of high speed optical connection is proposed by considering the effect of dispersion in the fiber.

The concept of QoS in communication system is closely related to the network performance of underlying routing system. Quality of service can be defined as the collective effect of service performance which determines the degree of satisfaction of user of the service. The physical layer impairments and issue challenges are considered in the way of optimum routing [8]. At the time of efficient connection provisioning various linear and non-linear impairments has to be considered without physical layer impairment awareness, a network layer provisioning algorithm should not guarantee for signal quality. Some of linear impairments are PMD, Chromatic dispersion, waveguide dispersion, modal dispersion, attenuation, Amplifier spontaneous emission, insertion losses. Some of non-linear impairments are self-phase modulation, cross phase modulation, four wave mixing,

stimulated Raman scattering etc. In this paper, Q-Factor is defined as the cost of the network. In the proposed algorithm, the QoS requirement is considered the bandwidth for each path and delay in the fiber due to pulse spreading. This paper discussed the improvement in the blocking probability for proposed algorithm for DJP and shortest path (STP). The QoS based optimum path provisioning mechanism for WDM network by considering maximum bandwidth and minimum delay for each path.

II. ROUTING MECHANISM

In this paper, the QoS is defined in terms of Q-Factor, which is computed in terms of maximum bandwidth and minimum delay associated with the optical fiber light path. The routing and wavelength assignments are necessary for improving the quality of service [6-7]. The maximum value for the Q-Factor is the optimum requirement for the connection request while calculating Q-Factor. The linear impairment factor dispersion is considered in this paper. Due to dispersion pulse is spreads and hence delay for the transmitted signal. The route with minimum delay are optimum path for routing and should have minimum number of node, for minimizing network cost but for the bandwidth, the optimum path is the path which provides maximum bandwidth value.

III. SYSTEM MODEL

The wavelength routed optical network consists of optical cross connects, optical add and drop multiplexers, which are connected through WDM links. This system consisting of three layers, the provider edge layer (PEL), optical core layer and client layer, shown in figure 1.

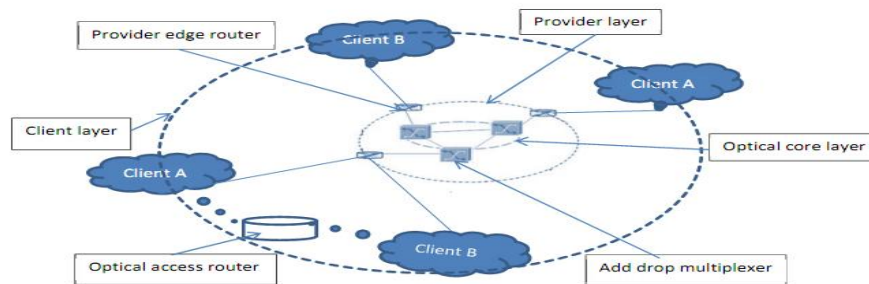


Figure1. System model topology

Provider edge router (PER) belongs to the light path client, which provides the light path services and interface between clients. The optical core router (OCR) is not connected to the client directly. In provider layer the PER are responsible for all non-local management function such as management of optical resource configuration and capacity management, addressing, routing, topology discovery, traffic engineering and restoration etc. PER maintain the traffic matrices (TM). The Traffic Matrices maintains the network as well as physical layer impairments (PLI). The PLI constraints are such as bandwidth, delay and dispersion and Q-factor matrices for all the possible light path connection in the network belongs to all the layers.

The virtual network model [1] is considered as shown in figure 2. In this network, a client (m) communicated with client (n) via source PER i to destination PER j. Connectivity in a system is determined by link and wavelength present or not. If link present between two nodes, connectivity is taken as 1 otherwise it is taken as 0. Similarly wavelength is available between two nodes is taken as 1 otherwise it is taken as 0.

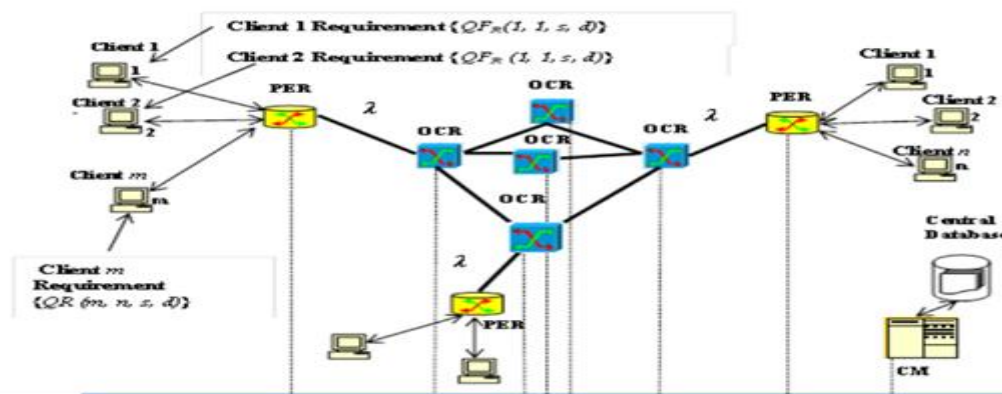


Figure2. Network topology

IV. REQUIRED Q-FACTOR FOR CLIENT POINT OF VIEW

The problem formulations are based on the different QoS parameters such as Q-factor in terms of bandwidth and delay. The Bandwidth and Delay requirements for client 'm' to client 'n' from light path source 's' to destination 'd' are respectively $BW(m, n, s, d)$ and $D_{PMD}(m, n, s, d)$. If $QF_R(m, n, s, d)$ is the required Q-Factor then it can be reformulated [4] as

$$QF_R(m, n, s, d) = \frac{BW(m, n, s, d)}{D_{PMD}(m, n, s, d)} \quad (1)$$

V. REQUIRED Q-FACTOR FOR SYSTEM POINT OF VIEW

The required Q-Factor has been computed in terms of bandwidth, delay and Q-Factor as follows;

a) Bandwidth computation for light path

Assume physical layer constraints are dispersion coefficient and link length. If $B(i, j)$ is the bandwidth between link 'i' and 'j' then it can be formulated [2] as

$$B(i, j) = \frac{\sigma}{DS_{pmd}(i, j) \times \sqrt{L(i, j)}} \quad (2)$$

Where σ , $DS_{pmd}(i, j)$, $L(i, j)$ are the pulse broadening factor, dispersion coefficient and link length of the fiber respectively.

b) Delay computation for light path

Differential time delay lies between two modes in the fiber. The delay is due to the effect of polarization mode dispersion. It can be formulated [1] as

$$DS_{pmd}(i, j) = DS_{pmd}(i, j) \times \sqrt{L(i, j)/2} \quad (3)$$

c) Q-Factor for light path

If $Q(i, j)$ is the computed Q-factor for a link pair 'i' and 'j', then it can be formulated as-

$$QF(i, j) = \frac{BW(i, j)}{DS_{pmd}(i, j)}$$

d) The total Q-Factor

If the minimum bandwidth and the maximum delay for every link (i, j) consisting of source to destination routes (s, d) are respectively $BW(m, n, s, d)|_{\min}$ and $DS_{pmd}(m, n, s, d)|_{\max}$. The total Q-Factor is formulated as

$$QF(m, n, s, d) = \frac{|B(m, n, s, d)|_{\min}}{|DS_{pmd}(m, n, s, d)|_{\max}} \quad (4)$$

VI. BLOCKING PROBABILITY

The blocking probability can be defined as the ratio of total number of connection blocked to the total number of connection required. If $BP(m, n, s, d)$ is the blocking probability from client 'm' to client 'n' via light path source 's' to destination 'd'. It can be formulated [5] as

$$BP(m, n, s, d) = \frac{TNCB(m, n, s, d)}{TNCR(m, n, s, d)} \quad (5)$$

Where TNCB is total number of connection blocked and TNCR is the total number of connection is required.

VII. ALGORITHMS AND FLOW CHART

In this paper two types of algorithms are compared are shown in figure 3.

1. Conventional shortest path algorithm (STP, $n=1$)
2. Proposed disjoint path algorithm (DJP, $n=1:N$)

The connections are blocked by two ways, if required Q-factor is greater than computed Q-factor ($QF_R > QF_C$) and links are busy.

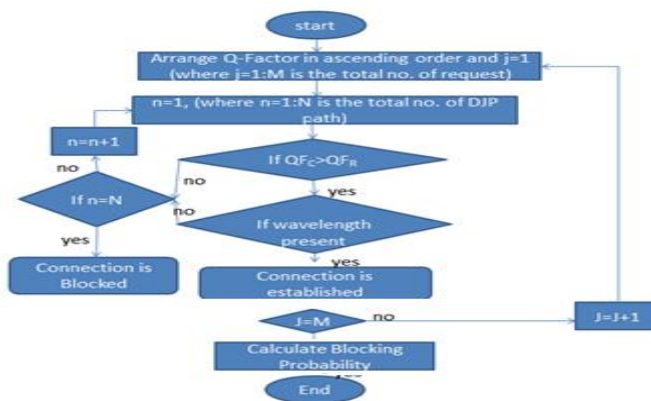


Figure3. Algorithm flow chart

The main steps in the algorithm are given below

Step1: To compute the entire disjoint path and the Q-factor for all these paths and arrange them in the ascending order of Q-factor.

Step2: To start $j=1$, for first request ($j=1: M$, where M is the total no. of request).

Step3: To start $n=1$, for first path ($n=1$ for STP, $n=1: N$, where N is the total no. of disjoint path)

Step4: To compare required Q-Factor with the computed Q-factor for the entire disjoint paths whenever it is satisfied go to step 6.

Step5: To Increase the path number $n=n+1$, and go to step 3. If entire path checked then connection is blocked.

Step6: To check availability for wavelength, then blocking probability is to be computed, if it not present go back to step 5 otherwise connections is established.

Step7: To Increase the path number $j=j+1$, and go to step 2.

Step8: To compute blocking probability. If entire request completed then end the program.

VIII. SIMULATION

Simulation is performed for WDM network with different nodes and links. The simulation model is shown in figure 4.

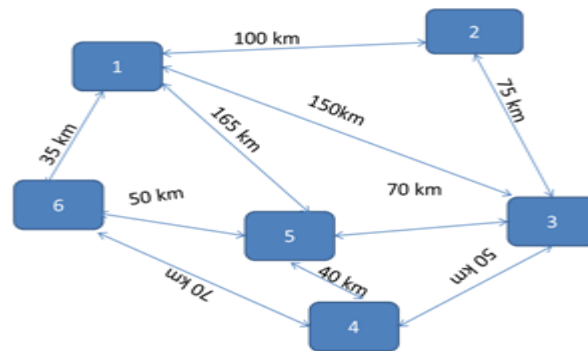


Figure4. Simulation model

This simulation model consists of 6 nodes and 10 links. In this simulation the value of various parameter are fixed. It is tabulated in table 1.

TABLE1: Simulation Parameter

Parameters	Parameter value
1. Polarization mode dispersion coefficient (ps/√km) DS _{PMD} (i, j)	0.2
2. Wavelength (nm) λ	1300-1600
3. Pulse broadening factor σ	0.1

The simulation result is for source 3 to destination 5. For this we considered 10 disjoint paths, and for each path computed minimum bandwidth and maximum delay is considered. In this paper Q-Factor is computed by taking ratio of minimum bandwidth to maximum delay for each path is shown in table 2. In this table, 4 optimum paths are chosen out of 10 paths. The paths, in which minimum and maximum Q-Factor are 35.4 and 70.7 respectively. The Q-factor for shortest path is 50.5.

TABLE 2: Simulation connection for STP and DJP

S.N	DISJOINT PATH	SHORTEST PATH	BW(l,j) (GHz)	Tpmd(i,j) (Pico sec)	QF(l,j)	DPS	SPS
1	3-1-5		38.9	1.82	21.4		
2	3-2-1-5		38.9	1.82	21.4		
3	3-4-6-1-5		38.9	1.82	21.4		
4	3-4-5		70.7	1.00	70.7	3-4-5	
5	3-5	3-5	59.8	1.18	50.5	3-5	3-5
6	3-1-6-5		40.8	1.73	23.6		
7	3-2-1-6-5		50	1.41	35.4	3-2-1-6-5	
8	3-4-6-5		59.8	1.18	50.5	3-4-6-5	
9	3-1-6-4-5		40.8	1.73	23.5		
10	3-2-1-6-4-5		40.8	1.73	23.5		

DPS: disjoint path selected, SPS: shortest path selected.

The comparison are shown in figure 5, in which single STP has 4 wavelength. The STP can handle maximum 4 request at time whenever it is greater than QF_R, but in case DJP entire requests are handled, due to more number of QF_C associated with DJP paths, are available.

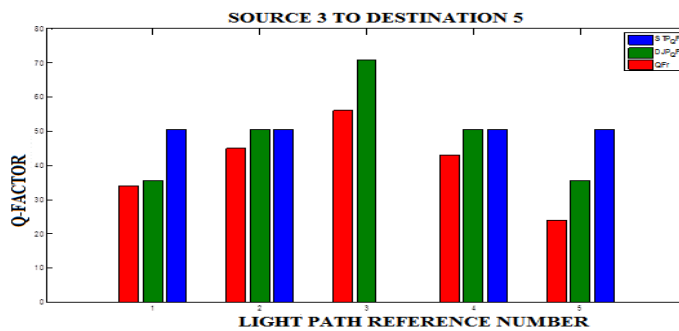


Figure5. Comparison of Q-Factors

In each path 4 wavelengths are available. As the number of request increased blocking probability are also increased for STP and DJP. The blocking probability is about 90% for STP and 60% for DJP. The improvements in blocking probability for disjoint path (DJP), over shortest path (STP) are shown in figure 6 (a). The QoS requirement from clients in the optical network are also analyzed for source-destination pair (1,5) and (2,5). The figure 6b and 6c shows the plot of corresponding blocking probability. The blocking probability is calculated from the number of call blocked and the total number of call generated as given in equation number 5. Our proposed algorithm helps to analyses both bandwidth and delay in terms of Quality Factor. This algorithm determine the best possible path between source and destination pair for each connection request and select the best possible path based on the requirement of the client.

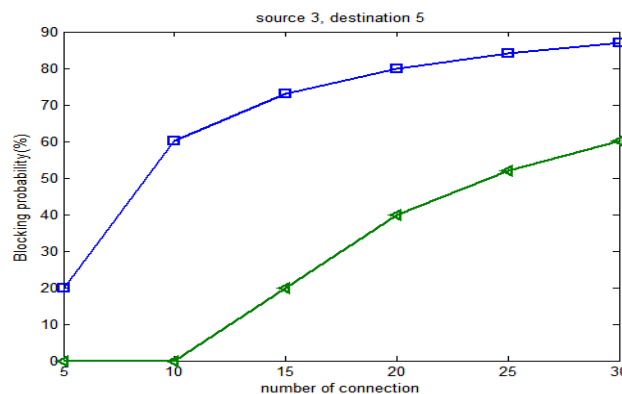


Figure 6a. blocking probability comparison for STP and DJP.

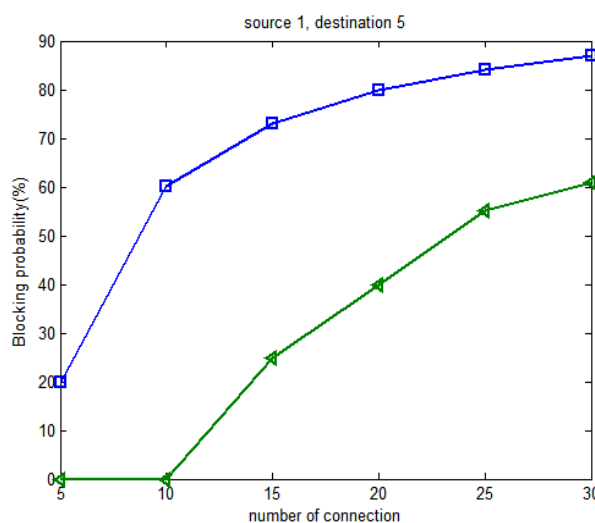


Figure 6b blocking probability for s-d pair(1,5)

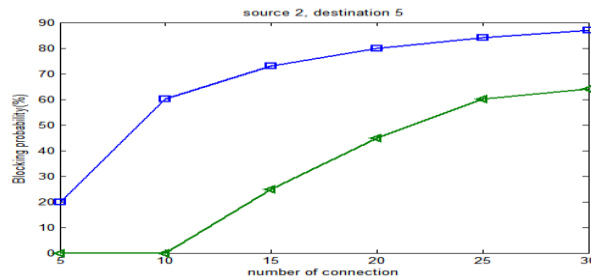


Figure 6c blocking probability for s-d pair(2,5)

IX. CONCLUSION

In this paper we have presented the improvement of DJP algorithm over traditional STP algorithm, by considering physical layer impairments. In case of light path, provisioning is based on Q-Factor. The responding path will be a guaranteed service. The proposed method provides a light path selection mechanism, which is flexible to the service provider as well as client.

REFERENCES

- [1] S.K. Das, Dhanya V.V. and S.K. Patra, "QoS based OVPN Connection Set up and Performance analysis", WSEAS transaction on Communication, issue 8, VOL 11, august 2012
- [2] S.K. Das, Dhanya V.V., "QoS based light path provisioning and performance analysis in WDM Network", international conference on computing, Electronics and Electrical Technologic, 2012, Tamilnadu, India
- [3] AneekAdhya and DebashishDatta, "light path topology design for wavelength-routed optical networks in the presence of four-wave mixing", opt. communication. And network vol. 4,no. 4, 2012
- [4] Das, Naik, and Patra, "Fiber material dependent QoS analysis and OVPN connection setup over WDM/DWDM network, TENCON 2011
- [5] A. Wason, R.S Kaler, "Wavelength assignment algorithms for WDM optical network," international journal for light and electron optics, vol 13, no. 1, pp. 877-880,2011.
- [6] R.M. Krishanaswami and K.N Sivrajan, "algorithm for routing and wavelength assignment based on solution of LP Relaxation," IEEE communication letters, VOL 5, no 10, OCT 2001
- [7] K.C., K.M. and E.C.V, "offline routing and wavelength assignment in transparent WDM Network", IEEE/ACM, VOL 18, no 5, OCT 2010
- [8] C.V. Saradhi. S. Subramaniam., "Physical layer impairments aware routing (PLIAR) In WDM optical networks; issue and challenges," IEEE communication survey and tutorials, vol.11 ,no.14 pp.109-130,2009
- [9] M.Yoo.,C.Qiao., "Anewopticalburstswitchingprotocolforsupportingqualityof service," SPIE Proceedings, All Optical Networking: Architecture, Control and Management Issue, vol. 3531, pp. 396-405, November1998.
- [10] B.Ramamurthy.,B.Mukherjee, "WavelengthconversioninWDMnetworking," IEEEJournal on Selected Areas in Communications, vol. 16, no. 7, pp. 1061-1073,1998.
- [11] M.Yang.,S.Q.Zheng.,D.Verchere., "Aqosupportingschedulingalgorithmfor optical burst switching in dwdm networks," Proceedings of GLOBECOM 2001,pp. 86-91,2001.
- [12] X.Huang.,F.Farahmandz.,J.P.Jue, "AnalgorithmfortrafficgroominginWDM mesh networks with dynamically changing light-trees," ProceedingsofIEEE Globecom, 2004
- [13] Provisioning With Y. Huang., J. P. Heritage., B. Mukherjee, "Connection Transmission impairment Consideration in Optical WDM Networks With High-Speed Channels," Journal of light wave technology, vol. 23, no. 3, pp. 982-993, 2005.
- [14] R.D.Der.,y.j.Jhong, "Delay-ConstraintSurvivablemulticastRoutingproblem on WDM Networks," Communicationsand Networkingin China (CHINACOM), 2010.
- [15] B. Abdelouab., H. Abdelhakim., G. Michel., T. Mariam., "Path-Based QoSProvisioning for Optical Burst Switching Networks," Journal of Lightwave technology, vol. 29, no. 13, July1, 2011



AshishKumar received his B.TECH degree in electronics and communication engineering from JSSATE, affiliated with GBTU, LUCKNOW, INDIA, in 2010 and M.TECH degree pursuing in electronics and communication engineering from Ajay Kumar Engineering College Ghaziabad, affiliated with UPTU LUCKNOW, INDIA. His research interests include design and analysis QoS routing in optical networks.



Prof. R.L.Sharma obtained M.Tech degree in Optoelectronics and Optical Fiber communication from Indian institute of technology Delhi (India) and Ph.D. degree from Singhania University. He has about 35 years of rich experience in maintaining, supervising and managing large communication networks involving HF, VHF, UHF and Data communication spread over the entire country, particularly far-flung and remote areas of northeastern regions and Jammu & Kashmir of India. For the past 5 years, he has been teaching optical fiber communication, Digital communication and optical networks in the department of ECE at A K G Engineering College, Ghaziabad, UP, INDIA. His research area is in the field of optical communication.

Cuckoo Search Based Threshold Optimization for Initial Seed Selection in Seeded Region Growing

M.Mary Synthuja Jain Preetha¹, Dr. L.Padma Suresh², M.John Bosco³

¹(ECE, Noorul Islam Centre for Higher Education, Kumaracoil, India)

²(Professor/EEE, Noorul Islam Centre for Higher Education, Kumaracoil, India)

³(Asst Prof/EEE, St, Xavier's Catholic College of Engineering, Chunkankadai)

ABSTRACT:

Image segmentation is the process of grouping pixels into different distinct regions. Seeded Region Growing (SRG) is a method of image segmentation, in which a pixel is used as seed pixel from which the regions start growing. Different seeds provide different results. In this paper we propose a threshold optimization technique using cuckoo search optimization algorithm for initial seed selection. The cuckoo search algorithm is used to find the optimal threshold values which maximize the fitness function.

KEYWORD: Seeded Region Growing, Cuckoo Search, Optimization

I. INTRODUCTION:

Image segmentation is the process of classification of pixels in an image into different clusters that exhibits similar features like color, intensity or texture. It should be noted that several general-purpose algorithms have been implemented for color image segmentation. A brief survey on image segmentation techniques is given in ref [1]. Segmentation process should be stopped when the region of interest is segmented from the input image. Image segmentation can be used in several applications and the region of interest may differ for different applications. Hence, none of the segmentation algorithms satisfy the global applications. Thus image segmentation is a challenging task for researchers. Image segmentation algorithms can be classified into four approaches namely: 1) Threshold-based 2) Boundary-based 3) Region –based 4) Hybrid-based techniques. Threshold-based techniques are based on the assumption that the neighboring pixels whose value lies below a certain range belong to same group[2]. Boundary-based techniques are based on the assumption that the pixels intensity change abruptly at the boundary between two regions [3,4]. Region-based techniques are based on the assumption that the neighboring pixels in the same region have similar features like grey-value, color-value or texture. Hybrid techniques integrate the results of both region based and boundary-based [5-7]. In region-based technique the performance of the segmented image mainly depends on the selected homogeneity criterion. Seeded Region Growing (SRG) technique is controlled by the set of initial seeds. Given the initial seeds, SRG tries to find the accurate segmentation of images into separate regions with the property that the neighboring pixels of a region meets exactly one of the seed. These initial seeds are the key point from which the regions start growing. Change in seed pixel will affect the final segmentation. Hence, selection of initial seed has a great impact on final segmentation. By optimizing the threshold values we can improve the accuracy of the segmented image. In this paper we propose an algorithm for initial seed selection which is optimized using cuckoo search algorithm.

Overview of the Algorithm: Fig:1 shows the general block diagram of our proposed algorithm. Initially the input color image is converted into grey scale image. Secondly, the histogram of the particular image is drawn. From the histogram thresholds are generated. From the generated threshold, using entropy as the fitness function optimal threshold is selected using cuckoo search algorithm for initial seed selection. Fig .2 shows the input image and the histogram of the gray scale image.

Threshold Optimization using Cuckoo Search: Optimization is a process of making something as fully perfect, effective or functional as possible. Optimization is restricted by the lack of full information about something and the lack of time to evaluate the full information. Hence optimization deals with finding best values of variables so that the values of a fitness function becomes optimum. This search starts with a random feasible solution, and then moves its neighborhood solution from its current position and accepts the new solution if and only if it improves the fitness function.

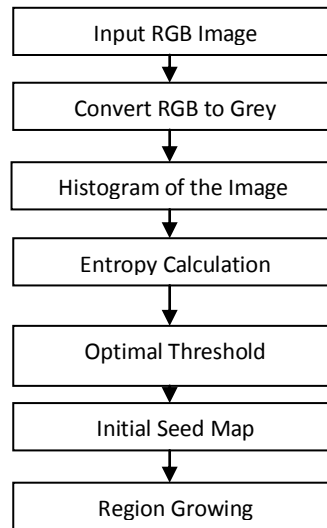


Fig 1: General Block Diagram



Fig 2: a) Input RGB Image b) Gray scale Image c) Histogram of the gray scale image

2.2 Cuckoo Search Algorithm: Cuckoos are brood parasite. They lay their eggs mostly in the nest of other host birds. If a host bird found that the egg in the nest is not their own, they will either destroy the eggs by throwing away or they will build a new nest elsewhere. Some cuckoo species can imitate the color and pattern of the eggs of the chosen nest. This mimicry will reduce the probability of cuckoo eggs being abandoned and therefore increases their re-productivity. Cuckoo search can be described by three generalized rule [8]: 1) Each cuckoo lays one egg at a time, and dump its egg in randomly chosen nest; 2) The best nests with high quality of eggs will carry over to the next generations; 3) The number of available host nests is fixed, and the egg laid by a cuckoo is discovered by the host bird with a probability $p_a = [0, 1]$. In this case, the host bird can either throw the egg away or abandon the nest, and build a completely new nest. For an optimization problem the fitness is proportional to the value of objective function.

2.3 Implementation: This proposed method is based on the search of thresholds that optimizes the objective function such as entropy. Entropy based thresholding considers the histogram of the image as a probability distribution and selects an optimal threshold value that yields maximum entropy. A best entropy thresholded image contains more information. In seeded region growing the initial seeds selected should contain more information about a particular region. So pixel values greater than the optimized threshold are selected as the initial seeds. The entropy calculation as described by T.Pun [9] is summarized here:

Let $x_1, x_2, x_3, \dots, x_n$ be the observed grey level and

$$p_i = \frac{x_i}{N}, \quad \sum_{i=1}^n x_i = N, \quad i = 1, 2, 3, \dots, N$$

Where n is the grey level and N is the total number of pixels. The entropy is given as

$$H'_n = -P_s \ln P_s - (1 - P_s) \ln(1 - P_s)$$

Where,

$$P_s = \sum_{i=1}^s P_i \text{ and } 1 - P_s = \sum_{i=s+1}^n P_i$$

Finally,

$$\frac{H'_n}{H_n} \leq f(s)$$

Where, $f(s) = \left[\frac{H_s \ln P_s}{H_n \ln[\max(P_1, P_2, \dots, P_n)]} + \left(1 + \frac{H_s}{H_n}\right) \frac{\ln(1-P_s)}{\ln[\max(P_{s+1}, P_{s+2}, \dots, P_n)]} \right]$ and $H_n = -\sum_{i=1}^n P_i \ln P_i$

This function f(s) is taken as the fitness function. S is the threshold value which maximizes the fitness function f(s). To implement cuckoo search, the population of the host nest $x_i = 1, 2, \dots, N$ is randomly initiated. From the population of the host nest, a cuckoo, say 'I' is randomly chosen and its fitness function F_i is evaluated. Choose a nest 'j' randomly and calculate its fitness function F_j . If $F_i > F_j$, replace j by the new solution 'I'. Thus a fraction of worst nest is abandoned as new ones are built. Keep the best solutions and find the current best. Thus the threshold for initial seed selection is optimized using cuckoo search and this optimized threshold is used for initial seed selection.

II. RESULTS AND DISCUSSION:

The performance of the proposed seed selection algorithm based on cuckoo search optimization technique is evaluated. Some experiments with test images from publically available Berkely dataset are presented to illustrate the key features of the proposed method.

Table 1: Optimal Threshold value and their fitness value



Input Image	Thresholds Generated	Optimal Threshold	Fitness value
	173	173	0.8448
	33		
	216		
	235		
	178		
	195		
	192		
	113		
	172		
	64		
	124	125	0.8398
	111		
	197		
	204		
	67		
	135		
	125		
	170		
	185		
	195		

Table: 1 shows the test image, number of thresholds generated and the optimal threshold values and the objective values achieved by the proposed method. Fig 3 and fig 4 shows the input image and the initial seed map for the optimal threshold.

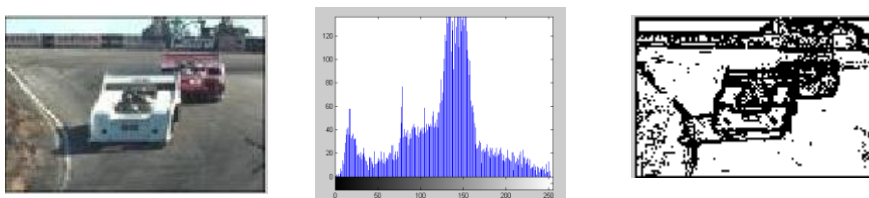


Fig 3: a) Input Image b) Histogram of gray scale image c) Initial Seed Map

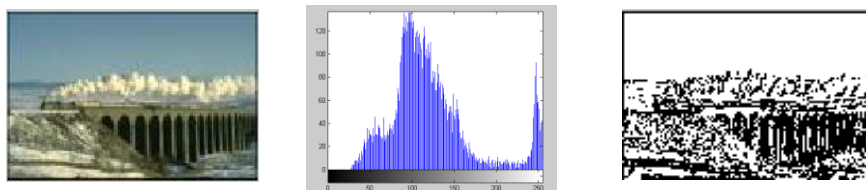


Fig 4: a) Input Image b) Histogram of gray scale image c) Initial Seed Map

III. CONCLUSION:

A seed selection algorithm using cuckoo search optimization is proposed in this paper. The population of the host nest is randomly initiated and from the population best threshold is chosen using the fitness function. This threshold is used as the optimal threshold for initial seed selection. A best entropy thresholded image contains more information. Hence, seeds generated using entropy thresholding will contain more information about a region and will provide better segmented image.

REFERENCES

- [1] H. Cheng, X. Jiang, Y. Sun, and J. Wang, "Color image segmentation: Advances & prospects," *Pattern Recognit.*, vol. 34, no. 12, pp.2259–2281, Dec. 2001.
- [2] Y. W. Lim and S. U. Lee, "On the color image segmentation algorithm based on the thresholding and the fuzzy C-means technique," *Pattern Recognit.*, vol. 23, no. 9, pp. 935–952, 1990.
- [3] M. Kass, A. Witkin, and D. Terzopoulos, "Snakes: Active contour models," in *Proc. 1st ICCV*, 1987, pp. 259–267.
- [4] P. L. Palmer, H. Dabis, and J. Kittler, "A performance measure for boundary detection algorithms," *comput. Vis. Image Understand.*, vol. 63, pp. 476–494, 1996. [5] T. Pavlidis and Y. T. Liow, "Integrating region growing and edge detection," *IEEE Trans. Pattern Anal. Machine Intell.*, vol. 12, pp. 225–233, 1990.
- [6] J. Haddon and J. Boyce, "Image segmentation by unifying region and boundary information," *IEEE Trans. Pattern Anal. Machine Intell.*, vol. 12, pp. 929–948, 1990.
- [7] C. Chu and J. K. Aggarwal, "The integration of image segmentation maps using region and edge information," *IEEE Trans. Pattern Anal. Machine Intell.*, vol. 15, pp. 1241–1252, 1993.
- [8] Yang XS, Deb S (2009) Cuckoo search via Lévy flights, In: *Proceedings of World Congress on Nature & biologically Inspired Computing (NaBIC 2009, India)*, 210-214.
- [9] T.Pun, "A new method for gray-level picture thresholding using the entropy of the histogram", *Signal processing* 2(1980), 223-237.

Development of Self Repairable Concrete System

Sahebrao.G.Kadam, Dr. M.A.Chakrabarti, S.V.Kedare
(Department of structural engineering, VJTI, Mumbai, India)

ABSTRACT:

This study aims to develop self repairable concrete as a new method for crack control and enhanced service life in concrete structure. This concept is one of the maintenance-free methods which, apart from saving direct costs for maintenance and repair, reduce the indirect costs. We are going to develop the self-repairing concrete by adding the materials from inside the concrete to repair. Our technique to develop self-repairing concrete consists of embedding repairing materials in hollow ducts in the repairing zone before it is subjected to damage. Therefore when cracks occurs this repairs materials will get released from inside and it will enter the repairing zone. Where it will penetrate into cracks and rebound to mother material of Structure and it will repair the damage.

KEYWORDS: Concrete – Serviceability – Cracks - Epoxy resins - Repairs

I. INTRODUCTION

The serviceability limit of concrete structures by cracking might be overcome by crack control methodologies; the enhanced service life of concrete structures would reduce the demand for crack maintenance and repair. In particular, the utilization of self-repairing technologies has high potential as a new repair method for cracked concrete. The usual approaches for repair of structural concrete are: polymer injection, prestressing, Geomembranes, and polymer wraps. These techniques seek a ductile, less brittle failure. All of them are based on addition of a repair material to concrete from the outside in; We add the materials from inside the concrete to repair. Our technique is to develop self-repairing concrete consists of embedding repairing materials in hollow ducts in the repairing zone before it is subjected to damage or crack. Therefore when cracks occurs this repairs materials will released from inside duct and it will enter the repairing zone. Where it will penetrate into cracks and rebound to mother material of structure. The cracking and damages are associated with low tensile strain capacity of concrete, get repaired with our chemical present inside. Thus we repair the problem where it occurs and just in time automatically without material intervention. Hence technique we utilized does precisely that it adds more materials to the concrete repair zone from inside upon demand when it is triggered by events such as cracking. Our approach consists to address the bonding problem of repair material from inside the concrete therefore definitely better technique compared to other methods. It is seen that self-repairing performs better because the resin is flexible itself and keep on releasing the each brittle failure that is cracks. The internal released stiff resins are less brittle, more ductile and stronger in tension as compare to concrete. This type of technique is useful for structural member subjected to bending, shear cracks, etc. This approach of self-repairing is useful for bridges having pre-stressed box girders where dynamics, moving loads cyclic loads are in huge quantity and development of minor to major cracks possibility is more.

II. WORK EXECUTED BY DIFFERENT RESEARCHERS

In literature survey last 20 years different research has develop the self-repairing techniques in different country under different climatic conditions, assumptions, and materials, etc. Out of which Dr. Carolyn Dry from USA has developed the practical technique of Development of self-repairing durable concrete [1]. In his work investigation was made into development of transparent polymer matrix composites that have the ability to self-repair internal cracks due to Mechanical loading. In his work focused on cracking of hollow Repair fibers disposed in a matrix and subsequent release of repair chemicals in order to visually assess the repair and speed of repairs in the impact test the polymer specimen was released in ten seconds. Similarly, Mihashi and Yoshio proposed incorporating glass pipes containing the repairing agent into the concrete for self-healing capabilities to restore strength and for the prevention of water leakage [2]. This concept was also utilized by Li et al. who incorporated hollow glass fibers containing ethyl cyanoacrylate, a thermoplastic monomer, into the mix [3]. This filled hollow-fiber method has been successful in other concrete systems as well as reinforced polymers and epoxies [4-10], but limitations such as a lack of ease in manufacturing have made these products undesirable for

commercial use. Sottos et al. have developed a polymer composite system that incorporates a catalyst into the polymer matrix phase with a microencapsulated repair agent [11]. The healing agent is released upon crack propagation through the microcapsule, resulting in as much as an 80% recovery of toughness after a fracture. This method has been successfully demonstrated in various polymer composite systems [12-14].

III. SELECTION OF MATERIAL

In development of self-repairable concrete system main component i.e. resin and hardener were selected such that, it will get mixed together after formation of crack and will get set within crack with addition of sealing it. Some criteria for the selection of resin considered are,

- a) The material should be able to repair different types and sizes of damages.
- b) It should be economically viable.
- c) It should be easily available in market.
- d) While using the chemical it should not cause hazardous effects.
- e) It should establish good quality assurance and reduce life cycle cost.
- f) It should withstand different forces and dynamic loads.
- g) It should have satisfactory properties like compressive strength, viscosity and pH.

pH value is such that it will not cause any corrosion to the reinforcement. Viscosity of both the chemical shall be such that it will seal the minor cracks like shrinkage or temperature cracks. Working temperature of both the solution shall be wide. Void former of polyurethane selected so that it can be easily removed from concrete specimen as there is no friction between surfaces. This void former material is elastic and easily available in various diameters.



Fig.1 Polyurethane pipe as void former 6mm outer diameter



Fig.2 Epoxy resin(Dropoxy 7250)



Fig.3 Hardener(Dromide 9340)

IV. TEST METHODOLOGY

The methodology is mainly designed for flexural member and for crack formation within that member due to different loadings. To carry out one point flexural test a concrete specimen of 300mm x 70mm x 1000mm with 6mm dia. mild steel bars is such selected so that it will be a flexural member with sufficient width so that matrix of hollow ducts can be laid along it on the tension side of section. In the initial stage of testing we have provided ducts in two layers along the length and width in cover area of reinforcement of member with the help of polyurethane material of 6mm diameter. This Ducts then alternately filled with epoxy solution and hardener. Idea behind is when crack formation under loading will take place this two solutions will get mixed with each other forming hard compound together which will seal the crack.



Fig.4 Shuttering for test specimen fitted with void formers

After fixing the void formers and reinforcement concreting was done in number of layers and successive vibration. After finishing with concreting specimen was allowed to set for 24 hr. After 24 hr. void former was removed by simple pulling from one end of specimen. Then slab specimen was separated from shuttering, one control specimen was also made same as main specimen but duct system was not provided. Slab specimen were then placed into the water curing tank for 28 days. After 28 days samples were taken out from curing tank and kept in air to dry it properly. This ducts then filled with alternate resin and hardener under gravity flow and it was ensured that no any air pocket will get formed. After filling of ducts with resin both end of specimen were sealed. After sealing ends, the slab specimen then tested with three point flexural loading. Load corresponding to hair crack formation, release of chemical through crack and proper visibility of solution noted along with deflection. After release of chemical from cracks, specimen then unloaded and kept for air curing for 7 days, this was done to allow chemical to get filled into the crack and seal the crack. Control specimen was also tested after 28 days curing, load corresponding to crack formation and also failure load was noted.



Fig.5 Slab specimen placed on one point flexure testing machine



Fig.6 Propagation of crack to soffit of slab



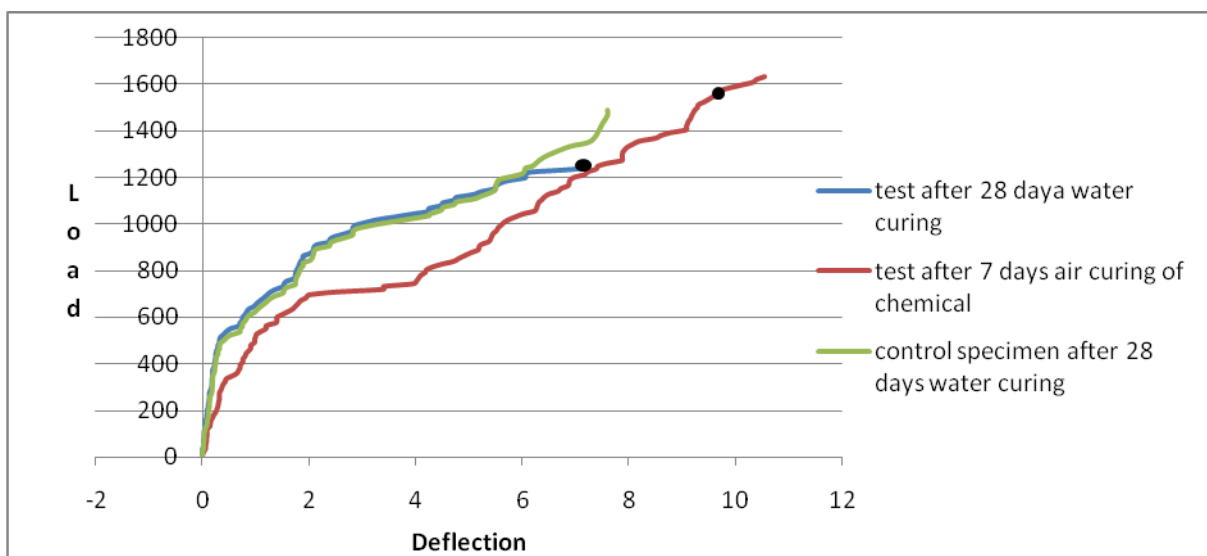
Fig.7 Chemical is released and appeared on surface



Fig.8 Crack sealed with resins and hardener

V. RESULTS AND CONCLUSION:

1. In this research work the load carrying capacity of plain member or control specimen and member with chemical in duct is same. Hence no reduction in strength by providing duct and chemical.
2. After loading and air curing of hardener and resins together, load carrying capacity increased by 15-20 % than control specimen member. Hence strength increases after reaction between hardener and resins by air curing.
3. Three point bending test was carried out on the specimen after 28 days of curing by feeling the resins. Load is gradually added till resin gets released through the cracks. Same test was again carried out after 7 days to ensure the curing with resins.
4. Application of research work is for the structures subjected to cyclic loads and dynamic loads. i.e Bridge Girders, etc.
5. Control specimen was also tested after 28 days curing Graph showing load vs. deflection of specimen.



Graphical representation of test data

From this graph of case one of loading some observations are made that are as follows:

- In case of first test chemical visible on surface for load of around 1248 kg and in case of second test chemical getting released for load of around 1548 kg.
- Theoretical value of load for crack formation matches with the experimental value.
- Chemical is getting released through the cracks in desired way.
- Crack getting filled with the solution in proper manner.
- Crack getting sealed properly where there is proper mixing of resin and hardener

REFERENCES

- [1]. Dr. Carolyn Dry Has Carried Out Lot Of Work On Development Of Self Repairing Durable Concrete. Natural Process Design, Inc. Winona, Minnesota (507-452-9113).
- [2]. Mihashi, H. and Y. Kaneko, Intelligent concrete with self-healing capability. Transactions of the Materials Research Society of Japan, 2000. 25(2): p. 557-560.
- [3]. Li, V.C., Y.M. Lim, and Y.-W. Chan, Feasibility study of a passive smart self-healing cementitious composite. Composites Part B, 1998. 29B: p. 819-827.
- [4]. Pang, J.W.C. and I.P. Bond, A hollow fibre reinforced polymer composite encompassing self-healing and enhanced damage visibility. composites Science and Technology, 2005. 65: p. 1791-1799.
- [5]. Dry, C.M., Alteration of matrix permeability and associated pore and crack structure by timed release of internal chemicals. Ceramic Transactions, 1991: p. 191-193.
- [6]. Dry, C.M., Passive tunable fibers matrices. . International Journal of Modern Physics, 1992. 6: p. 2763-2771.
- [7]. Dry, C.M. Smart building materials which prevent damage or repair themselves. in Proceedings of the Materials Research Society Symposium. 1992. California: Materials Research Society.
- [8]. Dry, C.M. Smart materials which sense, activate and repair damage; hollow porous fibers in composites release chemicals from fibers for self-healing, damage prevention, and/or dynamic control. in First European conference on smart structures and materials. 1992. Glasgow, Scotland.
- [9]. Williams, G., R. Trask, and I.P. Bond, A self-healing carbon fibre reinforced polymer for aerospace applications. Composites Part A, 2007. 38(1525-1532).
- [10]. Williams, G., R. Trask, and I.P. Bond, Bioinspired self-healing of advanced composite structures using glass fibres. Journal of the Royal Society Interface, 2007. 4: p. 363-371.
- [11]. Sottos, N.R., M.R. Kessler, and S.R. White, Self-healing structural composite materials. Composites Part A: Applied Science and Manufacturing, 2004. 34(8): p. 743-753.
- [12]. Yin Tao, e.a., Self-healing woven glass fabric/epoxy composites with the healant consisting of micro-encapsulated epoxy and latent curing agent. Smart Material Structures, 2008. 17: p. 15-19.
- [13]. Brown, E.N., N.R. Sottos, and S.R. White, Retardation and repair of fatigue cracks in a microcapsule toughened epoxy composite- Part II: In situ self-healing Composites Science and Technology, 2005. 65(15-16): p. 2474-2480.
- [14]. Yin, T., et al., Self-healing epoxy composites- Preparation and effect of the healant consisting of microencapsulated epoxy and latent curing agent. . Composites Science and Technology 2007. 67(2): p. 201-212.

Case Study on Injection Moulding Windsor 650 Machine Parameters on Wall Thickness Variation Defect

K. Raghavendra Kasyap¹ and M Subba Rao²

¹ M. Tech Student in MITS, Madanapalle

² Assistant Professor in Mechanical Engineering Department, MITS, Madanapalle

ABSTRACT:

In present scenario, injection moulding is most suitable manufacturing process for developing a plastic product. While developing a plastic product through injection moulding Windsor 650 machine, various defects are occurred internally and externally. Optimization of various parameters may reduce the defects of products and effect on the quality of the product. The purpose of this paper is studying the effect of various injection moulding Windsor 650 machine process parameters on Wall thickness variation defect. The Wall thickness variation is the most common defect which will form internally. To reduce the Wall thickness variation defect the various process parameters of injection moulding Windsor 650 machine are optimized by using Design of Experiments method.

KEYWORDS: Design of Experiments, Injection moulding, Optimization, Process parameters, Wall thickness variation defect.

I. INTRODUCTION

Injection moulding machine is most commonly used to producing plastic products. This process is most practical and cost effective to produce plastic products. During producing a product using injection moulding process various defects such as warpage, shrinkage sink marks and weld lines can be occurred. The optimization of injection moulding process parameters is very important to reduce these defects [1]. The process parameters for each defect are different, because of that while decreasing one defect may cause to increase another various defects [2]. So optimization of various process parameters is very essential for minimization of all the defects to get the quality product [3]. Common defects in injection moulding process are classified in to two ways. They are,

- [1] Dimensional related
- [2] Attribute related

Dimensional related defects can be considered by correcting the mould dimension. But attributed related defects are generally depends on process parameters of Injection moulding [4]. This paper presents the case study on injection moulding Windsor 650 parameters on wall thickness variation defect. Cavity pressure is the most common parameter in injection moulding process to compensate the shrinkage during cooling stage [5]. The mould temperature is one of the most efficient parameters in injection moulding to reduce warpage and shrinkage defects [6]. Holding time is another major effecting factor which influence the quality of the product produced. While temperature and pressure are constant some defects still arise due to effect of time [7].

II. TYPES OF WINDSOR INJECTION MOULDING MACHINE

There are three Windsor injection moulding machines which are most commonly used machines in the industries to produce plastic components. They are

- [1] Windsor sprint 180 machine.
- [2] Windsor sprint 350 machine.
- [3] Windsor sprint 650 machine.

Windsor sprint 180 machine: This type of machines is used for manufacturing a wide range of plastic products. This machine used to develop a plastic product which is small in size.
Example: Ribs, Bushes, vane plugs, pen caps etc.

Windsor sprint 350 machine: This type of machines is used for manufacturing a wide range of plastic products. This machine is used to develop a plastic product which is medium in size.

Example: Battery covers, Boxes etc.

Windsor sprint 650 machine: This type of machines is used for manufacturing a wide range of plastic products. This machine is used to develop a plastic product which is large in size.

Example: Battery containers, Buckets, Large plastic products.

III. WINDSOR SPRINT 650 MACHINES

The Windsor sprint 650 machine is one of the most commonly used injection moulding machine to produce a plastic product which is greater in size.

Procedure of Windsor sprint 650 machine

Like remaining processes, this machine is also simple to produce a wide range of variety of the products. The plastic granules are in the form of pellets are pre-heat in the dryer for 3 hours up to certain temperature. After preheating the pellets then poured in to the injection moulding machine through hopper.

In this machine there are mainly three stages for developing a plastic product,

They are

- [1] Injection stage.
- [2] Clamping stage.
- [3] Ejection stage.

Injection stage: In this stage the plastic granules comes through the hopper and feed in the form of pellets. A melting zone is there in this stage for melting the raw material at certain temperature and converts the pellets granules into liquid form. A reciprocating screw is located in the injection stage for inject the raw material in to the next stage. While screw moves backward the melted raw material moves forward. Now, the screw moves forward the raw material inject in to next stage through nozzle of the screw at certain temperature and certain speed. Injection moulding machine uses moulds to manufacture a plastic product. There are many components in the mould but it is split in to two halves. They are, mould core and mould cavity. When the mould is closed, the space between the mould core and mould cavity forms the part cavity. Multiple-mould is sometimes used, in which the two mould halves form several identical part cavities.

Clamping stage: When injecting the material in to the mould the two parts of mould must be securely closed by clamping stage. The mould core is attached to the injection chamber and mould cavity is attached to cooling chamber. While the material is inject in to the mould, the clamping stage pushes the two mould core and cavity together at certain force to close the mould.

Ejection stage: After some time, the cooled part is to be ejected from the mould by ejection system. While open the mould, a mechanism is used to push the plastic product out of the machine. Once the part is ejected, the mould will closed for the next shot of injection operation.

Defects in the product: Many factors can affect the quality of the plastic products during injection moulding process.

There are many defects that are formed internally and externally of the injection moulding plastic products. They are

- [1] Short fill.
- [2] Silver streak.
- [3] Colour variation.
- [4] Sink marks.
- [5] Weld lines.
- [6] Surface defects.
- [7] Flashes.
- [8] Warpage and
- [9] Wall thickness variation

1. Short fill

This means occurring of the short weight on the product. It is caused by insufficient filling of raw material in the mould.

Remedies of short fill are

- [1] Increase the short weight of the product.
- [2] Increase the injection pressure.
- [3] Decrease the cylinder temperature.
- [4] Increase the injection speed.
- [5] Decrease the rotation speed and reduce the back pressure of the screw.

2. Silver streak

It contains the moisture particles with in the raw material. It is in the form of silver colour which is to be formed on the product surface and which follow the flow direction of the raw material in the cavity.

It is caused by moisture occurred in the raw material.

Remedies of silver streak are

- [1] Pre – heat the raw material in the dryer for up to certain temperature for removing moisture particles.
- [2] Decrease the cylinder temperature and increase the injection pressure.
- [3] Increase the injection speed.
- [4] Increase the rotation speed and adjust the back pressure of the screw.
- [5] Ensure the proper melting duration of the raw material.

3. Sink marks

It is a local surface depression that typically occurs in the moulding with thicker sections or at locations above ribs, bosses and internal fillets.

Remedies of the sink marks are

- [1] Increase the hold on time, feeding time and cooling time.
- [2] Increase the injection pressure.
- [3] Extend the hold pressure duration.
- [4] Increase the screw forward time.
- [5] Decrease the melt temperature and
- [6] Decrease the mould temperature.

4. Weld lines

It is occurred when melt flow front collide in a mould cavity. It is very common and difficulty injection moulding defect to eliminate.

Remedies of the weld lines are

- [1] Increase the injection pressure.
- [2] Increase the injection speed.
- [3] Increase the cylinder temperature.
- [4] Make the position of where the weld line occurs more close to gate.
- [5] Change the gate position.
- [6] Change the part thickness.

5. Colour variation

It is occurred when insufficient mixing up of raw - material with master batch. Remedy is to take care of mixing proportions with accurate weight proportions.

6. Surface defects

The surface defects are mainly caused by either mould is heavy hot or in the form of heavy cold. The surface defects are mainly occurred at gates.

Remedies for surface defects are

When mould is hot

1. Cold the mould near gates.

When mould is cold

- [1] Increase the mould temperature.
- [2] Increase mould pressure and
- [3] Increase the injection speed.

7. Flashes

It is caused when excessive injection pressure and insufficient clamping force.

Remedies of flashes are

- [1] Decrease the injection pressure.
- [2] Decrease injection temperature.
- [3] Adjust the mould parting.
- [4] Increase the clamp force.

8. Warpage

It is caused when sharp variation occurs in the wall thickness of the plastic product.

Remedies of the Warpage are

- [1] Increase the melt temperature.
- [2] Decrease the volume of the product.
- [3] Decrease the injection pressure.
- [4] Decrease the injection time.
- [5] Adjust the gate sizes.
- [6] Adjust the part designs.

iv. Windsor 650 Machine Parameters on Wall Thickness Variation Defect:

The wall thickness variation is a common defect on injection moulding product. This is mainly occurred at internally of the plastic product. Hold on Pressure, Hold on speed, Hold on time and position of the raw material is the most efficient parameters of the wall thickness variation which will effect on the quality of the product.

Hold on Pressure: The hold on pressure holds the pressure against cooling the plastic in the cavity image while solidifies. It is one of the efficient parameter of injection moulding with range 50-80 bars. If hold on pressure increases, it result in over flash on the product. If hold on pressure decreases, it result in shrinkage.

Hold on Speed: It is the common parameter which causes the wall thickness variation defect in the injection moulding plastic product. Range of hold on speed is 20-40%. If hold on speed increases then shrinkage is avoidable on the product. If hold on speed decreases short fill occurs on the product.

Hold on Time: It is the common parameter which causes the wall thickness variation defect in the injection moulding plastic product. Range of hold on time is 5-8sec. If hold on time increases, it result in increasing the weight of the product. If hold on time decreases then short fill occurs on the product.

Position of raw material: It is the quantity of raw material which will feed for one stroke of injection rammer. It is the common efficient parameter in the injection moulding plastic product. If increasing and decreasing the position of raw material, it will affect in weight of the product and varying the wall thickness of the product.

v. CONCLUSIONS

This study is mainly focused on reduce the wall thickness variation defect in injection moulding product by optimizing various process parameters. Hold on pressure, hold on speed, hold on time and position of the raw material considered as most efficient parameters on the quality of the injection moulding product. By optimizing these parameters we can reduce the wall thickness variation defect in injection moulding Windsor 650 machine.

REFERENCES

- [1] R. Hussin, R. M. Saad, Razaidi Hussin, and M. S. I. M. Dawi, "An optimization of plastic injection moulding parameters using taguchi optimization method", *Asian Transactions on Engineering*, November 2012, Volume 02 Issue 05.
- [2] A. Akbarzadeh, and M. Sadeghi, "Parameter study in plastic injection moulding process using statistical methods and IWO algorithm", *International Journal of Modeling and Optimization*, June 2011, vol.1, No.2.
- [3] T. Eenzurumulu, and B. Ozcelik, "Minimization of warpage and sink mark index in injection - moulded thermoplastic parts using Taguchi Optimization method", *Materials and design* 27, 2006 853-861.
- [4] D. Mathivanan, M. Nouby and R. Vidhya, "Minimization of sink mark defects in injection moulding process – Taguchi approach", *International Journal of Engineering, Science and technology*, 2010 vol. 2, NO. 2.
- [5] M. Kurt, O.S. Kamber. Y. Kaynak, G. Atakok and, O. Girit, "Experimental investigation of plastic injection moulding: Assessment of the effects of cavity pressure and mould temperature on the quality of final products", *Materials and design* 30, 2009, (3217 - 3224).
- [6] Ko-Ta Chiang, "The optimal process conditions of an injection – moulded thermoplastic part with a thin shell feature using Fuzzy logic: A case study on machining the PC/ABS cell phone shell", *Materials and Design* 28 2007 1851 – 1860.
- [7] M.C. Huang, and C.C. Tai, "The effective factors in the warpage problem of an injection – moulded part with a thin shell feature" *Journal of Materials Processing Technology* 110, 2001, 1 – 9.

- [8] L.M Galantucci and, R. Spina, "Evaluation of filling conditions of injection moulding by integrating numerical simulations and experimental tests", *Journal of Materials Processing Technology* 141, 2003, 266 – 275.
- [9] H. Oktem, T. Enzurumulu, and Ibrahim uzman, "Application of Taguchi optimization technique in determining plastic injection moulding parameters for a thin – shell part", *Materials and Design* 28, 2007, 1271- 1278.
- [10] J. Cheng, Y. Feng, J. Tan, and W. Wei, "Optimization of injection mould based on Fuzzy mould ability evaluation", *Journal of Materials Processing Technology* 208, 2008, 222 – 228.
- [11] B. Ozcelik, "Optimization of injection parameters for mechanical properties of specimens with weld line of polypropylene using Taguchi method", *International Communications in Heat and mass Transfer* 38, 2011, 1067 – 1072.
- [12] Y.K Shen, C.W. Wu, Y.F Yu, and H. Wei- Chung, "Analysis for optimal gate design of thin-walled injection moulding", *International Communications in Heat and Mass Transfer* 35, 2008, 728 – 734.
- [13] B. Farshi, S. Gheshmi, and, E. Miandoabchi, "Optimization of injection moulding process parameters using sequential simplex algorithm", *Materials and design* 32, 2011, 414 – 423.